NASA-TM-111639

Clouds in Climate: Modeling and Satellite Observational Studies

March 1981

Report of Workshop
held at
NASA Goddard Institute for Space Studies,
New York, NY, October 29-31, 1980

National Aeronautics and
Space Administration

Clouds in Climate:
Modeling and Satellite Observational Studies

March 1981

Report of Workshop
held at
NASA Goddard Institute for Space Studies,
New York, NY, October 29-31, 1980

NASA
National Aeronautics and
Space Administration

CONTENTS

		Page
Preface		v
1.	Recommendations	1
2.	Introduction	4
3.	Clouds in Climate Models	8
	3.1 Cloud Generation in Climate Models	8
	3.2 Cloud Interactions with Other Elements	52
	3.3 Summary	112
4.	Satellite Observations	113
	4.1 Cloud Climatologies	113
	4.2 Data Compression	180
	4.3 Summary	197
5.	Recommended Studies	198
	5.1 Panel Discussion on Cloud/Climate Modeling Studies	198
	5.2 Panel Discussion on Analysis/Data Compression Schemes	199
6.	Appendices	201
	6.1 Organizing Committee	201
	6.2 Workshop Participants	202
	6.3 Availability of Data for Cloud Studies: R. Jenne	204
	6.4 Data Archives and Analysis/Data Compression Schemes: R. Jenne	212
	6.5 Cloud Climatology Needs of Climate Modelers: Summary of Recommendations: J. E. Hansen	217
	6.6 Selected Bibliography	220

PREFACE

The cloud-radiation problem has been identified as one of the high priority elements of the newly established World Climate Research Program (WCRP). The important aspects of this research element include:

- the sensitivity of climate to cloud-radiation feedback
- the primary problem of cloud generation in climate models
- the need for empirical studies of dependence of climate on cloudiness

The Joint Scientific Committee (JSC) of WMO/ICSU has endorsed the concept of a satellite derived cloud climatology project as a major new initiative under the WCRP. A major step forward in defining such a project was taken over the past year in preparing the document "The International Satellite Cloud Climatology Project." This report was prepared by a group of experts who met at Balatonalmadi, Hungary and at Fort Collins, Colorado in 1980 under the joint sponsorship of the IAMAP Radiation Commission and COSPAR. Plans are now underway to further define and implement this project.

The NASA sponsored workshop described in this report represents an attempt to bring together a group of producers and users of satellite derived cloud data to recommend priorities for research related to the cloud climatology problem. The user community participating in the workshop was restricted to the modelers; a subsequent workshop sponsored by the NOAA National Earth Satellite Service (NESS) involved in broader user community.

Within the U.S., responsibility for planning the national effort in support of this research will be under the National Climate Program's principal thrust in Solar and Earth Radiation, for which NASA has been assigned lead agency responsibility. International coordination will be through the NOAA Special Programs Office.

Robert A. Schiffer
Manager, Climate Research Program
Office of Space and Terrestrial Applications
NASA Headquarters

1. RECOMMENDATIONS

The general question of the role of clouds in the climate, understood primarily through modeling and data analysis, can be divided into two broad problems: measuring, modeling and understanding cloud *processes* and measuring, modeling and understanding the *climatology* of clouds. These two problems are, in fact, intimately intertwined in any research effort, but seem to require two distinct selections of the amount of detail and the spatial and temporal resolution required of data or modeling results. Neither selection is sufficient to define completely the role of clouds in climate nor is adequate to serve completely the purpose of the other. These two selections are complementary and of equal priority in the study of clouds.

Cloud process research primarily involves analysis of the kind of data obtained from an intensive field study like GATE and from modeling of individual clouds or mesoscale cloud complexes in isolation. Several such data sets are now available (e.g., GATE, CYCLES, MONEX), most especially those studies associated with FGGE. More such field studies are planned (e.g., STRATEX). Continued analysis of these data sets is vital support for a climatology effort.

Establishing and understanding the global climatology of clouds has not yet received the same coordinated and concerted effort to acquire the proper data that cloud process studies have; but planning for such a program is underway. Before we can collect the data to form a cloud climatology, we must define the best methods for obtaining it, consistent with our capabilities to measure the desired quantities, to process the data into a useful form, and to utilize the results effectively in climate models. There is a clear congruence of these capabilities, at present, in our improved ability to retrieve global atmospheric, surface and cloud optical properties from satellite measured radiances and to calculate and parameterize the radiative fluxes in climate models. Although other cloud processes in the atmosphere, such as convection or precipitation, are equally important to understanding the climate, neither our modeling of nor our ability to observe these processes has progressed as far as our understanding of the cloud-radiation interaction. Thus, *we recommend that the primary objective of cloud climatology research in the next decade be to define and obtain a global climatology of the radiative properties and interactions of Earth's clouds.* Obtaining a climatology of precipitation, small-scale convection or other related cloud/climate quantities should be considered secondary, though important, objectives of research during this period.

Before a program to collect data for a cloud climatology can be undertaken, research is required to answer four questions:

1. What are the most important optical and physical properties of clouds, atmosphere, and surface needed to determine the radiative properties and radiative interactions of clouds?
2. What quantities should be measured by satellites and conventional observing systems and with what spatial and temporal resolution and coverage in order to determine these radiative properties?

3. What is the best scheme for archiving as much of the original data stream as possible into a convenient format that does not have too large a volume?
4. What is the best analysis scheme for producing a cloud climatology that is small enough and informative enough to be effectively used by climate modeling research groups?

Interaction is required between studies of each question; e.g., to define the best archiving scheme requires understanding the nature of the final product of the analysis scheme. Thus, *we recommend the formation of a working group to coordinate a set of pilot studies to define the archiving and analysis schemes.* This working group should be composed of representatives from research groups and satellite operations groups that are *actively* pursuing studies of these four questions.

Task 1: Determination of Key Cloud-Radiation Parameters

Questions to be addressed:

1. What are the key cloud properties which govern cloud radiative interactions?
2. Which cloud and radiative parameters are most diagnostic of climate model performance?
3. Which quantities currently being measured by satellites are most important in determining the key cloud and radiative parameters?

Necessary pilot studies:

1. The treatment of cloud radiation interactions in climate models which predict cloud distributions should be improved consistent with current knowledge of these processes. Diagnostic analyses of data and model sensitivity studies should be performed to determine the key cloud and radiation parameters.
2. Model sensitivity studies should be performed to determine the parameters which govern the model radiation calculations, and which best test the model cloud predictions.
3. Tests of model sensitivity to uncertainties in quantities derived from current satellite observations should be performed to evaluate the required spatial and temporal resolution and coverage of the data for a cloud climatology.

Task 2: Definition of a Data Archiving Scheme

Questions to be addressed:

1. What are the basic *physical* quantities to be stored (e.g., radiances)?
2. What auxiliary information should be kept?
3. What volume should the archive have to be most useful?

Necessary pilot studies:

1. Access to a data base simulating the current operational data streams should be made available so that a few experimental archiving schemes can be tested to investigate the feasibility of real-time data compression. Scheme intercomparisons must be stressed.
2. The feasibility of storing the complete data stream, plus required auxiliary information, should be investigated. The usefulness of such an archive must be considered.

Task 3: Definition of Analysis Schemes

Questions to be addressed:

1. What are the basic cloud optical and physical properties that can be derived?
2. What supplementary information is needed to determine the cloud–radiation interaction?
3. What statistics and descriptions of the cloud distributions and variations should be retained in the climatology?
4. What volume should the climatology have to be most useful to research groups?

Necessary pilot studies:

1. Data from the FGGE period onward should be organized, corrected and documented to form data sets for testing analysis schemes.
2. *Coordinated* pilot studies testing the retrieval of cloud optical properties from different types of data should be performed with special emphasis on those types of data that will be available in mid–decade. These studies should produce preliminary cloud climatologies for scheme intercomparison and error analysis.
3. Wide dissemination of the results of these pilot studies is necessary.

Upon completion of such a coordinated set of pilot studies, a global, multi–year program to produce a global cloud climatology is the next necessary step in improving our understanding of the climate.

2. INTRODUCTION

This Cloud/Climate Workshop brought together representatives of the climate modeling and observational communities to determine guidelines for research on cloud-climate relationships over the next several years. Lack of understanding of the cloud processes linking the radiative, hydrologic and dynamic components of the atmospheric circulation is one major obstacle to understanding climate. The primary tools for investigations of climate are numerical models of varying complexity, but observations of cloud distribution and variation are necessary to improve model physics and to verify model simulations.

This Workshop was built on progress already attained by previous conferences, particularly, the 1974 JOC Study Conference on Climate and the 1978 JOC Conference on Parameterization of Extended Cloudiness and Radiation for Climate Models. The participants recommended a series of modeling and observational programs to attack, in particular, the problem of the radiative effects of clouds. The key modeling studies concerned determination of the model climate's sensitivity to variation of cloud properties and parameterizations and determination of the importance of cloud and related feedbacks to the model climate. The key observational programs were intensive field studies to improve understanding of cloud-radiation processes and large scale, long term studies to form global, seasonal cloud climatologies for model verification.

Several large field studies, most notably FGGE, have now been completed with data analysis underway. A few more such programs are already planned. With the continued development of climate models incorporating fully interactive clouds, assessment of data needed for further model development seems necessary. This document is a report of that assessment by the workshop participants. The most crucial requirement identified for further model development is for a global, seasonal cloud-radiation climatology to verify the performance of climate general circulation models (GCM's) which predict cloud distributions and variations.

Dr. Robert Schiffer, NASA Climate Program Manager, opened the Workshop by summarizing the key issues for discussion, as follows:

1. What is a cloud?
2. How well can we simulate cloud processes in climate models?
3. How well do we understand the physics involved?
4. What cloud data is needed to initialize/validate climate models?
5. What can we learn from further analysis of past/current satellite data?
6. Can we distinguish between significant cloud types and determine precipitation rates?
7. How should a global cloud data set be configured for climate model application?
8. What supplementary information should be included in the data set?
9. What research should be given the highest priority over the next several years?

Dr. Rex Fleming, Director U.S. GARP Office, further defined the context of the workshop by describing evolving plans for a WMO-sponsored project to collect and analyze five years of global satellite data to produce a cloud climatology for model verification. He suggested three preparatory tasks which should be the focus of research for the next several years:

1. Determine the capability to reduce the volume of satellite data without sacrificing "cloudiness signatures."
2. Develop optimum algorithms for translation of satellite radiance values to cloud properties.
3. Determine methods for satellite inter-calibration.

The first day of the workshop was devoted to presentations and discussion concerning cloud generation and interactions in climate models. Drs. Edward Sarachik (Harvard) and Peter Webster (CSIRO) presented reviews of these two topics. The second day was devoted to presentations and discussion concerning current methods of retrieving cloud properties and distributions from satellite data and possible data compression schemes. Drs. Eric Smith (Colorado) and Roy Jenne (NCAR) presented reviews. On the third day two panel discussions were organized about these topics, with the primary focus on the research needed to define the kind of satellite data and analysis required to produce a useful cloud climatology. A detailed agenda is shown below.

CLOUD/CLIMATE WORKSHOP
Goddard Institute for Space Studies
October 29-31, 1980
Agenda

Wednesday, October 29

OPENING REMARKS — 9:00 am – 9:30 am

R. Schiffer – NASA HQ
R. Fleming – U.S. GARP Office/NOAA

1. CLOUDS IN CLIMATE MODELS

Cloud Generation in Climate Models — 9:30 am – 12:30 pm

A. Arakawa – Chairman

E. Sarachik – Invited Review (45 min)

Contributed Papers

R. T. Wetherald and S. Manabe: A simulation of cloud cover with a global general circulation model of the atmosphere (20 min)

D. Rind: Cloud sensitivity experiments with the GISS GCM (25 min)

R. A. Reck and J. R. Hummel: Clouds in radiative-convective models: Assumptions, implications, and limitations (10 min)

R. S. Lindzen: Some remarks on cumulus parameterization (10 min)

Cloud Interactions With Other Climate Elements 2:00 pm – 5:00 pm

R. E. Dickinson – Chairman

P. Webster – Invited Review (45 min)

Contributed Papers

R. T. Wetherald and *S. Manabe:* Cloud cover and climate sensitivity (10 min)

V. Ramanathan and R. E. Dickinson: Stratus clouds and ocean energy budget: A preliminary GCM study (10 min)

G. F. Herman: A review of cloud-radiation experiments with the GLAS general circulation model (10 min)

J. Shukla and Y. Sud: Effect of cloud-radiation feedback on the climate of a general circulation model (10 min)

R. D. Cess: Low-latitude cloud amount and climate feedback (5 min)

G. L. Potter: Climate change and cloud feedback: The possible radiative effects of latitudinal redistribution (5 min)

A. Arking, M. D. Chou, and L. Peng: Sensitivity of climate to cloud parameter variations (5 min)

A. Gordon and R. Hovanec: The sensitivity of model-derived radiation fluxes to the monthly mean specification of cloudiness (5 min)

Thursday, October 30

2. SATELLITE OBSERVATIONS

Cloud Climatologies 9:00 am – 12:00 pm

A. Arking – Chairman

E. A. Smith – Invited Review (20 min)

Contributed Papers

E. Harrison: Examples of cloud cover and diurnal variation studies using GOES data (15 min)

J. A. Coakley: Errors in cloud amount obtained using threshold techniques (10 min)

M. T. Chahine: Comparisons of visible and infrared distributions of global cloud covers (15 min)

T. S. Chen, *L. L. Stowe,* V. R. Taylor, P. F. Clapp: Classification of clouds using THIR data from Nimbus 7 satellite (5 min)

W. B. Rossow: Preliminary global cloud properties retrieved from two-channel scanning radiometer data for July 1977 (10 min)

M. A. Atwater and *J. A. Parikh:* Satellite cloud analysis during GATE (5 min)

A. Arking: Detection of thin cirrus clouds and water/ice phase with the AVHRR (5 min)

J. T. Bunting: Sensing snow and clouds at 1.6 μm (5 min)

S. Warren, D. Hahn, J. London: Ground-based observations of cloudiness for cross-validation of satellite observations (15 min)

Data Compression 2:00 pm – 5:00 pm

P. K. Rao – Chairman

R. Jenne – Invited Review (30 min)

Contributed Papers

A. LeBlanc and F. R. Mosher: Data storage and compression of geostationary image data for cloud climatologies (15 min)

E. A. Smith, T. Vonder Haar and J. Graffy: The impact of GOES satellite data compaction on the estimates of cloud parameters (20 min)

Friday, October 31

3. RECOMMENDED STUDIES

Panel Discussion on Cloud/Climate Modeling Studies

R. E. Dickinson (Chairman), S. Manabe, D. Rind 9:00 am – 10:30 am

Panel Discussion on Analysis/Data Compression Schemes

R. Jenne (Chairman), J. A. Coakley, J. E. Hansen, P. K. Rao 10:30 am – 12:00 pm

3. CLOUDS IN CLIMATE MODELS

3.1 CLOUD GENERATION IN CLIMATE MODELS

REVIEW OF CLOUD GENERATION IN CLIMATE MODELS

Edward Sarachik
Center for Earth & Planetary Physics
Harvard University

The topic of cloud generation in climate models is too huge a subject, so I would like to limit myself to a very specific topic, which I believe is central and is probably the hardest question of all. In principle, clouds that can be resolved by the grids of numerical models are not a problem; we can sort of understand them.

Subgrid scale clouds, however, are a major issue, and in particular cumulus convection; this is the topic I would like to address myself to. The Global Atmospheric Research Program (GARP) many years ago identified cumulus convection as the single most important unsolved problem in the numerical modeling of climate. A large experiment, the GATE experiment, was done in order to find out about cumulus convection, and I would like to talk about that in particular.

You're probably wondering why I was chosen to give this talk and I was wondering that myself, so I asked the organizer of this conference, and I was told that it was because I had no ax to grind. There are a lot of people here with their own parameterizations, and since I have no parameterization attached to my name, presumably it is my job to be critical. On the other hand, I am also supposed to be fair, so I decided I would be equally critical of all models.

What we really want to ask is: what is a good parameterization of cumulus convection? In thinking about that, that question has never been asked in the sense of somebody choosing a cumulus parameterization on the basis of carefully comparing the performance of the models. The first cumulus parameterization was of necessity done when the first large numerical model that included a hydrological cycle was built; this was done by Dr. Manabe, and he said something in that paper which I find remarkably sensible.

"Two important processes which play a major role in general circulation of the atmosphere are the moist and dry convections. Unfortunately, we know very little about the dynamical and thermodynamic aspects of the macroscopic behavior of moist convection. Our ignorance on this subject does not seem to warrant the incorporation of a very sophisticated scheme of the convective process at this stage of the study of the general circulation by the use of numerical models. Therefore,

we use a simple convective adjustment of temperature and water vapor as a substitute for the actual convective process." (Manabe et al., 1965).

Now, he was basically saying that in lieu of any additional knowledge, you would use the simplest thing possible. What I would like to address myself to is, is there anything we have learned in the last fifteen years which would lead him to change his opinion on that. Now, Dr. Manabe is here and that leads me to propose an operational approach to the question.

You probably know that when the artificial intelligence people, the artificial intelligentsia, if you will (as compared to us who are the real intelligentsia), tried to decide the question of whether or not a computer can think, they devised the following solution. You would have a room and you would send messages into that room and ask this thing, whether a person or a computer, questions and if the responses were indistinguishable from something a real person could have said, then the computer was said to be thoughtful, could think. Presumably the computer would say something like, "Don't bother me, I've had a hard day," and we would attribute intelligence to this.

I propose that we can answer the question of choosing a parameterization by basically addressing ourselves to the question that Manabe raised. Is there something in light of everything we have learned in the last fifteen years which would lead him to change his opinion about convective adjustment, and at the end of this talk we will do that test.

It's a little difficult to give this talk because there are experts in the audience and there are non-experts, and I hope the experts will excuse me if I go over some introductory material, because after all, I would like to talk about some specific things about cumulus parameterizations.

What I want to do in this talk, therefore, is to look at the equations of motion and see where clouds enter. I would like to consider some kinematic properties of cumulus convection. This involves going over which properties are conserved, what cumulus clouds do, and this will take a fair amount of time, but the reason for doing that is the individual cumulus parameterizations, in fact, do refer to very specific processes.

Then I would like to talk about cumulus parameterizations and in particular to start off that discussion by talking about the general question of parameterizability. Can this thing be done that we want to be done? Can we parameterize the small-scale cumulus processes in terms of large-scale variables? Then I would briefly like to review the existing cumulus parameterizations.

Basically, they can be classified as a) convective adjustment, b) moisture convergence, c) the parameterization due to Kuo, and d) the parameterization due to Arakawa. I believe that almost every parameterization suggested is in one way or another a modification or variant of one of these parameterizations.

Then I would like to discuss some of the physical processes not included in these parameterizations. These parameterizations, as we will see, are highly specific to an assumed cloud model, and I would like to discuss what we have learned since then that could modify this, and then I would like to talk about the general problem of verifications of parameterizations, and, this seems to me to be the key

to the entire thing. There is a real question about whether an individual parameterization can be verified. It's not a trivial question at all, and it seems that it is one of the things we should probably spend most of our discussion on. And then I will give some conclusions, and then Dr. Manabe will give you his opinion.

Equations of Motion. The quantities Q_1 and Q_2 are conventionally defined as a large-scale heat source and a large-scale moisture sink.

$$Q_1 \equiv \rho\left[\frac{\partial \bar{s}}{\partial t} + \bar{\mathbf{V}} \cdot \nabla \bar{s} + \bar{w}\frac{\partial \bar{s}}{\partial z}\right] = L(\bar{c} - \bar{e}) - \frac{\partial}{\partial z}\overline{(w's')\rho} + Q_R \qquad (1a)$$

$$-Q_2 \equiv L\rho\left[\frac{\partial \bar{q}}{\partial t} + \bar{\mathbf{V}} \cdot \nabla \bar{q} + \bar{w}\frac{\partial \bar{q}}{\partial z}\right] = L(\bar{e} - \bar{c}) - \frac{\partial}{\partial z}\overline{(w'q')\rho L} \qquad (1b)$$

$$\rho\left[\frac{\partial \bar{\mathbf{V}}}{\partial t} + \bar{\mathbf{V}} \cdot \nabla \bar{\mathbf{V}} + \bar{w}\frac{\partial \bar{\mathbf{V}}}{\partial z} - \mathbf{k} \times f\mathbf{V}\right] = -\nabla p - \frac{\partial}{\partial z}\overline{(w'\mathbf{V}')\rho} + \text{Friction} \qquad (1c)$$

where $s = gz + C_pT$ is the dry static energy, overbars denote averages over cloud and non-cloud areas, and $\mathbf{V}$ is the horizontal velocity.

The quantities on the right-hand side are presumably properties of clouds with the exception of radiation, which we will just consider an external variable.

In general, if we have upward motion and the potential temperature or $\bar{s}$ is increasing with height, the $\bar{w}\ \partial\bar{s}/\partial z$ term in (1a) will be cooling and therefore Q_1 will essentially need a source to balance it, so that the clouds will heat in order to balance the source.

Q_2, however, is defined conventionally the other way. $\bar{q}$ is usually decreasing with height, so that upward motion will tend to moisturize, and we need a sink in order to remove it. So clouds basically remove moisture from the large scale -- it's a sink -- by condensing it, taking vapor and condensing it into water.

The terms on the right-hand side of (1a) are the rate of condensation $\bar{c}$, rate of re-evaporation $\bar{e}$, and an eddy term, which is basically the divergence of cloud heat transport.

Similarly, in the moisture sink (1b), there will be evaporation, $\bar{e}$, which is a source of water vapor, condensation, $\bar{c}$, which is a sink of water vapor, and there will be an eddy term, which is a convergence of the eddy moisture flux.

And I have also included a momentum equation (1c) because clouds can transport momentum -- clouds in fact can transport horizontal velocity and deliver it upwards, and we will have to include the eddy term.

So, the cumulus clouds will enter the equations in these various terms which are not resolvable in most numerical models. It is going to be our job to parameterize them.

To summarize; clouds heat by condensation and convergence of the sensible heat transport; and they cool by re-evaporation of cloud liquid water. They moisturize by re-evaporation of cloud liquid water. They dry by subsidence – we'll see what that means – basically from this point of view, we can say they dry by condensing vapor into liquid water. You might not think of liquid water as something that dries, but remember that these are equations for the vapor. Clouds transport momentum. They cool radiatively or heat radiatively and this is a great issue, and they block solar radiation so that they affect the solar flux.

Now, in terms of these definitions, Q_1 and Q_2 can be measured by measuring the large-scale variables, and this has been done basically twice. There are only two tropical data sets from which we can actually get those measurements and this has been done in the Western Pacific, as a result of the Marshall Islands radiosonde network set up to monitor the nuclear tests in the 60's and this was also done in GATE (Figure 1). Basically you see that clouds heat with a vertical distribution that on an average seems to be different in the Atlantic and in the Pacific. In the Pacific, the peak of the heating is somewhere above 500 millibars while in the Atlantic it seems to be lower. Some people would

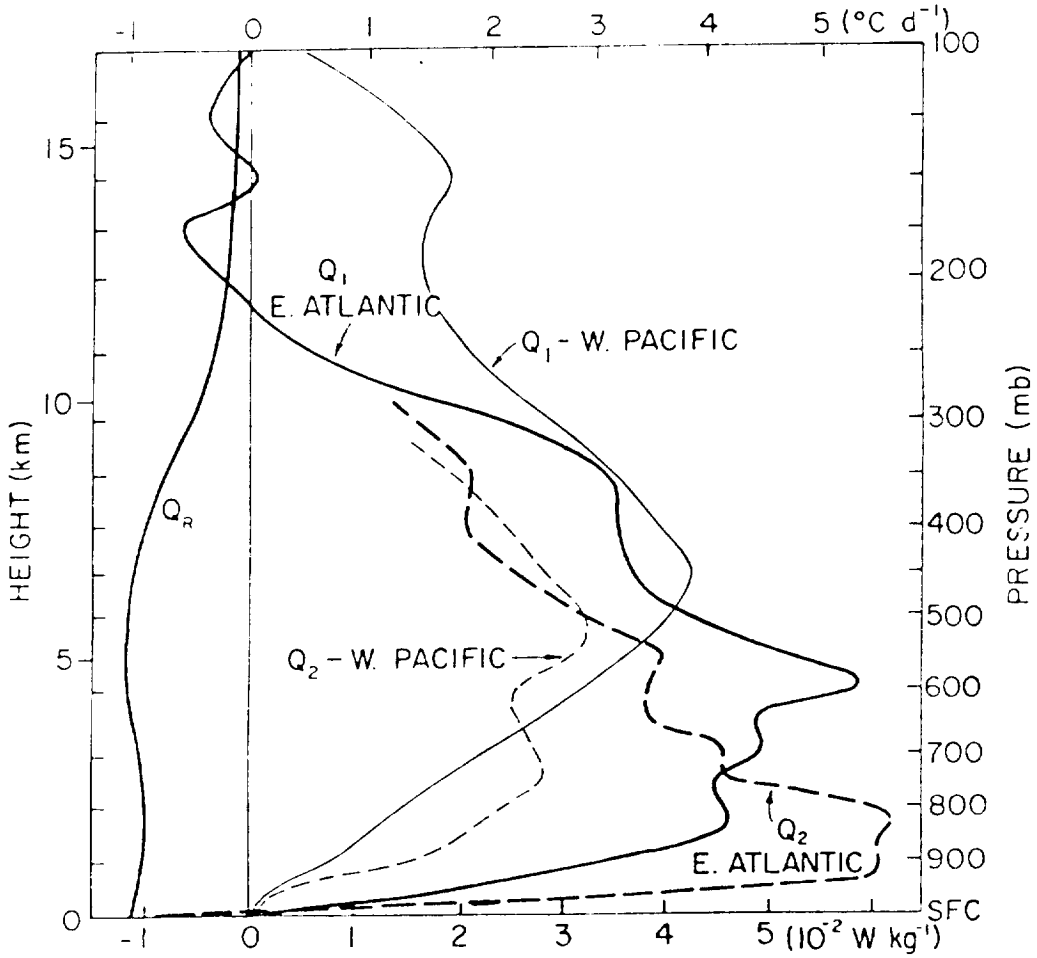

Figure 1. Heating rates associated with cumulus convection over the Pacific and Atlantic tropical oceans. (Taken from Thompson, et al., 1979)

say that the Atlantic tends to be more stable because of warm Saharan air and things like that, but the point is that the heating profile is not a universal constant, presumably is one of the things that we would like to predict.

A VOICE: What type of errors are you going to put on those curves? Maybe they are roughly the same.

DR. SARACHIK: They could be the same. I don't know what kind of error bars.

So, if we wanted to solve the equations of motion, we would have to be able to get the various terms on the right-hand side of Eq. 1 and presumably for parameterization we would like to get those terms in terms of the large-scale parameters.

There is a problem which I can't really address myself to, and that is in order to perform the radiative transfer calculations we would like to get cloud cover. Being able to parameterize cumulus convection in terms of the sources on the right-hand side of the equation is not the same as getting the cloud cover. Presumably a lot of the liquid is going to be detrained and remain as cloud.

We know that active cumulus clouds cover something like three percent of fractional area of the tropics, while the cloud cover can be as much as 40 or 50 percent. They are really connected to different problems. In order to really derive the cloud cover, we would require a detailed liquid water equation on the large scale. As far as I know, this really hasn't been done in any of the numerical models. Cloud cover is not usually parameterized in terms of cumulus convection. It is not really solved. I would like to leave that to the discussion; it is not something I can address myself to here.

Kinematics of Cumulus Convection. We will have to talk a little about the kinematics of cumulus convection, because the individual cloud parameterizations that I am going to talk about later in fact will refer to a lot of these quantities. There are two standard quantities which are conserved in dry and moist adiabatic ascent:

$$s = C_pT + gz \quad \text{conserved in dry adiabatic ascent;}$$

$$h = C_pT + gz + Lq \quad \text{conserved in moist ascent.}$$

You know that when a moist parcel is raised, it cools and eventually becomes saturated. When it becomes saturated, the quantity h is then conserved. In other words, as the vapor condenses into liquid, the temperature changes in such a way that h stays constant with height. So that s being constant with dry adiabatic ascent, $\partial s/\partial z$ going to zero gives you the dry adiabatic lapse rate, and if we define $(\ )^*$ to be the saturation value at a given temperature, h^* is the saturated moist static energy and that is conserved in moist adiabatic ascent so that the $\partial h^*/\partial z = 0$ is the moist adiabatic lapse rate. Note that h^* only depends on temperature.

Now the tropical atmosphere typically looks like Figure 2. s will be increasing with height in some way, and h^* will have a minimum in the troposphere. Now you can show that the buoyancy of the saturated parcel (as long as the temperature are not too different from the environment) is

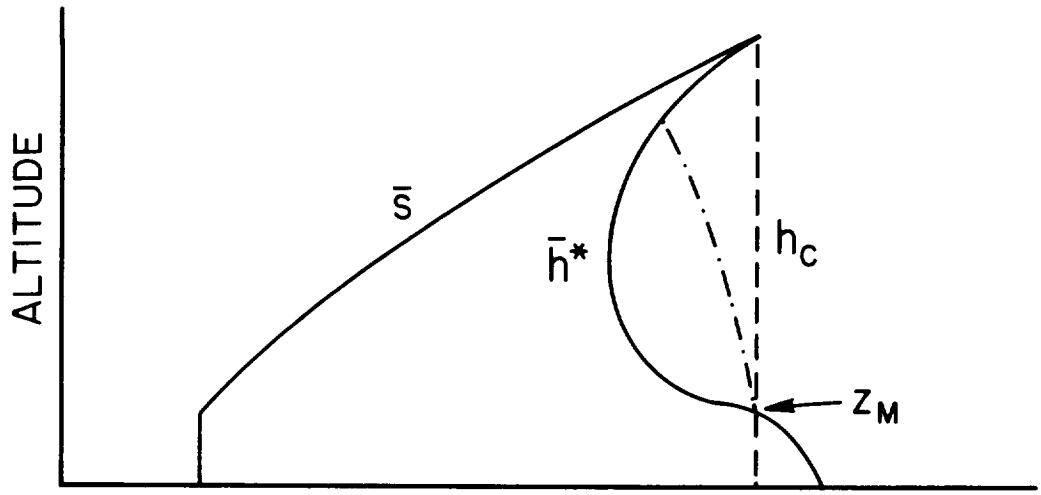

Figure 2. Schematic of the vertical variation of dry static energy, $\bar{s}$, and moist static energy, $\bar{h}^*$, over tropical oceans.

proportional to the cloud moist static energy minus the saturation moist static energy of the environment. So that when a cloud rises without detrainment, conserving its moist static energy, as the dotted line shows, it will have positive buoyancy above z_m, and negative buoyancy below that point.

That means if we can raise the parcel to z_m it will take off, because it will be positively buoyant. It turns out that the tropical atmosphere is always CIFK, which is conditionally unstable (Conditional Instability of the First Kind). That might not mean much to you if you don't know what the second kind is; simply consider it as conditional instability. The tropical atmosphere is almost always conditionally unstable.

In the presence of entrainment, h_c, the cloud static energy, is not conserved and in fact as you entrain into the clouds some drier environmental air, an ascending cloud might behave like the dashed dotted line, and therefore entraining clouds lose their buoyancy lower down; non-entraining clouds reach higher up.

A lot of the kinematics of cumulus convection depends on the fact that active cumulus clouds cover a fractional area smaller than unity, $\sigma \ll 1$. An active cumulus cloud is a cloud that is growing. After it grows, it just sort of sits there and dies and you can still see it; these dead clouds and other cloud detritus cover a much larger area, 40 or 50 percent, but active cumulus clouds cover only a few percent. This enables many approximations to be done: this fact is the essence of cumulus-environment interaction. It is the sort of a thing that makes it all possible.

We define $(\bar{\ })$ as an average over cloud and non-cloud areas, such that, for example,

$$\bar{s} = \sigma\, s_c + (1 - \sigma)\, \tilde{s} \approx \tilde{s} + 0(\sigma)$$

where $\sim$ is the average over non-cloud areas only. Therefore the static energy averaged over both

cloud and non-cloud areas will be approximately equal to the static energy over the non-cloud areas only, as a consequence of $\sigma \ll 1$.

On the other hand, when we calculate the fluxes due to clouds, which we remember are on the right-hand side of Eq. 1 and are the things we have to parameterize, we have

$$\overline{\rho w' s'} = M_c (s_c - \tilde{s}) + O(\sigma)$$

$$= M_c (s_c - \bar{s}) + O(\sigma)$$

where M_c is the mass flux in the clouds $(\rho w)_c$. The mass budget averaged over cloud and non-cloud areas is

$$\overline{\rho w} = M_c + \tilde{M}$$

and here we see that the average must include the clouds because $w_c = O(1/\sigma)\ \bar{w}$, where $\bar{w}$ is simply the mean vertical velocity. In the absence of any mean motions, $\bar{w} = 0$, and if there is going to be mass flux in the clouds, in order to conserve mass, there has to be mass flux coming down outside the clouds, which is called compensating subsidence. We look at the right hand side of the heat equation (Eq. 1a) in order to see how clouds heat:

$$Q_1 = L(\bar{c} - \bar{e}) - \frac{\partial}{\partial z} \overline{\rho (s' w')}$$

Now

$$-\frac{\partial}{\partial z} \overline{\rho (s' w')} = -\frac{\partial}{\partial z} [M_c (s_c - \bar{s})]$$

$$= -\frac{\partial}{\partial z} (M_c s_c) + \left(\frac{\partial}{\partial z} M_c\right) \bar{s} + M_c \frac{\partial \bar{s}}{\partial z}$$

At this point we have to specify a model of clouds in order to evaluate the derivatives. Just for this purpose, let me specify the simplest possible ensemble of clouds and that is one in which everything that condenses in the cloud falls as precipitation and none of it re-evaporates, $\bar{e} = 0$. Also assume that the clouds do not entrain, so that the mass flux is constant with height, and that this ensemble is completely steady. I just want to show how to evaluate the cloud flux divergence. So I am making up an ensemble, which is the simplest way of doing this. The ensemble heat equation is then

$$\frac{\partial}{\partial z} (M_c s_c) = L \bar{c}$$

$$= M_c \frac{\partial s_c}{\partial z}$$

since we have assumed no entrainment. When there is no condensation, s_c becomes conserved as we noted previously. When there is condensation, s_c is no longer conserved and increases with height in the clouds.

This enables us to evaluate the flux divergence term

$$-\frac{\partial}{\partial z}\,\overline{\rho\,(s'\,w')} = M_c\,\frac{\partial \bar{s}}{\partial z} - L\,\bar{c}$$

and therefore the entire right-hand side of the heat equation

$$Q_1 = M_c\,\frac{\partial \bar{s}}{\partial z}\,.$$

In other words, the heating has a term in it which is given by the mass flux in the cloud acting on the environmental lapse rate. Now, this is sometimes called compensating subsidence. It isn't. You can see where compensating subsidence is by looking at how temperature changes occur

$$\rho\,\frac{\partial \bar{s}}{\partial z} \cong (M_c - \rho\bar{w})\,\frac{\partial \bar{s}}{\partial z} = -\tilde{M}\,\frac{\partial \bar{s}}{\partial z}$$

in the absence of horizontal temperature gradients.

Now, M_c could be less than $\rho\bar{w}$, it can be greater than or it can be equal. We defined M_c minus $\overline{\rho w}$ as an environmental subsidence $\tilde{M}$ and in fact, temperatures will change when there is subsidence, but just because we have clouds heating does not necessarily mean there is going to be subsidence or temperature changes. What could happen is that all the mass that gets converged on the large-scale can go up in clouds, and there would be no temperature change and no compensating subsidence.

Now, I made up a cloud ensemble model in order to evaluate the terms just in order to be able to specify what the clouds are doing. The canonical, if you will, cloud ensemble, which was given in seminal papers by Ogura, Arakawa and Shubert (1974) and others, is an ensemble that is steady, that entrains continuously, but detrains only when the cloud loses its buoyancy at the very top; this is a highly specific cloud ensemble, and they wrote the equations in the following way, using this specific ensemble:

$$Q_1 = M_c\,\frac{\partial \bar{s}}{\partial z} + D\,(s_D - \bar{s} - L\ell_D) + Q_R$$

$$Q_2 = -M_c\,\frac{\partial}{\partial z}(L\bar{q}) - D\;L\,(q_D^* - \bar{q} + \ell_D).$$

s_D and q_D^* are the detrained static energy and moisture, D is the rate of detrainment and ℓ_D is the detrained liquid water.

The thing I would like to emphasize is that this is the starting point of most parameterizations, but in fact it has already assumed properties of the cloud ensemble. That is important. Many of the modifications that we will see in a moment, in fact, use different ensembles.

To finish up the kinematics of cloud ensembles, we have to note that there is a profound connection of the cloud ensemble with the boundary layer, and in fact if we write a schematic boundary layer equation – and this is something I just can't get into in detail – one can consider that the boundary

layer near the surface is being driven by evaporation, and it's being held down by, almost everywhere, by the subsidence, if any.

$$\frac{dH}{dt} \propto \tilde{w} + \text{Evaporation}$$

It is a sort of balancing process; when the evaporation exceeds the subsidence that holds it down, the boundary layer tends to rise. When it is less, the boundary layer tends to fall.

The key thing about the boundary layer is that all the moisture that goes up in the clouds has to pass through the boundary layer and it ultimately had to come from various combinations of evaporation, plus convergence. As it is usually said, cumulus clouds have their roots in the mixed layer.

Cumulus Parameterizations. Having talked about the kinematics of cumulus, I'd like to at least briefly describe the existing cumulus parameterizations.

Let me start by talking about the general question of parameterizability, namely, is what we are trying to do possible to do. Is it obvious that it is possible to do? What we would like to do is derive properties of the cloud ensemble in terms of the large scale variables.

We know that something like parameterizability *has* to exist because we know that there are large-scale budgets. The precipitation that gets rained out in a cloud had to be evaporated and/or had to be converged in. So in some sense, parameterizability in that sense is assured just by the existence of budgets. If we know what the large-scale is doing, if the large scale is converging in moisture over long periods of time, say, and if there is evaporation, we know it has to precipitate. So we have some properties of the cloud ensemble, some gross properties, just from the large scale. In that sense there is parameterizability.

On the other hand, can we get *all* the properties of the cloud ensemble from the large scale? Can we get vertical distribution, can we get the liquid water detrainment, can we get every single property that appeared on the right-hand side of Eq. 1? That is *not* quaranteed – it may come out and it may not come out. The test of a parameterization is whether or not it gives you, not only the gross properties, which are assured by the equations of motion and the large-scale budgets, but also the detailed vertical distribution. We have to judge parameterization basically on these grounds: does it give you all the quantities in terms of large scale, which are needed on the right-hand side of these equations in order to drive the equations of motion?

Now, I would like to briefly describe some of the parameterizations and I will very briefly give you some pros and cons of each of these parameterizations.

We will start with the first, convective adjustment. When the moist static energy gradient is unstable and the atmosphere is saturated, i.e., when $\partial\bar{h}^*/\partial z < 0$ and $\bar{q}/\bar{q}^* \geqslant 1$, then the temperature profile in the adjustment is brought back to neutral $\partial\bar{h}^*/\partial z = 0$ in such a way that $\bar{q}/\bar{q}^* \leqslant 1$ in the adjustment.

In other words, when we are both saturated and conditionally unstable, the profile is adjusted to a neutral lapse rate in such a way that you never exceed 100 percent relative humidity. In this process you transport heat upwards, which means you are heating above and you are cooling below. As you cool below, the relative humidity will go above 100 percent because the air has less ability to hold water, and therefore you have to drop out some rainfall; the rainfall is calculated this way.

It is a very simple scheme; as Manabe pointed out, it's the simplest scheme. But it says almost nothing about clouds, and it is sort of unphysical in the sense that it is known that the tropical atmosphere is always conditionally unstable, even where it is not raining and even where there is no cumulus convection. In the real atmosphere conditional instability exists without cumulus convection and it's beginning to look like it is the clouds that are producing the conditional instability rather than the conditional instability which is producing the clouds.

So what's the argument for it? Well, *individual* clouds do precisely what convective adjustment says, so that, if, for example, in a numerical model only a small number of those grid points adjust, then the individual grid points which are adjusting are acting like clouds. If it only takes a few clouds to define an ensemble on the large scale then convective adjustment is sort of mimicking the actual effects of clouds. If that argument is at all valid (and numerical models that use convective adjustment don't look terribly unreasonable), it indicates, to me at least, that very few clouds, very few adjusted points, are necessary to define statistical properties of the cumulus ensemble.

The second parameterization is moisture convergence. On long enough time scales such that not a whole lot of moisture can be stored in the atmosphere, the net precipitation rate has to be proportional to the total amount of moisture that is converged in, plus what is locally evaporated.

$$P = E + \int \nabla \cdot (\bar{\mathbf{V}}\bar{q}\rho)\, dz .$$

If we have a well mixed layer in moisture up to z_m, say, then

$$P = E + (\rho w)_{z_m} q_m$$

The advantages of this parameterization are that it is simple and that it cannot be wrong – it is simply a statement of the budget.

What it does not do is give me a vertical distribution of the heating, which is one of the things we require. So somehow we have to externally specify what that vertical distribution has to be. Thus, in some sense moisture convergence by itself is not a complete parameterization unless I give you a rule, a method, to determine the vertical distribution.

VOICE: You mean mixed layer, not some other level?

DR. SARACHIK: I mean mixed layer. I am just giving this as an example. In general it would be chosen as the top of the moist layer.

DR. ARAKAWA: Don't you have to keep track of the stored moisture?

DR. SARACHIK: That's right. On short time scales there can also be storage and we would need an additional model for the storage. A model for the storage might say that the relative humidity is always 80 percent. So, you are right, moisture convergence is not complete by itself, you have to specify the vertical distribution and you have to specify the storage.

The third parameterization I will talk about is one investigated by Kuo, and it's important to realize, and I never had until I went back and prepared this talk, that Kuo did not parameterize all the terms on the right-hand side of Eq. 1; he only parameterized the condensation term $\overline{c}$ and assumed that the divergence of the flux term equals zero.

Now, you recall that we saw that the flux term was

$$-\frac{\partial}{\partial z}\ \overline{\rho\,(s'\,w')} = M_c\,\frac{\partial\,\overline{s}}{\partial\,z} - L\,\overline{c}$$

and there seems to be no a priori reason why it should be zero.

If we integrate the heat and moisture equations vertically, we see that the integral of Q_1 is basically going to be given by the net latent heat of the precipitation reaching the surface, minus the sensible heat leaving the surface. By neglecting this term, we ignore the sensible heating from the surface. Similarly, the integral of Q_2 is given by the net precipitation rate, reaching the surface minus the net evaporation rate. So that in some gross sense Kuo, by leaving this out, has neglected evaporation from the surface.

In troughs of waves, where convergence might exceed evaporation by a factor of five, that might be quite reasonable. But otherwise it will not.

Therefore it's not obvious, a priori, that these flux terms should be small. The key thing is that he is parameterizing only the condensation term, not the flux term. He specifies, by various arguments, that it is proportional to the moisture convergence and that the vertical distribution is basically given as if these clouds grew and then mixed into the environment:

$$\overline{c}\ \propto\ (T_c - \overline{T})\ \int \nabla\ \cdot (\rho \overline{V}\overline{q})\,dz\ .$$

The vertical distribution is given by the temperature in the clouds minus the temperature in the environment, and the condensation is proportional to the moisture convergence. In a sense he has to get the net condensation rates correct, because he built it in.

The final parameterization I will describe is the one by Arakawa. Arakawa wants to specify the vertical distribution by dividing the clouds into a steady ensemble of clouds of various heights, the idea being, that if we can predict the clouds at various heights, all the quantities on the right-hand side of the heat and moisture equations will be known. If you remember I said that the clouds that entrained a lot detrained lower down, so he divided the mass flux of the ensemble we are trying to

parameterize in terms of sub-ensembles of constantly entraining clouds.

$$M_C = \int m(\lambda)\, d\lambda$$

Clouds of entrainment rate λ are assumed to detrain only at the level at which they lose buoyancy.

Then he assumes that an equilibrium between the large scale and the small scale exists separately for each sub-ensemble characterized by the parameter λ. The arguments are fairly involved but he assumes that there is a quantity for each sub-ensemble, $A(\lambda)$, which is basically proportional to the buoyancy of that sub-ensemble;

$$A(\lambda) = \int_{z_M}^{z_D(\lambda)} \frac{g}{C_p \bar{T}}\, \eta(\lambda, t)\, [s_{vc}(z, \lambda) - \bar{s}_v(z)]\, dz$$

where $\bar{s}_v$ and s_{vc}, are the virtual dry static energy of the environment and cloud respectively, and $\eta(\lambda, t)$ is the shape function $m(\lambda, z)/m_m(\lambda)$ of clouds that start at the mixed layer z_m with mass flux $m_m(\lambda)$. The quantity $A(\lambda)$ is called the cloud work function.

The Arakawa parameterization is that the equilibrium between cloud and large scale manifests itself in the constancy of the quantity $A(\lambda)$;

$$\frac{dA(\lambda)}{dt} = 0.$$

The interpretation of this condition is that as the large-scale motions destabilize the atmosphere, the clouds of parameter λ draw on this instability in such a way as to keep $A(\lambda)$ constant.

By inserting the equations of motion into this parameterization condition to eliminate the time derivatives, an integral equation for the cloud mass flux $m(\lambda)$ in terms of the large-scale fields is obtained. $m(\lambda)$ and some assumptions about the amount of liquid water detrained (which I can't go into here) is enough to determine all the cloud quantities on the right-hand side of the equations of motion.

The point I wish to make now is that there is nothing in this assumption which guarantees what the vertical distribution will turn out to be. It is therefore a test of this parameterization to see whether or not the vertical distribution of the heating and moistening comes out right.

Additional Physical Effects. Now that we've briefly surveyed the existing parameterizations, we turn to those aspects left out of existing parameterizations.

a) *Convective scale downdrafts.* Clouds not only have updrafts they have downdrafts. These downdrafts are known to be saturated. The equations for heat and moisture are modified in that the term for re-evaporation of liquid water, $\bar{e}$, is less because some of the liquid re-evaporates in the downdrafts within the cloud rather than being released to the environment. You may wonder how liquid can evaporate into a downdraft if it is saturated. The point is that it is saturated because the liquid has evaporated. What happens is that these downdrafts form, they are unsaturated, if you will, because as you move air down it gets warmer. Therefore, their capacity to hold water is greater, and since there is so much water around, a lot of that water re-evaporates into the downdrafts and saturates them.

These downdrafts are not symmetrical with the updrafts, because the updrafts are entraining as you move up, but the downdrafts are entraining as you move down. So that leads to a modification of the cloud mass flux, and it leads to a modification of the evaporation term $\bar{e}$. As far as I know no cumulus parameterization has included that.

b) *Life cycle effects.* The cloud ensemble used by Arakawa and various other people, assumes that the clouds detrain only when they lose buoyancy, but we sort of know that's not true because we see clouds out there and they hang around for a long time and sort of fade away. This means that some of their liquid water is evaporating *in situ*, this is usually referred to as mixing of dying clouds with their environment. Various people have investigated properties of cloud ensembles assuming averages over the entire life cycle of the cloud. Cho derived the following modified moisture equation

$$Q_2 = -L \int \frac{\sigma(p')}{\tau_{p'}} [q_c(\tau_{p'}) - \bar{q}] \, dp'$$

where τ_p is the lifetime and $\sigma(p)$ the fractional area of clouds that grow to height p. We see that shallow clouds contribute most because of their short lifetime. No cumulus parameterization has taken life-cycle effects into account.

c) *Mesoscale organization.* Finally, one of the major outcomes of GATE is that clouds are not these individual ensembles of growing clouds, but they are organized into mesoscale systems. In fact, most rainfall in GATE occurred in these mesoscale systems, and these mesoscale systems have very characteristic structures. Figure 3 shows the characteristic structure of the mesoscale systems observed during GATE. Air moves into the cumulus front from the left. To the rear of the system we see an immense anvil cloud from which falls something of the order of 40% of the total rainfall in the system.

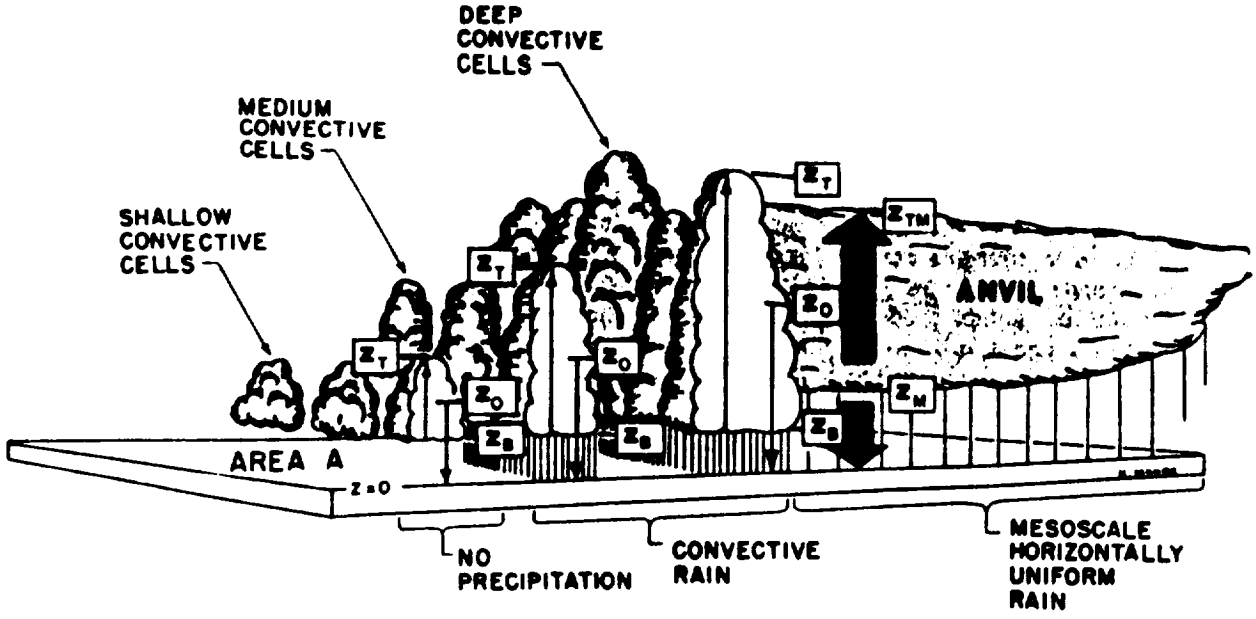

Figure 3. Schematic of a typical population of clouds over a tropical ocean. Thin arrows represent convective-scale updrafts and downdrafts. Wide arrows represent mesoscale updrafts and downdrafts. (Taken from House et al., 1980.)

There are now two possibilities. The anvil cloud could have gotten all of its vapor from the cumulus cloud and just rained it out, in which case there would be no modification to the equations; or there could be some dynamics involved such that the anvil, in fact, has updrafts which condense. In that way the dynamics gets changed and it's not obvious in that case that we can parameterize the effect of the mesoscale system by a random distribution of cumulus clouds, because there is now some mesoscale dynamics. This can change the vertical distribution of heating and moisturizing.

The parameterization problem in addition becomes harder. It is no longer clear that a statistical equilibrium between large and small scale exists because so few of these systems exist.

In fact, for each wave there might only be three or four systems gradually moving through the wave. What we are now talking about is parameterizing the effects of mesoscale systems on the large-scale, the mesoscale systems themselves still being subgrid scale. Needless to say, the effect of mesoscale systems has not been included in any cumulus parameterization.

There is some question about whether this dominant role of mesoscale systems was also true in the original analysis by Reed and others in the Pacific and I have verbal assurances that in fact most of the rainfall in the Pacific did come from a few mesoscale systems.

Verifications. Finally, I would like to talk about some verifications. And this is perhaps the hardest question of all. What do you verify a cumulus parameterization with respect to?

The first requirement is that it should be physical, but one man's physical is another man's unphysical. You can't decide that a priori. There are various possibilities. You can put a cumulus parameterization in a numerical general circulation model, but then what do you compare the results to?

You can compare with climatology, but climatology may or may not be determined by the details of the cumulus cloud parameterization. You can compare with observations, but you are never sure that some other thing in the general circulation model is not causing the deviation between reality and your numerical model.

You can compare cumulus parameterizations directly with data and I would like to talk a little bit about such diagnostic comparisons. Here you assume you have a lot of data and you assume it's good. But you would like to compare the Q's you get from large-scale data, with that which you would get by predicting the properties of a cumulus ensemble using some cumulus parameterization scheme.

That means you will get things like mass fluxes, spectra, etc. Unfortunately, these are not things you can compare with observations. GATE could not give us a spectrum of clouds, could not give us the individual mass flux, it couldn't tell us how many updrafts or downdrafts were in a cloud. It's the sort of data which doesn't exist and probably never will.

As an example, Johnson (1980) diagnosed the properties of a cumulus ensemble assuming no downdrafts at all, cumulus downdrafts only, or both cumulus and mesoscale downdrafts. The Figure 4 shows that the diagnosed environmental subsidence changes by a factor of 5 depending on which

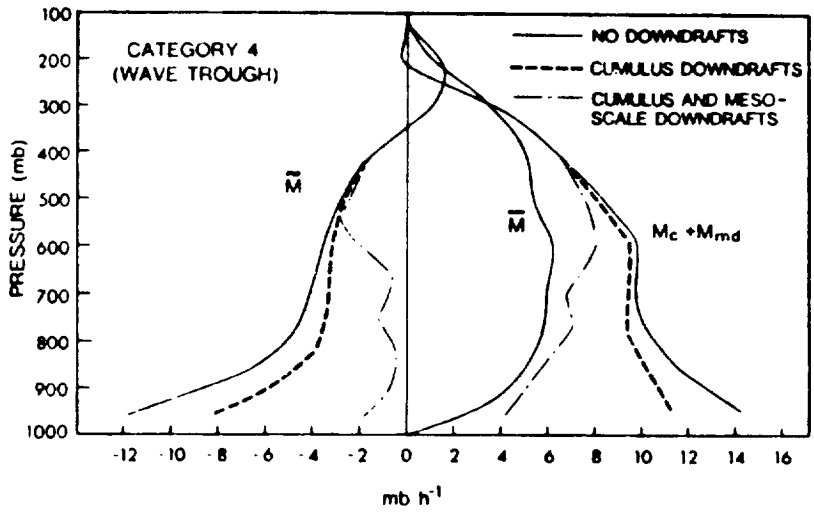

Figure 4. Environmental mass flux $\tilde{M}$, mean mass flux $\bar{M}$, and net convective mass flux $M_c + M_{md}$ for category 4 for cases with and without downdrafts. (Taken from Johnson, 1980).

assumption was made. This is clearly of importance since the properties of the boundary layer, for example, depend directly on the environmental subsidence. On the other hand, since there is no direct way of verifying the mass flux, all we can conclude is that *if* there are downdrafts, *then* these are important.

This is less trivial than it sounds because such diagnoses have shown that certain things don't matter. For example, people have worried that cumulus clouds do not detrain at a sharp level but seem to bounce around their level of detrainment. Diagnoses have indicated that cumulus ensembles with and without this feature yield approximately the same mass fluxes and spectra.

Thus diagnostic comparisons to data are useful for determining what doesn't matter but they can never verify the properties of cumulus ensembles where things can matter. Diagnoses have indicated that only three things need be included in future cumulus parameterizations: life cycle effects, downdrafts, and mesoscale organization.

People have compared precipitation rates as given by various cumulus parameterizations to observed precipitation rates from GATE.

This figure is from Krishnamurti (Figure 5) and he claims – I put this graph in to illustrate one of the dangers of this whole business – he claims convective adjustment predicts precipitation rates an order of magnitude larger than observed.

What he did, was at every time step he assumed that things would convectively adjust, because diagnostically the adjustment occurs only in response to instantaneous properties of the observed system. When actually used in numerical models, of course, you would solve the equations of motion, so that after each convective adjustment the system would take some time to restore itself and would

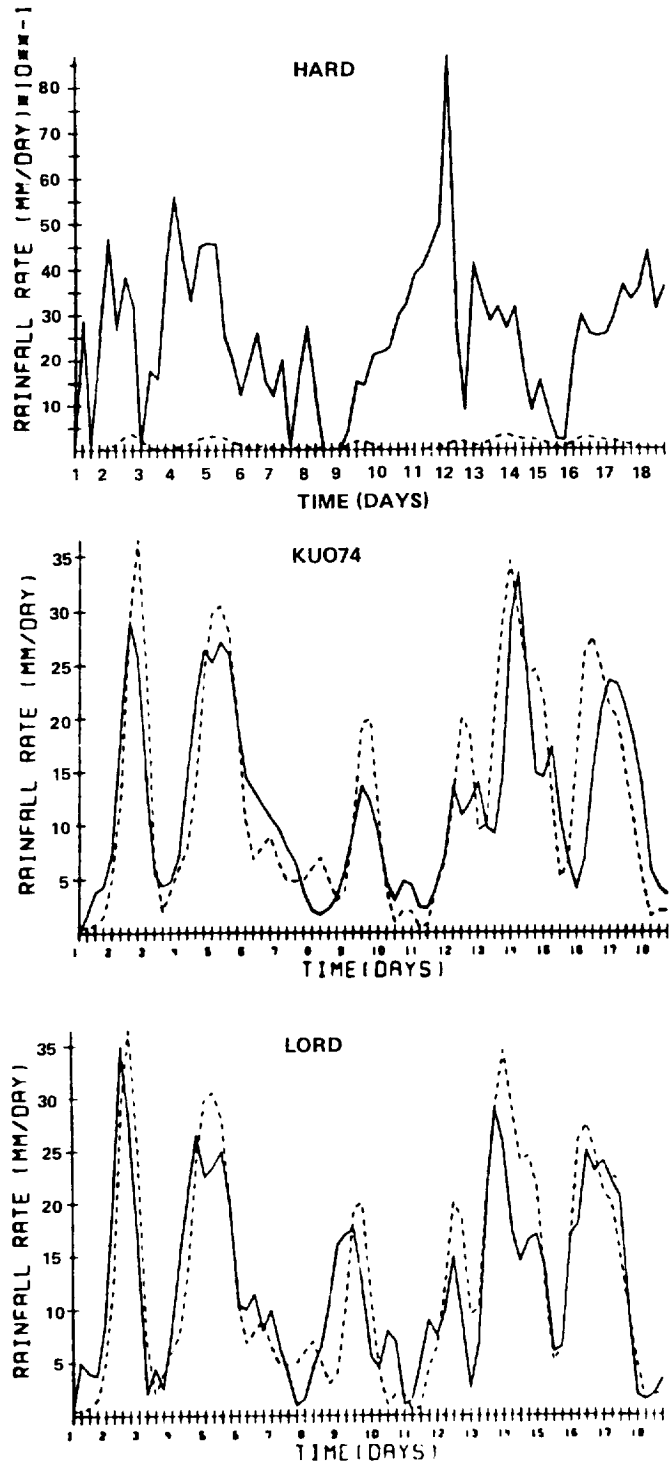

Figure 5. Comparison of observed (dashed line) and predicted (solid line) rainfall rates (μm day^{-1}) using (a) hard convective adjustment, (b) Kuo's (1974) scheme and (c) Lord's formulation of the Arakawa-Schubert scheme. Days 1 to 18 correspond to the third phase of GATE between 1 September and 18 September 1974. Data are for 6 hr intervals beginning with 0000 GMT 1 September. (Taken from Krishnamurti et al., 1980.)

not precipitate during this restoration period. Krishnamurti applied the method in a way that violated the equations of motion so that it is not a fair test of convective adjustment.

The second figure in Figure 5 is using the Kuo parameterization. Now, Kuo, if you remember, parameterized the precipitation in terms of moisture convergence, and if there is not much storage he had to get the right answer. It turns out in waves there isn't that much storage, and the results turned out well in regions where evaporation was also not major.

The next figure compares the Arakawa parameterization with observed precipitation rates. It seems to me the Arakawa parameterizability assumption uses the equations of motion, and therefore has to in a gross sense satisfy some budgets. So it is not clear to me that this is a test of the Arakawa parameterization either. It's not clear to me it isn't, but it's not clear to me it is. Perhaps Prof. Arakawa can respond to this.

You may recall that the vertical structure was an important property and what Lord (1980) basically did (Figure 6) was take the large-scale variables, deduce the properties of the cumulus ensemble using a version of the Arakawa parameterization, reconstitute Q_1 and Q_2 using only the properties of the derived cumulus ensemble, and compare them to the Q_1 and Q_2 gotten directly from large-scale observations. As you can see from the figure, the Arakawa-Shubert prediction did not agree with the observed profiles, which were the input to that same calculation.

I do not take this as a vote of confidence, because it seems to me that is something that had to be gotten correctly. Now I may have misunderstood what he did, but it seems to me he used Q_1 and Q_2, derived the properties of the cumulus ensemble, then reconstituted Q_1 and Q_2 and they did not agree.

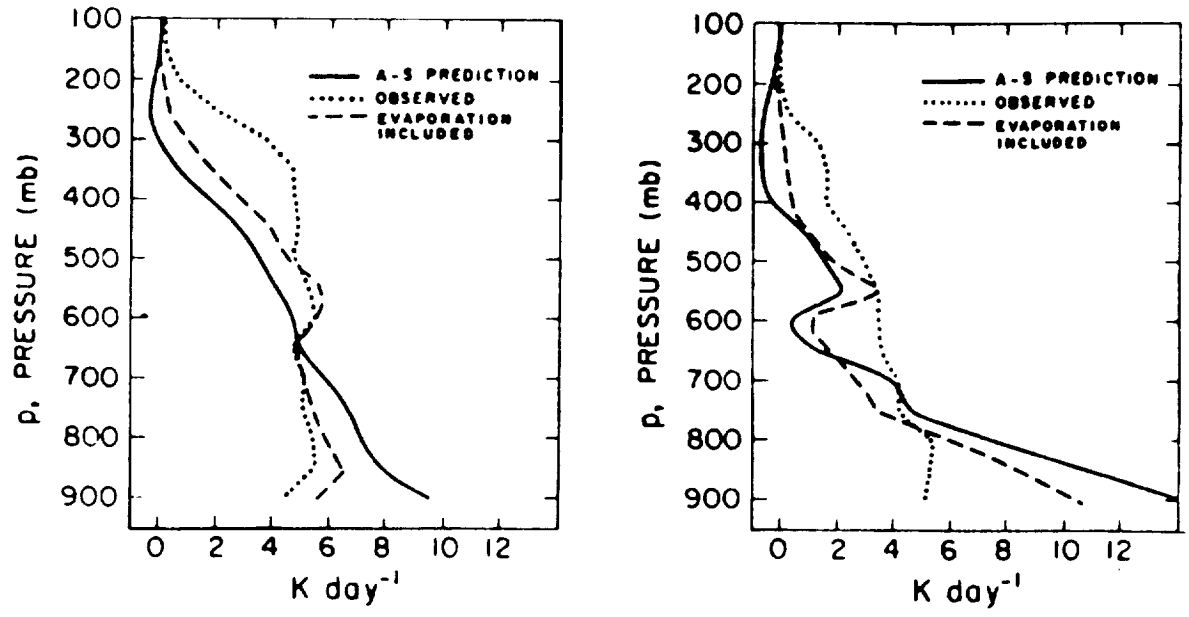

Figure 6. Time-averaged vertical distribution of the calculated and observed (a) heat source, $Q_1 - Q_R$, and (b) moisture sink, Q_2, due to clouds. (Taken from Lord, 1980.)

As a final test of parameterizations, you can compare them in general circulation models and see if it makes a difference. Now I only know of one example in the literature which has compared various cumulus parameterizations, and it is a simulation by Miyakoda and Sirutis (1977), which is extremely hard to read, and it's a little bit hard to know precisely what they did. They say they compared convective parameterizations and various boundary layer turbulence parameterizations in a general circulation model with the results shown in Figure 7.

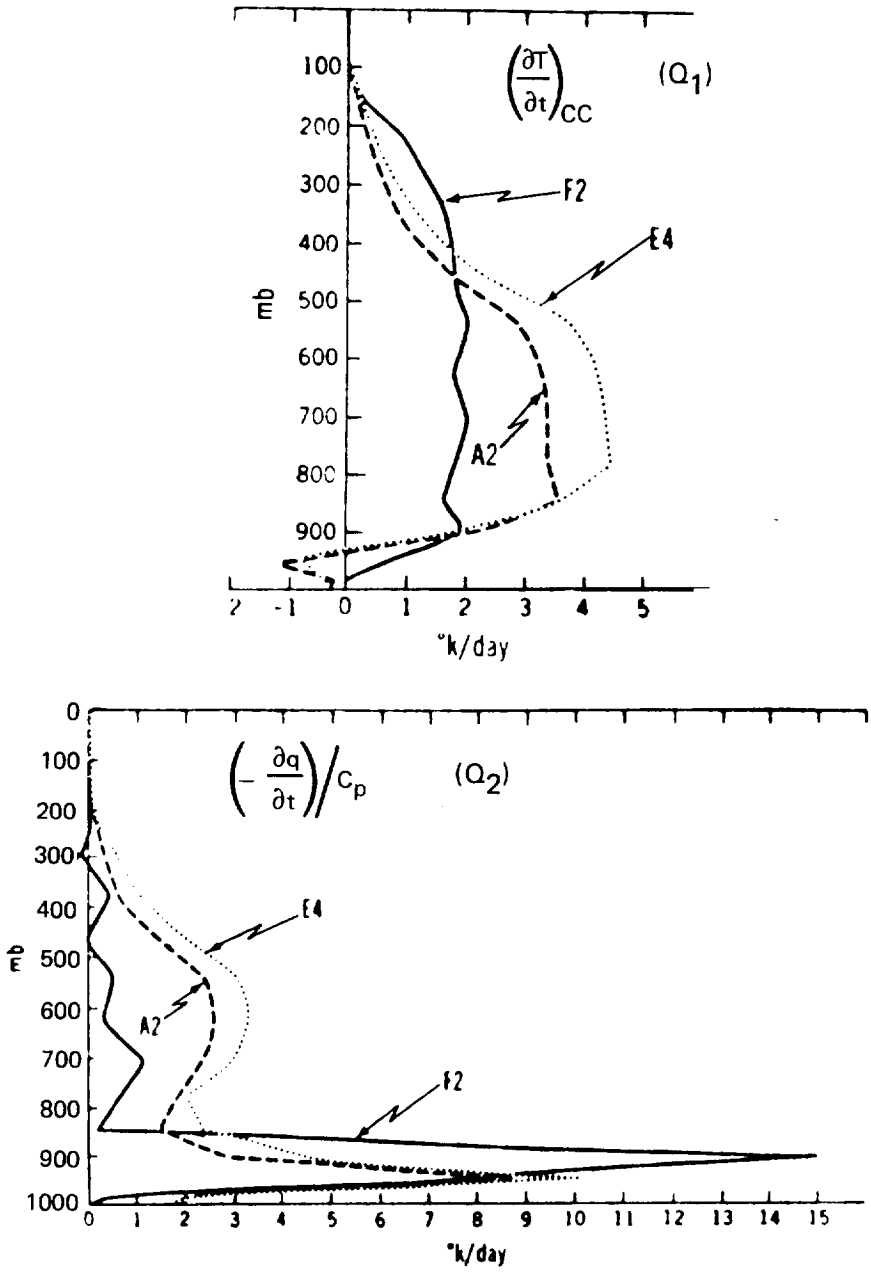

Figure 7. Vertical distribution of (a) heating and (b) moisture sink due to cumulus convection processes at about 5°N, averaged zonally and temporally for 13 days in the three models. (Taken from Miyakoda and Sirutis, 1977.)

(F2 is the Arakawa-Schubert parameterization, A2 and E4 are convective adjustment parameterizations differing only in the parameterization of boundary layer turbulence.)

Notice the convective adjustment gives you a peak of the heat source which is fairly low compared to observations, but that might be correct in the model. The Arakawa parameterization yields a much more uniform heat source but its magnitude seems much too small.

The final, and perhaps best, test of a cumulus parameterization would be in numerical weather prediction models. Using the same (observed) initial conditions, models differing only in their cumulus parameterizations could be run and the end state compared to observations. To my knowledge, this has not yet been done.

Let me conclude this somewhat pessimistic survey of the art of cumulus parameterization by proposing one of my own. I had a lot of fun thinking about it because it has to be wrong. It actually makes no sense, but nobody has been able to tell me precisely why.

I thought of it in the following way: When we do a diagnosis, we take the observed large-scale heat sources Q_1 and Q_2. We derive a parameterization and the parameterization for the cumulus ensemble we get has to agree with Q_1 and Q_2. Now in the numerical model we already have Q_1 and Q_2. So why not use it? That's my parameterization. It has to be right, right?

Thank you.

Acknowledgment: This work was supported by NASA Grant NGL-22-007-228 at Harvard University.

References

Arakawa, A., and W. Schubert, 1974: Interaction of cumulus cloud ensemble with the large-scale environment, Part I. *J. Atmos. Sci., 31,* 674-701.

Houze, R. A., C.-P Cheng, C. A. Leary, and J. F. Gamache, 1980: Diagnosis of cloud mass and heat fluxes from radar and synoptic data. *J. Atmos. Sci., 37,* 754-773.

Johnson, R. H., 1980: Diagnosis of convective and mesoscale motions during Phase III of GATE. *J. Atmos. Sci., 37,* 733-753.

Krishnamurti, T. N., Y. Ramamathan, H.-L. Pan, R. J. Pasch and J. Molinani, 1980: Cumulus parameterization and rainfall rates I. *Mon. Wea. Rev., 108,* 465-472.

Kuo, H. L., 1974: Further studies of the parameterization of the influence of cumulus convection on large-scale flow. *J. Atmos. Sci., 31,* 1232-1240.

Lord, S., 1980 in *Proceedings of the Seminar on the Impact of GATE on Large-Scale Numerical Modeling of the Atmosphere and Ocean,* held at Woods Hole, August 20-29, 1979, published by National Academy of Science, Washington, D.C.

Manabe, S., J. Smagorinsky, and R. F. Strickler, 1965: Simulated climatology of a general circulation model with a hydrologic cycle. *Mon. Wea. Rev., 93,* 769-798.

Miyakoda, K., and J. Sirutis, 1977: Comparative integrations of global models with various parameterized processes of subgrid-scale vertical transports: Description of the parameterizations. *Beit. Phys. Atmos., 50,* 445–487.

Thompson, R. M., S. W. Payne, E. E. Recker and R. J. Reed, 1979: Structure and properties of synoptic-scale wave disturbances in the intertropical convergences zone of the eastern Atlantic. *J. Atmos. Sci., 36,* 53–72.

SIMULATIONS OF CLOUD COVER WITH A GLOBAL GENERAL CIRCULATION MODEL OF THE ATMOSPHERE

R. T. Wetherald and S. Manabe
Geophysical Fluid Dynamics Laboratory/NOAA
Princeton University, Princeton, N. J.

1. INTRODUCTION

The purpose of this small paper is to describe simulations of global cloud cover obtained from a general circulation model.

2. DESIGN OF EXPERIMENT

In the present study, a simple method of cloud prediction is incorporated into a global model of the atmosphere with realistic geography and sea surface temperature. The model employed for this study is, essentially, the spectral model described in Manabe et al. (1979). The method of cloud prediction consists of placing clouds in those layers where the relative humidity exceeds 97%. Two separate time integrations are performed, one for the month of July and the other for the month of January. The cloud parameterization used is calibrated such that it minimizes the difference between the simulated and observed (Ellis and Vonder Haar, 1976) fluxes of net solar and terrestrial radiation at the top of the model atmosphere for the month of July. The same parameterization is, then, applied to the January case. The results for the July calibration are shown in Figure 1.

3. CLOUD COVER SIMULATION

Figures 2 and 3 show the zonal mean latitude-height distributions of the computed cloud amounts for the months of July and January, respectively. In general, one may identify three separate regions of maximum cloud amount which correspond to the upward motion branches of the Hadley and Ferrel cell circulations for the two hemispheres. On the other hand, the areas of minimum cloud amounts in the model subtropics correspond to the downward motion branches of the Hadley cells. The relatively thin layer of large cloudiness near the earth's surface is mainly due to the

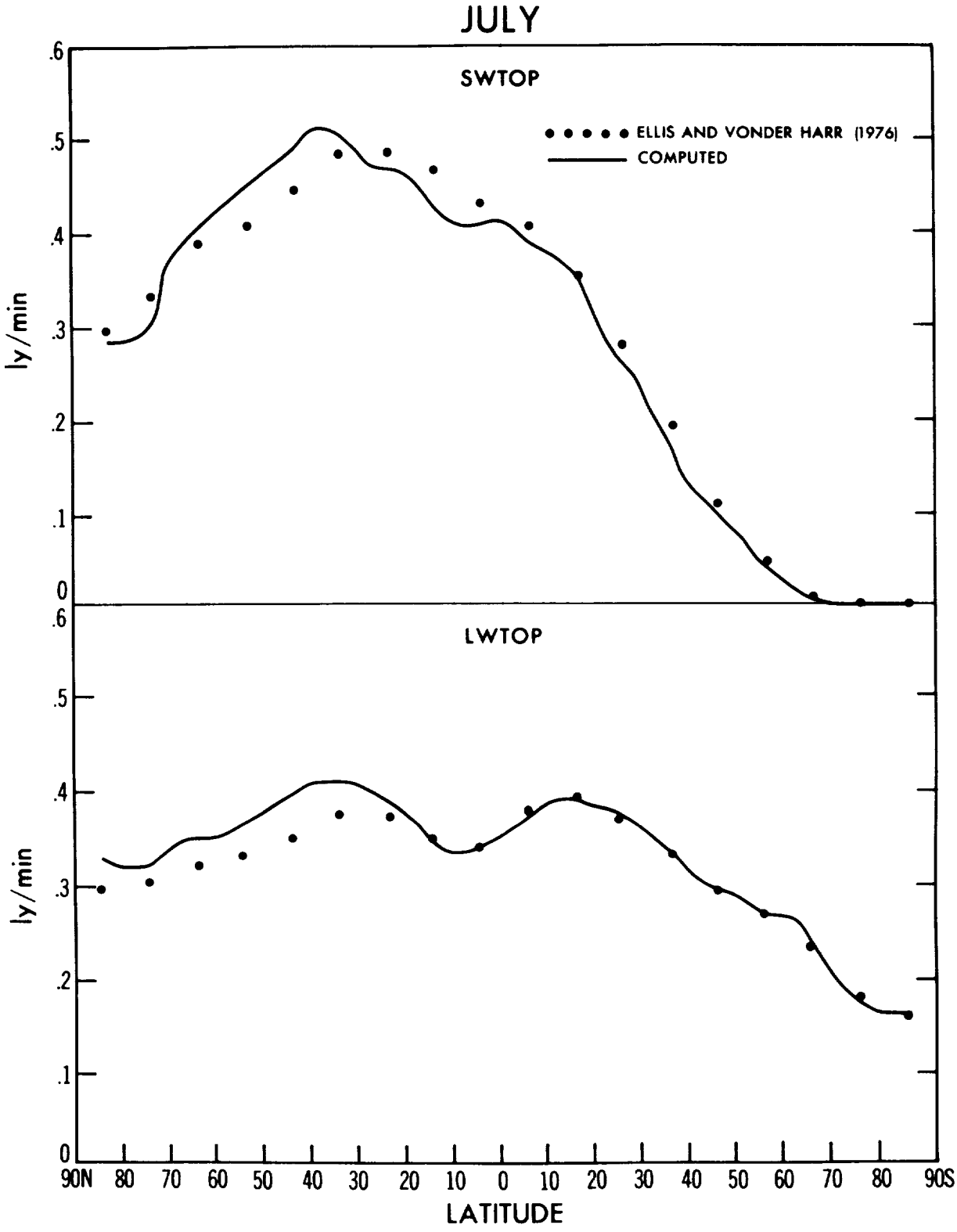

Figure 1. Zonal-mean computed and observed distributions of net solar (SWTOP) and terrestrial (LWTOP) radiative fluxes at the top of the model atmosphere for the month of July.

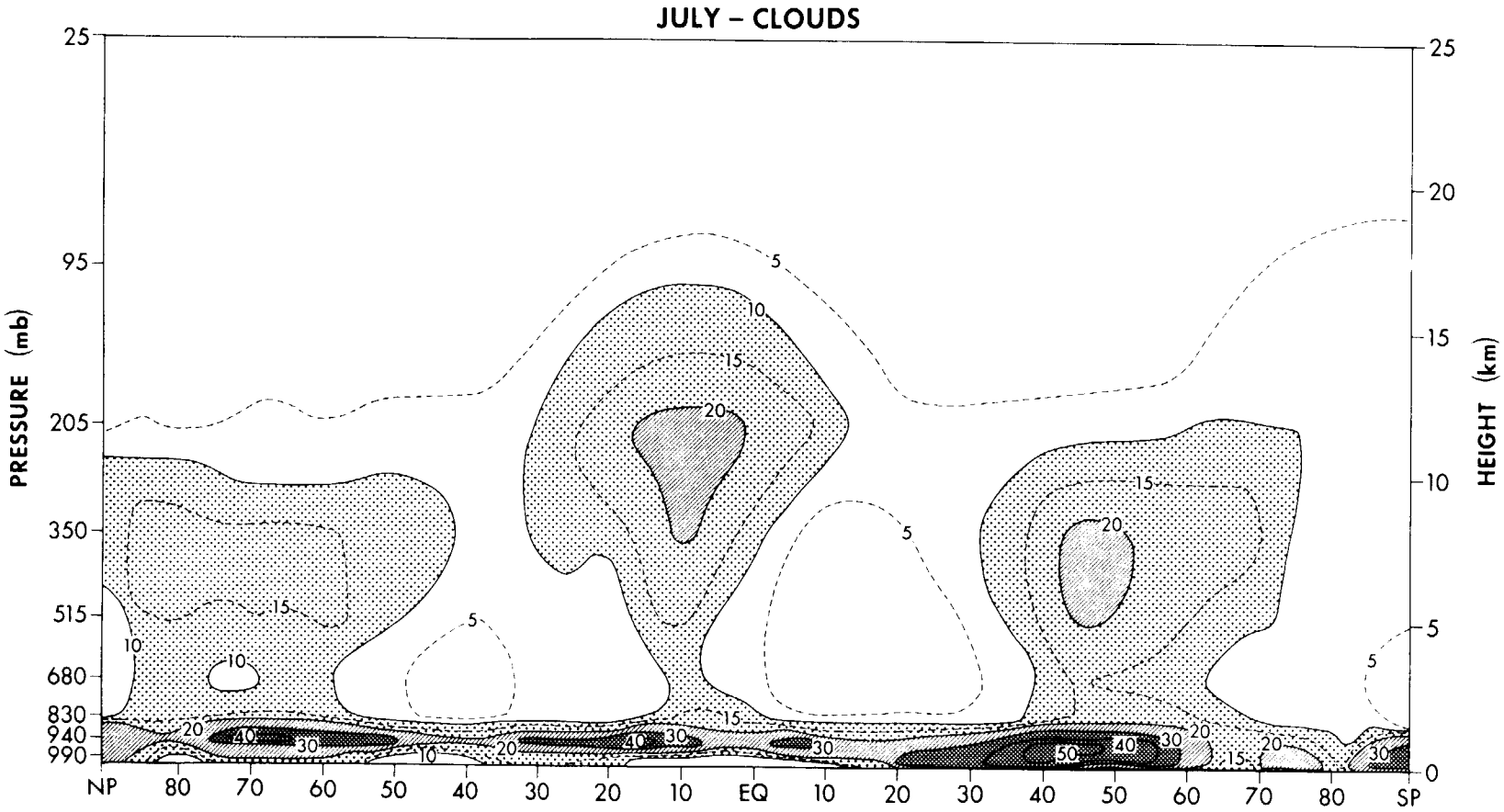

Figure 2. Latitude-height distribution of zonal mean total cloud amount (%) for the month of July.

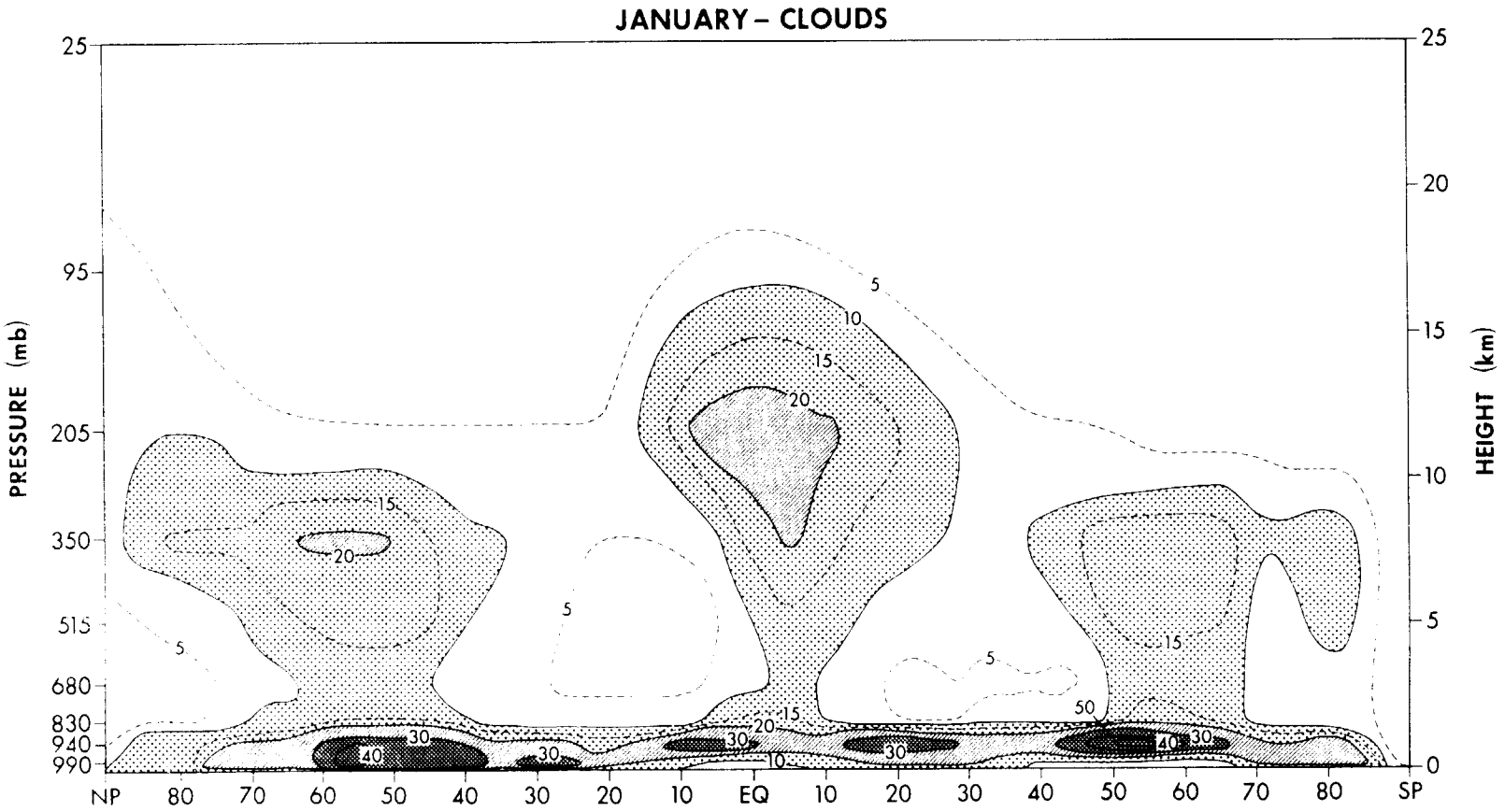

Figure 3. Latitude-height distribution of zonal mean total cloud amount (%) for the month of January.

trapping of moisture there by the relatively stable stratification in high latitudes and the subtropics. In addition, one may identify the upper tropospheric cloud maximums at ~12 km in the tropics to ~6 km in the high latitudes as "cirrus" clouds. A more complete discussion on this subject is contained in a study by Wetherald and Manabe (1980) where a similar method of cloud prediction is used.

It is found that both of these time integrations successfully reproduce many of the features of the global distributions of cloud cover which are obtained from observations. Figures 4 and 5 show the distributions of global total cloud cover derived from the July and January integrations, respectively, along with the corresponding observed distributions by Berlyand and Strokina (1974). It may be seen that in both simulations, areas of small cloud amount, such as the deserts of Africa, Australia, and the southwestern United States are well reproduced along with the semi-permanent low pressure areas with a relatively large cloud cover in the winter hemispheres. Exceptions to this are a general lack of a low stratoform cloud layer just off the western coasts of the United States, South America, and northern Europe and a general underprediction of total cloud amounts in higher latitudes in summer hemispheres as compared with observation. Also, the simulated cloud cover distributions indicate an ITCZ (inter-tropical convergence zone) in the tropical Pacific Ocean, whereas the observed distributions show no such maximum there. The discrepancies concerning underprediction of cloud cover off the western coasts of the continents and in higher latitudes are attributed, in part, to a shortcoming of the boundary layer formulation over the oceanic surfaces. Much of the difference in the tropics, on the other hand, may be due to a low or coarse resolution of the observed cloud data in the vicinity of the very narrow tropical rainbelt regions.

References

Berlyand, T. G. and L. A. Strokina, 1974: Cloudiness regime over the globe. *Physical Climatology*, MGO, Trudy, Vol. 338, 3–20.

Ellis, J. S. and T. H. Vonder Haar, 1976: Zonal average earth radiation budget measurements from satellites for climate studies. Atmos. Sci. Paper No. 240, Colorado State University, Fort Collins, Colo.

Manabe, S., D. G. Hahn and J. L. Holloway, 1979: Climate simulation with GFDL spectral models of the atmosphere. GARP Publication Series No. 22, World Meteorological Organization, Geneva.

Wetherald, R. T., and S. Manabe, 1980: Cloud cover and climate sensitivity. *Jour. Atmos. Sci., Vol. 37,* 1485–1510.

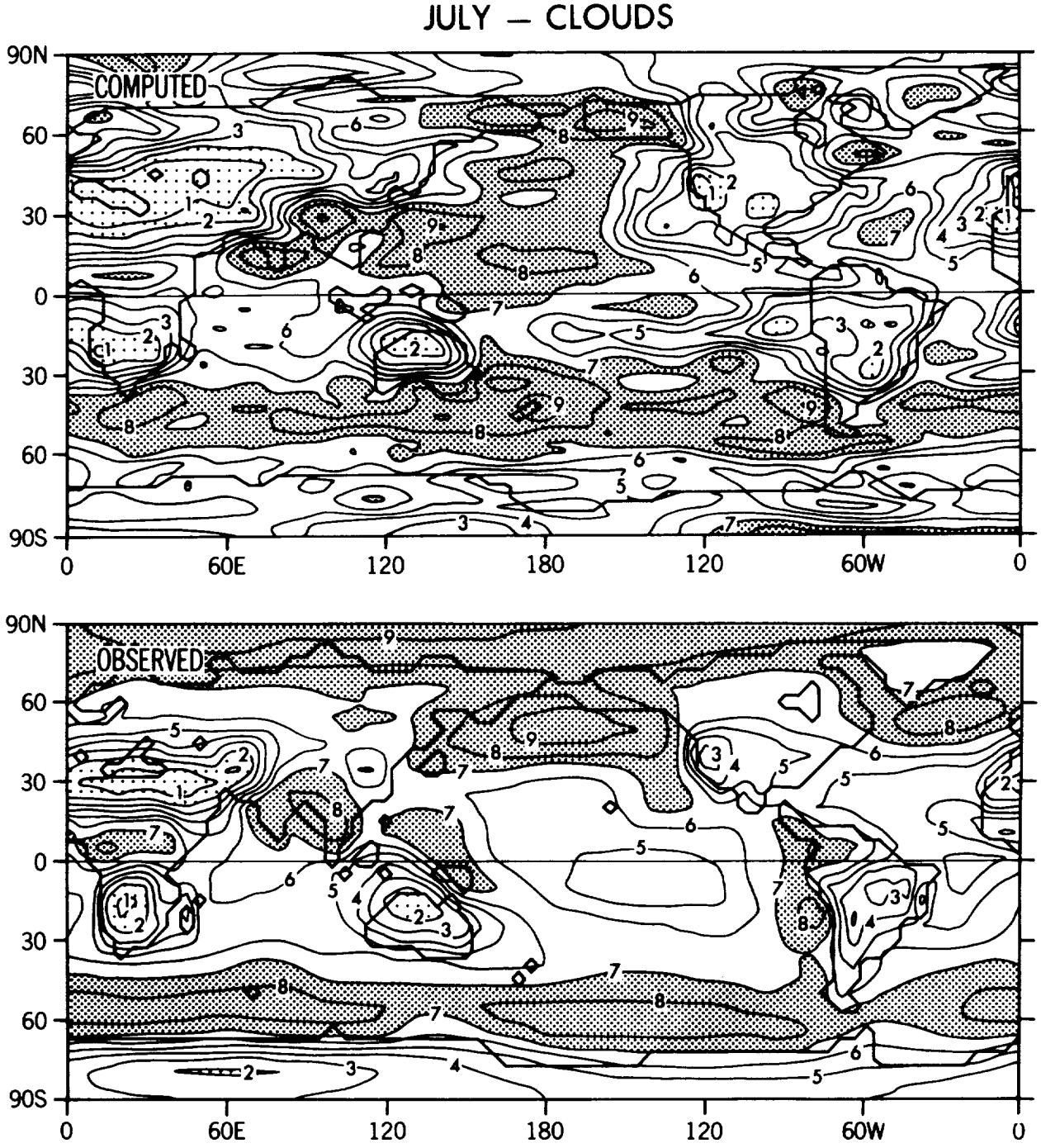

Figure 4. Global distributions of computed and observed total cloud amount (in tenths) for the month of July. Dark shade signifies values of 70% and greater. Light shade signifies values of 20% and smaller. Contour interval is 10%.

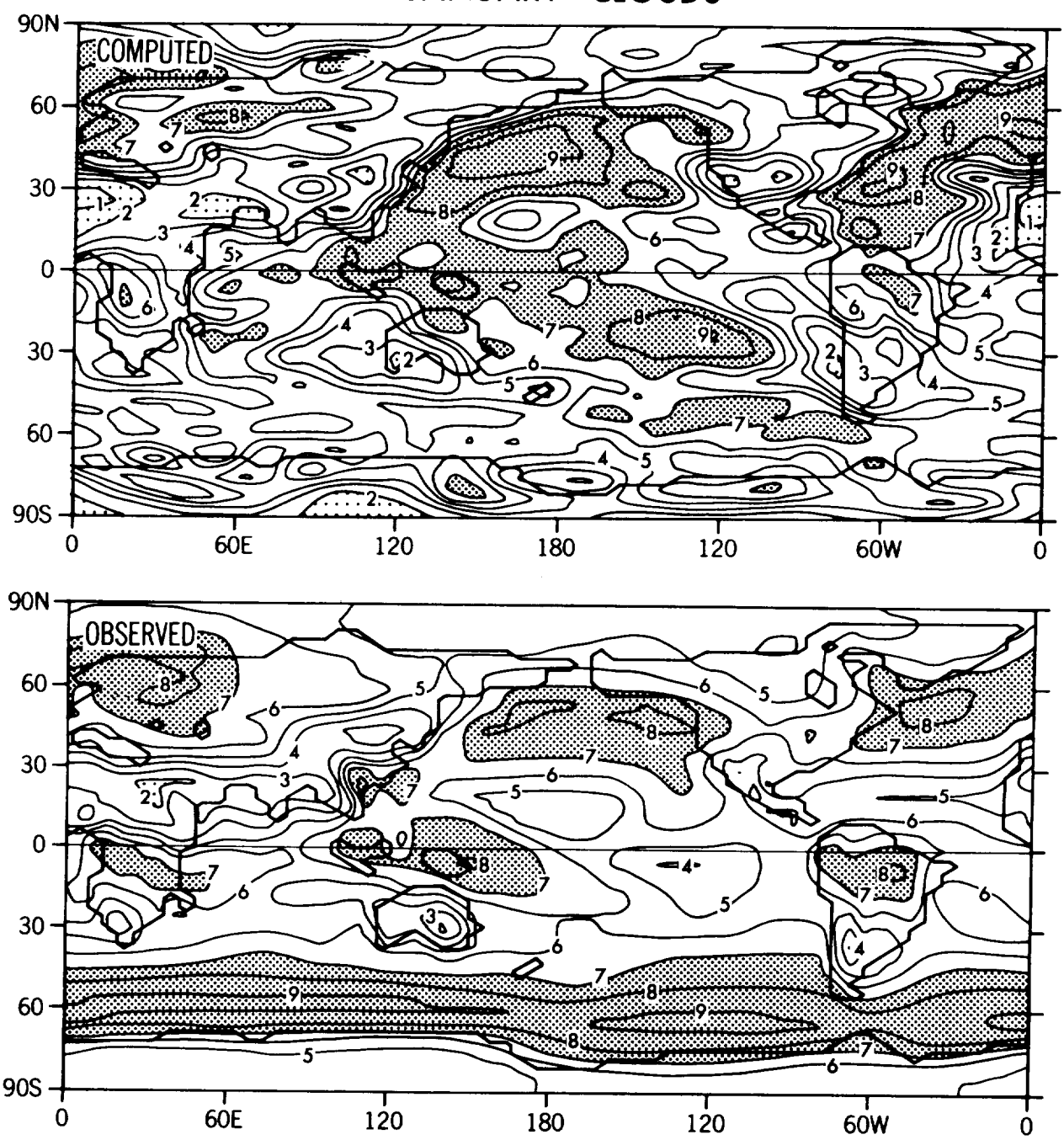

Figure 5. Global distributions of computed and observed total cloud amount (in tenths) for the month of January. Dark shade signifies values of 70% and greater. Light shade signifies values of 20% and smaller. Contour interval is 10%.

CONVECTION SENSITIVITY EXPERIMENTS WITH THE GISS GCM

D. Rind
NASA Goddard Institute for Space Studies
New York, New York 10025

One of the most important choices for any general circulation model concerns the parameterization for convection, a subgrid scale process which cannot be simulated explicitly. Convection is responsible for mixing heat, moisture and perhaps momentum and so plays an important role in determining the time-averaged temperature, moisture and wind fields. This means that the form of many of the other parameterizations of physical processes, decided upon by comparing model results to observations, is highly dependent upon the convection scheme employed. Thus the choice of convection scheme strongly impacts the entire structure of the general circulation model.

In order to evaluate this dependence we have employed several different convection schemes in the 8° x 10° version of the GISS GCM. Each experiment was run for nine months starting on December 1, 1976; the results noted below are for the third month, but were consistently observed throughout the (Northern Hemisphere) winter months. The control run for these experiments was run for five years and it was possible to determine the noise level for various parameters from the interannual variation. This defined the standard deviation referred to below.

Consider an atmosphere which is conditionally unstable, i.e., the moist static energy decreases with height but the dry static energy increases with height. In such a background a parcel of air will rise until it is saturated. In experiment I the parcel rises until it is just stable, and there is compensatory subsidence of an equal amount of air from the higher layer(s). Since the descending air was initially at a higher potential temperature than the ascending air, the subsidence will produce warming in the lowest layer. The convection will have transported moisture vertically, as the moist static energy profile was unstable. We can thus expect that the result of the convection is to warm and dry the lower layer, while moistening and perhaps cooling the upper layer.

In contrast, consider the process known as "moist adiabatic adjustment." Given the same background situation the procedure in this type of scheme is to simply equalize the moist static energy profile, raining out any moisture in excess of saturation. There is no subsidence considered. After this process the lower layer has lost moist static energy and since it is still saturated this means it has lost both heat and moisture, while the upper layer gains. The result then is to cool the lower layer and maintain a saturated state while warming the upper layer. This, experiment II, should then produce effects directly opposite to that of experiment I.

Both of these schemes differ from that normally employed in the control run which hypothesizes a subgrid scale temperature variance with a distribution extrapolated from the resolvable scales. The supposition is that in spite of the mean profile determined by values averaged over the course grid, a certain proportion of the grid will most likely be unstable while another portion will be stable. Given a conditionally unstable atmosphere, the subgrid scale temperature variation causes part of the grid to be warm enough to be absolutely unstable – the dry static energy would decrease with height, and the compensatory subsidence would produce cooling. However, for the remainder of the unstable portion of the grid, the scheme would operate as in experiment I, and warm the lowest layer. The net effect should then be intermediate to that of experiment I and experiment II.

Figure 1 shows the difference in moist convective heating between experiment I and the control run during February. As expected there is greater subsidence warming in the lowest layer in experiment I, and greater cooling aloft. The changes are 5–10σ, with the standard deviation determined from the five year control run. Figure 2 shows the cloud cover decreases in the lowest layers (4–6σ), again as expected. The heating of the subtropical lower layers provides upward motion there (Fig. 3) reducing the intensity of the Hadley Circulation and moistening desert areas (3–6σ changes).

In contrast moist adiabatic adjustment produces cooling in the lowest layer compared to the control run as a response to convection (Fig. 4), in agreement with the analysis. However it leaves the atmosphere in a saturated state and when one adds the effect of large scale supersaturation heating, the net effect is to produce warming at low levels (Fig. 5). This is an example of an often encountered GCM phenomenon: feedbacks in the system more than compensating for the (correctly expected) initial change. This heating distribution increases the Hadley Circulation, with greater rising air at low latitudes and sinking in the subtropics (Fig. 6). Finally, if one calculates clouds with this process the result is a huge increase, especially at the lowest levels (Fig. 7). These last two effects are in direct contrast to those of experiment I, even though both ultimately produced low-level heating.

The choice of convection scheme can be seen to result in large differences in the mean meridional circulation, the cloud cover and, although not discussed here, the temperature, precipitation, and wind fields as well. Given any one scheme, subsequent choices for parameterizations are made against the background of these effects to produce a model which simulates the real world. Different models will most likely have different sensitivities to climate change mechanisms. It can thus be argued that a realistic convection scheme should be one of the first priorities in developing a general circulation model.

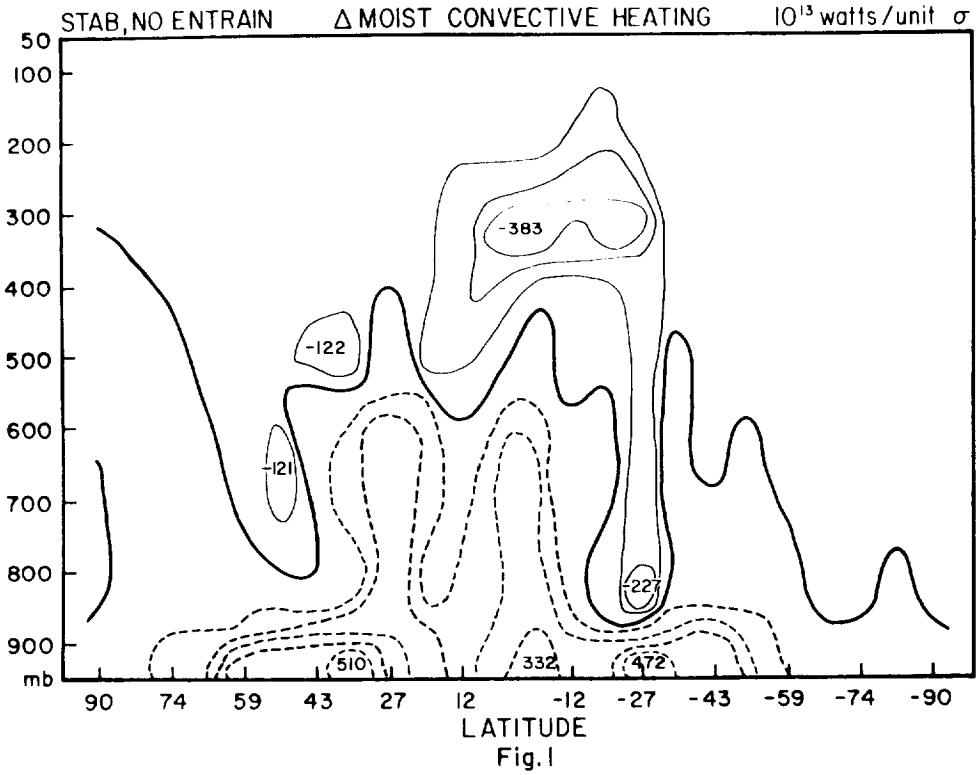

Fig. 1

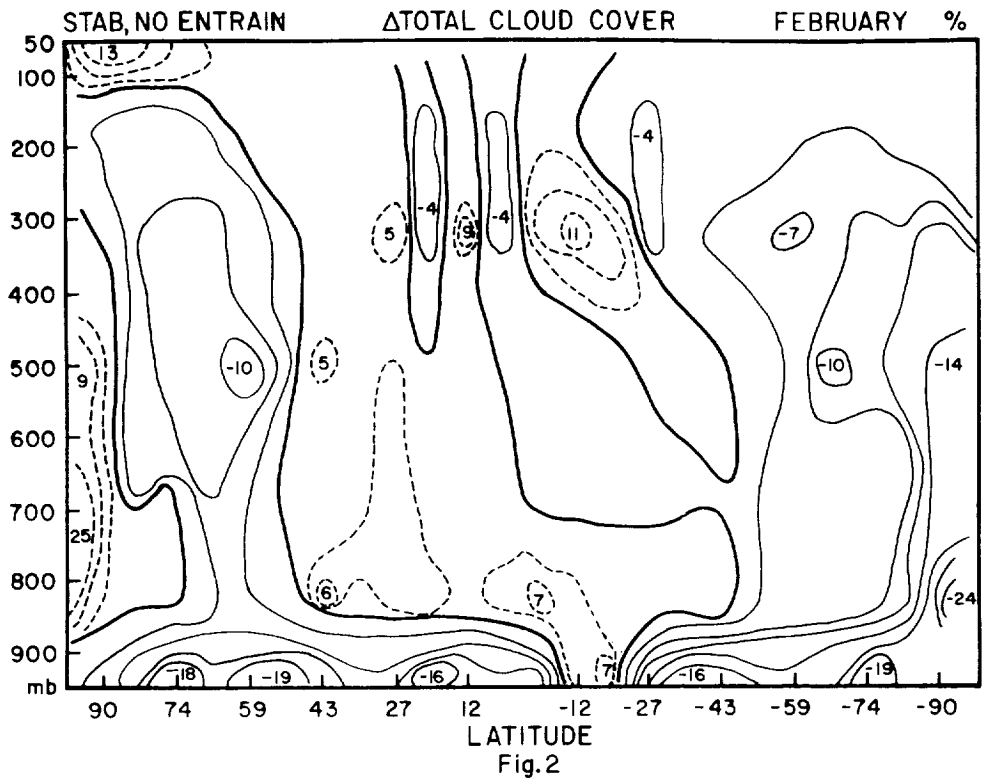
STAB, NO ENTRAIN
ΔTOTAL CLOUD COVER
FEBRUARY %
50
100
200
300
400
500
600
700
800
900
mb
3
-4
5
-4
-4
11
-4
-7
-10
5
9
-10
-14
25
6
7
-24
-18
-19
-16
7
-16
-19
90 74 59 43 27 12 -12 -27 -43 -59 -74 -90
LATITUDE

Fig. 2

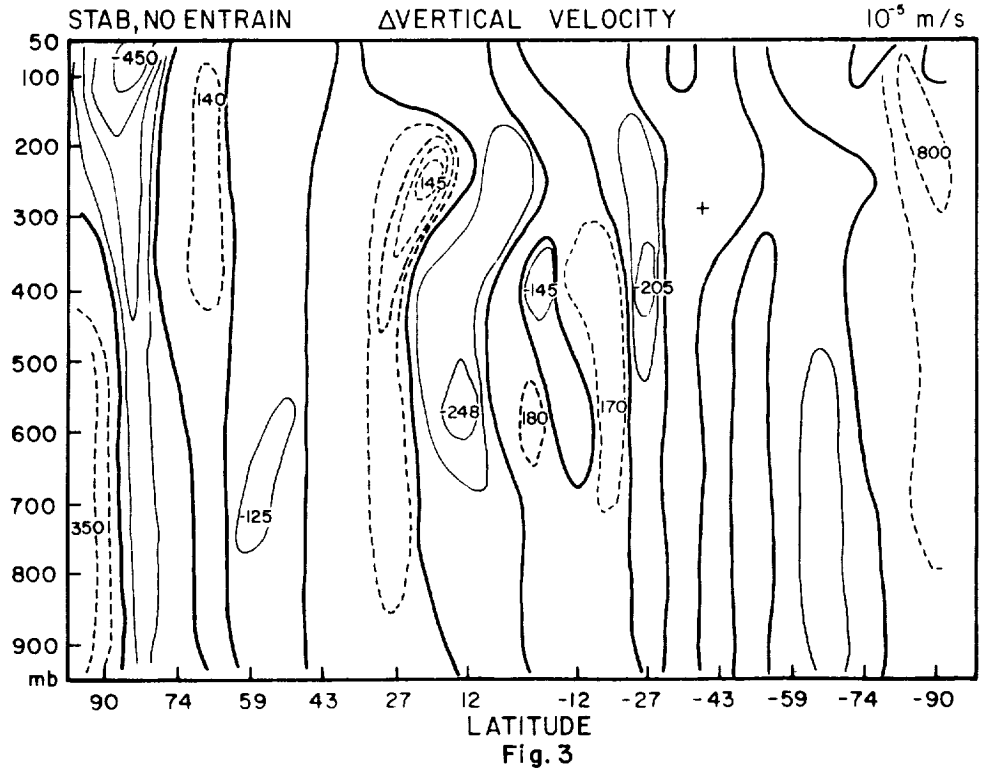
STAB, NO ENTRAIN
ΔVERTICAL VELOCITY
10⁻⁵ m/s
50
100
200
300
400
500
600
700
800
900
mb
450
140
145
800
145
205
248
180
170
350
125
90 74 59 43 27 12 -12 -27 -43 -59 -74 -90
LATITUDE

Fig. 3

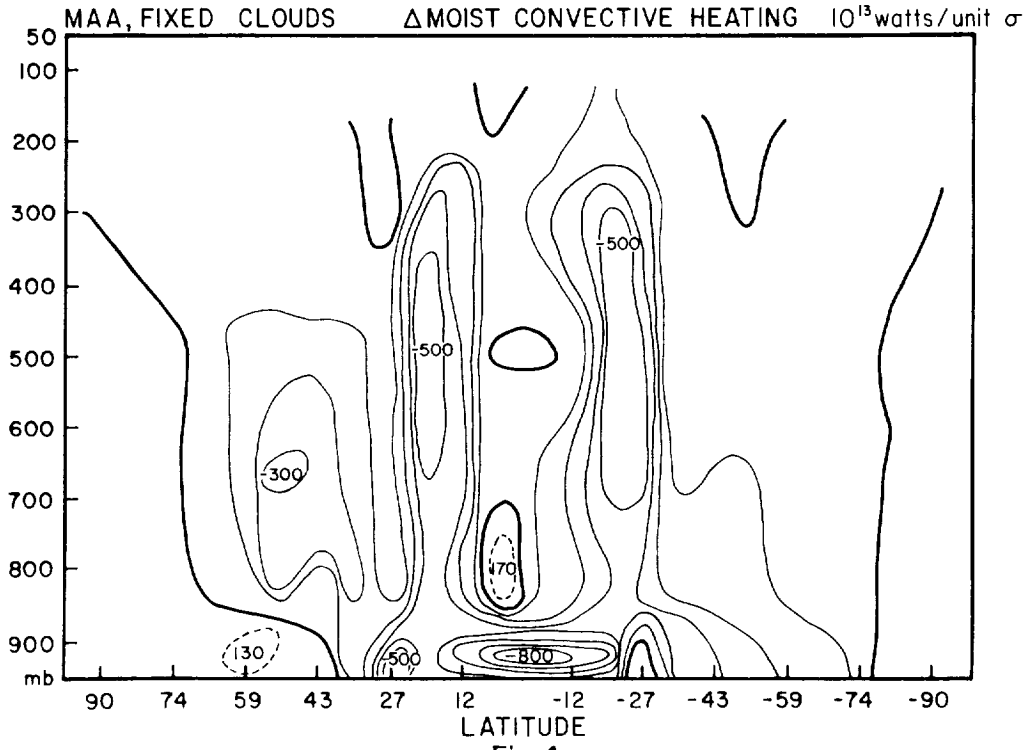
MAA, FIXED CLOUDS
ΔMOIST CONVECTIVE HEATING
10^13 watts/unit σ
50
100
200
300
400
500
600
700
800
900
mb
-500
-500
-300
-470
-130
-500
-800
90
74
59
43
27
12
-12
-27
-43
-59
-74
-90
LATITUDE

Fig.4

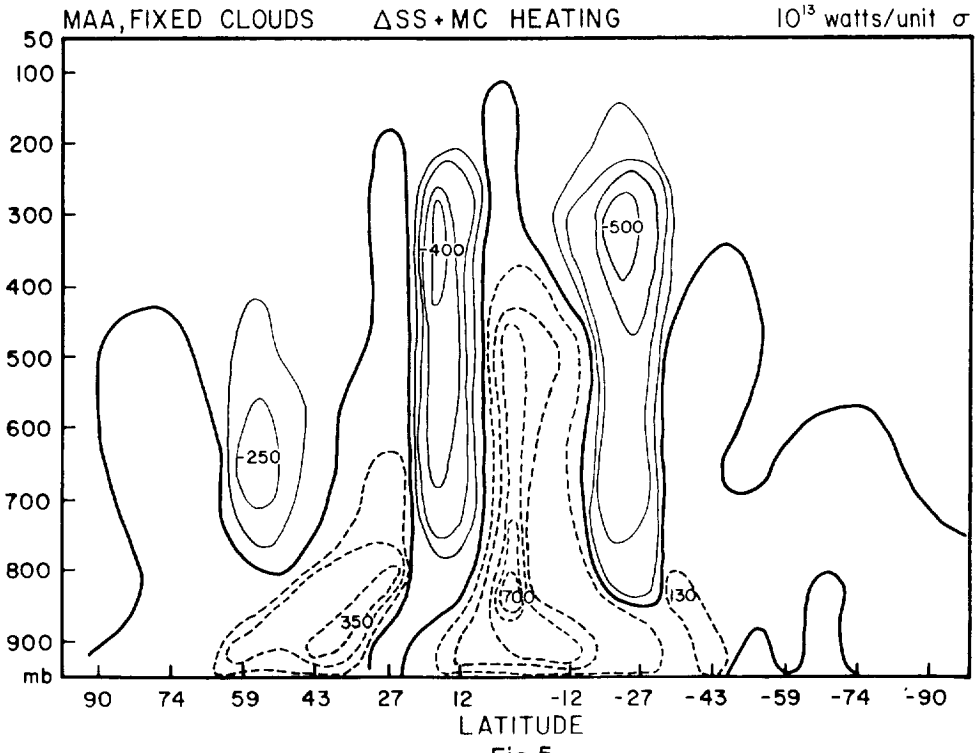
MAA, FIXED CLOUDS
ΔSS + MC HEATING
10^13 watts/unit σ
50
100
200
300
400
500
600
700
800
900
mb
-500
-400
-250
-700
-350
-130
90
74
59
43
27
12
-12
-27
-43
-59
-74
-90
LATITUDE

Fig.5

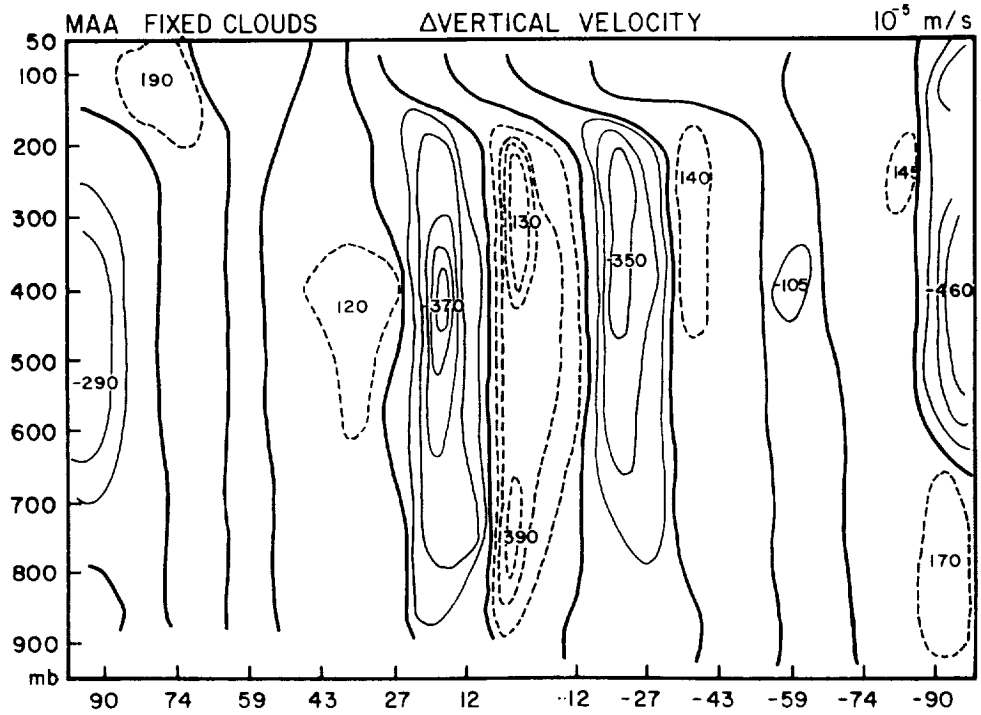
MAA FIXED CLOUDS
ΔVERTICAL VELOCITY
10^{-5} m/s
50
100
200
300
400
500
600
700
800
900
mb
190
120
-290
-370
130
390
-350
140
-105
145
-460
170
90 74 59 43 27 12 -12 -27 -43 -59 -74 -90
LATITUDE

Fig. 6

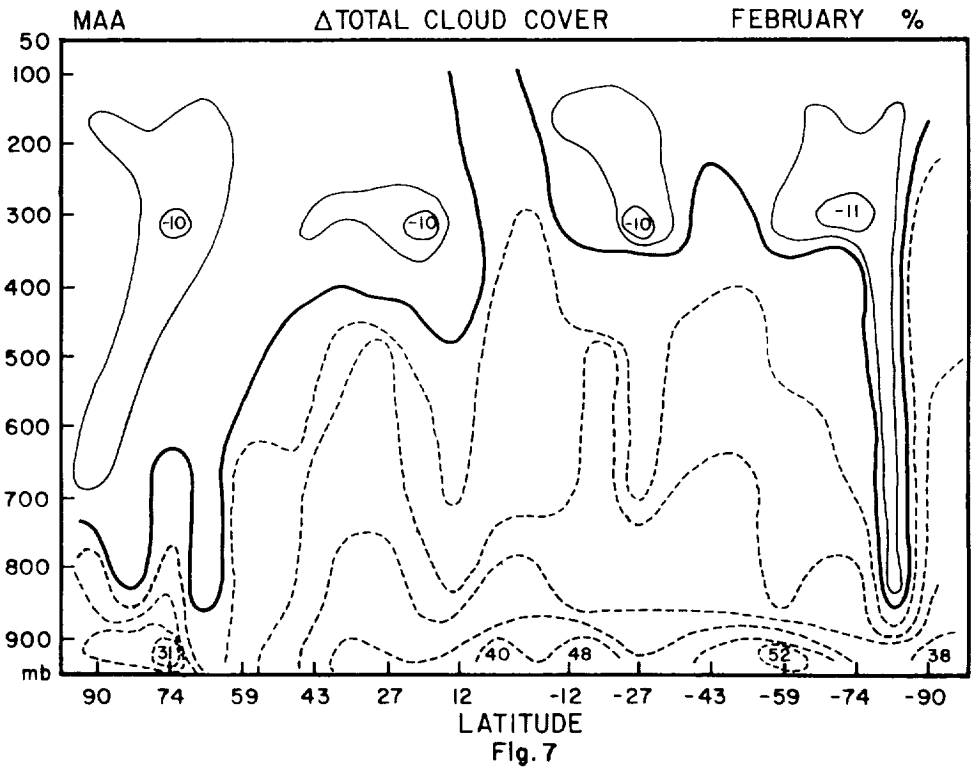
MAA
ΔTOTAL CLOUD COVER
FEBRUARY %
50
100
200
300
400
500
600
700
800
900
mb
-10
-10
-10
-11
31
40
48
52
38
90 74 59 43 27 12 -12 -27 -43 -59 -74 -90
LATITUDE

Fig. 7

CLOUDS IN RADIATIVE-CONVECTIVE MODELS: ASSUMPTIONS, IMPLICATIONS, AND LIMITATIONS

Ruth A. Reck and John R. Hummel
Physics Department
General Motors Research Laboratories
Warren MI 48090

In one-dimensional radiative-convective models the radiative impact of clouds is typically the only element of the cloud-climate relationship that is considered. However, it is well known that in the real atmosphere clouds also furnish a major latent heat contribution to the energy balance, a key link in the hydrologic cycle.

Water Vapor Profiles and Cloud Locations

Most simple models assume a linear relationship between pressure (p) and the relative humidity (h) of the form

$$h(p) = h_s(p_o)\ \frac{p/p_o - 0.02}{0.98},$$

where h_s refers to the surface relative humidity and p_o is the surface pressure. Based upon clear and cloudy sky weighted averages and assuming cloud formation at 100% relative humidity there is a limited region where clouds are thermodynamically acceptable (e.g. see Figure 1). In this case a

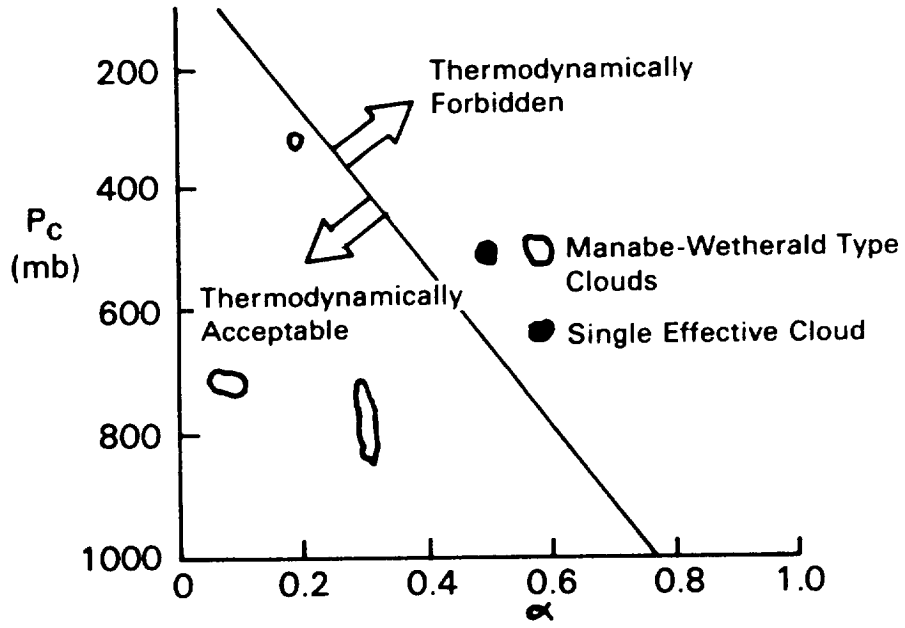

Figure 1. Calculation of the pressure P_c for which the clear sky relative humidity $\rightarrow 0$ for a given cloud abundance α.

single effective cloud at 5.5 km (used in many 1-D calculations) falls within the thermodynamically forbidden region and even for three layers of clouds and global average conditions (including 50% cloud cover) the precipitable water is five times less than the apparent measured global average value. This occurs partly because the calculated global average temperature is so low (280 K) and because the distribution of water vapor with latitude is highly non-linear. By inclusion of cloudy sky upward transport and clear sky downward transport of water vapor (defined by the vertical velocity calculated from the Richardson equation) Hummel and Kuhn have developed a 1-D model which calculates cloud altitudes and which also obtains good agreement with measured humidity profiles and surface temperature. Reck has previously demonstrated with the Manabe-Wetherald model that the height of the assumed clouds is critical since the sensitivities calculated with a fixed cloud top temperature are ~1.5 times those calculated with a fixed cloud top pressure model.

Cloud Optical Properties

The sensitivity of the Manabe-Wetherald 1-D model to cloud albedo, absorption and abundance has also been calculated (Fig. 2 and 3). These results show the greatest sensitivity to low and high cloud albedo and abundance. However, the magnitude of the cloud abundance sensitivity varies with surface albedo. The calculated surface temperature T_S may be fit to ~0.1 K by a relationship of the form

$$T_S = A + B\omega_S + C\alpha + D\omega_S\alpha + E\omega_S^2 + F\alpha^2$$

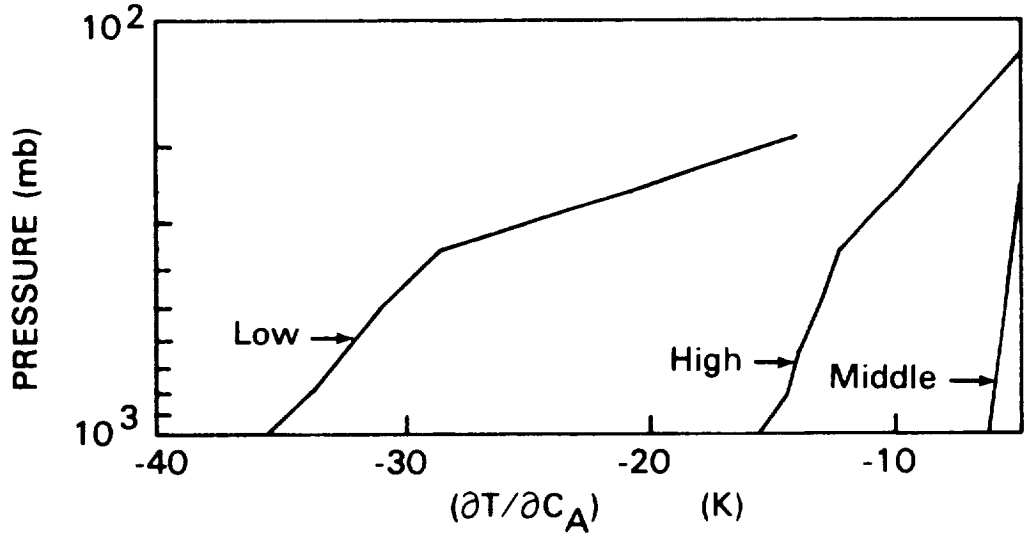

Figure 2. Calculation of the temperature sensitivity of the Manabe-Wetherald 1-D model to cloud shortwave albedo, C_A.

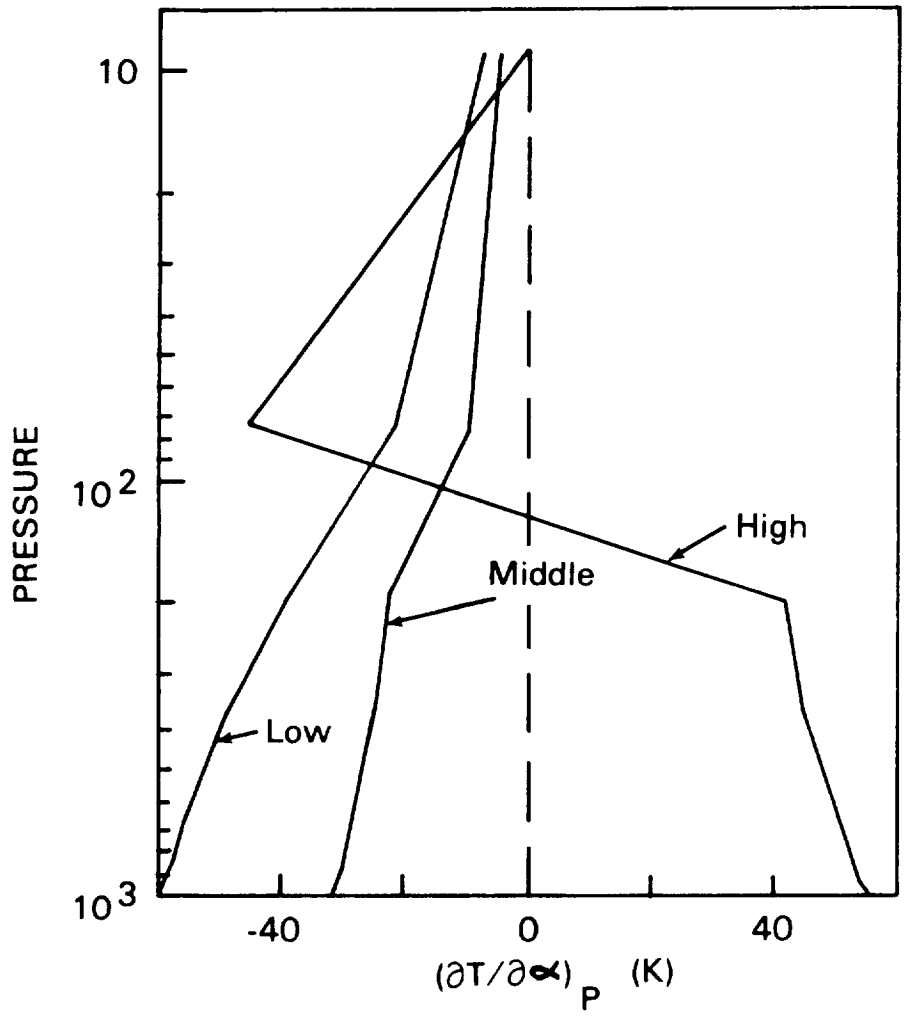

Figure 3. Calculation of the temperature sensitivity of the Manabe-Wetherald 1-D model to cloud abundance α.

where the constants have the values

	A	B	C	D	E	F
Low Clouds	313.081	-96.695	-56.530	61.449	-54.052	-13.172
Middle Clouds	298.637	-83.779	-45.537	38.496	-51.027	10.208
High Clouds	286.880	-70.985	41.890	-35.248	-54.832	50.068

This empirical relationship may be useful to demonstrate the relative importance of independent variations in cloud α abundance and surface albedo ω_s

$$\delta T_s = (C + D\omega_s + F\alpha)\,\delta\alpha + (B + D\alpha + 2E\omega_s)\,\delta\omega_s$$

as well as to predict total cloud abundance which produces a calculated surface temperature for a given surface albedo.

SOME REMARKS ON CUMULUS PARAMETERIZATION

R. S. Lindzen
Center for Earth and Planetary Physics
Harvard University
Cambridge, MA 02138

Dr. Sarachik, in the opening paper of this session, has noted that the total precipitation (or equivalently the atmospheric heating) associated with cumulus convection is generally accurately represented by a simple moisture budget:

$$\text{Precipitation} = \text{Evaporation} + \text{Convergence of Moisture} \qquad (1)$$

The relevant convergence appears to be that which occurs in the lower troposphere – below the trade inversion where such a feature exists. Such a budget has been observed in the western Pacific (Ogura and Cho, 1973) and during all phases of GATE (1980). The total cumulus heating is simply the latent heat of condensation, L, times the precipitation.

We shall discuss the above budget later in this note. Clearly, such a budget cannot be true always; otherwise there would be no way for humidity in the lower troposphere to change. For the moment, however, let us ignore this problem. As noted by Sarachik, (1) fails to give us the vertical distribution of heat release. Some additional closure conditions are needed to obtain such a distribution. The question arises as to whether we need a detailed specification of the vertical distribution of cumulus heating. The answer to this question is not entirely clear. Stevens, *et al.* (1977) concluded that the vertical distribution was not too important for fully developed easterly waves because of the important role of cumulus friction. The same insensitivity may not hold for weaker developing waves (Stevens and Lindzen, 1978). Furthermore, the ability of latent heat release in the tropics to force stationary waves in middle latitudes intuitively ought to depend on whether the latent heat is deposited in the lower troposphere where we have prevailing easterlies or at upper levels where prevailing westerlies may exist (Charney and Drazin, 1961). At least in some circumstances, therefore, we *do* expect the vertical distribution of latent heat release to be important.

Among the various closures suggested for obtaining this distribution is that due to Arakawa and Schubert (1974). This particular approach is difficult (if not impossible) to solve for, and its physical basis is not at all clear. An attempt to apply the Arakawa-Schubert scheme to GATE data has been made by Lord (1978). Lord was unable to obtain a solution to the Arakawa-Schubert scheme. However, using simplex methods, Lord obtained answers close (in some sense) to being solutions. A comparison between the predicted distribution of heating (using Lord's approach) and observations is shown in Figure 5 of Sarachik's paper in this volume. The agreement is quite poor. The Arakawa-Schubert scheme predicts a concentration of cloud heating near the surface; observations show fairly uniform heating between the ground and 300 mb. In view of our remarks on tropical forcing of stationary waves we might anticipate serious problems arising from this misrepresentation.

We may next ask whether this failure implies that a more effective parameterization will prove still more complicated than the Arakawa-Schubert scheme. I doubt it. I will attempt to show, in this

note, that an almost trivial but plausible scheme provides a rather good simulation of the observed heating. The basic approach is that described in Appendix 1 of Stevens and Lindzen (1979). As shown by Ooyama (1971) and Arakawa and Schubert (1974) (see Sarachik's lecture for further details), cumulus heating can be expressed

$$H = M_c \frac{\partial s}{\partial z} = \rho Q \tag{2}$$

where

Q = Htg. in deg/day

M_c = mass flux in cumulus clouds

$\frac{\partial s}{\partial z}$ = dry static energy gradient in air outside clouds ($s = c_p T + gz$)

The specification of the vertical distribution of heating becomes equivalent to the specification of M_c's distribution. Certain aspects of M_c's distribution are fairly clear: for example, M_c should not extend beyond a height, z_T, where

$$c_p T(0) + Lq(0) = c_p T(z_T) + gz_T \tag{3}$$

where

$$c_p T(0) + Lq(0) = h(0) = \text{moist enthalpy } (s+Lq) \text{ at the ground}$$

and

$$c_p T(z_T) + gz_T = s(z_T) = \text{dry static energy at } z_T.$$

Equation (3) defines z_T. Equation (1) gives us that

$$\int_0^{z_T} M_c \frac{\partial \theta}{\partial z} dz = L(E + \text{conv. of water vapor}) \tag{4}$$

The simplest choice of M_c consistent with (3) and (4) would be to make M_c a constant between $z = 0$ and $z = z_T$. Such a choice would lead, via (2), to a better fit to the observed heating during GATE than that obtained by Lord. However, it would do poorly for the Marshall Islands. Following an admittedly *ad hoc* procedure, one can do much better. In Figure 1 we show s, h and h* (saturated moist enthalpy) *vs.* p for GATE and the western Pacific (during the Marshall Islands nuclear tests of the late 1950s). (Note that s is very nearly linear in p -- rather than z. This implies that $\partial s/\partial z \propto \rho$ and hence Q will follow M_c rather than M_c/ρ.) Clearly, air above the minimum in h cannot participate significantly in cumulus convection. We shall assume (counter to the most straightforward arguments) that all air below the minimum can participate in cumulus convection,[1] and that the

[1]Conventional reasoning (Holten, 1972) would hold that only air with values of h such at h* at some greater height is less than h can become convectively buoyant. However, Augstein, *et al.*, (1974) show that at any instant the minimum in h arises from a precipitous drop in h from larger values below, and that all the air below can be convectively unstable (*viz.* Figure 2). The layer in which the precipitous drop occurs is identified with the trade inversion. The broad minimum in Figure 1 seems likely to be the result of averaging over a trade inversion which is moving up and down.

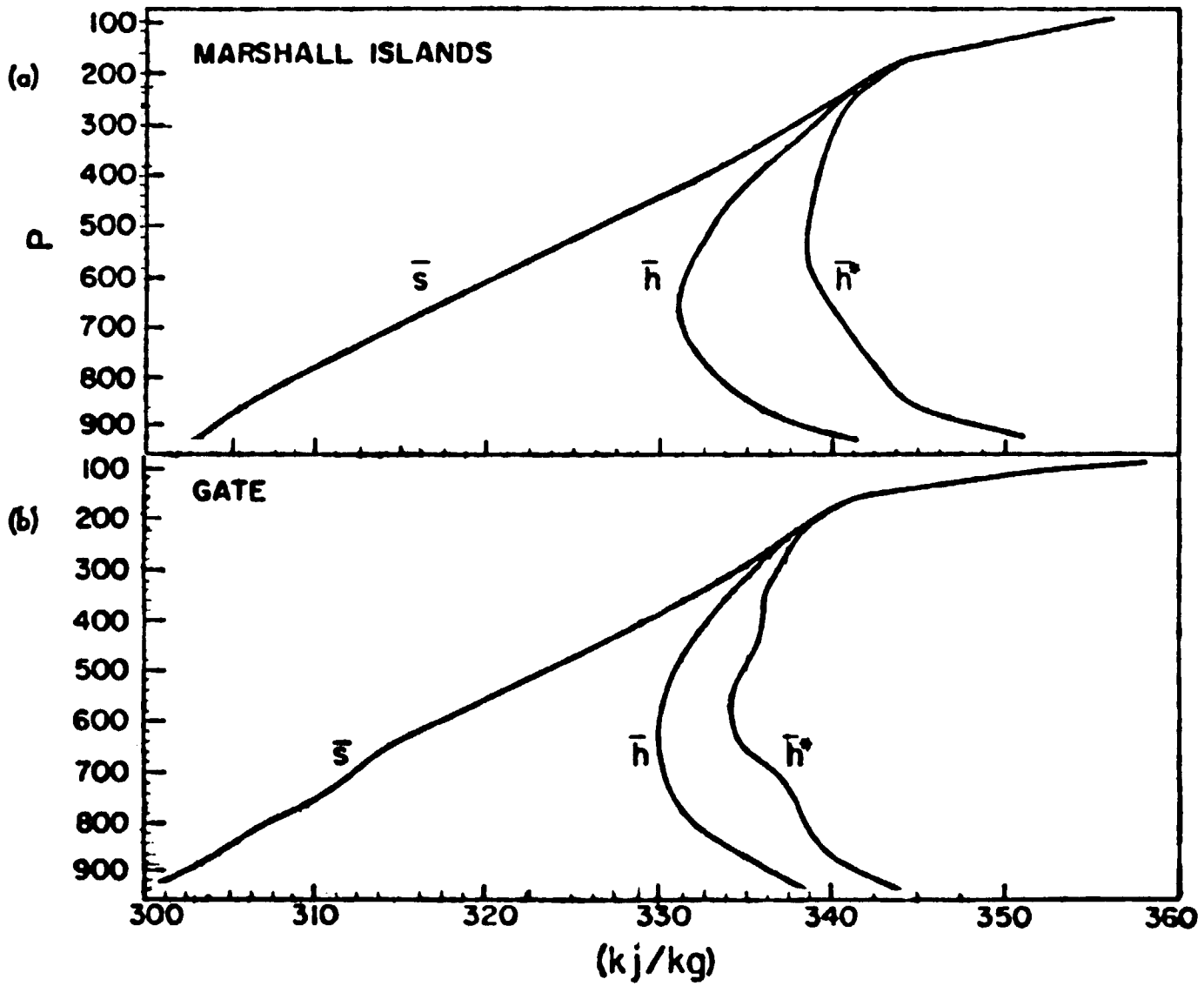

Figure 1. Dry static energy, $\bar{s}$, moist static energy, $\bar{h}$, and saturation moist static energy, h^*, in units of kj kg^{-1} *vs.* height (mb). From Fig. 4.7 in Lord, 1978.

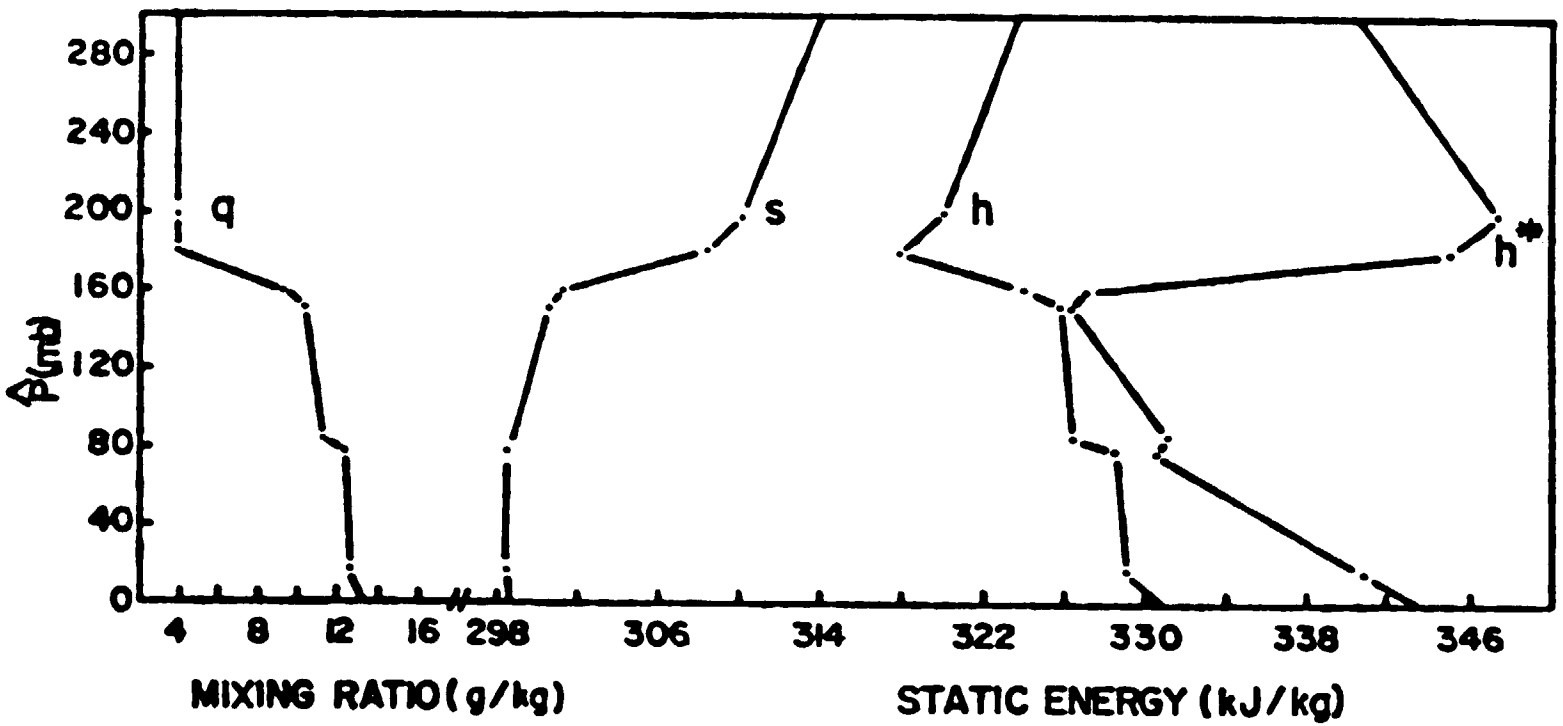

Figure 2. Vertical profiles of mixing ratio, dry static energy, moist static energy, and saturation static energy for the ship Planet, February 7–12, 1969 (Augstein, *et al.*, 1974).

moisture convergence referred to in Eq. (1) is that which takes place below the minimum in h. We next assume that portion of M_c which arises from evaporation, $M_{co} = E/q_o$ (where E = surface evaporation and q_o = specific humidity of surface air) detrains at z_T (*viz.* Eq. (3)), while that portion of the air converged between some z and δz, $\delta(\rho w)$ gives rise to a $\delta M_c = \delta(\rho w)$ which detrains at that z_d where $s(z_d) = h(z)$. This procedure completely specifies the vertical distribution of M_c. The above procedure is unambiguous when low level convergence is occurring. Its application is schematically illustrated in Fig. 3. Additional considerations must be applied when we have divergence. Indeed, when divergence exceeds evaporation, drying must occur. For the purposes of this brief note divergence will be ignored.

We shall use data from the Marshall Islands (Reed and Recker, 1971) and from the third phase of GATE (Lord, 1978) to calculate the vertical distribution of cumulus heating. For both GATE and the Marshall Islands it was the case that evaporation was small (~20% of convergence in trough regions), and, hence, we will ignore M_{co}. Figure 1 gives the vertical distribution of s and h for both cases. The distributions do not change markedly during the passage of an easterly wave. Hence this figure can be used to determine at what height air converged below h's minimum will eventually detrain. Figure 4 shows ω (p-velocity ~ $-\rho w$) *vs.* p for the convergent phases of easterly waves in the Marshall Islands (taken from Fig. 8 of Reed and Recker, 1971) and during GATE (taken from Fig. 5.6 of Lord, 1978). Note that during GATE convergence (increasing $\rho\omega$ with height) was confined far more closely to the surface than during the Marshall Islands tests. We now calculate M_c using the approach described above and in Fig. 3. The results are shown in Figs. 5 and 6. Also shown is the cumulus heating given by Eq. (2) – using $\partial s/\partial z$ from Fig. 1. Note that the vertical distribution of heating is very different in the two cases – largely but not totally reflecting the different distributions of M_c. The differences in M_c arise from differences in the large-scale low-level convergence.

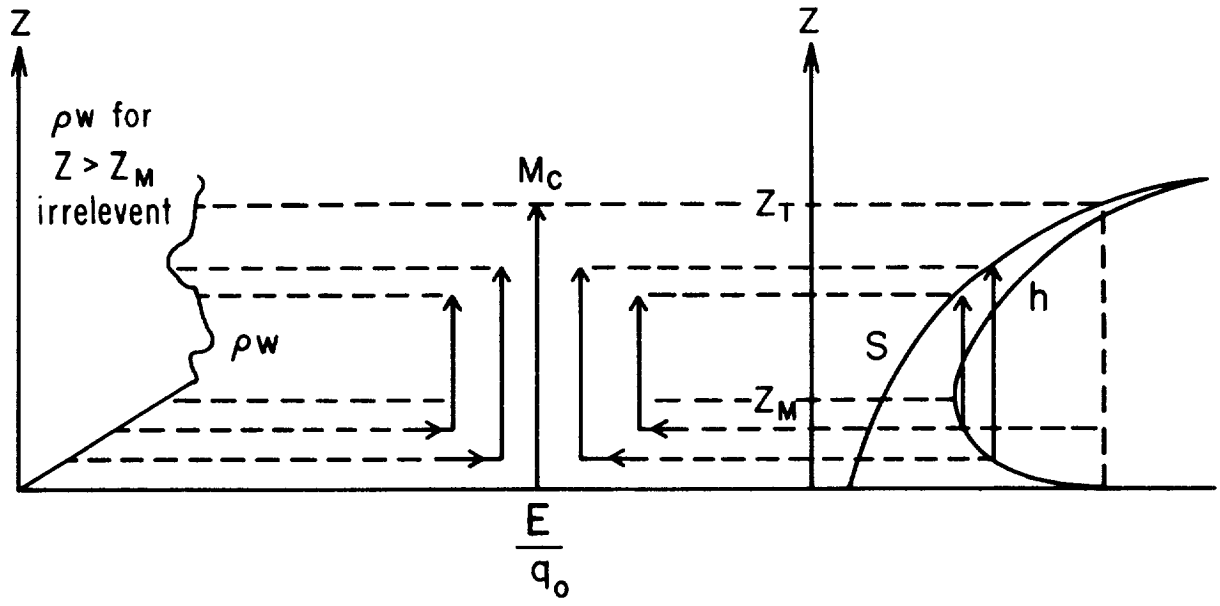

Figure 3. Schematic illustration of how M_c is related to distribution of s, h and $\rho\omega$ ($\wedge\vee - \omega$).

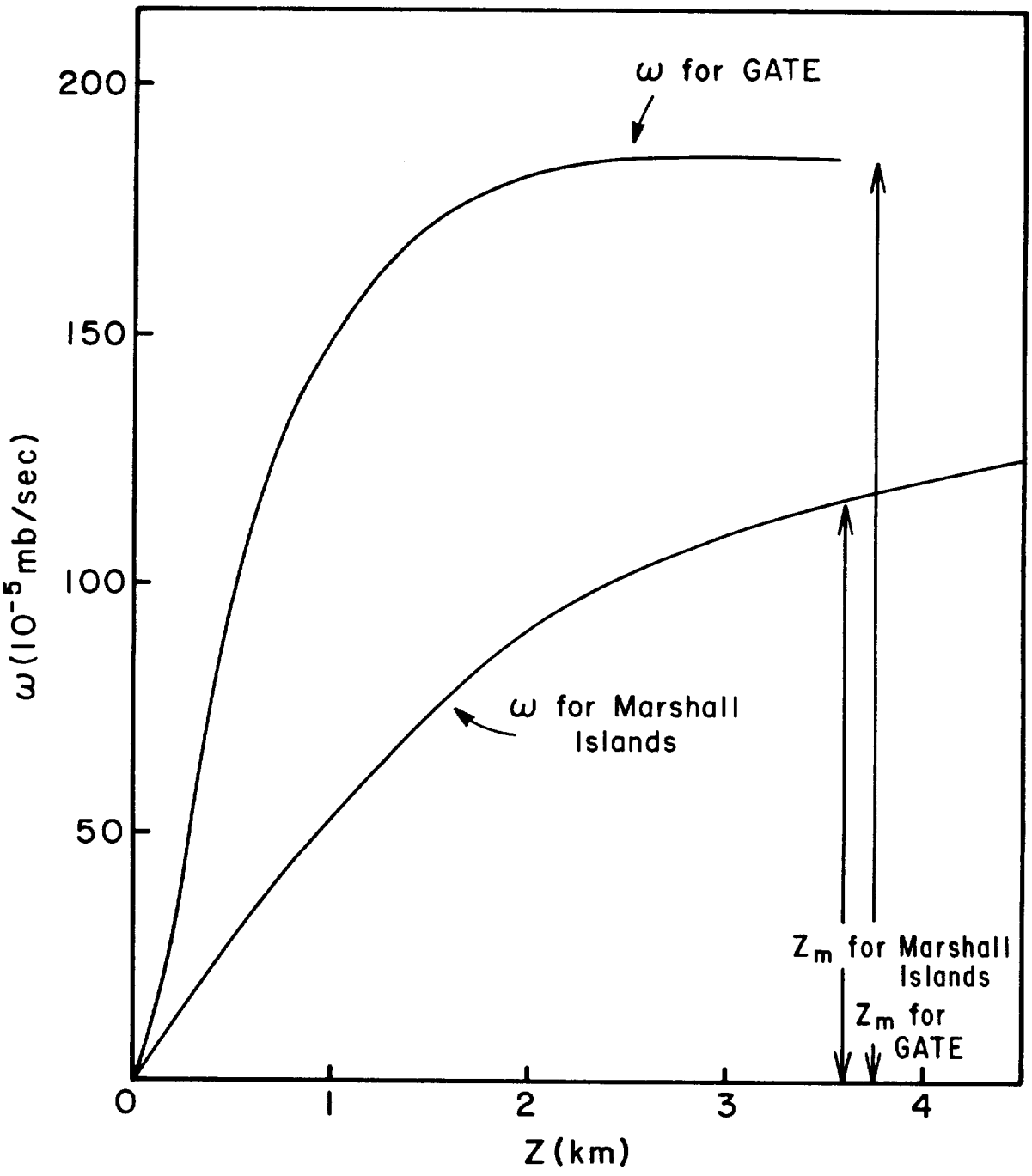

Figure 4. Vertical distribution of $-\omega$ (10^{-5} mb/sec) during convergent phase of easterly wave.

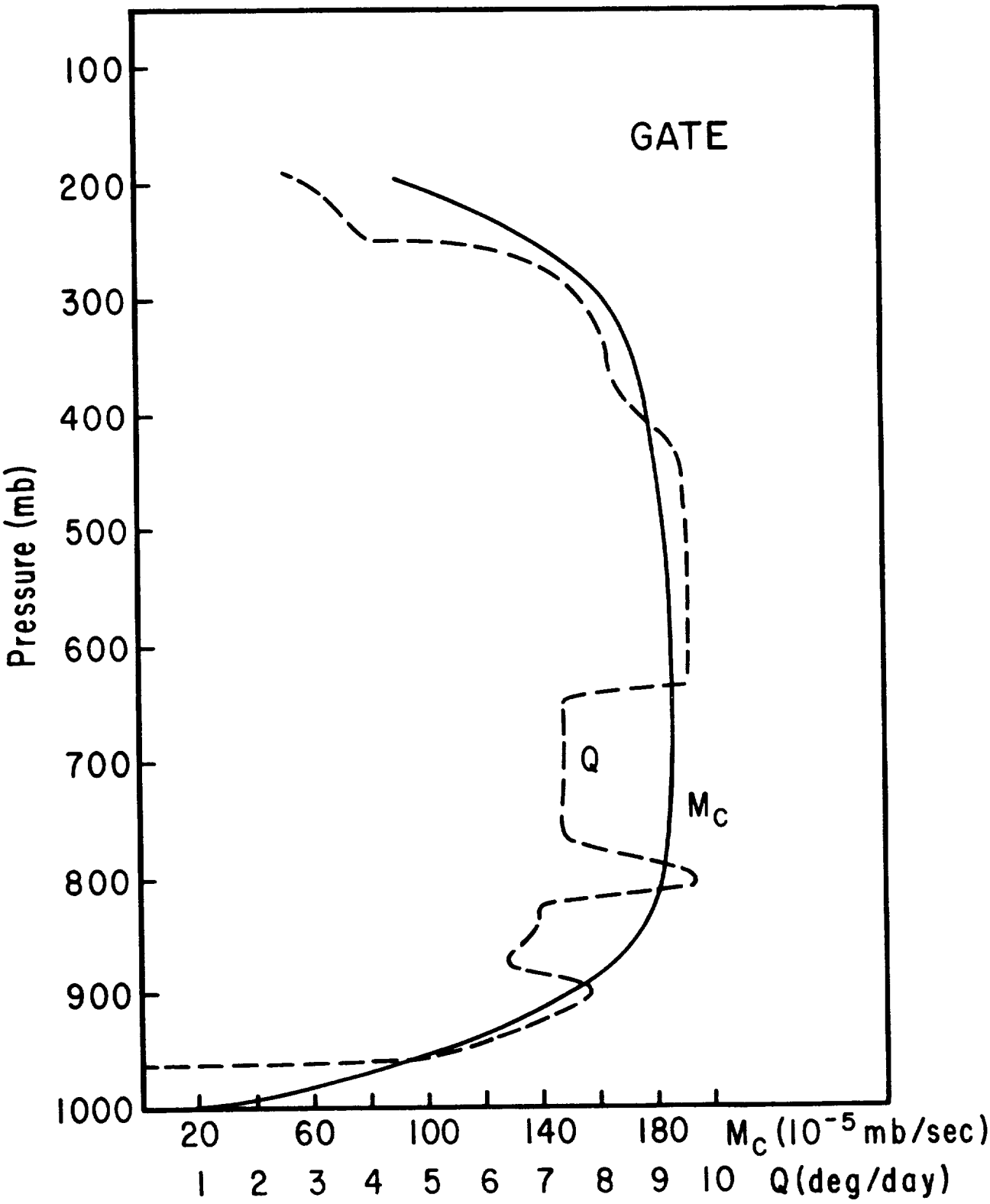

Figure 5. Predicted M_c and Q for GATE.

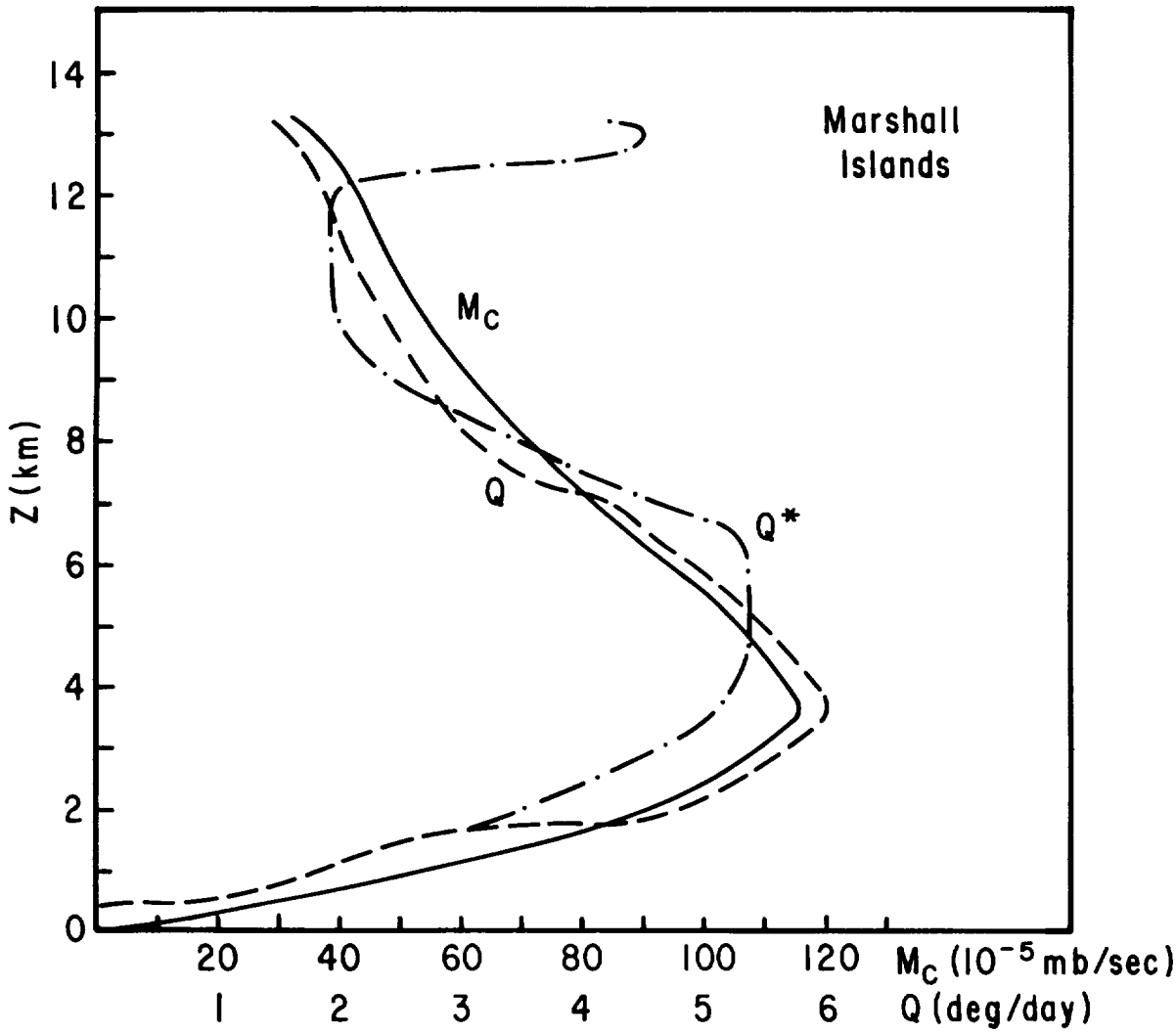

Figure 6. Predicted M_c, Q and Q* for Marshall Islands.

For the GATE case large-scale convergence is confined to a region well below the minimum in h. The converged air, therefore, has a large value of h and does not detrain until it reaches the upper troposphere. In between there is a large region of constant M_c. For the Marshall Islands large-scale convergence occurs throughout the region below the level of minimum h, and hence detrainment begins shortly above this level. Interestingly, in both cases the predicted profiles are very similar to the observational estimates of cumulus heating (*viz.* Fig. 14 in Reed and Ricker, 1971 and Fig. 5 in Sarachik). This measure of agreement in two very different cases supports the notion that the vertical distribution Q depends strongly on the distribution of low-level convergence. In contrast, the Arakawa-Schubert scheme, wherein the distribution of Q depends strongly on the distribution of ω at upper levels (Stark, 1976), yields extremely poor agreement with observed distributions. Thus, in addition to being so obscure, the Arakawa-Schubert scheme seems to be in conflict with observations.

To be sure, the results in Figs. 5 and 6 are not in perfect agreement with observations – obviously observations are not perfect either. First there is a small underestimate of total heating in both cases (~0 (10-20%)) which almost certainly results from ignoring evaporation. Finally, in Fig. 5, for the Marshall Islands, the peak in Q is 1-2 km lower than observed, while in Fig. 6, for GATE, the low-level wiggles are somewhat more extreme than those observed. These modest discrepancies are associated with small variations in $\partial s/\partial z$ with height (*viz.* Fig. 1, and Eq. (2)). While such variations of $\partial s/\partial z$ are probably not of fundamental consequence (and probably not very measurable), they do effect the detailed structure Q. In Fig. 7 we show the observed zonally averaged distribution of s (from Oort and Rasmusson, 1971) for the equatorial region. The use of this profile rather than that in Fig. 1 (for the Marshall Islands) does not greatly alter the distribution of M_c, but does lead to a new heating distribution – labelled Q* in Fig. 5. Q* peaks at an altitude in agreement with observation but has a second (unobserved) peak in the upper troposphere. There is no reason to worry about this upper level peak; the heating would rapidly alter s so as to eliminate the peak.

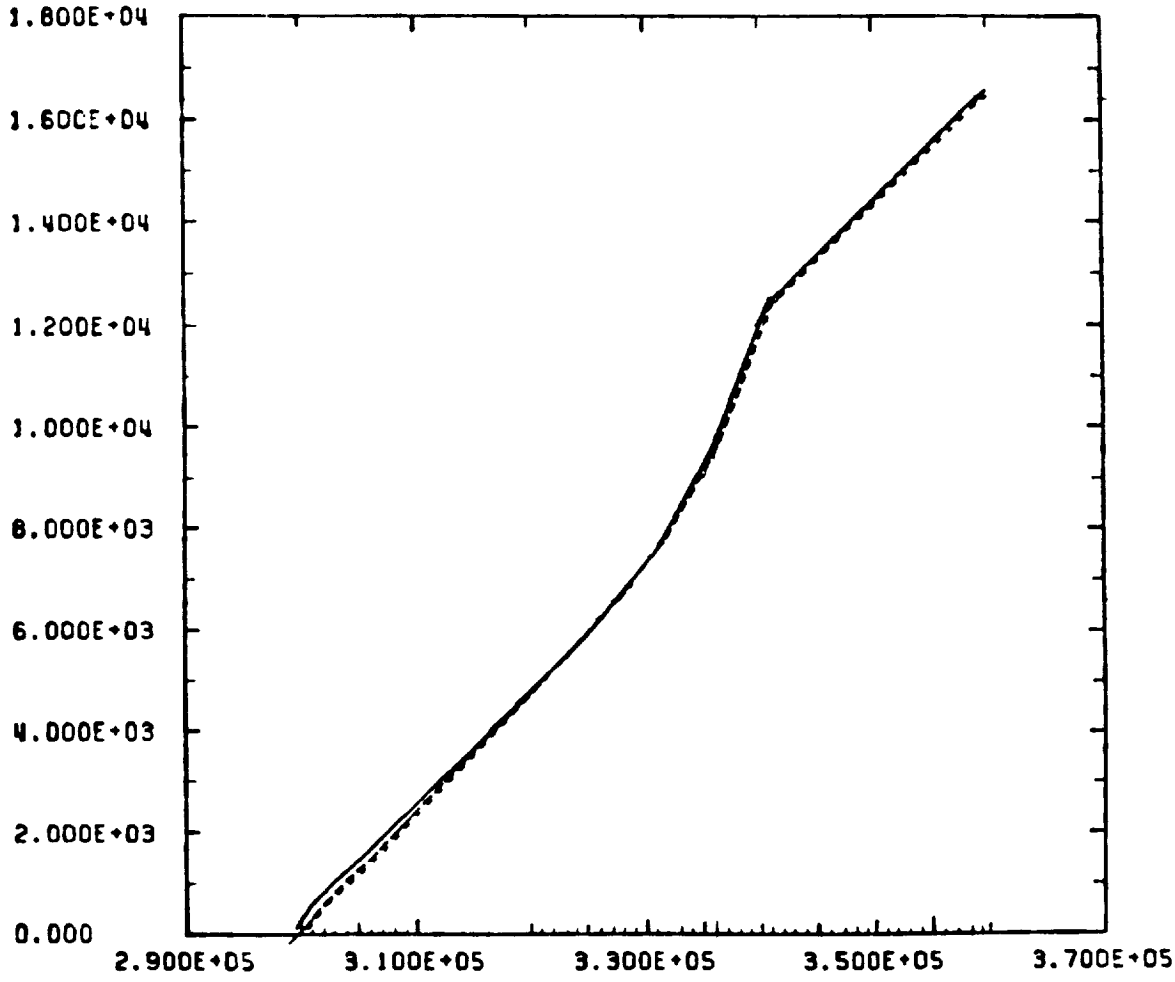

Figure 7. s *vs.* z from Oort and Rasmusson (1971).

In conclusion, our results suggest that the physically accurate parameterization of cumulus heating may be relatively simple – rather than a hopelessly difficult task. There does remain one difficulty mentioned at the beginning of this note. Namely, the detailed validity of the moisture budget given by Eq. (1). Intuitively, it seems that the development of deep instabilities from previously stable configurations might prove difficult in the presence of such a budget constraint. In addition, we know that shallow cumulus clouds do *not* rain efficiently. Thus it might suffice to replace (1) with a relation

$$\text{Precipitation} = f(z_T)\left\{\text{Evaporation} + \text{Convergence of Moisture}\right\} \qquad (5)$$

where (3) defines z_T, and $f(z_T)$ is less than one, approaching one as z_T approaches the upper troposphere. At the moment, the determination of $f(z_T)$ is *ad hoc*, but, it should not be difficult to tune.

Acknowledgments: The work described here has been supported by the National Science Foundation under Grant ATM-78-23330 and by the National Aeronautics and Space Administration under Grant NGL-22-007-229.

References

Arakawa, A. and W. H. Schubert, 1974: Interaction of a cumulus cloud ensemble with the large-scale environment, Part I. *J. Atmos. Sci., 31,* 674–701.

Augstein, E., H. Schmidt, and F. Ostapoff, 1974: The vertical structure of the atmospheric planetary boundary layer in undisturbed trade winds over the Atlantic Ocean. *Boundary-Layer Meteor., 6,* 129–150.

Charney, J. and P. Drazin, 1961: Propagation of planetary-scale disturbances from the lower into the upper atmosphere. *J. Geophys. Res., 66,* 83–110.

GATE, 1980: Proceedings of the NAS Symposium on the Impact of GATE on Large-scale Numerical Modelling of the Atmosphere and Ocean. Woods Hole Oceanographic Institution, 1979.

Holton, J. R., 1972: Introduction to Dynamical Meteorology. Academic Press, NY, 391 pp.

Lord, S. J., 1978: Development and Observational Verification of a Cumulus Cloud Parameterization. Ph. D. Thesis in Atmospheric Sciences, UCLA, 359 pp.

Ogura, Y. and H. R. Cho, 1973: Diagnostic determination of cumulus cloud populations from observed large-scale variables. *J. Atmos. Sci., 30,* 1276–1286.

Oort, A. and E. M. Rasmusson, 1971: Atmospheric Circulation Statistics. NOAA Professional Paper, *5*, 323 pp.

Ooyama, K., 1971: A theory of parameterization of cumulus convection. *J. Meteor. Soc. Japan, 49,* Special Issue, 744–756.

Reed, R. J. and E. E. Recker, 1971: Structure and properties of synoptic scale wave disturbances in the equatorial western Pacific. *J. Atmos. Sci., 28,* 1117–1133.

Sarachik, E. S., 1980: Report for GISS Cloud/Climate Workshop, NASA-GISS, New York, 1980. To appear.

Stark, T. E., 1976: Wave-CISK and cumulus parameterization. *J. Atmos. Sci., 33,* 2383–2391.

Stevens, D. E., R. S. Lindzen, and L. J. Shapiro, 1977: A new model of tropical waves incorporating momentum mixing by cumulus convection. *Dyn. Atmos. and Oceans, 1,* 365–425.

Stevens, D. E. and R. S. Lindzen, 1978: Tropical wave-CISK with a moisture budget and cumulus friction. *J. Atmos. Sci., 35,* 940–961.

3.2 CLOUD INTERACTIONS WITH OTHER CLIMATE ELEMENTS

REVIEW OF CLOUD INTERACTION WITH OTHER CLIMATE ELEMENTS

Peter J. Webster
Division of Atmospheric Physics
CSIRO
Australia

Summary

An attempt is made to assess the manner in which clouds interact with other elements of the climate of the earth system. It is shown that some observations hint at a strong relationship between cloud processes and the modification and redistribution of components of the total diabatic heating field. Such hints assume some consequence as variations in the diabatic heating distribution lead to the generation of eddy available potential energy which would imply a direct cloud–climate association.

Because of the difficulty in establishing control experiments, the observed relationships between clouds and dynamics may be circumstantial, especially with regard to their influence on the radiative heating component. It is argued that the development of physical and mathematical analogues of the climate system (i.e. models) are essential in order to overcome the observational shortcomings.

Two types of models are identified; open and closed loop models. Open-loop models usually possess few degrees of freedom and require the stipulation of a cloud structure, height, type and amount. Closed-loop models, on the other hand, develop their own cloud field by parameterization. Closed-loop models are usually substantially more complicated than the open-loop systems and generally appear less sensitive to cloud variations. Examples of the various sensitivities are presented in some detail and compared with a few observational studies which use satellite data.

1. Cloud Distributions

The distribution of cloud in the atmosphere possesses substantial temporal and spatial variability. Figure 1 shows the distribution of cloud in the tropical sector to the south of Asia during a five-day period of the Winter Monsoon Experiment in December 1978 (see Webster and Stephens, 1980). Not only is there a unique spatial variation, but there is substantial vertical structure. The predominant cloud species near the equator are the upper tropospheric extended clouds which are probably the cirrus canopies of convective systems. Away from the equator, low-level clouds predominate. The cloud distribution shown in Figure 1 changes in character from one five-day period to the next (Webster and Stephens, 1980) and from one season to the next. Even this region, which is the most persistent convective region on the earth, shows substantial *interannual* variability. The mean annual cloudiness fields for four successive years are shown in Figure 2.

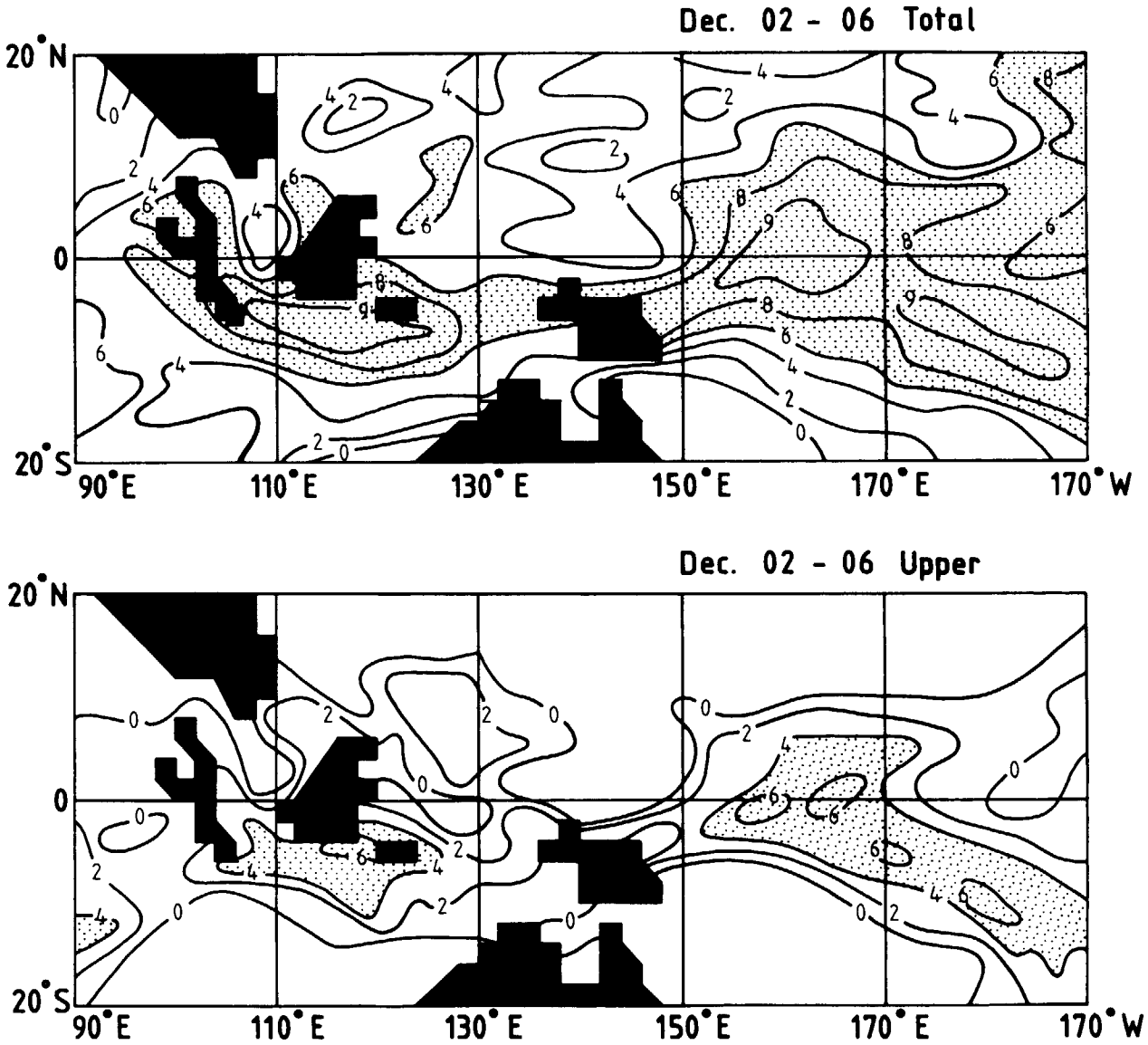

Figure 1. Five-day average cloudiness distributions for total (upper panel) and upper (lower panel) cloud. Shaded areas denote >0.6 total cloudiness or 0.4 upper level cloudiness. Period is 02-06 December and the data is from the GMS. Diagram from Webster and Stephens (1980). Cloudiness in tenths.

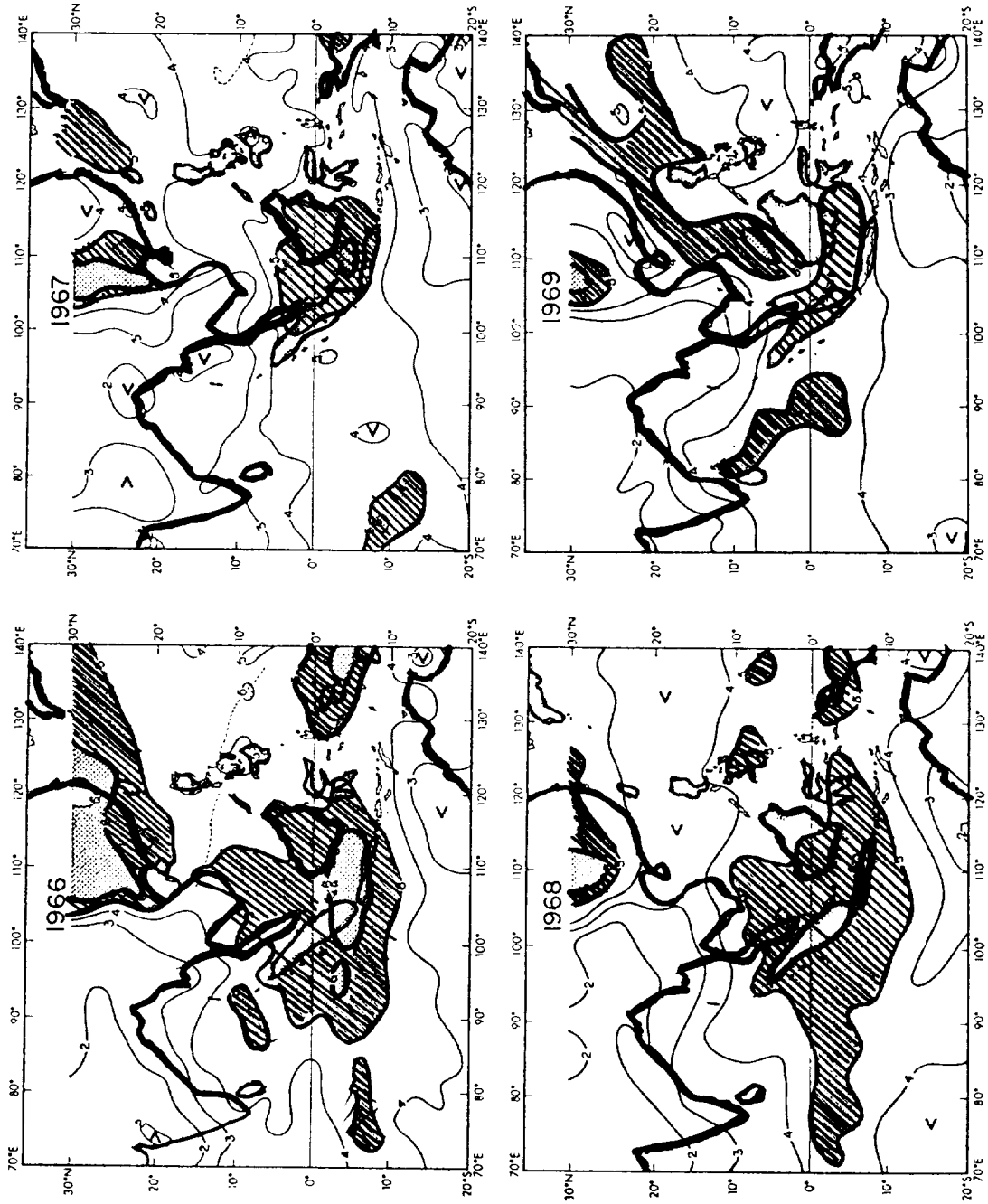

Figure 2. Annual average cloudiness for four years 1966–1969 over the South-east Asian region. Cloudiness in eighths. Cloudiness greater than five-eighths is hatched. Diagram from Sadler and Harris (1970).

The temporal and spatial variations of the mean cloudiness distributions do not appear to be merely random variations of a variable field. Some evidence does exist that the cloud variations are associated with distinct climatic events. An example is given in Figure 3 which shows the difference in sea surface temperature and mean cloudiness between a "normal" December in the eastern Pacific Ocean (1971) and the December of an El Nino year (1972). Significant cloud differences appear to exist between the two years which are well correlated with the anomalous sea surface temperature.

Many other examples are available showing the variability of cloudiness and their apparent association with climate events. However in all examples it is impossible to tell whether or not the cloud field is a passive climatic variable changing its distribution as a response to other climate variables, or whether clouds are a significant interactive parameter which enters into system feedbacks which alter the climatic state. The reason for this uncertainty is that it is difficult to construct meaningful controlled observational experiments to tackle the problem of cloud interaction. Because of this we are required to construct mathematical and physical analogues of the system.

2. Clouds and the Total Diabatic Heating Field

Clouds appear to be intrinsic features of processes associated with the modification and redistribution of the components of the total diabatic heating field of the atmosphere. Such associations are identifiable in the list of Arakawa (1975) which shows how clouds may effect climate. The basic processes of Arakawa are:

(i) The coupling of dynamic and hydrological processes through the release of latent heat and by evaporation, and by the redistribution of sensible and latent heat and momentum;

(ii) The coupling of radiative and dynamical-hydrological processes in the atmosphere through the reflection, absorption and emission of radiation;

(iii) The coupling of hydrological processes in the atmosphere and in the ground via precipitation, and;

(iv) The influencing of couplings between the atmosphere and the ground through the modification of radiation and the turbulent transfers through the surface.

Modifications and redistribution of the diabatic heating are apparent in all four processes. For example, (ii) describes the modification by cloud of the incoming and outgoing radiative stream whilst (iii) describes the manner in which the radiative heating enters the hydrology cycle by providing heat for evaporation tending to the eventual release of latent heat in cloud structures.

The need to understand the role clouds play in the maintenance and modification of the diabatic heating is essential because of the importance of the heating field to the generation of potential energy in the atmosphere.

The overall role of diabatic processes emerges from consideration of the global energy budget. If K represents the total kinetic energy of the system and P the available potential energy then we can write:

$$\frac{dK}{dt} = \{P.K\} - E$$

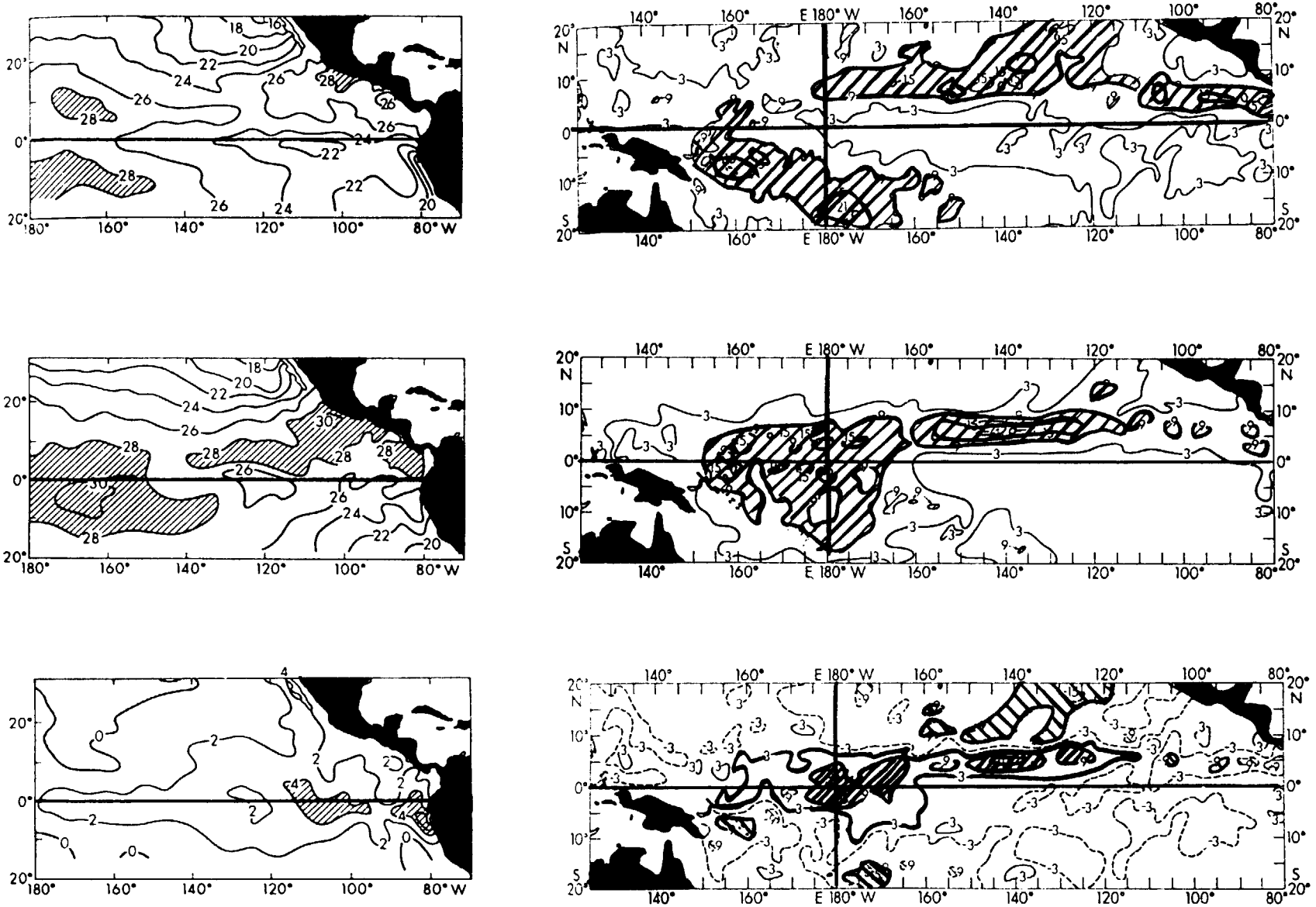

Figure 3. Mean December sea surface temperature and cloudiness for the two years 1971 (upper panel) and 1972 (lower panel). The differences of temperature and cloudiness between the two Decembers are shown in the lower panel. From Ramage (1975).

and

$$\frac{dP}{dt} = - \{P.K\} + G$$

so that the total energy equation of the system is given by:

$$\frac{d}{dt} (K + P) = G - E \qquad (1)$$

where G and E are the available potential energy generation and kinetic energy dissipation terms. For a quasi-geostrophic system G may be written as:

$$G = \int_v \frac{f_o^2}{\sigma} R \frac{\partial \psi}{\partial p} dv \qquad (2)$$

where f_o and σ are Coriolis and stability parameters, R the diabatic heating and $\partial\psi/\partial p$ is a measure of the temperature of the column. $\int dv$ indicates a volume integration. Eq. (1) states that the rate of change of the total energy is given by the difference between the generation of available potential energy due to the correlation of diabatic heating (R) and the temperature ($-\partial\psi/\partial p$) and the kinetic energy dissipation by surface friction. The implication of Eqs. (1) and (2) to climate research is obvious. If R is large then a sound knowledge of both G and E will be necessary in order to accommodate an adequate energy conservation.

The problem is underlined to some extent in Figure 4 which shows the vertical distribution of the zonally averaged heating rates attributable to transport mechanisms as a function of latitude. Calculations were made using data from Oort and Rasmussen (1971) and Newell et al. (1972) for the northern hemisphere summer (i.e. June–August). At all latitudes the radiative cooling to space

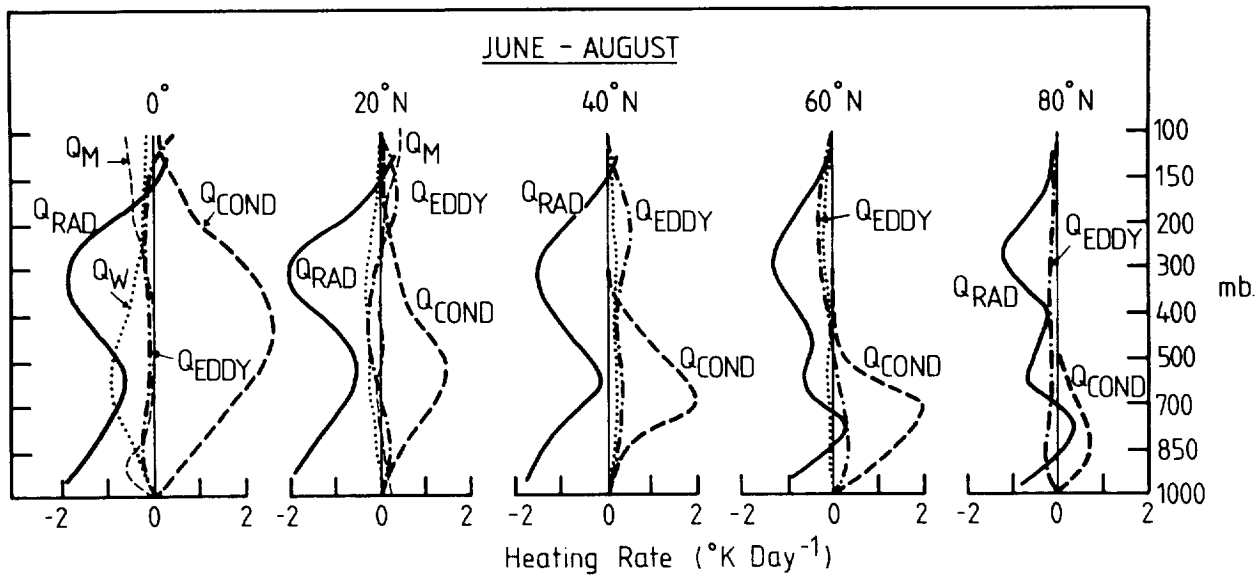

Figure 4. Vertical distribution of heating rates attributable to zonally averaged transport mechanisms of various latitudes in July. Q_{RAD}, Q_{COND}, Q_M and Q_{EDDY} refer to heating due to radiation, condensation, mean motion heat convergences and eddy heat convergences.

($\dot{Q}_{RAD}$) and/or the condensational heating are major processes. Dynamic transports appear as small residuals. The profiles suggest that both the radiative effects and the condensational heating must be well known in order to calculate the residual with some accuracy. What is not apparent from Figure 4 or from the data from which it evolved is the role clouds play in the establishment of the form or magnitude of the components of the diabatic heating fields.

The problem is compounded when the longitudinal or eddy structure of the diabatic heating is considered. If a zonal mean is defined ($^-$) and a deviation from that zonal mean ($'$) we may write down a mean available potential energy ($\bar{P}$) equation and an eddy available potential energy (P') equation. These are:

$$\frac{d\bar{P}}{dt} = -\{\bar{P}.P'\} - \{\bar{P}.\bar{K}\} + \underline{\{\bar{R}.\bar{P}\}} \tag{3}$$

and

$$\frac{dP'}{dt} = \{\bar{P}.P'\} - \{P'.K'\} - \underline{\{P'.R'\}} \tag{4}$$

The first two terms on the right-hand sides of Eqs. (3) and (4) refer to the energy conversions between the indicated energy forms. For our discussion the most important terms are underlined and refer to (respectively) the generation of mean zonal available potential energy and of eddy zonal available potential energy. The two terms are defined as:

$$\{\bar{R}.\bar{P}\} = -\int_v \frac{f_o^2}{\sigma} \bar{R} \frac{\partial \bar{\psi}}{\partial p} \, dv \tag{5}$$

and

$$\{R'.P'\} = \int_v \frac{f_o^2}{\sigma} R' \frac{\partial \psi'}{\partial p} \, dv \tag{6}$$

Eq. (5) simply states that $\bar{P}$ is generated if mean zonally averaged diabatic heating correlates positively with the zonal mean temperature. As the net diabatic heating *abundance* occurs in the *warm* equatorial regions (i.e. latent, sensible and radiative effects) and the diabatic *deficit* occurs in the *cool* higher latitudes, then $\{\bar{R}.\bar{P}\}$ is positive. In a similar manner if eddy heating correlates with longitudinal variations in temperature then P' is generated (i.e. $-\{P'.R'\} < 0$). Oort and Rasmussen (1971) estimate by residual methods that $\{P'.R'\}$ is roughly 25% of $\{\bar{R}.\bar{P}\}$ in magnitude and 25% of either $\{\bar{P}.P'\}$ or $\{P'.K'\}$. Consequently the term is important from large-scale energetic considerations.

Figure 5 shows a partial representation of energy transports and heating rates for three locations (I, the arid regions of Saudi Arabia, II, the Arabian Sea and III, the Bay of Bengal). Radiational cooling is important at all the three adjacent locations but with a variation of form from the relatively dry and cloudless Arabian region to the moist, convective and cloudy Bay of Bengal.

Convective heating is a maximum in the Bay of Bengal column and radiative cooling over the Arabian desert region. Large local imbalances between the radiational and condensational heating are apparent and the compensatory (longitudinal and latitudinal) dynamic transports are considerably larger than evident in Figure 4. What emerges are strong zonal and meridional transports ($\dot{Q}_M$(N-S) and $\dot{Q}_M$(E-W)) or, in other words, vigorous thermally forced dynamic modes.

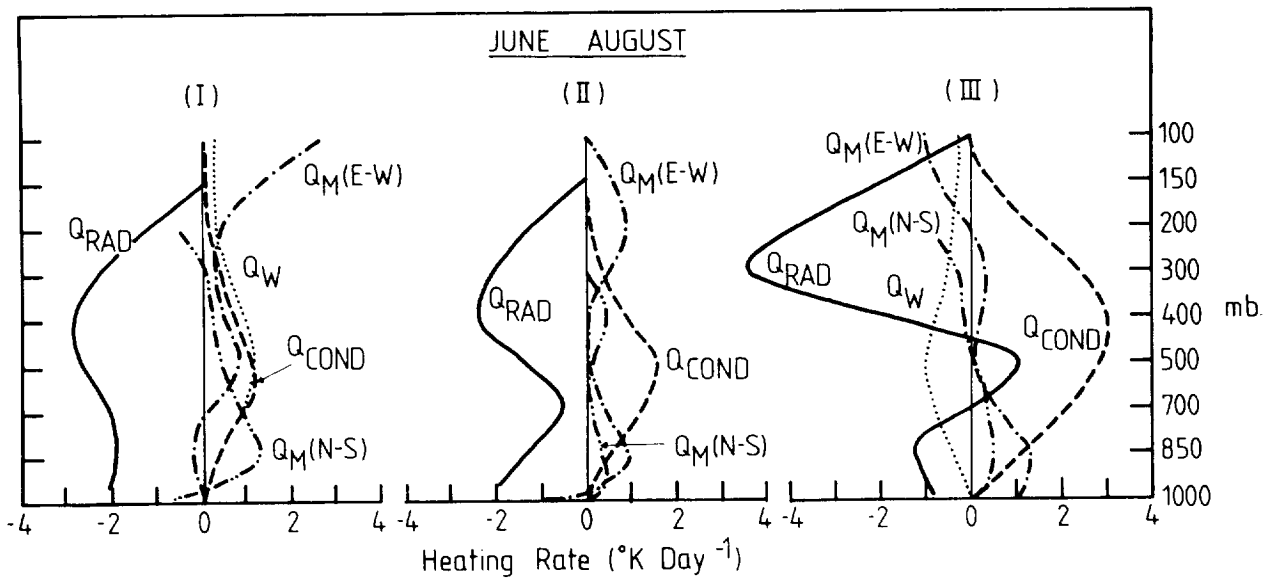

Figure 5. Same as Figure 1 for heating rates along 25°N in July. Q_{RAD} and Q_{COND} Q_M(E-W) and Q_M(N-S) refer to heat convergences by zonal mean motions and meridional mean motion. Locations I, II, and III, refer to Saudi Arabia, the Arabian Sea and the Bay of Bengal.

The longitudinal variation of the radiative diabatic heating component is shown in Figure 6 where the distribution of net radiative flux (positive into the atmosphere) at the top of the atmosphere using NIMBUS III data for July 1969 is plotted. The desert regions on the latitudinal section (small dashed curve) between 0°E and 180°E (upper abscissa scale) appears as net radiative heating sinks whereas the active convective region (80°E – 180°E) appear as net radiative heating sources. Most importantly, however, is that Figure 6 illustrates that the longitudinal gradient of the net radiation is *equal* in magnitude to the latitudinal gradient. That is, it is not sufficient to consider that the radiation heating field is merely a function of latitude.

Figures 4–6 indicate an important point. The total diabatic heating of a column is made up of large compensatory components. The residual heatings are responsible for the generation of eddy available potential energy (as shown in 3 and 4) which, ultimately, will determine the phase and amplitude of the long quasi-stationary climatic features of the atmosphere. It becomes an essential point to determine how sensitive the observed profiles of heating are to variations in cloudiness. Such knowledge serves the purpose of setting some of the important bounds on the required complexity of climate models.

3. Model Types for Estimating Cloud–Climate Sensitivities

We may express a climate system in the following manner:

$$L = L(X) = L(X_1, X_2, \ldots; C, \ldots) \tag{7}$$

where

$$C = C(L, X) = C(L, X_1, X_2 \ldots) \tag{8}$$

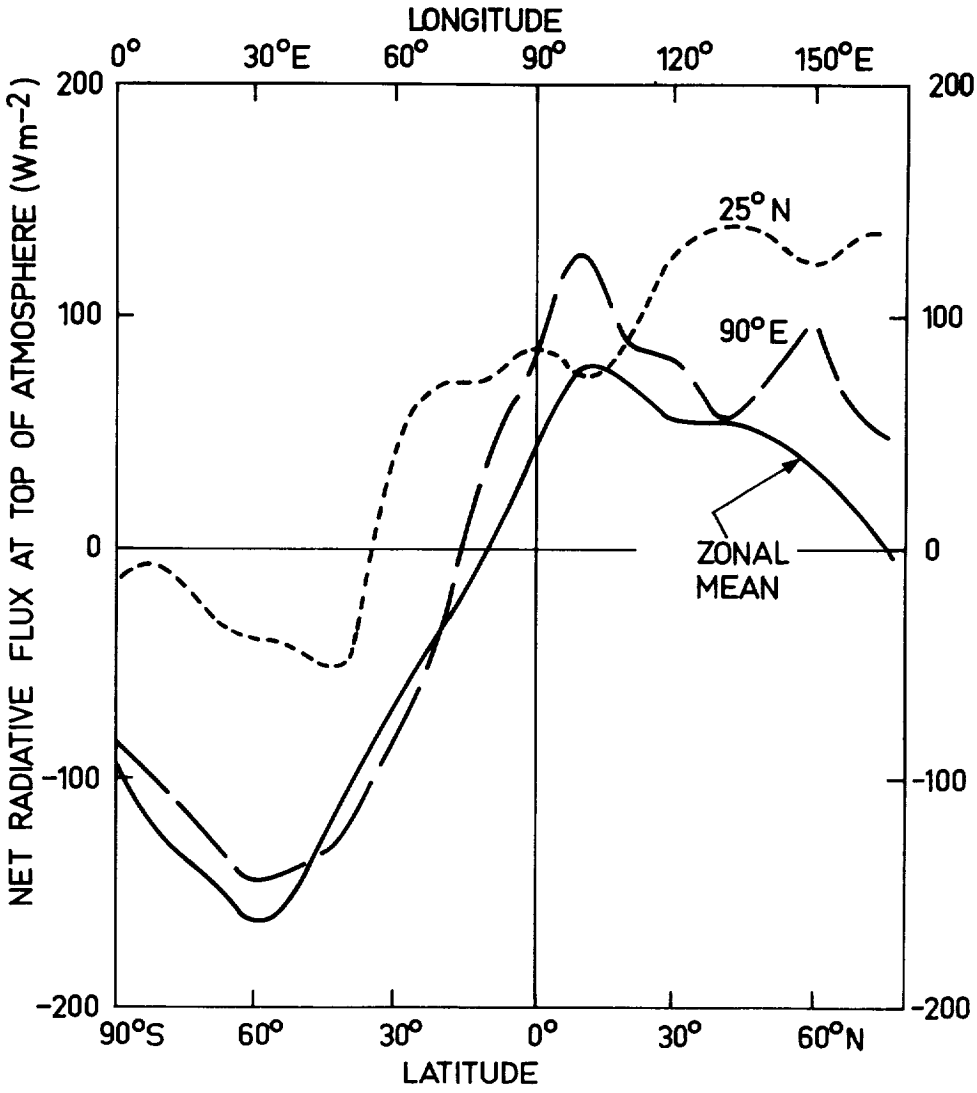

Figure 6. Net radiative flux at the top of the atmosphere as determined by NIMBUS 3 in July 1969. Shown are the pole-to-pole sections along 90°E, the zonal mean and a *latitudinal* section along 25°N between 0°E and 180°E. Net flux is positive into the atmosphere (from Stephens and Webster, 1979).

In this non-linear system, L describes a family of climate variables which depend on X_i, one of which is the cloudiness of the atmosphere, C. In a fully interactive system C may also be a function of L_i and X_i.

Models which are used to study the sensitivity of the climate system to variations in cloud amount, height or composition fall into two main groups. The first group is comprised of models in which the climate-cloud feedback is left open. That is, C in Eq. (7) is constant and in Eq. (8) $C \neq C(L,X)$. That is, changes to the climate system which are produced by a change in a cloudiness specification

are not allowed to feed-back into the cloud structure. The second group of models allow the climate system to be fully coupled as described by Eqs. (7) and (8). These are referred to as the closed-loop models. Figure 7 shows a schematic of both model groups.

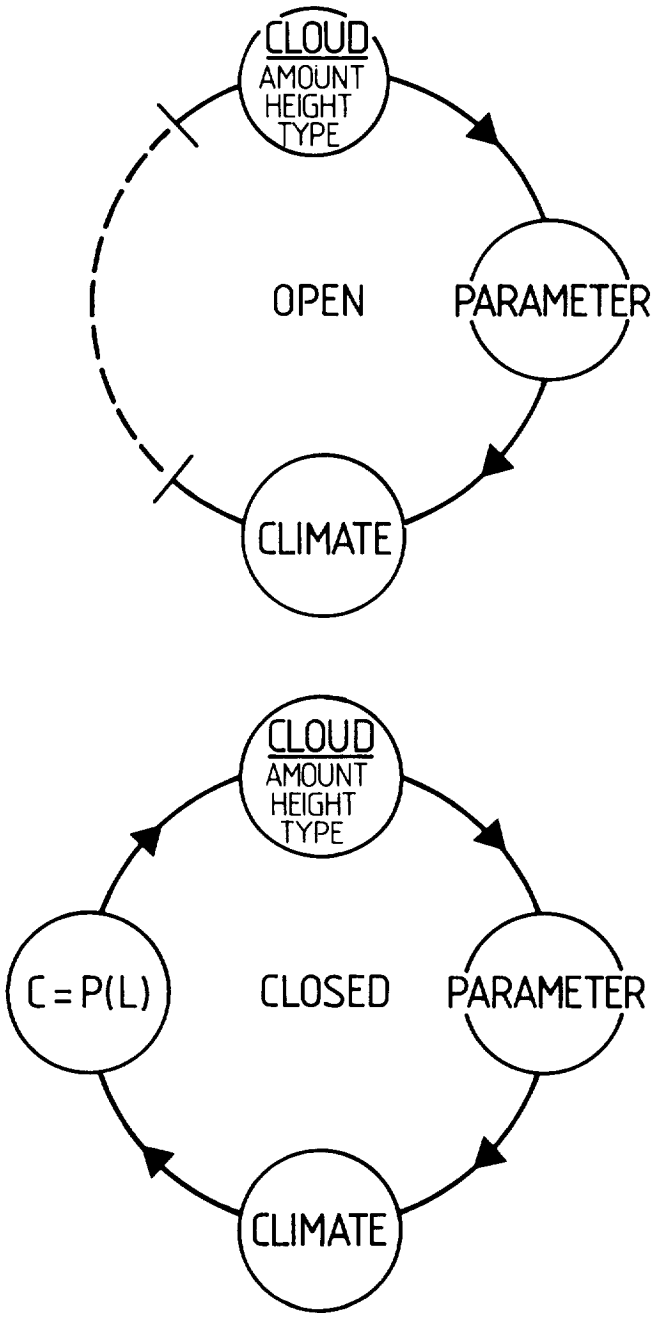

Figure 7. Schematic representation of open-loop models and closed-loop models.

There are a number of model types which make up the two groups. These may be summarized as follows:

(1) 1 parameter energy balance models. The one parameter is normally surface temperature. All atmospheric structure is expressed as a form of the surface temperature. Basic physics involve surface energy balance and horizontal heat diffusion.

(2) (a) 1 parameter radiative-convective models. The parameter is the vertically-dependent atmospheric temperature (including surface temperature). A dynamic correction may be applied. Temperature profile is corrected to ensure convective stability in the vertical.

(b) Radiative-convective models with simple 1 dimensional ocean.

(3) Multi-parameter radiative-dynamic models: These are usually multi-dimensional, contain full dynamics and (occasionally) an interactive ocean.

Generally the open-loop group of models is comprised of types (1) and (2) and the closed-loop group with the type (3). However Hunt (1978) performed a cloud sensitivity experiment with a type (3) model in which clouds were specified invariant features.

The open-loop model group possesses the following attributes:

(i) Although it is not necessary, the open-loop models are usually of low degrees of freedom. This simplicity allows the possibility of a fine grid resolution, especially in the vertical. The simplicity of the model renders the results relatively easy to understand.

(ii) An extremely detailed cloud parameterization may be attached to the fine grid resolution. The amount of cloud, the cloud height and their optical properties may be carefully specified.

(iii) The open-loop model allows careful controlled experimentation.

However, open-loop studies have the following drawbacks:

(i) The very simplicity of the model makes it difficult to compare the model results with the real climate.

(ii) As the climate-cloud feedback loop is left open the results may be interpreted, at best, as the initial tendencies of the real climate system to the change in a particular cloud property. Because of this, open-loop models tend to be considerably more sensitive than closed-loop models.

(iii) It is probably impossible to develop parallel observational studies with open-loop models.

The closed-loop model group possesses a number of attractive features. These are:

(i) The physical complexity of the parent climate model allows a greater confidence in the similitude between the model and the real climate system.

(ii) The estimate of the system sensitivity to cloudiness is beyond the initial tendency of the system. That is, secondary adjustments are allowed to take place.

(iii) Similarities between the model and the real climate system allow comparisons between observational studies and the model climate.

But, on the negative side;

(i) Because of the physical complexity of the model the grid resolution of the system is rather coarse. Consequently there is a model limitation on cloud detail. This appears to be particularly critical in determining the cloud height.

(ii) The success of climate simulation depends on how well clouds are parameterized. Generally this is achieved by a simple one parameter scheme involving the relative humidity with an allowance for atmospheric stability. In an unstable atmosphere convective penetration is often allowed.

(iii) There are a number of ways to interpret climate sensitivity. Do the model results imply a real climate sensitivity or a parameterization sensitivity?

4. Open-Loop Model Studies

A fairly large literature exists on closed-loop studies. We will utilize a series of studies [Stephens and Webster (1979, 1980) and Webster and Stephens (1980a, 1980b)] to illustrate system sensitivities to variations in cloudiness. We emphasize these studies because the same cloud and radiation models were used throughout. This consistency of parameterization facilitates simpler comparisons.

Figure 8 shows the cloud albedo-cloud effective emissivity relationships used in the three studies. The albedo and emittance are plotted as functions of liquid water path allowing the expression of both the long-wave and short-wave optical properties of the clouds as functions of one parameter. The parameterization originates in the study of Stephens (1978). Along the upper abscissa are the ranges of liquid water path which the various clouds possess. The essential feature of the parameterization is that the clouds become optically black at much lower values of liquid water path than when the cloud asymptotes to maximum albedo. This disparity between the long-wave and short-wave properties of a cloud result in high thin clouds being relative warmers of the surface whereas other thicker clouds tend to be net coolers.

Figure 9 shows the variation of the net radiative flux in an atmospheric column between totally covered and clear skies as a function of latitude for three cloud species. The figure is from Webster and Stephens (1980a) and the results were obtained using the static radiative transfer model of Stephens and Webster (1979). The static model, the first open-loop model used in the series of studies, sought the radiative structure of the atmosphere which was consistent with a set temperature profile and a specified cloud distribution. In this case the temperature structure was varied from the mean tropical atmosphere to the mean arctic atmosphere and the equilibrium structure flux sought for each cloud layer. At low latitude the greatest change in the radiative structure of the atmosphere is brought about by middle and high clouds. Returning to Figure 1 it will be remembered that the predominant cloud form at low latitudes was the upper tropospheric extended cloud decks. If this simple radiative model can be believed, it would appear that the radiative structure of the tropical atmosphere is considerably dependent on its cloud form.

It is possible to use the Stephens-Webster static model to gauge the role of clouds in determining the *longitudinal* variation of radiative structure noted in Figures 5 and 6. Mean temperature and moisture profiles and surface albedos were used to represent the Saudi Arabia, Arabian Sea and Bay

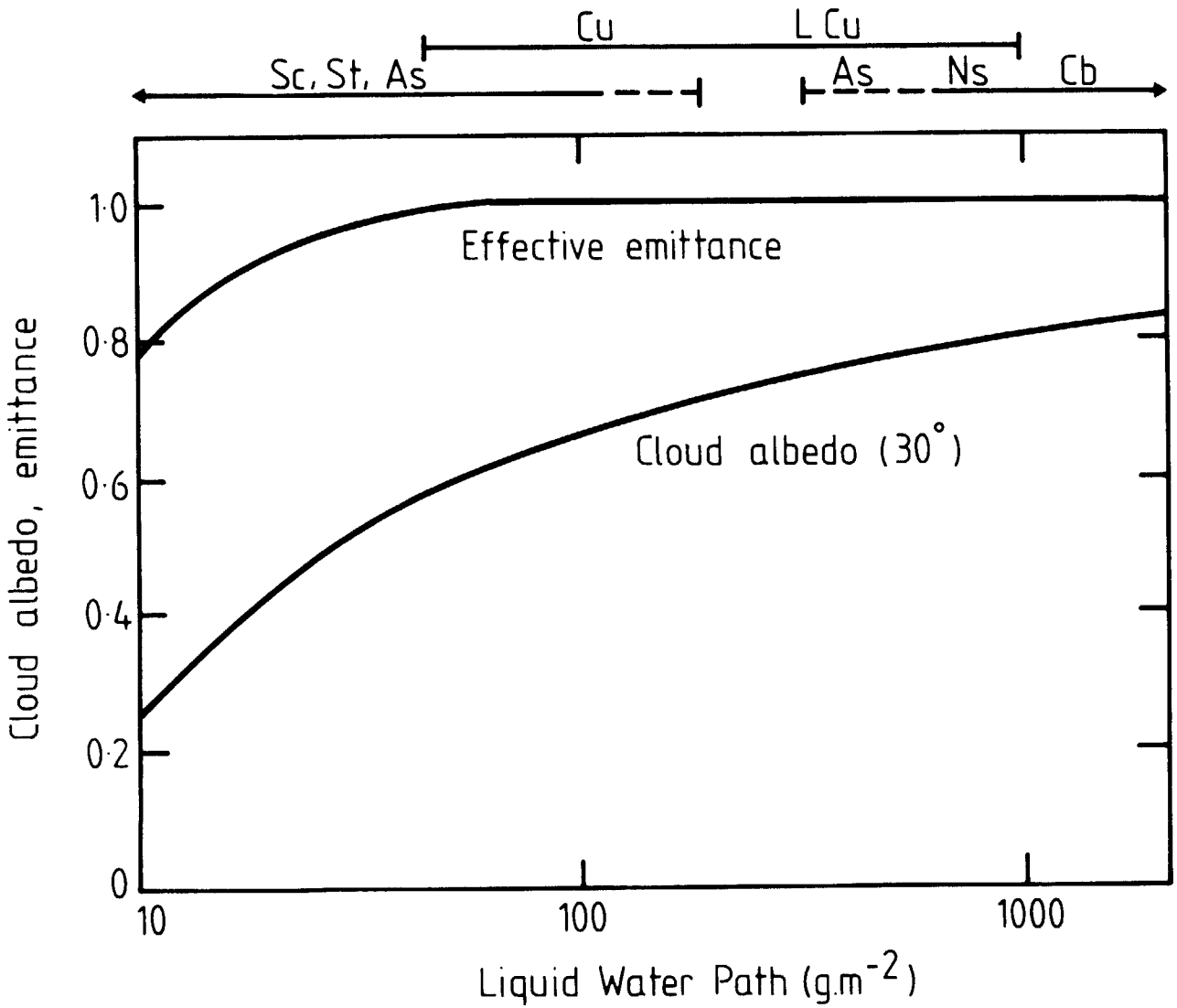

Figure 8. Albedo and effective emissivity relationships as a function of liquid water path (gm^{-2}). Curves represent the basic cloud optical property parameterization of Stephens (1978).

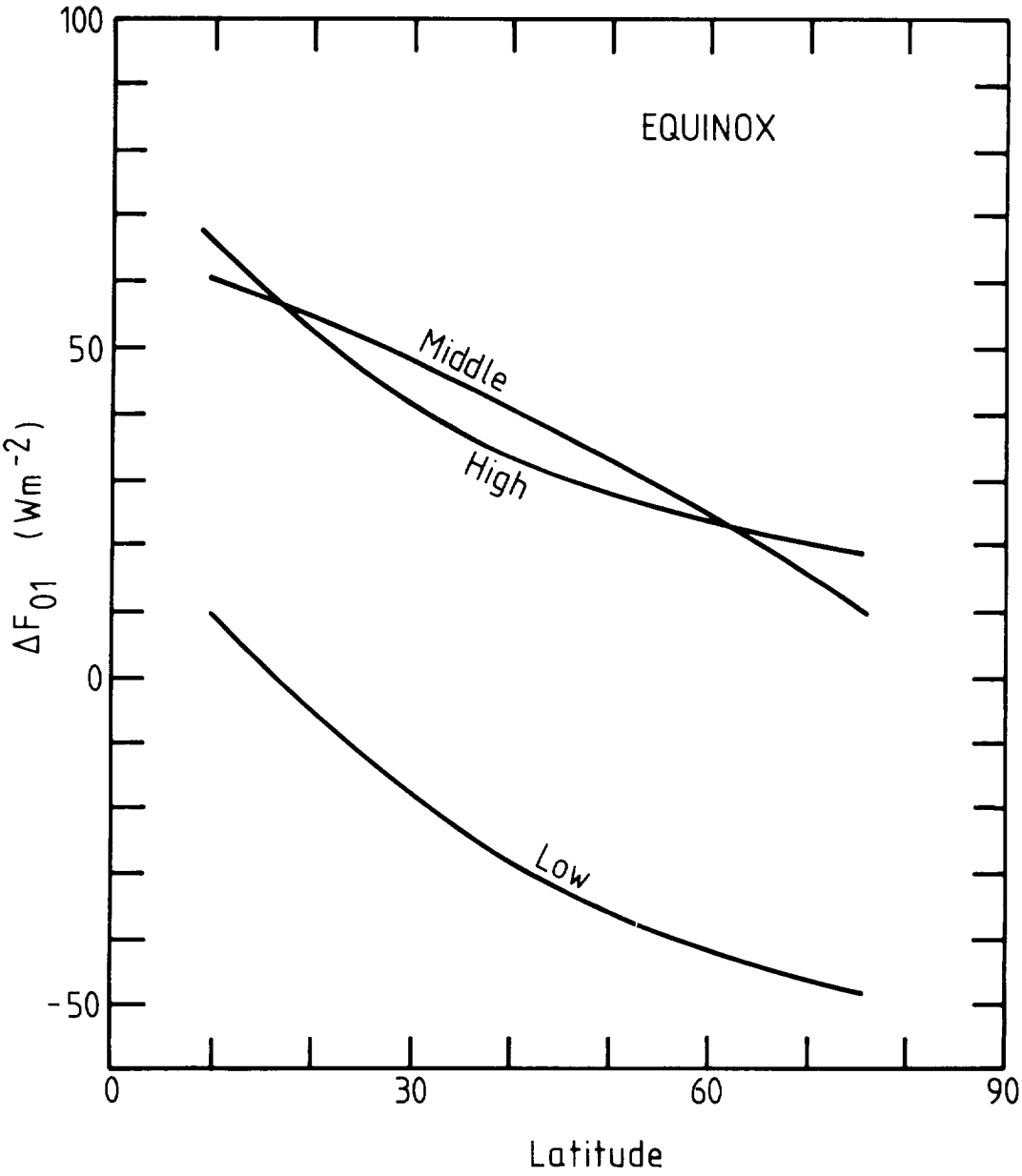

Figure 9. Variation of net radiative flux in an atmospheric column between totally covered and clear skies as a function of latitude for three cloud species (see Webster and Stephens, 1980).

of Bengal conditions. The results are shown in Figure 10 for three cloud structure scenarios. These were no cloud (curve a, Figure 10), zonally averaged cloud (curve c) and "variable" cloud (curve b) where longitudinally varying mean values were used. Curve c of Figure 10 compares quite well with the 25°N curve of Figure 6. Comparison with curves a and b suggests a poorer fit. The implication is that it is not only necessary to provide the variation of water vapor and temperature with longitude but also the longitudinal variation of cloud amount in order to model the radiative heating of the atmosphere in an adequate manner.

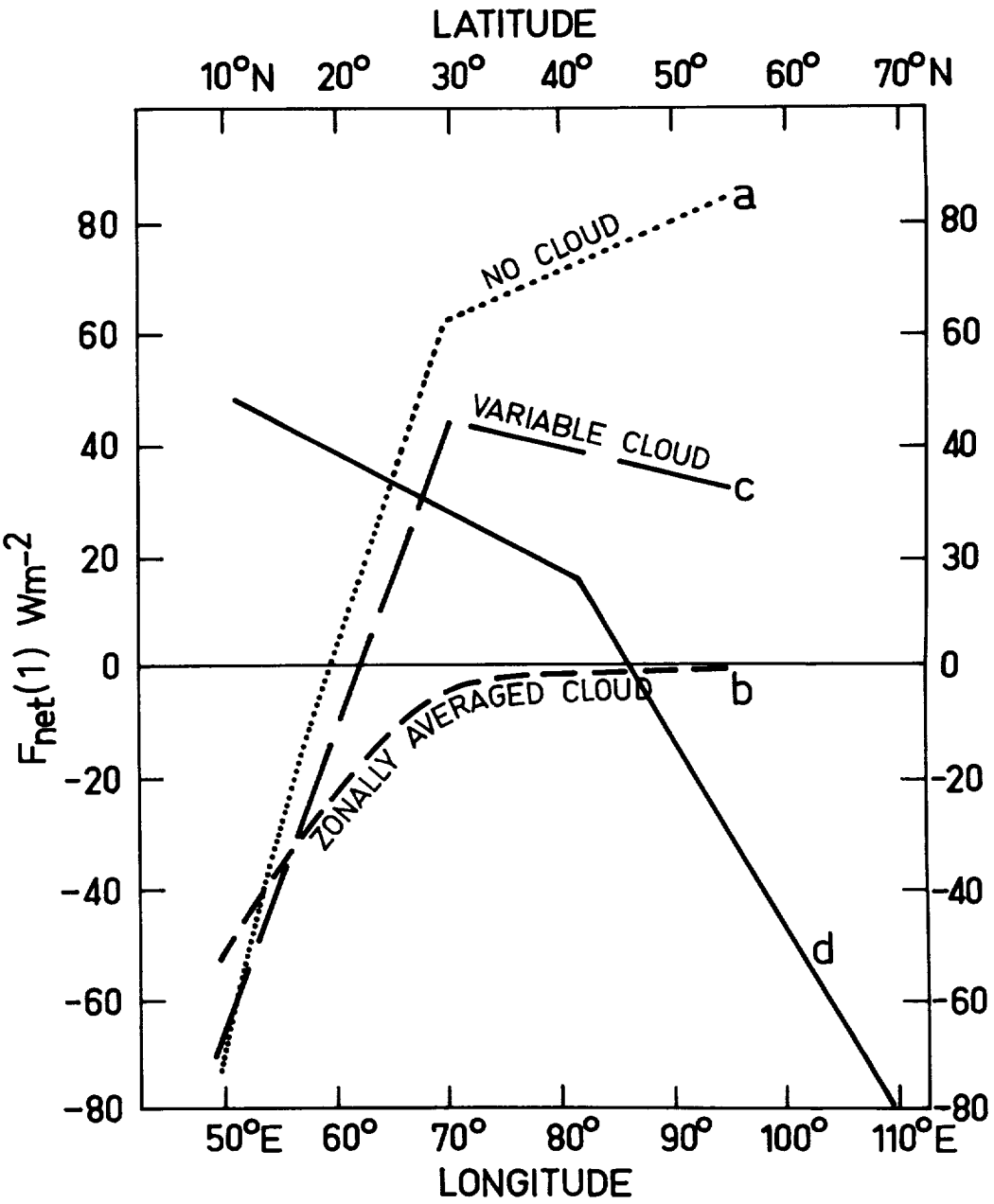

Figure 10. The net radiative flux directed into the top of the atmospheric column along latitude line 25°N between longitudes 50°E to 110°E for the cases of no cloud (dotted line), a zonally average cloud amount (dashed line) and variable cloud (broken line). Stephens and Webster (1979).

In summary, the static radiative transfer model of Stephens and Webster (1979) implies a significant sensitivity of the radiative heating component of the diabatic heating. To test other sensitivities we require a slightly more complicated model; in this case a radiative-convective model.

In developing a radiative convective adjustment model, Stephens and Webster (1980) removed the constraint of the static radiative model of a fixed thermodynamic state. The model differed slightly from other radiative convective adjustment models in that a climatological dynamic heating correction is made to allow for horizontal eddy transports. The equilibrium profiles of T(z) for clear skies with and without the climatological dynamic heating input are shown in Figure 11. 35°N winter insolation values were used.

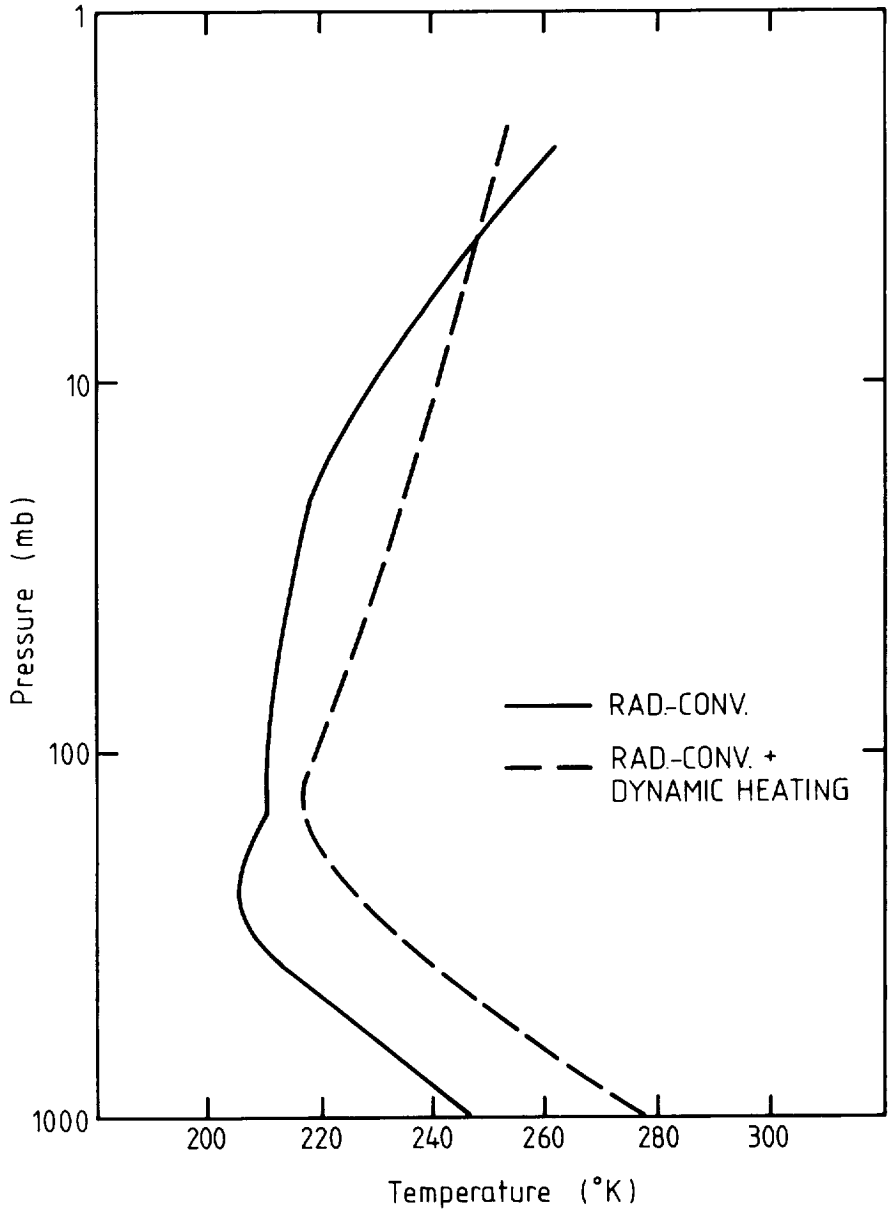

Figure 11. Equilibrium temperature profile for 35°N in January calculated using the one dimensional radiative convective model (solid line). Modified profile which includes dynamic sensible heat convergence is shown as the dashed curve. From Stephens and Webster (1980).

The radiative convective model was used to test the sensitivity of a number of climate factors to cloudiness. Unless otherwise specified, low clouds are constrained to be between the 913 and the 854 mb levels, middle clouds between 632 and 549 mb and high clouds between 381 and 301 mb. In interpreting the results it must be remembered that the only *interactive* dynamics which are allowable in this model are convective overturnings necessary to insist on gravitational stability.

(i) *Sensitivity to Cloud Amount:* The variation of surface temperature for two insolation values (January and July at 35°N) and three cloud species are shown in Figure 12. Each species shows a different gradient of temperature with respect to change in cloud amount. Middle and low clouds tend to decrease the surface temperature as cloud amount is increased whereas high clouds show the opposite trend. The reason for the difference may be seen in Figure 8. The middle and low cloud

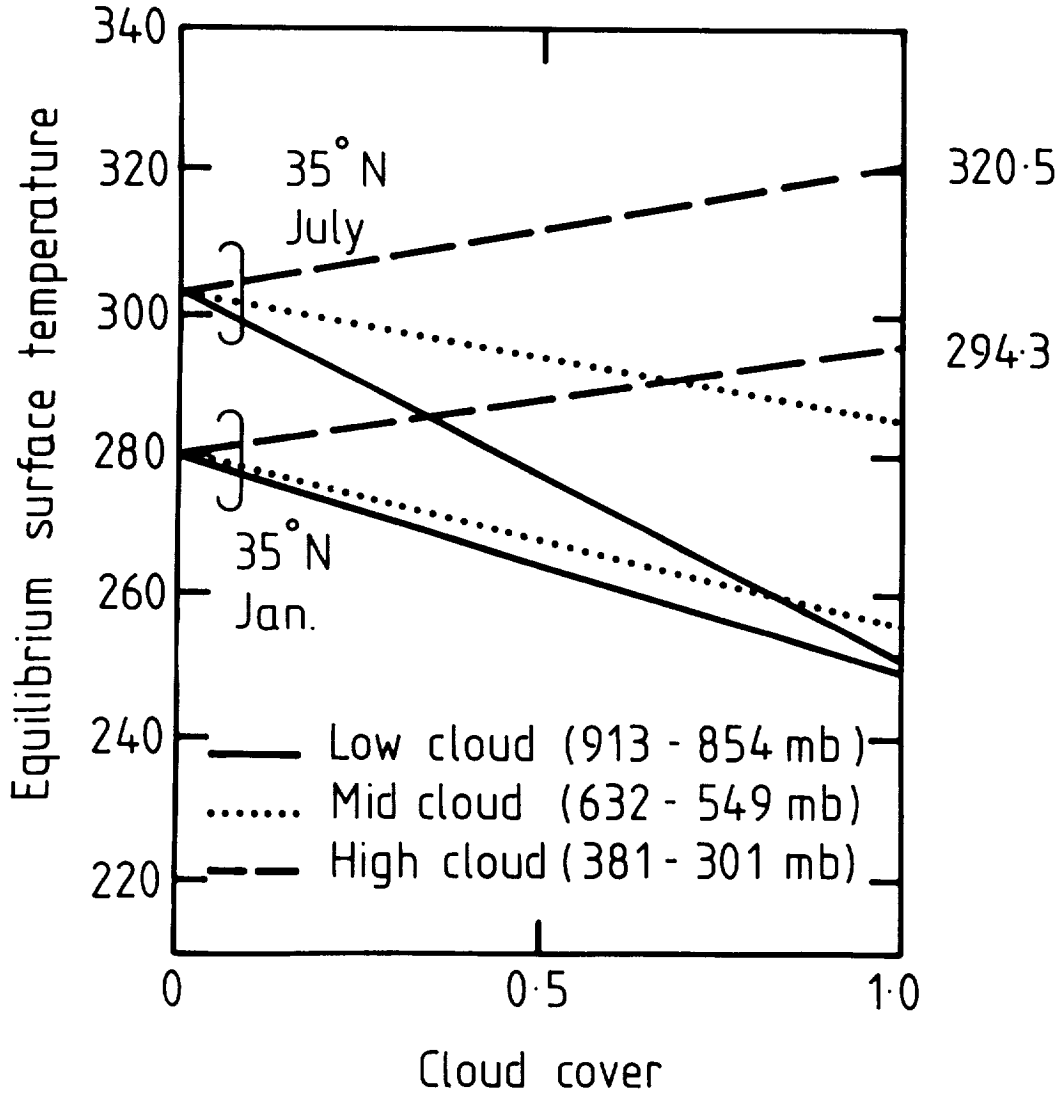

Figure 12. Equilibrium surface temperature distribution as a function of cloud amount for three cloud layers using summer and winter solstice conditions at 35°N.

values possess liquid water paths which are greater than 100 gm^{-2} which typifies an emissivity of unity and a high albedo. The high clouds have liquid water paths of <15 gm^{-2} which corresponds to a reduction in cloud albedo by a factor of four but an emissivity reduction of only 20%. Thus in the case of low and middle clouds the albedo effects dominate over the emissivity effects and the net energy input to the surface is decreased as cloud amount is increased. However with the high clouds the emissivity effect dominates and only a small percentage of the incident solar stream is reflected. Consequently, an increase in high cloud amount tends to raise the surface temperature.

(ii) *Sensitivity to Cloud Property:* The change in surface temperature due to low and high cloud of various cloud albedo and emittance values (or by Figure 8, by liquid water paths) is shown in Figure 13. In the diagram isopleths of surface temperature change induced by an overcast cloud are plotted as functions of cloud albedo and cloud emittance. Regions of strong cooling and heating are apparent. The solid curves are merely alternative representations of the emittance-albedo relationship seen earlier in Figure 8.

(iii) *Sensitivity to Cloud Height:* Figure 14 shows the variation of surface temperature for an overcast sky induced by the change in cloud height. Generally, for a given liquid or ice water path, the

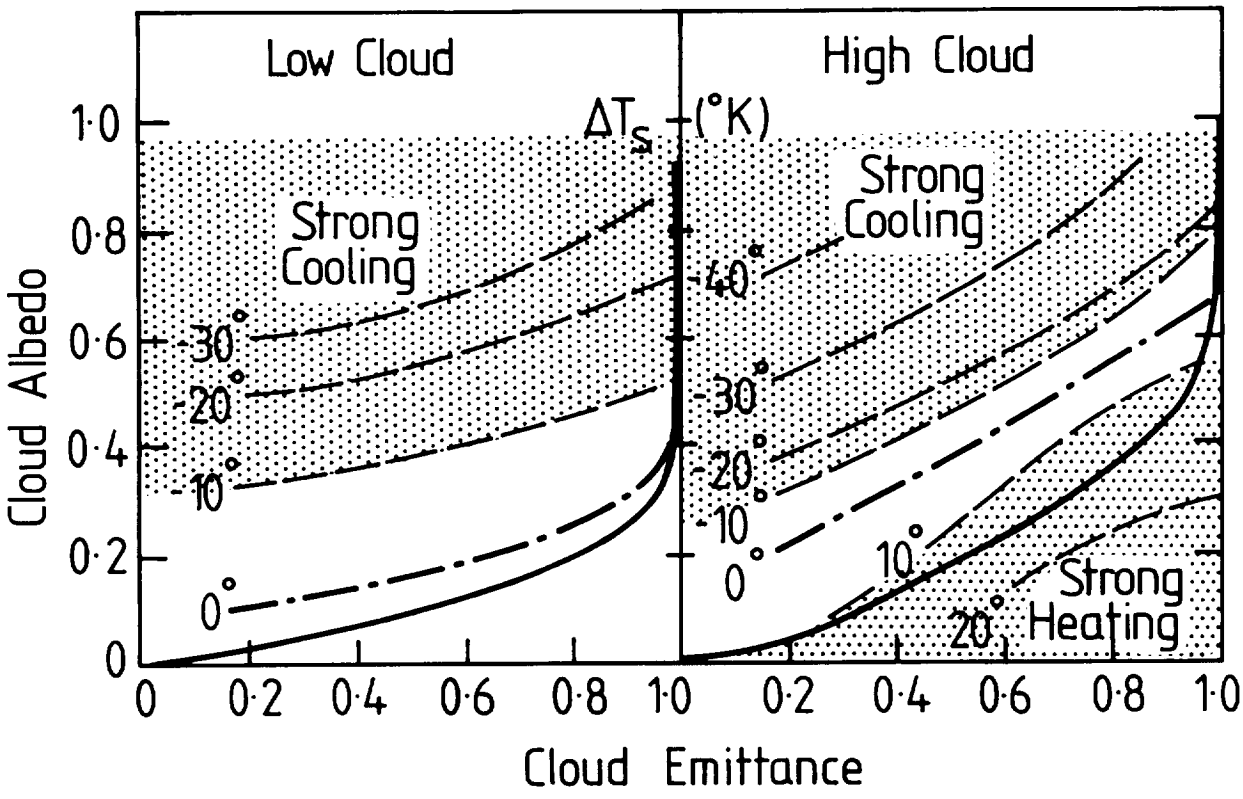

Figure 13. Surface temperature differences between clear and overcast low and high cloud as a function of cloud albedo and emissivity. Stippled region indicates strong heating or cooling. Solid line indicates the albedo emittance relationship of Figure 8.

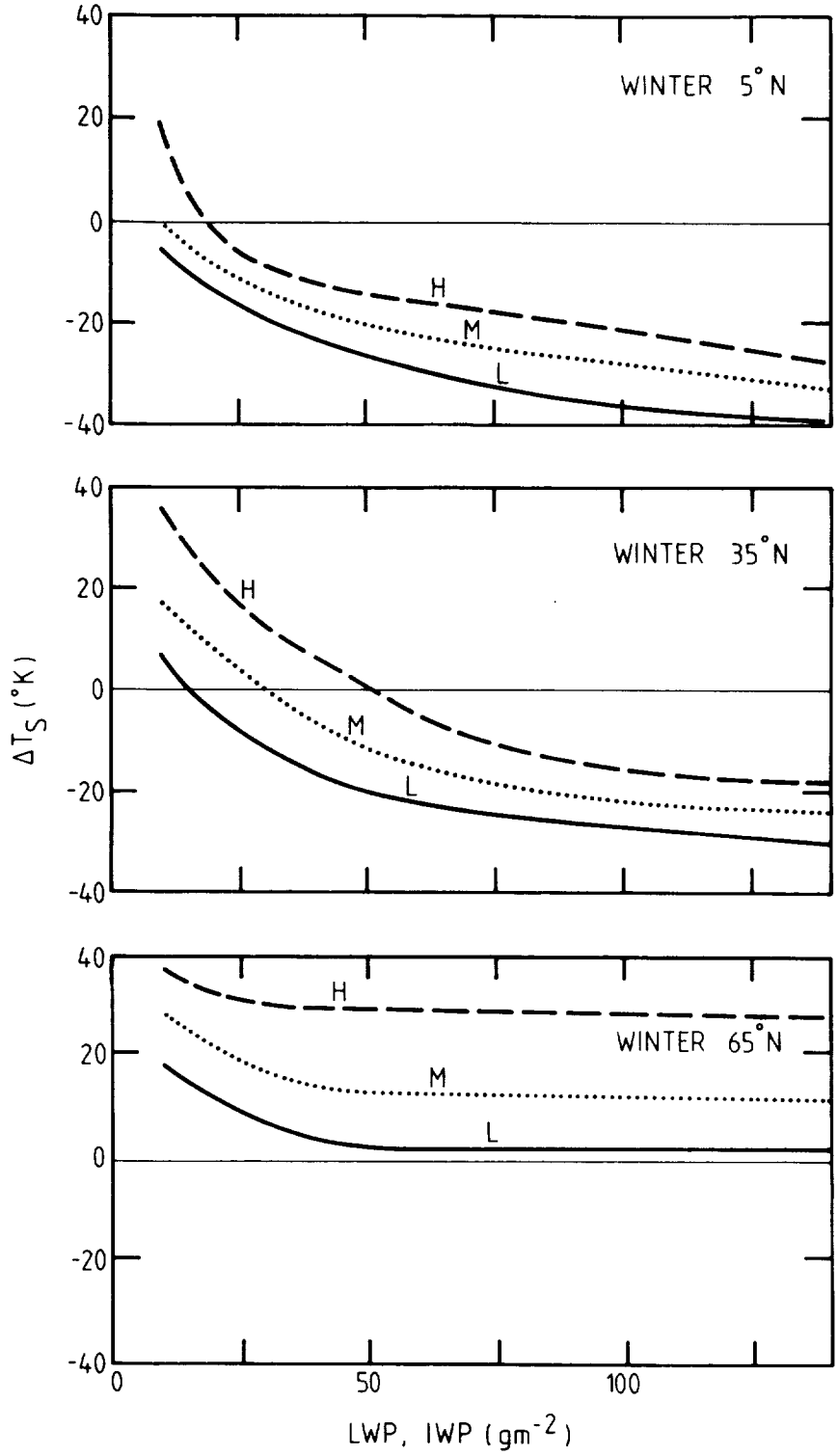

Figure 14. Surface temperature difference between clear and overcast conditions as a function of water or ice-water path (gm^{-2}) for three cloud layers. Results are shown for 5°N, 35°N and 65°N in winter with a surface albedo of 0.102. Stephens and Webster (1980).

effect of an increase in the cloud height is to decrease the cooling effect of the cloud or increase the warming effect. The reason for this is rather simple. Except for slightly different absorption profiles, the short-wave effect of the clouds is much the same irrespective of height. However, as the cloud top assumes the ambient temperature of the atmosphere, the radiative loss to space by the system is reduced as the cloud top is raised.

(iv) *Cloud-radiation Surface Albedo Sensitivities:* In a cloud-free atmosphere the effect of surface albedo on surface temperature is dramatic; increases cause a substantial cooling at the surface. However when clouds are included in the system, the effect is changed considerably.

Figure 15 shows the difference in equilibrium surface temperature between a clear and overcast sky of the indicated cloud type as a function of surface albedo. Because of the albedo effect, a cloud with a specified liquid water path (and therefore albedo and emittance) *can change from being a net cooler to being a net warmer of the surface.* For example, at 35°N middle and low level clouds of 140 gm^{-2} are usually net surface coolers. However with surface albedoes greater than about 0.5 the clouds tend to warm the surface. This is important because these surface albedos are in the range observed over continental regions in winter. The effect probably has palaeoclimatological implications. Stephens and Webster (1980) develop analytic expressions for the critical albedo.

(v) *Clouds and Atmospheric Sensitivity to Composition Changes:* The effect of doubling the atmospheric CO_2 concentration on the equilibrium temperature profile of a radiative convective atmosphere is shown in Figure 16 for a cloudless atmosphere. The results show little difference to the Manabe and Wetherald (1967) experiments with a tropospheric temperature increase of about 2.5°K and a stratospheric cooling of about twice that amount. The temperature increase results from enhanced CO_2-H_2O emission in the stratosphere.

With the introduction of cloud the heating and cooling distributions change (Webster and Stephens, 1980b). Figure 17 plots of the difference in the vertical profiles of equilibrium temperature between the two CO_2 concentrations for the clear case and for various cloud species. The clear case plot is merely a different expression of Figure 16. Generally above the cloud layer the temperature changes are similar to that of the clear case but in the sub-cloud layer the temperature changes are significantly smaller. In fact, tropospheric surface temperature changes have decreased from about 2.6°K in the clear atmosphere to about 0.5 to 1.0°C for optically thick clouds and to even smaller values for high thin clouds. It appears that the effect of cloud is to *reduce* the sensitivity of the lower part of the model atmosphere to CO_2 effects. The physical mechanism which accomplishes the reduction is the effective partitioning of the stratosphere and the troposphere by the cloud layer. With the enhanced stratospheric IR emission impeded by the cloud layer, the surface temperature will only increase by an amount which is determined by increased IR emission originating in the *sub-cloud layer.*

The various surface temperature sensitivities discussed in the preceding paragraphs are summarized in Table I. Sensitivities are expressed as the surface temperature change (°K) which would be produced by a 1% change in some parameter. The table indicates the fact that the model climate appears most sensitive to cloud amount changes. In fact a 5% decrease in cloudiness would be equivalent to a 1% change in solar constant. Likewise the temperature increase produced by the doubling

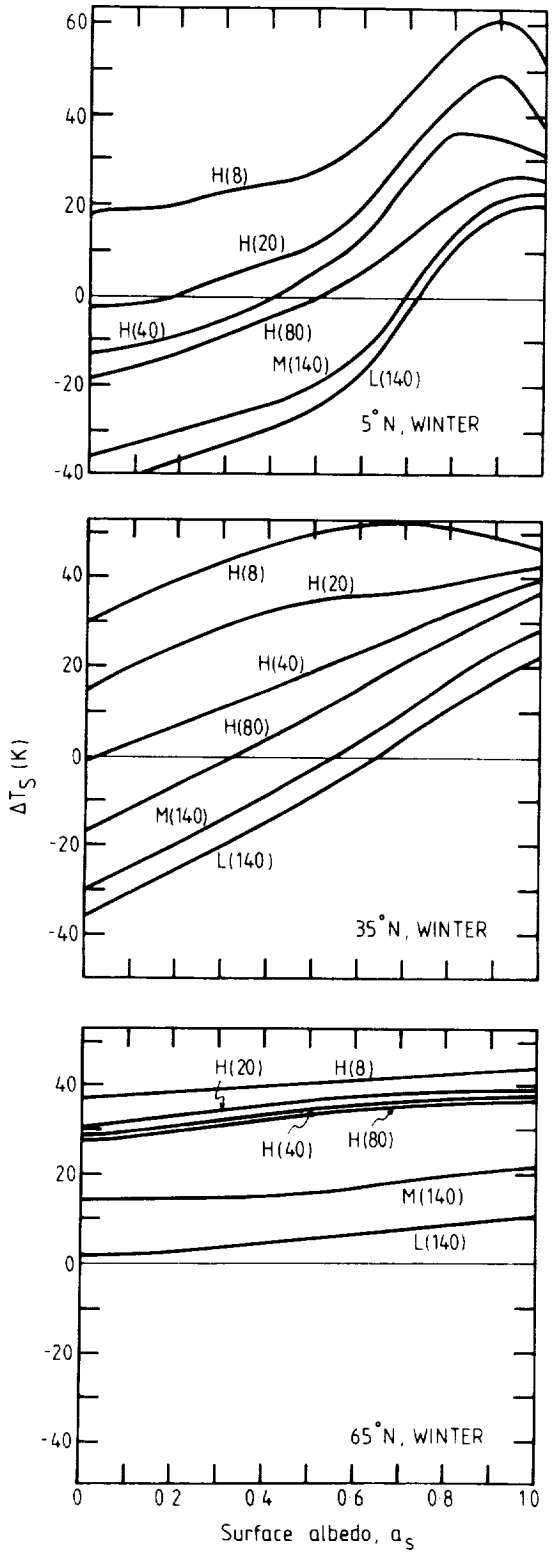

Figure 15. Surface temperature difference between clear and overcast sky conditions as a function of surface albedo. Results are for 5°N, 35°N and 65°N. Parentheses enclose liquid water path value of low (L), middle (M) and high (H) cloud. Stephens and Webster (1980).

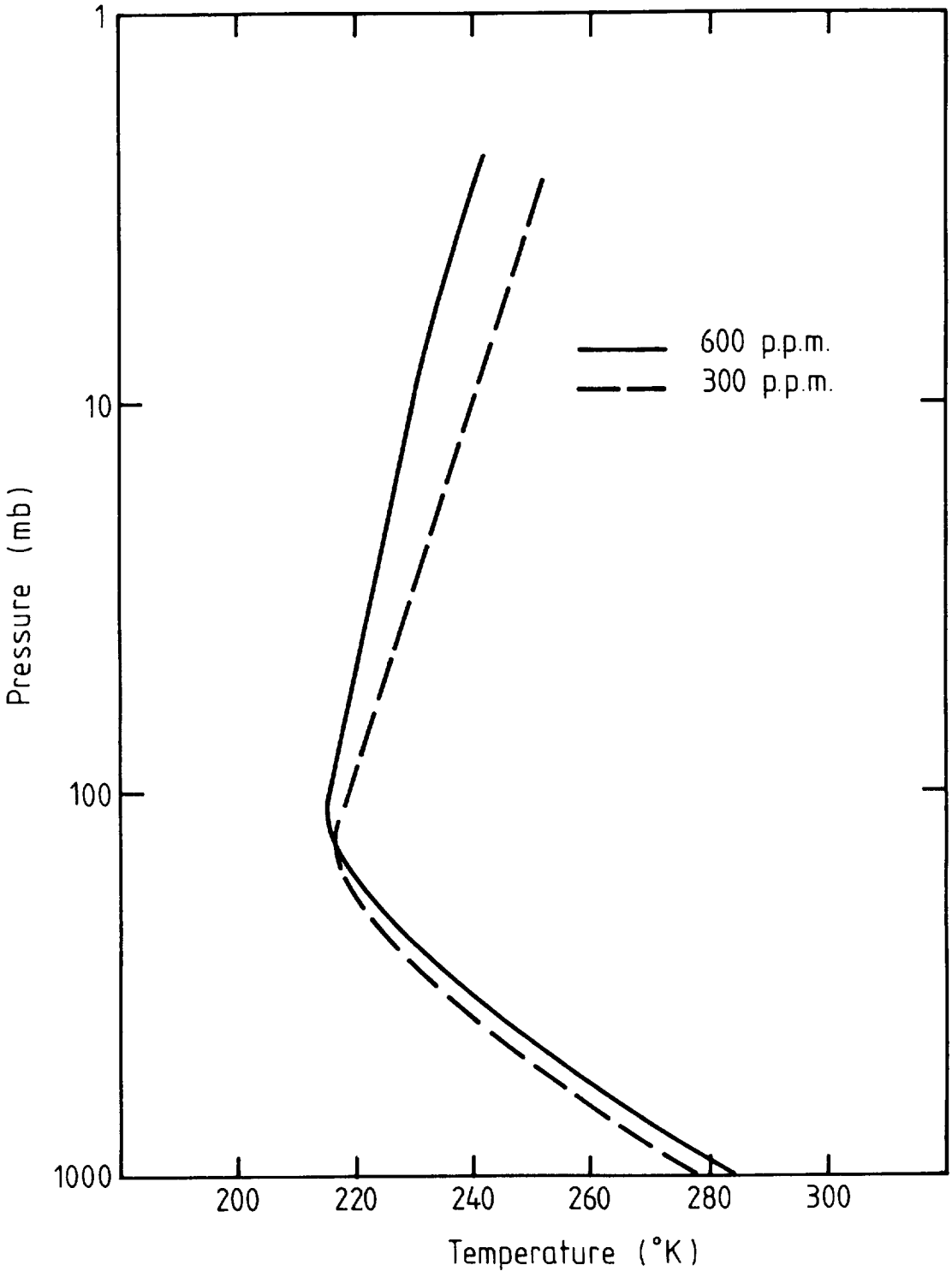

Figure 16. Vertical profiles of the equilibrium temperature distribution for CO_2 concentrations of 330 ppm and 600 ppm for a cloudless atmosphere at 35°N in winter. Webster and Stephens (1980)

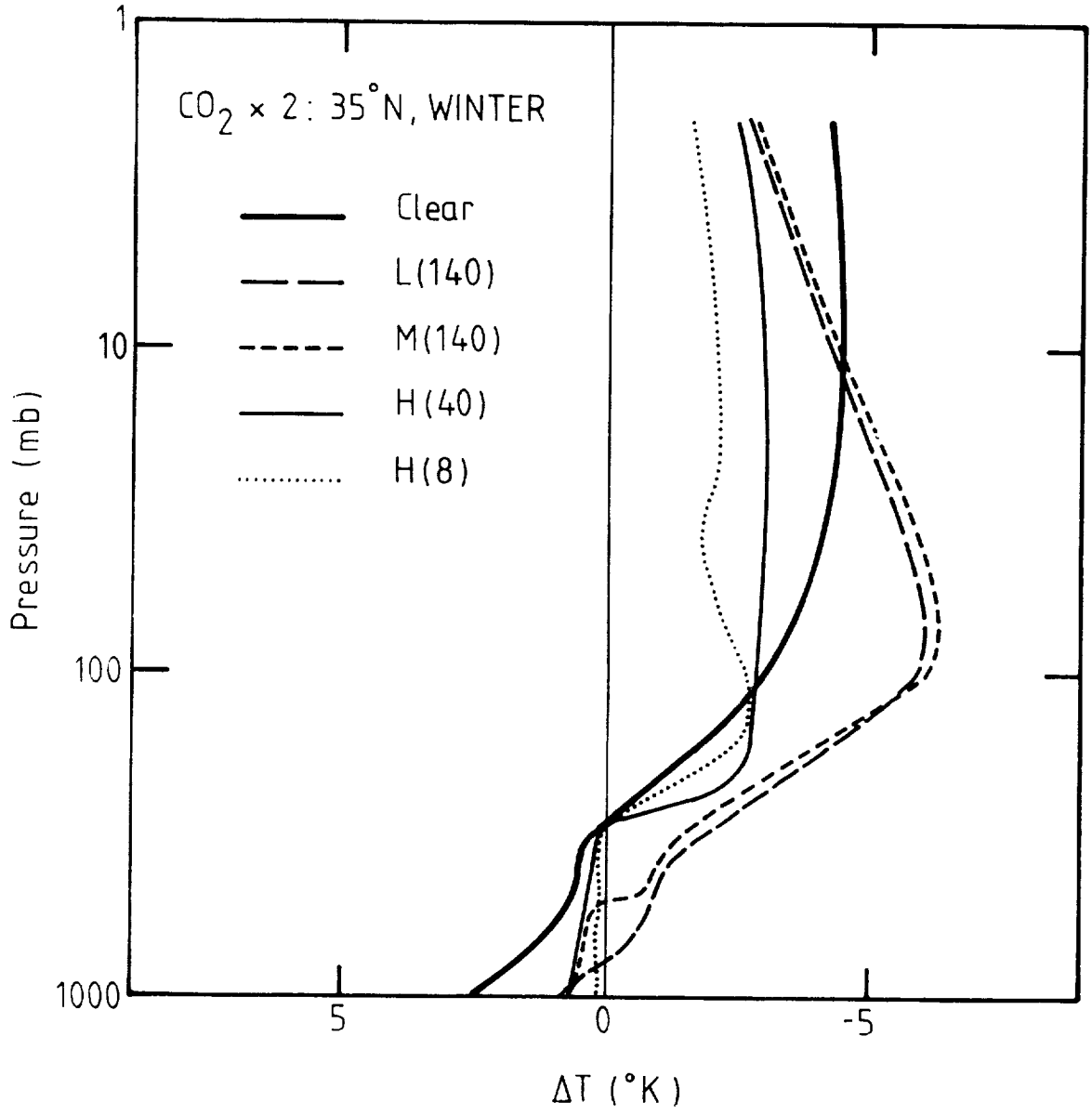

Figure 17. Vertical structure of the difference between equilibrium temperature profiles for atmospheres possessing 300 and 600 ppm CO_2 concentrations for clear skies and for overcast conditions. Webster and Stephens (1980).

Table I

Surface temperature sensitivities to changes in various parameters at 35°N in winter. Implications from open-loop studies.

Sensitivity $\frac{\alpha}{100}\frac{dTs}{d\alpha}$

	Clear	L(140)	M(140)	H(40)	H(8)
Parameter α					
Solar Constant	+1.26	+1.20	+1.20	+1.25	+1.27
Cloud Amount	–	-0.28	-0.22	+0.04	+0.26
Surface Albedo					
As<0.5	-0.8	-0.13	-0.17	-0.30	-0.46
As>0.7	-0.9	-0.14	-0.18	-0.40	-1.20
CO_2	+0.026	+0.006	+0.005	+0.004	+0.004

of CO_2 could be offset by a 10% increase in low cloud amount or a 10% in high cloud. The latter figures are listed in Table 2.

Arguments about compensatory climatic parameters are difficult to develop when it is realized that we have little idea whether cloudiness would tend to increase or decrease with an induced column temperature rise. The problem is compounded further when it is realized that high cloud and low cloud work in opposite directions a feature which originates from the different albedo-emittance relationships of high and low clouds. Of course, this conclusion says nothing of the *sign* of the cloud amount variation with a changing atmospheric temperature. These are the problems the *closed-loop models* must tackle.

Table 2

The percent variation in cloudiness which would be required in order to match a temperature change of (A) 2.6°K and (B) 0.5°K by a CO_2 atmospheric concentration doubling. Implications from open-loop studies.

	(A) 2.6°K Increase			(B) 0.5°K Increase		
	L(140)	M(140)	H(8)	L(140)	M(140)	H(8)
Cloud Amount (%)	+9.3	+11.8	-10.0	+1.9	+2.3	-1.9

5. Closed-Loop Model Studies

It may be expected that the magnitudes of the sensitivities disclosed by the open-loop studies may be modified by models which are considerably more complicated and which may contain closed cloud feedback loops. However it is difficult to imagine that the sign of the sensitivities will change. Consequently, the open-loop studies provide a clear warning of the difficulty which may be anticipated in cloud parameterizations to be used in closed-loop studies if they are to be of any use in climate research.

An example of the difficulty may be obtained by considering once again the CO_2 problem; a problem tackled by a number of closed-loop studies (e.g. Manabe and Wetherald, 1975, 1980 and Manabe and Stouffer, 1979). The major implication of the open-loop studies is the necessity to obtain the correct distribution of cloud. We noted from Table 2 that a decrease of 10% of low cloud or a 10% increase of high cloud is one method of compensating for the effect of a CO_2 doubling. Consequently a correct modelling of the total cloud amount is insufficient! A closed-loop model must also forecast the variation of the cloud amount of the various layers of cloud.

With these reservations in mind we may quickly review the "CO_2 papers" of Manabe and Wetherald (1975, 1980). These studies are mentioned as they are the best examples of the closed-loop studies showing what may be achieved with sophisticated climate models. At the same time, they underline some of the problems which must be reckoned with at some stage. A large number of cases were run by Manabe and Wetherald utilizing a variable cloud scheme (i.e. model generated). The cloud parameterization depended principally on the relative humidity distribution. Manabe and Wetherald concluded that ". . . modelling variable clouds had a relatively minor effect on the sensitivity of the models' climate (to CO_2 variations) . . .". These conclusions agreed with (or perhaps were the cause of?) the recent NAS Reports on CO_2 which suggested that cloud variation was probably a second order effect in the CO_2–Climate relationship. Given the extreme sensitivity implied by the open-loop studies and the simplicity of the parameterizations of cloud variability used in the closed-loop studies, the question of the meaning of these results and the relation of model and climate sensitivity needs to be reexamined. However, despite relative insensitivities with respect to cloudiness variations, the GCM's have managed to show the same sign of variation of climate with other variables and have shown some interesting longitudinal and latitudinal distributions of climate change.

Similar dispute exists in the few observational "closed-loop observation studies". Using satellite data Cess (1976) found that the short-wave loss due to clouds almost exactly balanced the long-wave gain. The implications from this study would be that the climate would be *insensitive* to cloud amount variation. That is, clouds would be climatically passive. However, Ohring and Clapp (1980) suggested that generally the short-wave loss was larger than the long-wave gain. That is, clouds are climatically significant; an increase in cloud amount leads to a cooling of the surface. But it seems that the question remains to be resolved as Hartman and Short (1980) have pointed out that Cess may have been looking at the total derivative of net flux radiation at the top of the atmosphere with respect to cloud whereas Ohring and Clapp may have been calculating the partial derivative!

6. Some Concluding Remarks

The simpler open-loop studies almost universally suggest a considerable sensitivity of climate to variations in various cloudiness parameters. These findings coincide with expectations obtained from diabatic heating studies and observations discussed earlier. Observational studies using satellite data tend to produce ambiguous support and the GCM's offer little encouragement to the results of the simpler studies.

There are a number of reasons why there may be differences in the results between the various model modes. For example, are the GCM's stating the sensitivity of the real climate system or the insensitivity of the cloud parameterization? On the other hand, how much larger than reality are the sensitivities portrayed by the open-loop studies?

The most troublesome aspect of the problems raised above is how to approach a solution. How do we know when the GCM is performing well and when it is producing a consistent cloud set? For example, in the Manabe-Wetherald (1980) study considerable tuning was required in order to compare "fixed" and "variable" cloud cases. Also despite claims of insensitivity, mean tropospheric surface temperature differences of about 1.5°C were found between the fixed and variable cloud cases which is 70% of the calculated CO_2 doubling warming effect. The tuning of the model was achieved by using a solar constant which was 105.5% of the normal value which resulted in a "correct" temperature gradient although Manabe and Wetherald produce a cloudiness gradient which is a strong function of solar constant as shown in Figure 18 (taken from Manabe and Wetherald (1980). These points are discussed here to point out the difficulty in performing control experiments with the existing large-scale closed-loop models.

In order to overcome of the problems listed above, the following recommendations may be of use:

(i) It appears necessary to develop more exact parameterization of cloud production. Such parameterizations will require subtlety in order to represent cloud height and cloud structures which appear to be important in modifying the radiative heating profiles. Probably the use of a radiative convective model with a *hydrology cycle,* as proposed by Sarachik (1978), will be useful in the developmental phase.

(ii) Observational studies carried out at the same time as model experimentation are necessary. "Control" experiments such as those undertaken by Ohring and Clapp should be developed. It is difficult to understand how useful the proposed cloud climatology studies will be to the development of cloud variation parameterization. As the satellite is the principal tool of the climatology exercise, the only information to be compiled will be the cloud top height and temperature and the net flux at the top of the atmosphere. Whereas such data has a certain physical importance it does not define a unique state of the column and as a consequence it may not be of much use to the modeller who is developing parameterizations which must describe the complete cloud structure. Perhaps for specific periods the satellite-based cloud climatology can be meshed with other observing techniques.

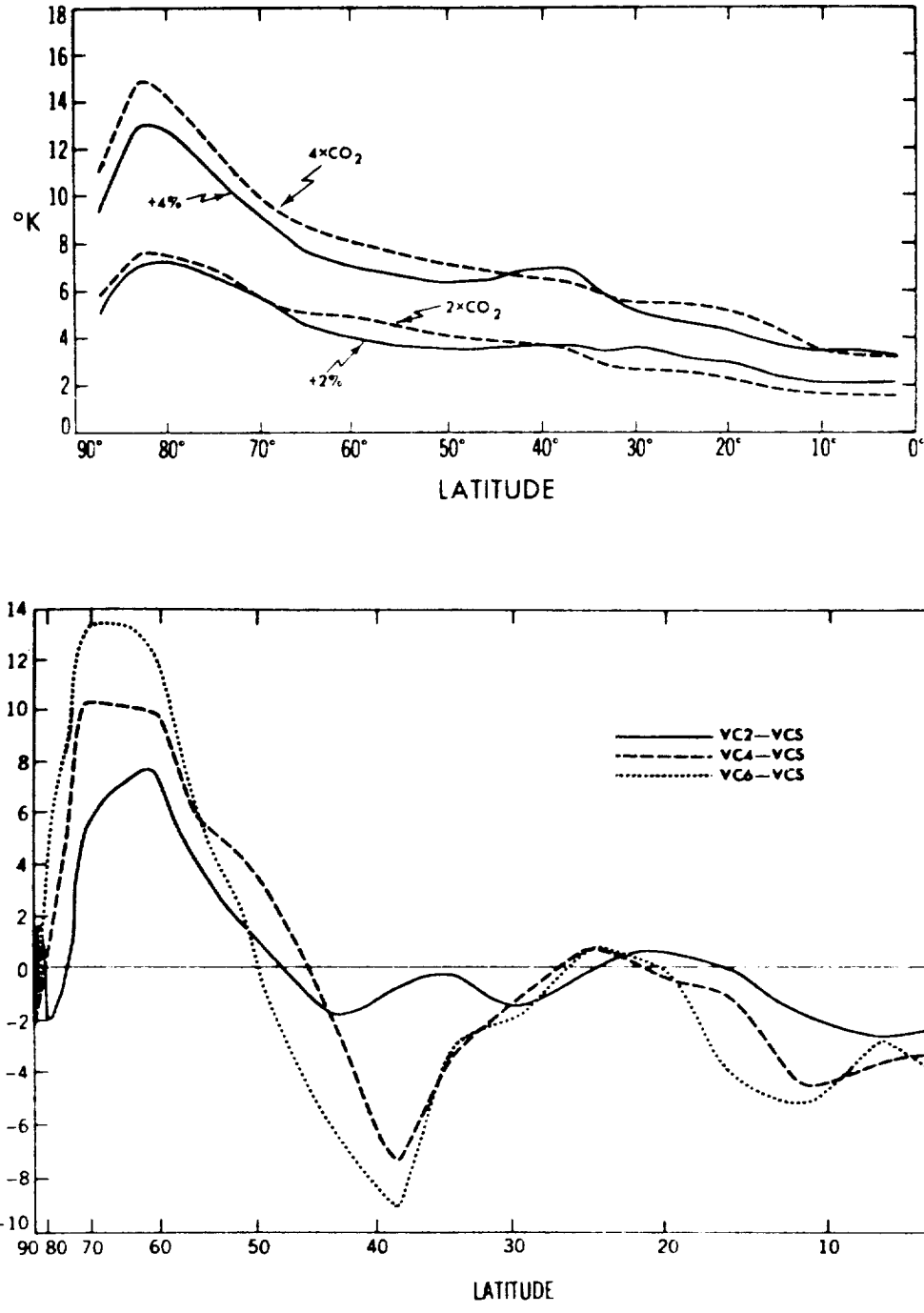

Figure 18. *Upper panel:* Latitudinal distribution of the zonal-mean change of surface air temperature in response to a 2% and 4% increase of the solar constant, and a doubling and quadrupling of the CO_2 content (after Manabe and Wetherald, 1980). *Lower panel:* Latitudinal distribution of zonal mean difference in total cloudiness (%) between a number of experiments, (after Manabe and Wetherald, 1980).

References

Arakawa, A., 1975: Modelling clouds and cloud processes for use in climate models. GARP Publication Series No. 16 (ICSU/WMO) pp. 183–197.

Cess, R. D., 1976: Climate change: An appraisal of atmospheric feedback mechanisms employing zonal climatology, *J. Atmos. Sci., 33,* 1831–1843.

Hartman, D. L. and D. A. Short, 1980: On the use of earth radiation budget statistics for studies of clouds and climate. *J. Atmos. Sci., 37,* 1233–1250.

Hunt, B. G., 1978: On the general circulation of the atmosphere without clouds. *QJRMS* 104, 91–102.

Manabe, S. and R. J. Wetherald, 1967: Thermal equilibrium of the atmosphere with a given distribution of relative humidity. *J. Atmos. Sci., 24,* 241–259.

Manabe, S. and R. J. Wetherald, 1975: The effects of doubling of the CO_2 concentration on the climate of a general circulation model. *J. Atmos. Sci., 33,* 3–14.

Manabe, S. and R. J. Wetherald, 1980: On the distribution of climate change resulting from an increase in CO_2 content of the atmosphere. *J. Atmos. Sci., 37,* 99–118.

Manabe S. and R. J. Stouffer, 1979: A CO_2-climate sensitivity study with a mathematical model of the global climate, *Nature, 282:* p. 491.

Newell, R. E., J. W. Kidson, D. G. Vincent and G. J. Boer, 1972: The General Circulation of the Tropical Atmosphere and Interaction with Extratropical Latitudes, 1. The MIT Press, 258 pp.

Ohring, G. and P. F. Clapp, 1980: The effect of change in cloud amount on the net radiation at the top of the atmosphere. *J. Atmos. Sci., 37,* 447–454.

Oort, A. J. and E. Rasmussen, 1971: Atmospheric circulation statistics. NOAA, Pub. Pap. No. 4, U.S. Department of Commerce, 323 pp.

Ramage, C. S., 1975: Preliminary discussion of the meteorology of the 1972–73 El Nino, *B.A.M.S., 46,* p. 4–15.

Sadler, J. and B. E. Harris, 1970: The mean tropospheric circulation and cloudiness over southeast Asia and neighbouring areas. Technical report, Hawaii Institute of Geophysics, University of Hawaii, Contract No. F19628-69-C-0156.

Sarachik, E. S., 1978: Tropical sea surface temperature: an interactive one-dimensional atmosphere-ocean model. *Dynamics of Atmosphere and Oceans, 2,* 455–469.

Stephens, G. L., 1978: Radiative properties of extended water clouds: II. Parameterizations. *J. Atmos. Sci.,* 2123–2132.

Stephens, G. L. and P. J. Webster, 1979: Sensitivity of radiative forcing to variable cloud and moisture, *J. Atmos. Sci., 36,* 1542–1556.

Stephens, G. L. and P. J. Webster, 1981: Clouds and Climate: Sensitivity of Simple Systems. To appear in *J. Atmos. Sci.,* February 1981.

Webster, P. J. and G. L. Stephens, 1980a: Tropical upper tropospheric extended cloud: Inferences from Winter MONEX. *J. Atmos. Sci., 37,* 1521–1541.

Webster, P. J. and G. L. Stephens, 1980b: Gleaning CO_2-Climate. Relationships from Model Calculations. *Carbon Dioxide and Climate: Australian Research.* Editor, G. I. Pearman; Australian Academy of Science. 185–195.

CLOUD COVER AND CLIMATE SENSITIVITY

Richard T. Wetherald and Syukuro Manabe
Geophysical Fluid Dynamics Laboratory/NOAA
Princeton University
Princeton, New Jersey 08540

This study discusses how the sensitivity of climate may be affected by the variation of cloud cover based upon the results from numerical experiments with a highly simplified, three-dimensional model of the atmospheric general circulation. The model explicitly computes the heat transport by large-scale atmospheric disturbances. It contains the following simplifications: a limited computational domain (Figure 1), an idealized geography, no heat transport by ocean currents and no seasonal variation. Two versions of the model are constructed. The first version includes prognostic schemes of cloud cover and its radiative influences, and the second version uses a prescribed distribution of cloud cover for the computation of radiative transfer. Two sets of equilibrium climates are obtained from the long-term integrations of both versions of the model for several values of the solar constant. Based upon the comparison between the variable and the fixed-cloud experiments, the influences of the cloud cover variation upon the response of a model climate to an increase of the solar constant are identified.

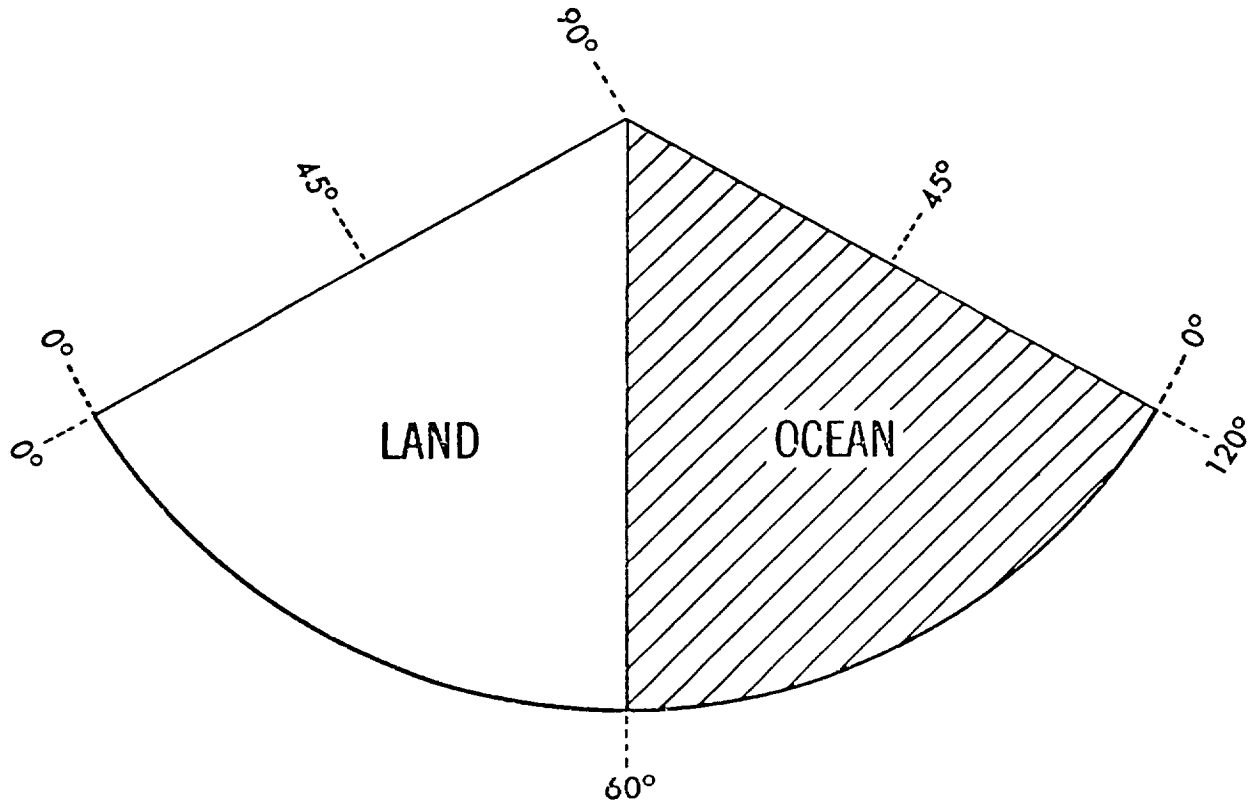

Figure 1. Computational domain of the model. The oceanic region is hatched. Cyclic continuity is assumed in the atmosphere between the two meridional boundaries.

The results from this analysis indicate that the following changes in cloudiness occur in the model atmosphere in response to an increase of the solar constant (see Figure 2). In the upper and middle troposphere of the model, both zonal-mean relative humidity and cloudiness decrease because of the increase in the variance of vertical velocity. Owing to the saturation and the condensation of water vapor, the moistening in the region of upward motion tends to be smaller than the drying in the region of subsidence. Thus, the reduction of area-mean relative humidity occurs in the layers of intensified vertical velocity. In high latitudes and the subtropics where the atmospheric static stability in the planetary boundary layer of the atmosphere is relatively stable, enhanced evaporation from the warmer surface contributes to the increases in both relative humidity and non-convective cloudiness at the near-surface level where the warming due to increased insolation is less than the surface warming. In the lower stratosphere of the model, nonconvective cloudiness increases particularly in high latitudes. It is suggested that the large reduction in static stability around the tropopause level, which results from the large difference in warming between the troposphere and stratosphere, enhances the upward moisture transport across the tropopause and raises both the relative humidity and cloudiness in the lower stratosphere where the warming is relatively small. In summary, cloudiness decreases in the upper and middle troposphere of the model at most latitudes but increases near the earth's surface and lower model stratosphere in high latitudes in response to an increase of the solar constant.

Because of the change described above, total cloud amount reduces in most of the region equatorwards of 50 degree latitude with the exception of a narrow subtropical belt. However, it increases in the region polewards of this latitude (see Figures 3a and 3b). Thus, the net change in the area-mean total cloudiness turns out to be very small. It is found that, in both regions, the cloud-induced changes in net incoming solar radiation and upward terrestrial radiation at the top of the atmosphere tend to compensate with each other. For example, equatorwards of 50 degrees latitude, the reductions of cloud amount and effective cloud top height contribute to the increase in the effective emission temperature of the upward terrestrial radiation and enhance the cooling of the model atmosphere. On the other hand, the aforementioned reduction of cloud amount results in a decrease of reflected solar radiation (or increase of net incoming solar radiation) and thus increases the absorption of incoming solar radiation and contributes to the warming of the earth-atmosphere system of the model.

Poleward of 50 degrees latitude, the increase of total cloud amount contributes to the reductions of both net incoming solar radiation and outgoing terrestrial radiation. Although the effective height of cloud top does not change as it does in lower latitudes, the change of the outgoing terrestrial radiation almost compensates with that of reflected solar radiation owing to the smallness of insolation in high latitudes.

The present study appears to indicate that the influence of the cloud feedback mechanism upon the sensitivity of the global mean temperature may not be as large as originally suspected because of the compensation mechanism identified above. In assessing the relevance of the present results to the sensitivity of the actual atmosphere, it is, however, necessary to recognize that the method of cloud prediction used for this study is highly idealized. Furthermore, the optical properties of the clouds assumed for the model may not be sufficiently realistic. As a matter of fact, the degree of compensation between solar and terrestrial radiation at each latitude depends upon the specific choice of

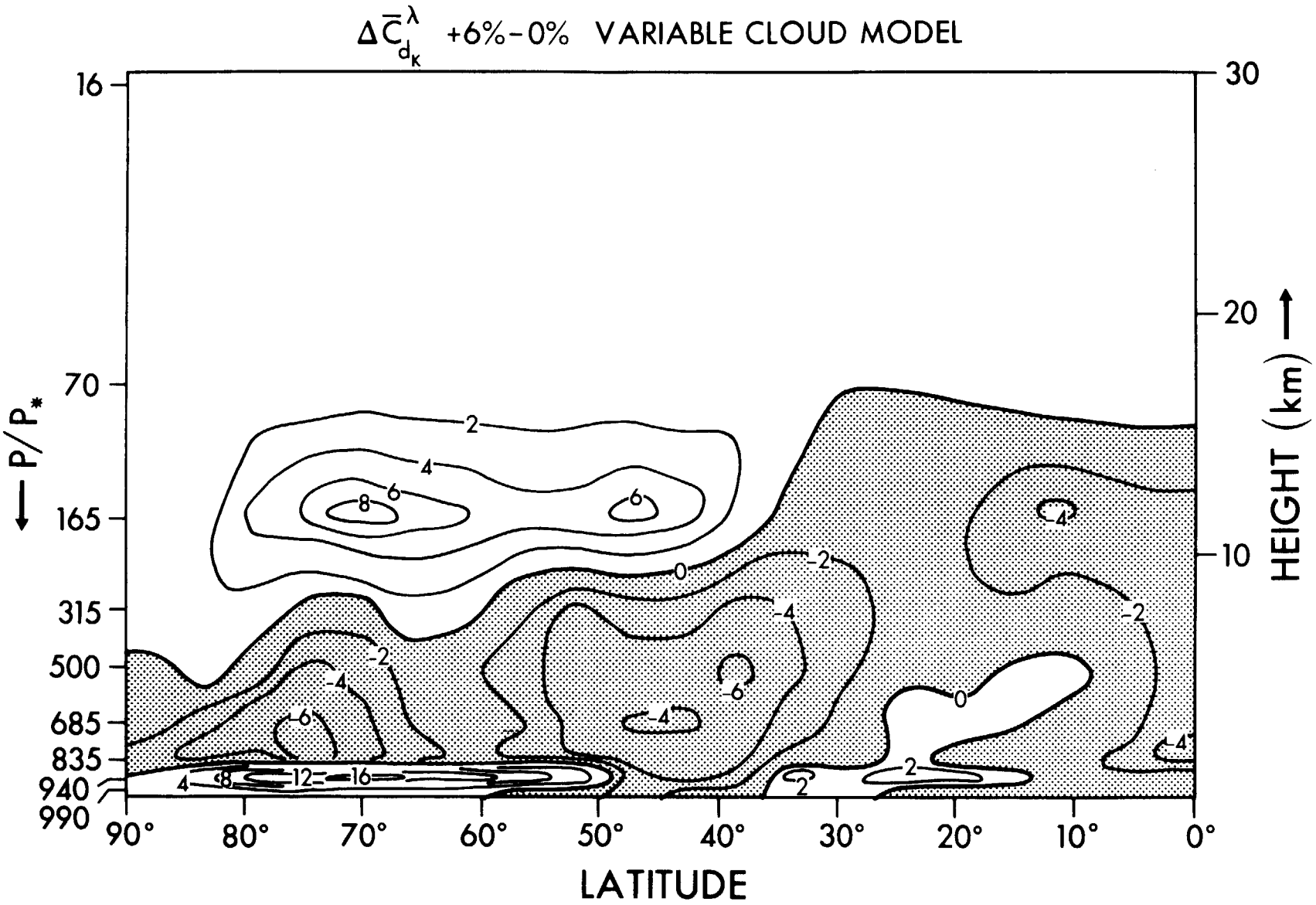

Figure 2. Latitude-height distribution of the change in zonal-mean cloud amount (c_d) in response to a 6% increase in the solar constant. Shaded areas indicate negative values. Units are in percent.

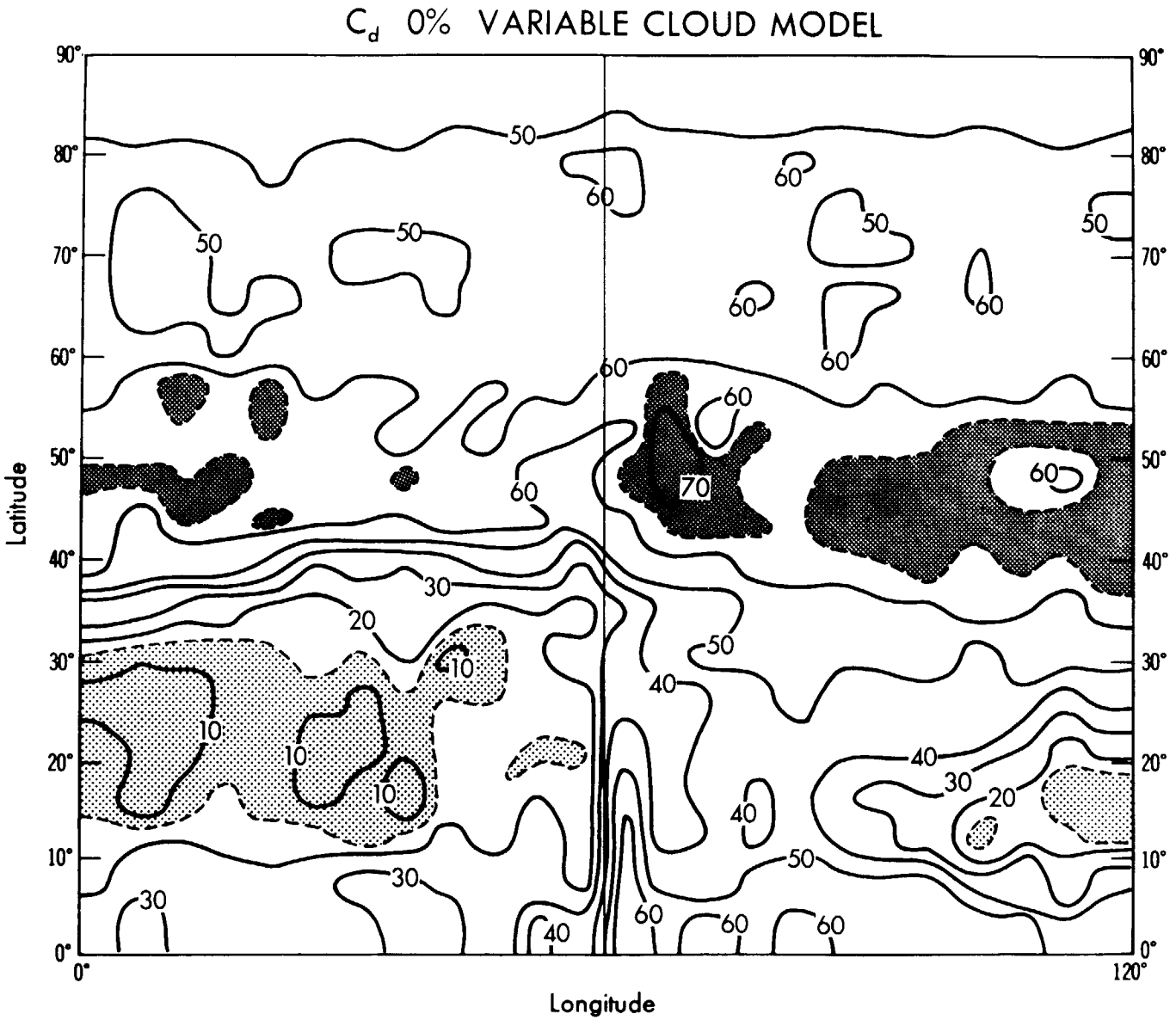

Figure 3a. Horizontal distribution of total cloud amount (c_d) from the standard experiment. Units are in percent.

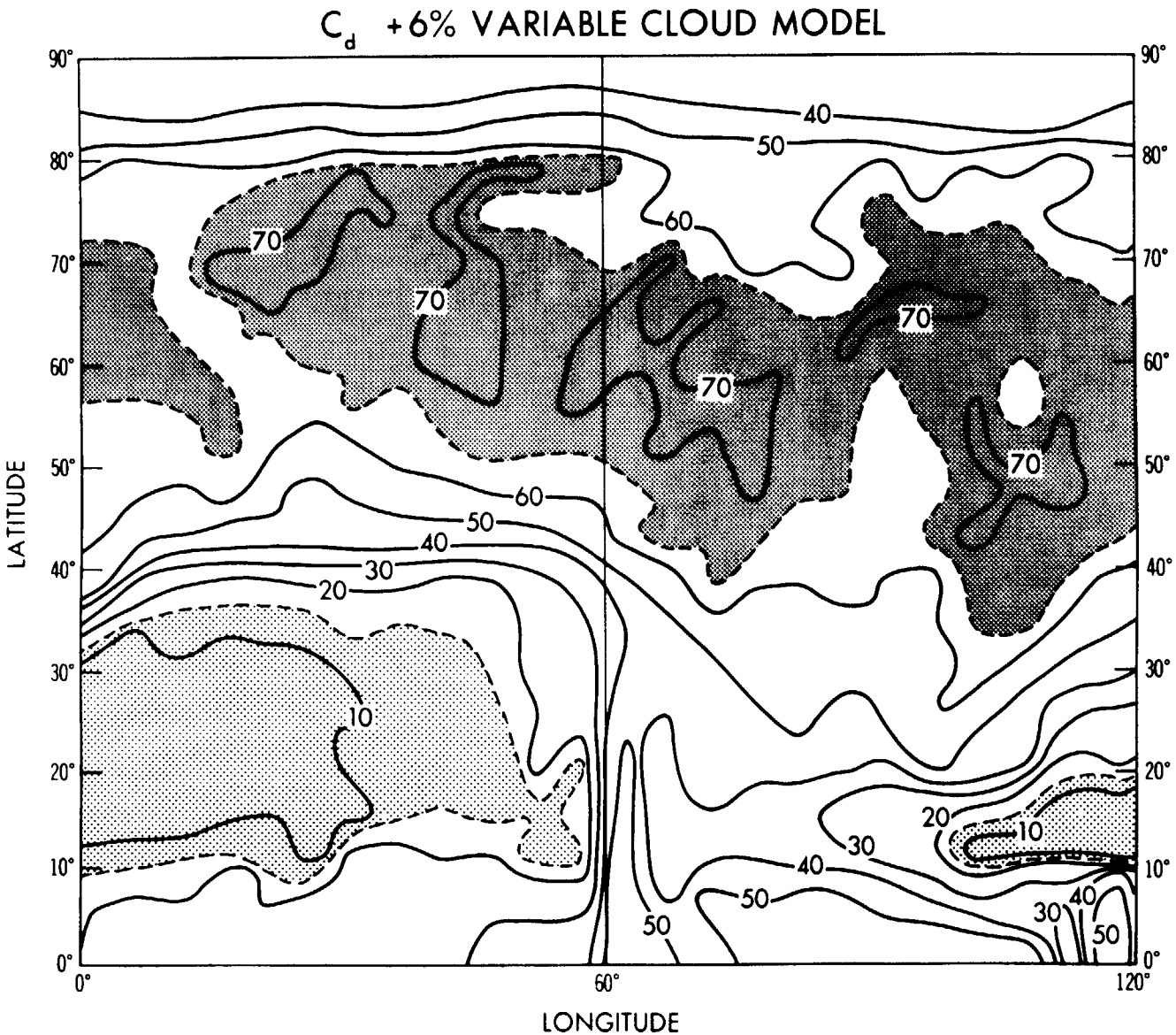

Figure 3b. Horizontal distribution of total cloud amount (c_d) from the experiment in which the solar constant is increased by 6%. Units are in percent.

optical properties of cloud cover. Therefore, further study is required before one can determine whether variable clouds have an amplifying, damping or neutral effect upon the sensitivity of global climate. For more details of this study, see Wetherald and Manabe (1980).

References

Wetherald, R. T. and S. Manabe, 1980: Cloud cover and climate sensitivity. *J. Atmos. Sci., Vol. 37,* 1485-1510.

A SCHEME FOR FORMING NONPRECIPITATING LOW-LEVEL CLOUDS IN GCMS

V. Ramanathan and R. E. Dickinson
National Center for Atmospheric Research
Boulder, Colorado 80307

Low-level clouds such as marine stratocumulus and trade cumulus which form during undisturbed atmospheric conditions play an important role in determining the ocean energy budget. Numerous 1-dimensional model studies of these low-level clouds have improved our understanding of the processes that are responsible for their formation and maintenance. Based on the theoretical framework provided by these 1-D model studies, we are testing a simple scheme for forming stratocumulus and trade cumulus clouds in the NCAR GCM. Preliminary GCM results of cloud distributions will be described here.

The GCM used in this study is described in Washington et al. (1979). The parameterization scheme for forming low-level clouds is illustrated in Figure 1. The NCAR GCM has 8 layers with each layer approximately 3 km thick. The lowest model layer extends from the surface to about 700 mb and as shown in Figure 1, three types of nonprecipitating clouds are formed within this layer. Deep cumulus: when the lowest layer and the layer above it are conditionally unstable, i.e., $\partial\theta_e/\partial z$, where θ_e is the equivalent potential temperature, and when the relative humidity (RH) exceeds a critical relative humidity, deep cloud extending upward from 850 mb is assumed to form. If the two layers mentioned above are stable then either stratocumulus or trade cumulus clouds are formed provided the conditions shown in Figure 1 are satisfied. The symbols in Figure 1 denote the following: $\partial\theta/\partial z$ is the gradient of dry potential temperature between surface and 850 mb. EVP is the surface evaporation; LCL is the lifting condensation level defined as the pressure level at which a parcel with the mixed layer humidity, q_M, will exceed saturation humidity assuming dry adiabatic ascent; θ and q are respectively potential temperature and specific humidity and the subscript M denotes mixed layer value. As can be inferred from the vertical profiles of θ and q in Figure 1. The scheme basically assumes that stratocumulus cloud is imbedded within the mixed layer whereas the trade cumulus is above the mixed layer.

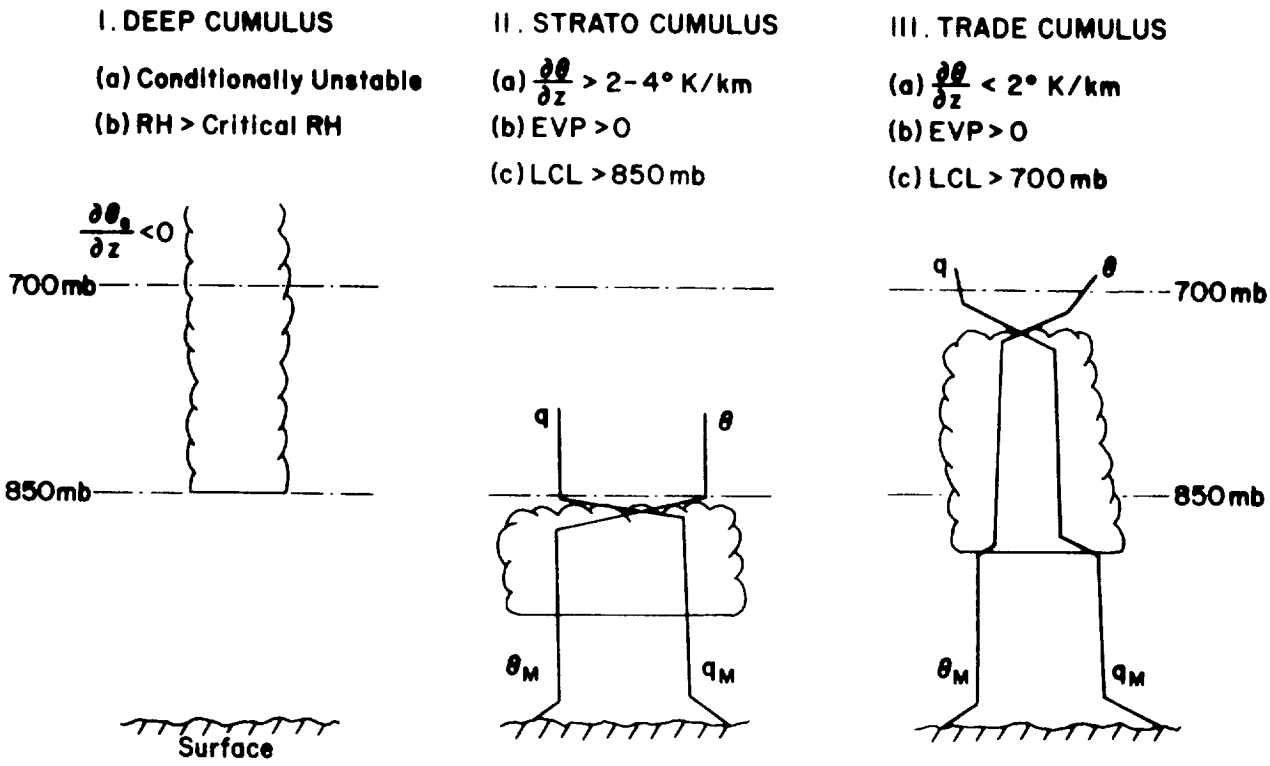

Figure 1. Non-precipitating low-level clouds.

Figure 2 shows the simulated monthly mean stratus geographical distribution of stratocumulus by the GCM for August and January. The GCM was integrated in time for six months (starting from the July initial conditions) with seasonally varying (but prescribed) sea surface temperatures and solar insolation. From Figure 2, the model simulates the gross features of the observed stratocumulus clouds on the eastern boundary of the Pacific off the coast of California and South America in August and the summertime arctic stratus. It is encouraging to note the disappearance of these clouds in January. The predicted trade cumulus cloud distributions are shown in Figure 3 along with observed trade wind systems. The regional locations of simulated trade wind cumulus seem consistent with the observed trade wind systems. Note also by comparing Figures 2 (August simulation) and 3 that in the region extending southwestward into the Pacific from the California coast the model simulates the transition of stratocumulus into trade cumulus.

The scheme proposed here for forming these low-level clouds is admittedly crude and glosses over several important dynamical constraints (e.g. entrainment), but the results of our preliminary attempt seems encouraging.

Reference

Washington, W., R. Dickinson, V. Ramanathan, T. Mayer, D. Williamson, G. Williamson, and R. Wolski, 1979: Preliminary atmospheric simulation with the third-generation NCAR general circulation model: January and July. *Report of the Joint Organizing Committee Study Conference on Climate Models: Performance, Intercomparison and Sensitivity Studies,* 95-138 (WMO Publication).

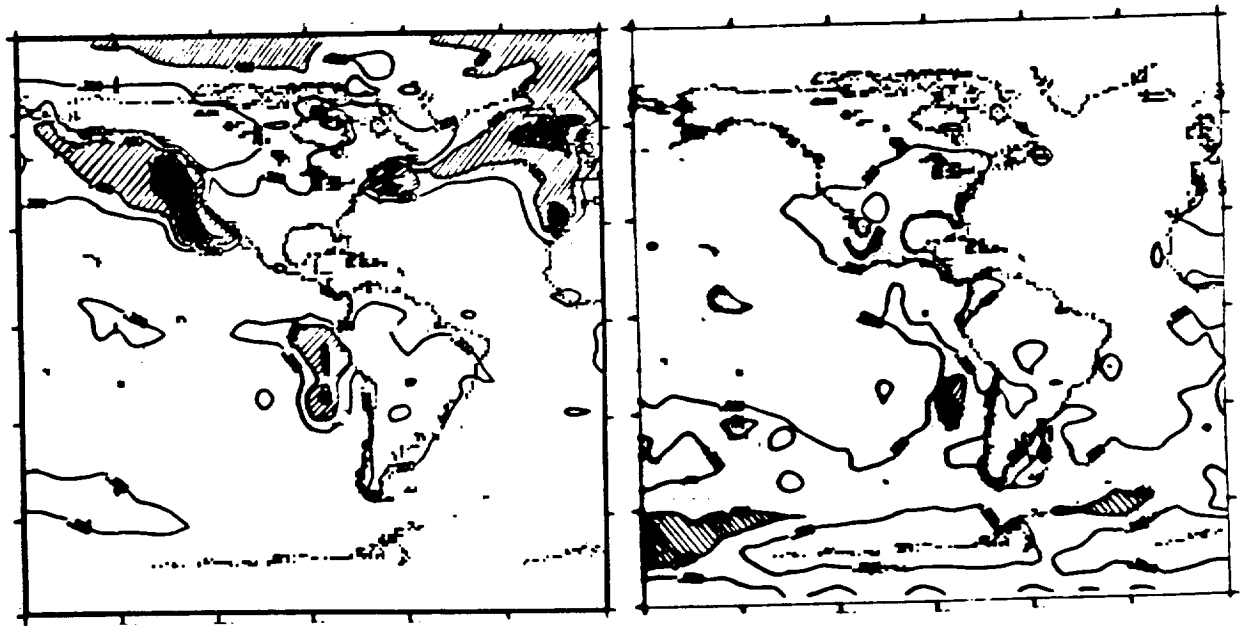

AUGUST JANUARY

Figure 2. Simulated stratus and stratocumulus. (Hatched area – greater than 40% cloud fraction. Darkened area – greater than 60% cloud fraction.

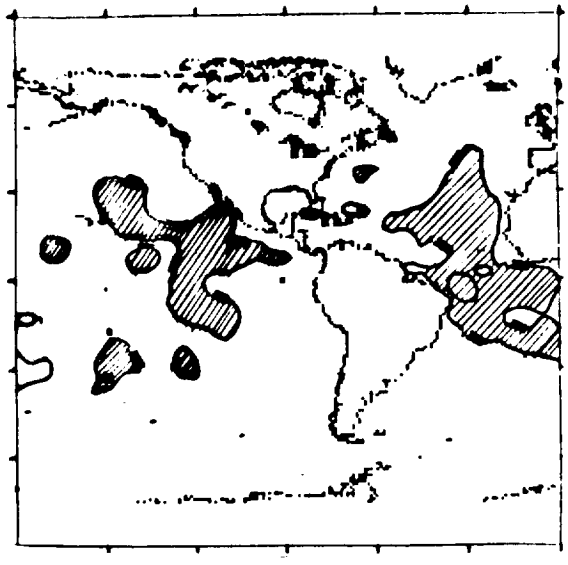

SIMULATED TRADE CUMULUS DISTRIBUTION

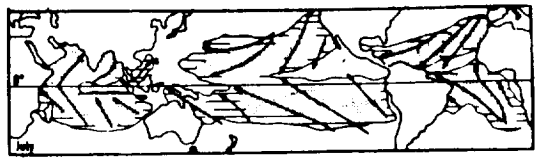

TRADE WIND OBSERVATIONS
World Trade Wind Systems (Crowe, 1971)

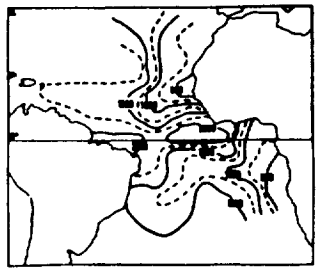

WEIGHT OF TRADE INVERSION IN METERS
(Riehl, 1954)

Figure 3.

CLOUD-RADIATION EXPERIMENTS CONDUCTED WITH GLAS GENERAL CIRCULATION MODELS

Gerald F. Herman
Department of Meterology
University of Wisconsin, Madison 53706

NASA Goddard Laboratory for Atmospheric Science
Greenbelt, Maryland 20771

The second order general circulation models (GCMs) developed at NASA's Goddard Laboratory for Atmospheric Science (GLAS) have been used in a variety of sensitivity and simulation studies to illustrate the relationship between cloudiness, radiation, and the large-scale dynamics of the model. The cloud and radiation budgets of the model are reviewed, and are assessed with respect to currently available observational data. Four cloud feedback experiments that were conducted with GLAS GCMs are reviewed, and their implications for further modelling and observational needs are discussed.

Cloud formation processes in the model are fully coupled to cloud radiative processes insofar as clouds grow and dissipate in response to changes in temperature, stability, and surface heating, and these depend in part on the flux and flux divergence of solar and thermal radiation. Cumulus cloud formation in the model is calculated with Arakawa's three-level parameterization (see Helfand, 1980, *J.A.S., 36,* p. 1827), while stratiform clouds occur simply when a grid element becomes supersaturated. Solar radiation is treated with an algorithm developed by Lacis and Hansen (1974, *J.A.S., 31,* 118-133), and thermal radiation with a technique developed by Kaplan and Wu (see Wu, 1980, *J.G.R., 85,* p. 4084).

The zonally-averaged cloud frequencies obtained with the model for the January-February and July periods are shown in Figures 1 and 2. The general character of the observed cloud distribution (obtained from Beryland and Strokina, *Trudy VGO, 338,* and Gates and Schlesinger, 1977, *J.A.S., 34,* p. 36) as a function of latitude is simulated, *e.g.* mid-latitude and tropical maxima, sub-tropical minimum, but major discrepancies do exist. The most notable of these are the excessive supersaturation cloud formed by the model north of 45°N in winter, the failure of adequate high-latitude cloudiness to develop in July, and the unrealistically small amplitude of the ITCZ migration from January to July. The observed maxima of cloudiness over Indonesia, South America, Central Africa, and the high-latitude oceans are well simulated.

The solar radiation absorbed by the model's earth-atmosphere system generally agree well with the recent observations of Winston *et al.* (1979, NOAA, U.S. Dept. Commerce) except in the Southern Hemisphere summer, where the model's absorption is overestimated. The infrared flux at the top of the model's atmosphere (see Figure 3) is systematically too low during both seasons by 40-60 W m^{-2}, and this deficiency is attributed to the model's inability to treat subgrid scale fractional cloudiness, or true optical properties of tenuous clouds, such as cirrus.

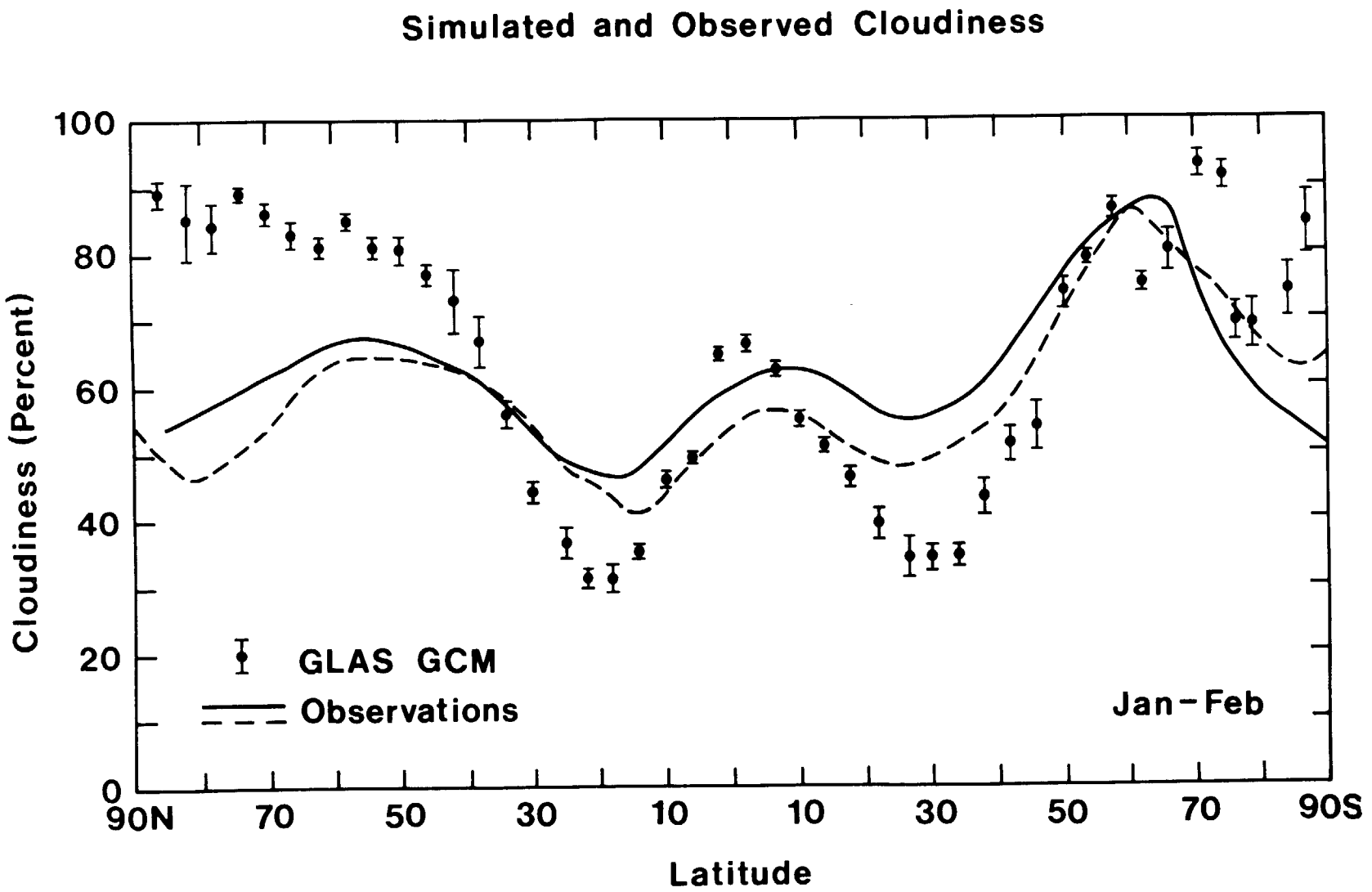

Figure 1. Observed zonal cloudiness from Berlyand and Strokina (solid line) and as compiled by Gates and Schlesinger (1977). Bars indicate the inherent variability of model-generated cloudiness.

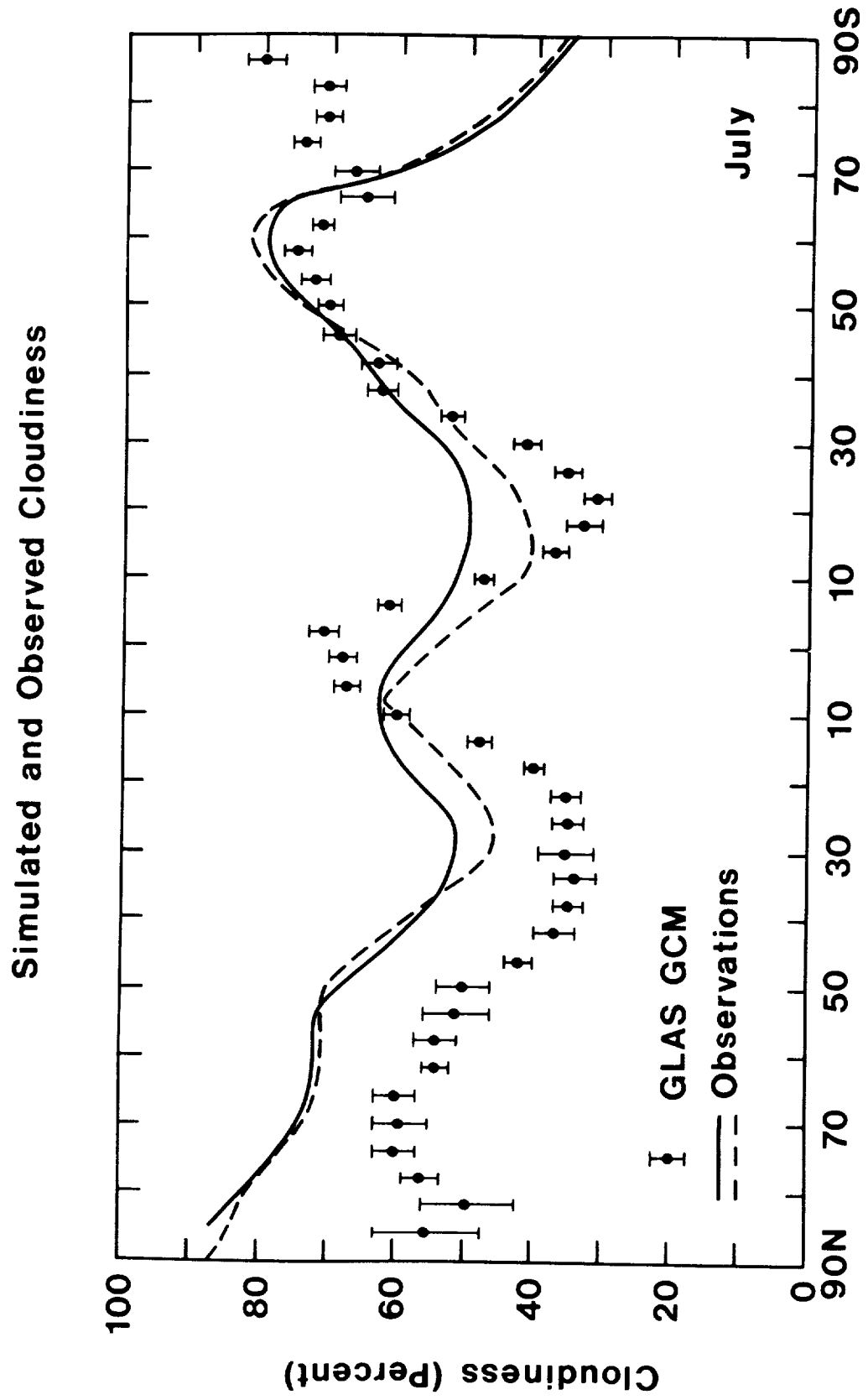

Figure 2. As in Figure 1, except for July.

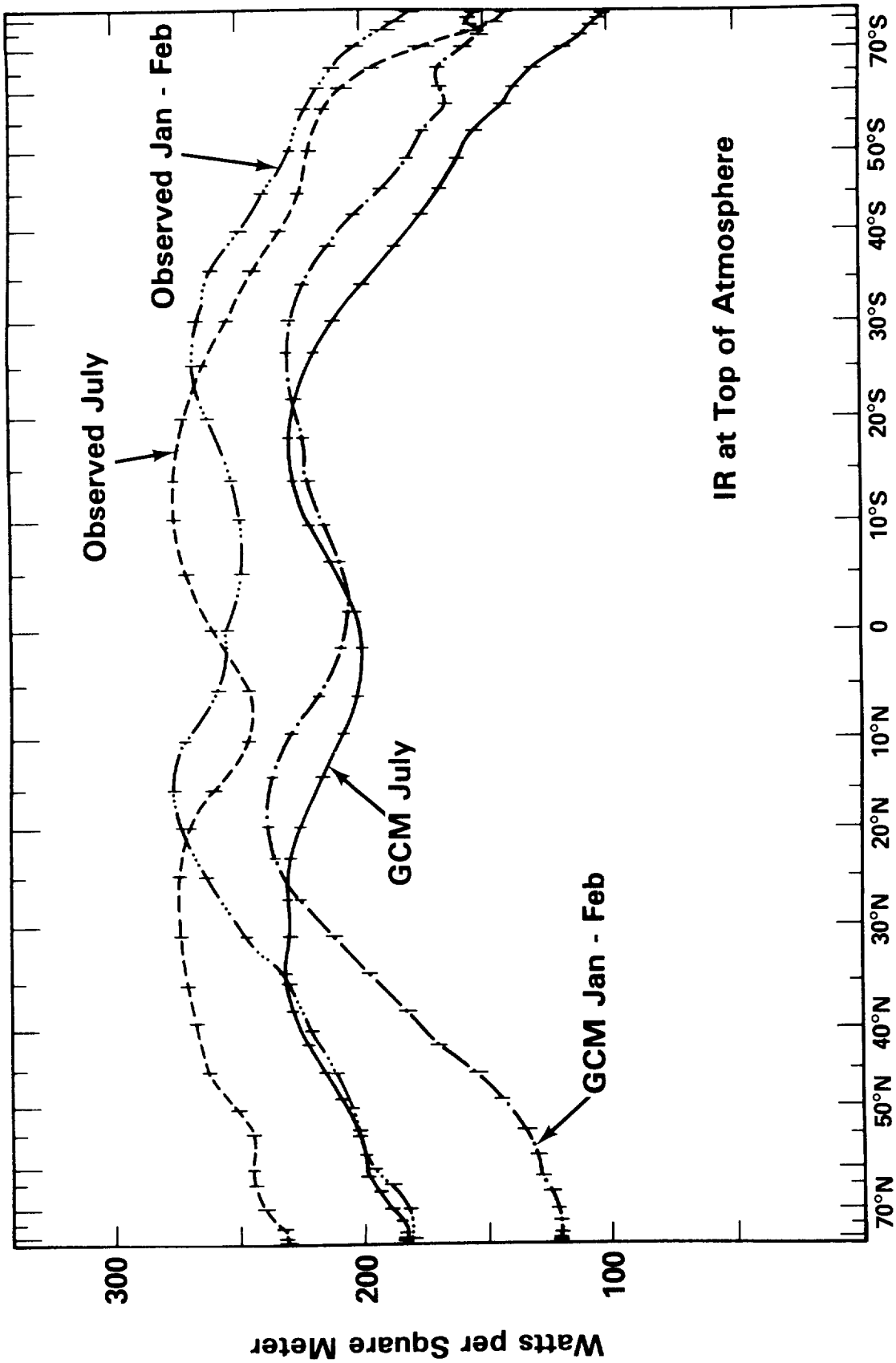

Figure 3. Observed and simulated net longwave radiation at the top of the atmosphere. Key: Simulated July ——; Observed July – – – –; Simulated January–February —·—·—; Observed January —··—··—.

The principal results of cloud-feedback experiments with the GLAS GCM are reviewed. Stated briefly they are:

(1) In the desert-albedo experiments of Charney *et al.* (1977, *J.A.S.*, *34*, p. 1366) the depletion of the surface radiation balance was due solely to albedo changes when cloud feedback was minimal, but was due to an enhanced infrared loss when cloud feedback was included. In both cases a decrease of precipitation accompanied the albedo increases.

(2) In the transparent cloud experiments of Herman *et al.* (1980, *J.A.S.*, *37*, p. 1251) it was shown that on a global basis cloud albedo effects dominated cloud greenhouse effects, although the situation was reversed in high latitudes of the winter hemisphere. Cloud formation over water was suggested to occur as a positive feedback component of the climate system, while cloud formation over land was thought to be negative.

(3) In the fixed vs variable cloud experiments of Shukla and Sud (1980, *J.A.S.*, submitted for publication) statistically significant differences occurred between runs either having clouds fixed, or varying according to internal model dynamics.

(4) A possible relation was suggested between cloud formation, the surface radiation budget, and the intensity of the wintertime Asiatic high.

A complete description of the results presented here will appear in the *Proceedings of the Workshop on Radiation and Cloud-Radiation Interaction in Numerical Modelling*, held at the European Center for Medium Range Weather Forecasting, 15-17 October, 1980.

EFFECT OF CLOUD-RADIATION FEEDBACK ON THE CLIMATE OF A GENERAL CIRCULATION MODEL

J. Shukla and Y. Sud
Goddard Laboratory for Atmospheric Sciences
NASA/Goddard Space Flight Center
Greenbelt, Maryland 20771

The General Circulation Model (GCM) of the Goddard Laboratory for Atmospheric Sciences (GLAS) was integrated for 107 days starting from the initial conditions of May 15. In this run, clouds were continuously generated according to the model parameterization, and therefore they were varying in space and time. Then starting from day 76 of the control run, the model was again integrated for 31 days during which cloudiness for radiative-cloud interaction was spatially prescribed and was invariant in space and time. This run is referred to as the 'fixed-cloud run'. The spatial distribution of clouds in the fixed run was chosen to be such that the aggregate cloudiness frequency over all the grid points at each vertical level and each latitude circle remained nearly same

for the control and the fixed cloud run. This condition implied that the cloud frequency in a grid cell was either 0 percent (no cloud) or 100 percent (permanent cloud) in the fixed cloud case. Clouds were prescribed on grid cells which produced the highest cloud frequency in the control case. It may be emphasized that the statistically averaged cloudiness fields were very similar in both the cases. The only difference in the two runs was that in the fixed-cloud case, the cloudiness for radiative cloud interaction was held constant for the period of integration. The 31-day mean simulation of the second run (fixed clouds) is compared with the last 31-day mean simulation of the first run to study the effects of cloud radiation feedback on the mean monthly circulation, atmospheric energy cycle and the hydrological cycle, evaporation and precipitation and the local climate.

Various meteorological fields were analyzed to study the difference between the two runs. In order to examine the significance of these differences, the model natural variability from the July simulations was also examined. The predictability experiments in which only the initial wind fields at each of the nine model levels were randomly perturbed with a Gaussian error field having a standard deviation of 3 m/sec. For each predictability experiment, the model was integrated for 45 days, and the monthly means for the last 31 days were used to calculate the natural variability of the model. It is assumed that the standard deviation (with Bessel correction) among the four runs (1 control and 3 predictability runs) is a measure of the natural variability of the model. Results from these experiments show significant changes in the simulated large-scale dynamical circulation of the global model. We present four key results in this abstract.

Figure 1 shows the differences in 500 mb geopotential height fields. Large differences are noticed in the latitude belt of 40°-60° S. This is perhaps due to the combined effects of baroclinicity which is maximum in this latitude belt (winter circulation) and the generation of eddy available potential energy (EAPE) due to large longitudinal asymmetry of the fixed-cloudiness field at this latitude. Large differences are also seen in this field at 40°-60° N. In the northern hemisphere (summer circulation) baroclinicity is relatively weak but zonally asymmetric heating in the fixed-cloud run would be more because of larger solar flux. The differences in these fields are also 2-3 times the model's natural variability (Figure 1).

Figure 2 shows the energy cycle of the northern hemisphere. There are four sections of this figure: the energy cycle for the control run, the fixed cloud run, their differences and the corresponding model variability. In the southern hemisphere, (not presented), the model variability of all the energy conversions (EAPE to EKE, ZAPE to EAPE, ZKE to EKE and ZAPE to ZKE) were larger than their corresponding differences between the two runs. However, the situation in the northern hemisphere is quite different. For the control run in the northern hemisphere (summer circulation) baroclinic energy conversion from EAPE to EKE is not so strong. This, of course is due to the reduction of a vigorous baroclinically unstable wave activity during summer. However, the differences in the atmospheric energy cycle between the control run and the fixed-cloud run are comparatively larger than the natural variability of the model. For example, the differences in EAPE and EKE for the northern hemisphere are more than four times the natural variability. The presence of fixed clouds is equivalent to an asymmetric heat source which enhances the generation of EAPE and its conversion to EKE. The changes in other energy conversions are not so significant.

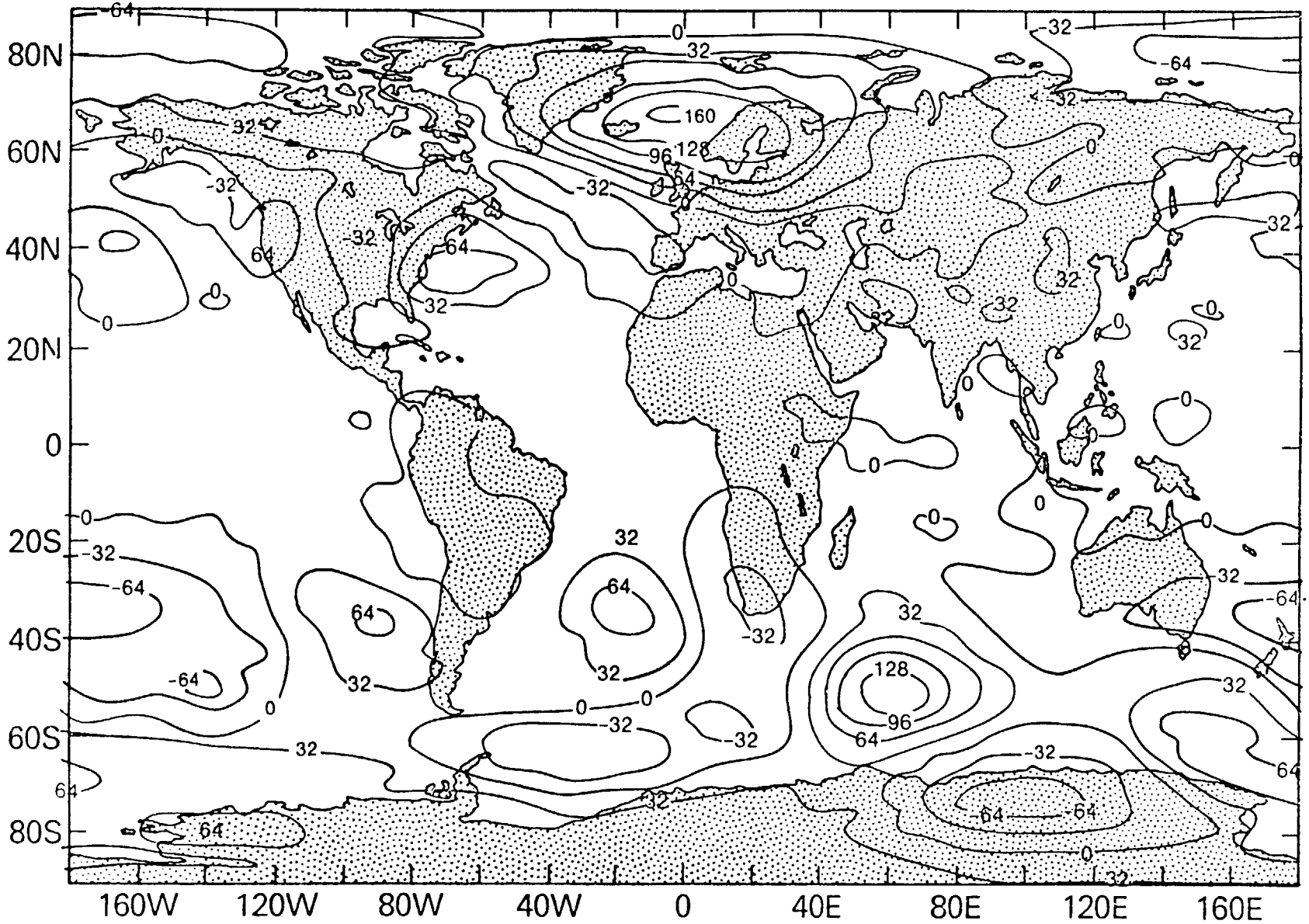
80N
60N
40N
20N
0
20S
40S
60S
80S
160W
120W
80W
40W
0
40E
80E
120E
160E

Figure 1

N. HEMISPHERE

ENERGY CYCLE

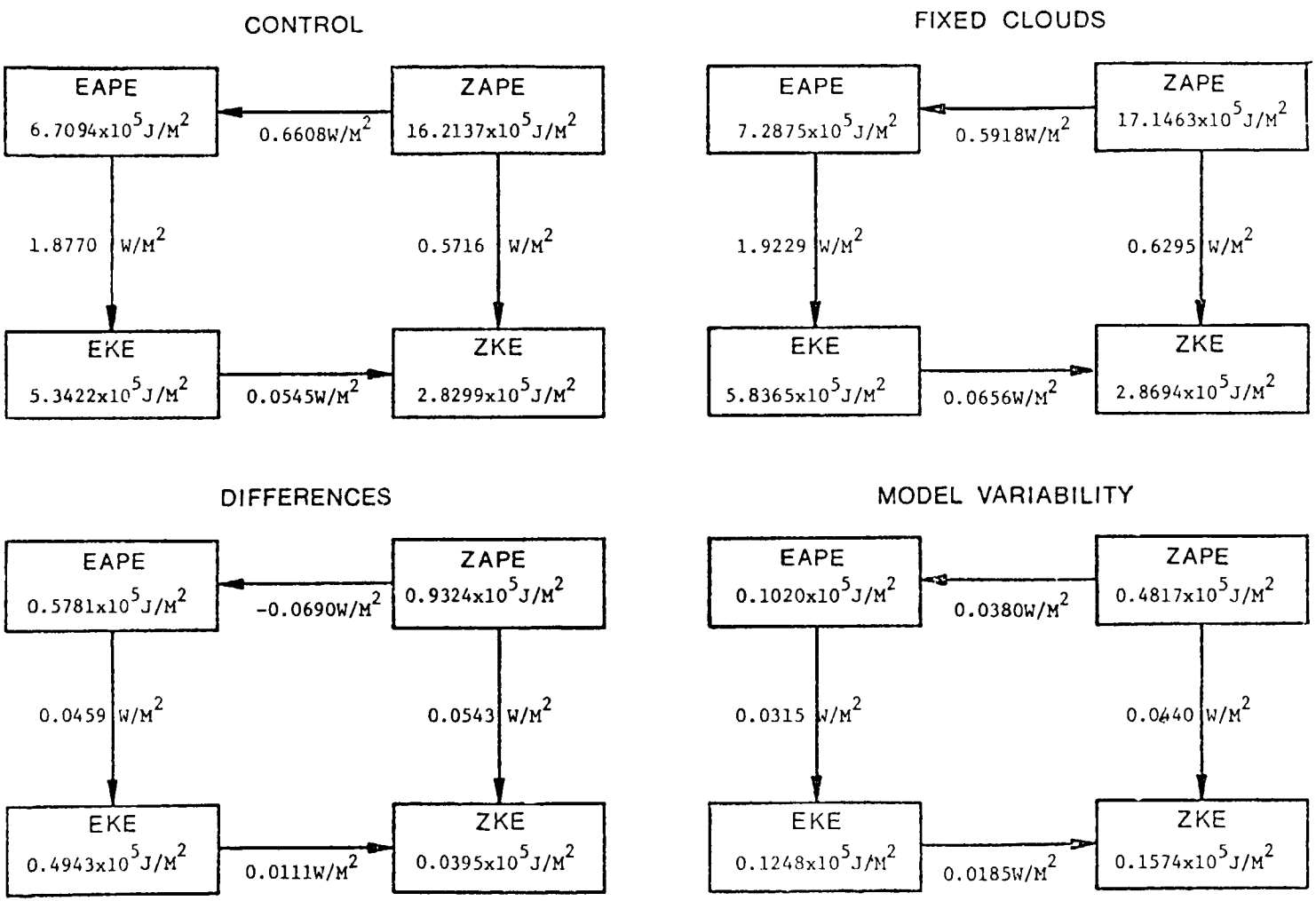

Figure 2

The differences in the energy cycles of the two runs suggest a mechanism through which cloud-radiation interaction can provide significant feedbacks to the dynamical circulation which, in turn, gives rise to significantly different local climate.

Figures 3 and 4 show the zonal root mean square differences in the evaporation and precipitation fields for the control and the fixed-cloud runs and its comparison with the average of the zonal root mean square difference between the control run and each of the three predictability runs. Between the latitudes 10°S-35°N, the differences between the control and the fixed-cloud run are twice as large as the difference between the control and the predictability runs. It should be pointed out, however, that the local variability is much larger than that inferred from the zonal averages and that variability over oceans is larger than that over the land. The differences between land and ocean evaporation and sensible heat flux (not presented) were also large. Although the sea surface temperatures were prescribed identically in both integrations, the changes in evaporation and precipitation were found to be much larger over the oceans compared to that over the land.

We suspect that this happened because the ground temperature was determined by the model's heat balance at the earth's surface and therefore internal model adjustments do not allow the hydrologic cycle over land to be very different between the fixed-cloud run and the control run. Based on these calculations, this study suggests that the processes of cloud radiation feedback are important in the general circulation of the model atmosphere and these should be adequately parameterized for a realistic interpretation of predictability and sensitivity studies carried out with a general circulation model.

Although it is well understood that the zonally asymmetric thermal forcing (heat sources and sinks) plays an important role in the dynamics of stationary and transient components of the general circulation, the contribution of radiation toward the total asymmetric thermal forcing is generally considered not to be significant. This study suggests that the radiative forcing, through cloud radiation interaction and associated changes in the hydrologic cycle, can be a significant component of the asymmetric thermal forcing.

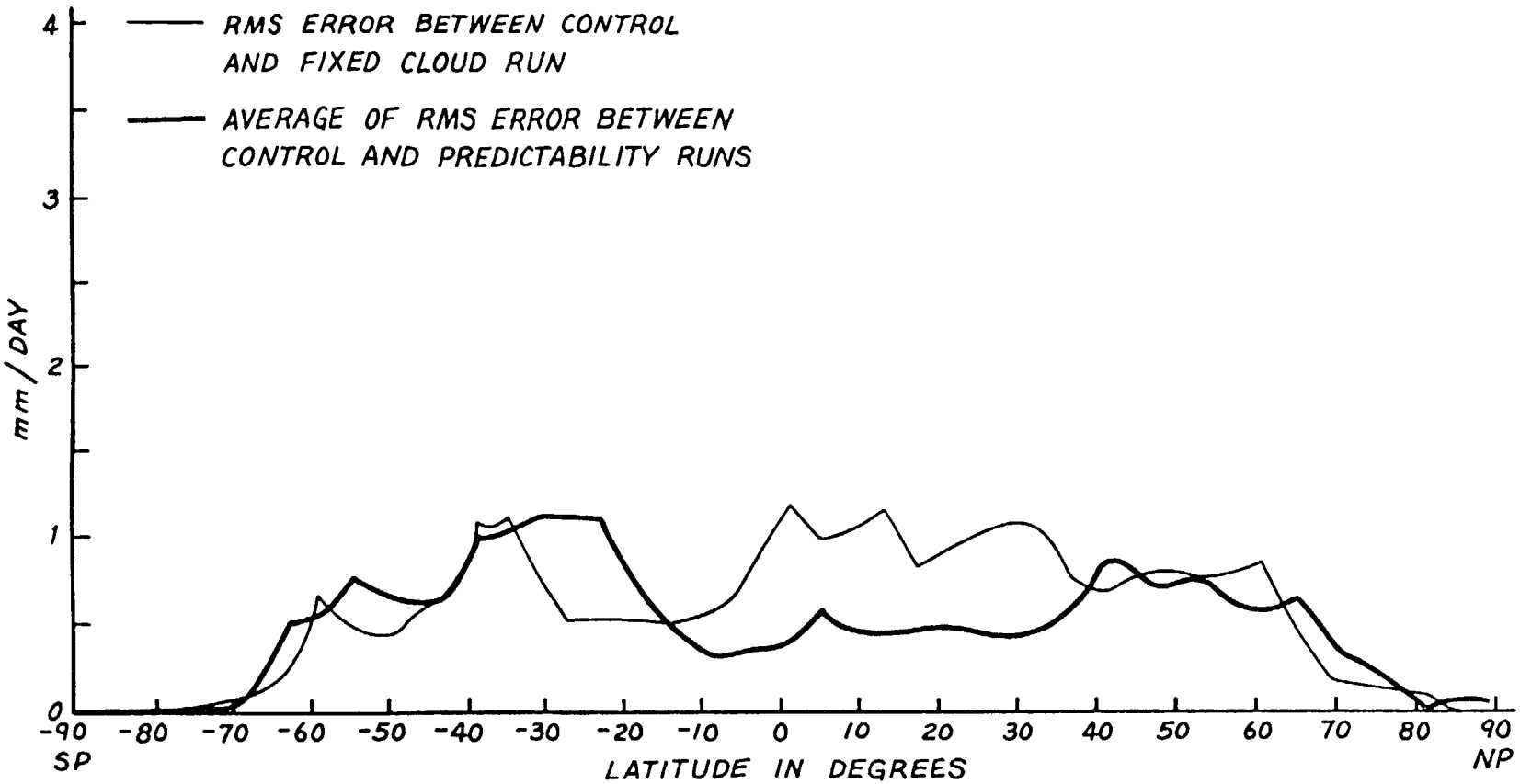
RMS ERROR BETWEEN CONTROL AND FIXED CLOUD RUN
AVERAGE OF RMS ERROR BETWEEN CONTROL AND PREDICTABILITY RUNS
mm / DAY
0
1
2
3
4
-90 -80 -70 -60 -50 -40 -30 -20 -10 0 10 20 30 40 50 60 70 80 90
SP
NP
LATITUDE IN DEGREES

Figure 3

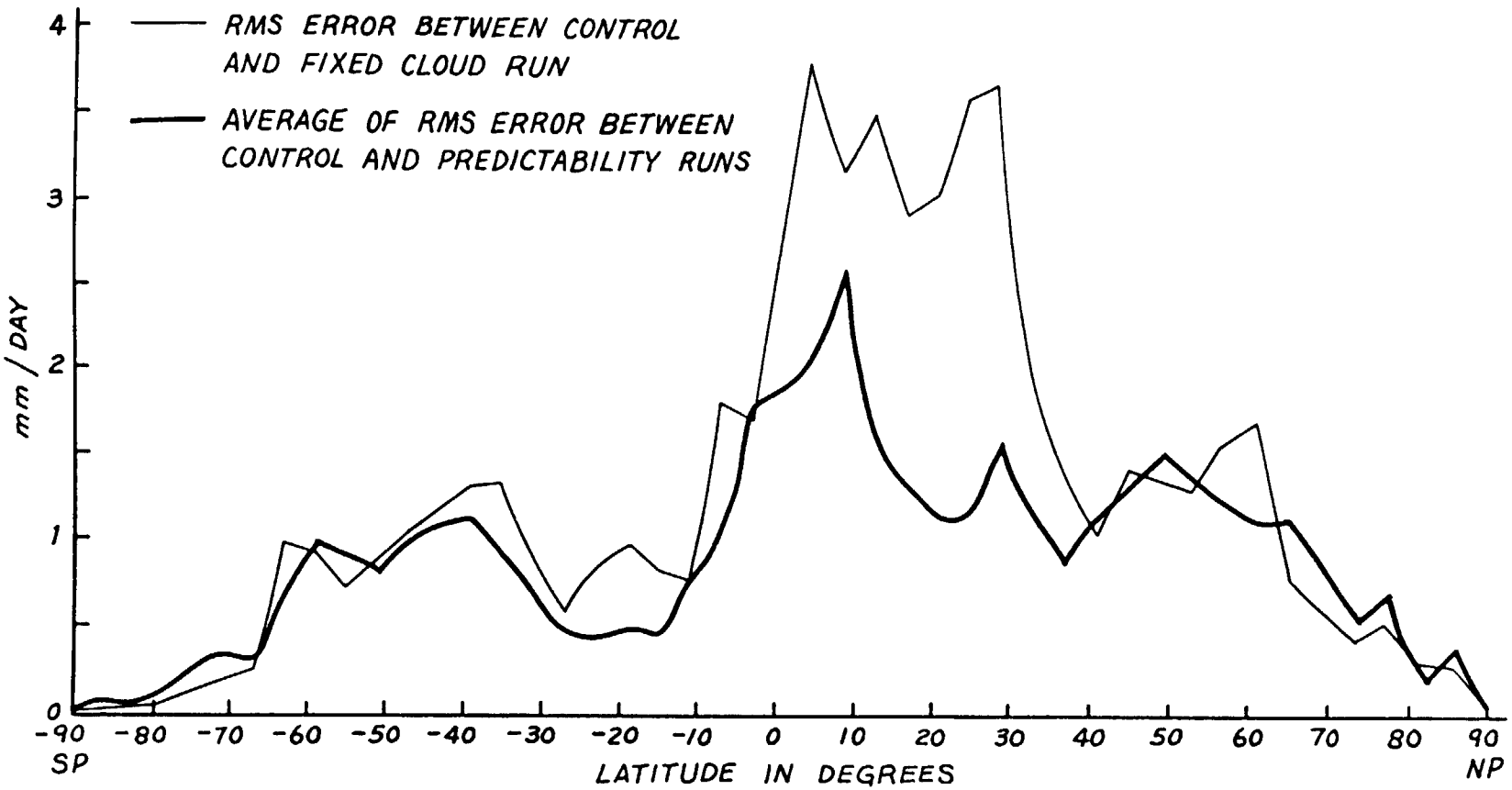
RMS ERROR BETWEEN CONTROL AND FIXED CLOUD RUN
AVERAGE OF RMS ERROR BETWEEN CONTROL AND PREDICTABILITY RUNS
mm / DAY
0
1
2
3
4
-90 -80 -70 -60 -50 -40 -30 -20 -10 0 10 20 30 40 50 60 70 80 90
SP
NP
LATITUDE IN DEGREES

Figure 4

LOW-LATITUDE CLOUD AMOUNT AND CLIMATE FEEDBACK

Robert D. Cess
Laboratory for Planetary Atmospheres Research
State University of New York
Stony Brook, New York 11794

Satellite observations of the outgoing infrared flux at the top of the atmosphere indicate that, at low latitudes, the flux is a maximum in winter and a minimum during the summer. This constitutes an anticorrelation with seasonal cloud amount, indicating that the major seasonal influence upon the outgoing flux comprises seasonal variability in cloud cover. This suggests the following "climate experiment" for estimating, at least for low-latitude seasonal cloud variability, the relative roles of albedo and atmospheric infrared opacity modifications due to changes in cloud amount.

Let F* denote the seasonal outgoing infrared flux for which the small (for low latitudes) contribution due to seasonal variations in surface air temperature has, through a model calculation, been removed. Thus, at least to first order, seasonal variability in F* is due to cloud amount variability. Moreover, let Q_a* represent the seasonal absorbed solar radiation, but with variability due to seasonal insolation and zenith angle effects having been removed. Thus, as with F*, the seasonal variation in Q_a* should be due mainly to seasonal cloud variability. The derivative dF^*/dQ_a^* would then represent the relative role of infrared versus solar modifications of the radiation energy budget due to cloud variability.

Employing monthly zonal values of F and Q_a, for low latitudes and from Ellis and Vonder Haar (1976), with subsequent conversion to F* and Q_a*, it is found that $dF^*/dQ_a^* \cong 1$, implying that the separate infrared and solar modifications to the radiation budget, for variable cloudiness, are compensatory. On the other hand, employing F and Q_a results from the NOAA-NESS data, quite a different result is obtained, $dF^*/dQ_a^* \cong 0.5$. These results are summarized below, with no values given for 5°N, since there was an insufficient seasonal signal at this latitude.

Summary of dF^*/dQ_a^*

Lat.	Ellis & Vonder Haar	NOAA-NESS
15°N	1.1	0.5
5°S	1.2	0.5
15°S	1.1	0.4

Interestingly enough, the above results are consistent with three totally different approaches to estimating dF^*/dQ_a^*. Ohring and Clapp (JAS, 1980), employing interannual variability in regional monthly means from NOAA-NESS data, and attributing this variability as due to interannual variability in cloud cover, estimate that globally $dF/dQ_a^* \cong 0.4$. In a related study, employing regional

day-to-day variability from NOAA-NESS data, Hartmann and Short (JAS, 1980) estimate that globally $dF^*/dQ_a^* \leq 0.5$. On the other hand, using latitudinal variability from the annually averaged Ellis and Vonder Haar data, Cess (JAS, 1976) estimates that $dF^*/dQ_a^* \cong 1.0$. Clearly conclusion concerning the relative infrared and solar modifications to the radiation budget, for variable cloudiness, are strongly dependent upon the satellite data which is employed.

CLIMATE CHANGE AND CLOUD FEEDBACK*

G. L. Potter
Lawrence Livermore National Laboratory
University of California
Livermore, California 94550

The sensitivity of outgoing longwave flux to changes in cloud cover ($\partial F/\partial A_c$) as defined by Cess (*J. Atmos. Sci., 33,* 1831-1843, 1976) must be evaluated carefully to avoid discrepancies arising from the interchange of averaging conventions. In a recent zonal atmospheric model experiment the global value of $\partial F/\partial A_c$ was negative. This behavior was traced to a latitudinal redistribution of cloud amount and height that occurred in the doubled CO_2 experiment.

We see from Figure 1 that the LLNL Statistical Dynamical Model (SDM) produced large cloud increases at 60°N and 40°S for the experiment. If the value of $\partial F/\partial A_c$ is calculated as a global number using the global values of δF and δA_c, then the ratio of $\partial F/\partial A_c$ is 76. However, if $\partial F/\partial A_c$ is calculated at each latitude and then averaged for the globe, the value is -99 which is in accordance with satellite observations (Cess, 1976). In addition to the averaging technique, the major reason for this difference is the latitudinal variation in cloud amount. The low latitudes, where the cloud amount decreased, are quite warm and the reduction in cloud amount further enhanced the already large longwave loss to space. The higher latitudes have much cooler temperatures and an increase in cloud amount there did not compensate sufficiently for the enhanced longwave radiation loss at the lower latitudes. The total global cloud fraction increased slightly because of the larger increase in the higher latitudes.

*This work was performed under the auspices of the U.S. Department of Energy by the Lawrence Livermore Laboratory under contract No. W-7405-Eng-48.

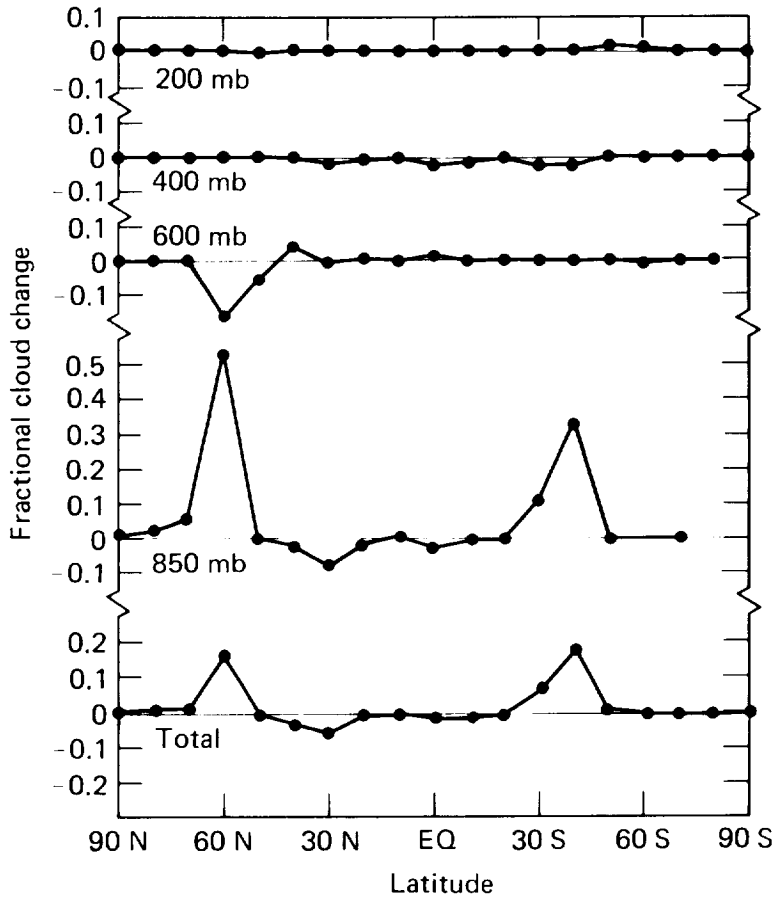

Figure 1. Change in cloud cover due to doubled atmospheric CO_2 at each of the heights where clouds are computed. The lowest line is the change in total cloud cover.

SENSITIVITY OF CLIMATE TO CLOUD PARAMETER VARIATIONS

Albert Arking and Ming-Dah Chou
Laboratory for Atmospheric Sciences
Goddard Space Flight Center
Greenbelt, MD 20771

and

Li Peng
Applied Research and Systems
Annapolis, MD 21401

A multi-layered zonally and annually averaged climate model with highly accurate radiation routines (Peng, et al., 1980) has been used to determine the sensitivity of climate to variations in cloud parameters. The results suggest a moderate sensitivity to changes in cloud amount, with the sign and magnitude highly dependent upon how the changes are distributed with respect to cloud type.

The variation in sensitivity is illustrated by two examples: (1) a 10% increase in cirrus clouds yields a change in the hemispheric mean surface temperature $\overline{\Delta Ts} = +.75°C$, and (2) a 10% increase of all cloud types yields $\overline{\Delta Ts} = -.74°C$. This study shows that for cirrus clouds the infrared "greenhouse effect" is dominant over the opposing solar "albedo effect", while the reverse is true for the middle and low level clouds.

Examination of the sensitivity of the radiative fluxes at the top of the atmosphere to cloud cover changes also reveals a very high dependence upon cloud type. The net sensitivity parameter for the two examples above are $\delta_1 = +84$ w/m^2 and $\delta_2 = -16$ w/m^2; for changes restricted to middle and low level clouds the sensitivity parameter is -92 w/m^2. This extreme variation with cloud type may explain why different answers are obtained when different methods are used to extract the parameter from climatological data. For example, the high sensitivity value for all clouds obtained by Ohring and Clapp (1980), -57 to -67 w/m^2, can be explained by the bias of their methods against cirrus clouds, which, if properly included, tend to cancel the effects of lower level clouds.

The latitudinal and vertical distribution of the response to changes in cloud cover amount or cloud height bears a close resemblance to that caused by a variety of other radiative forcings (e.g., change in solar constant, doubling of CO_2, enhancement of the stratospheric aerosol layer): in the lower troposphere the maximum response occurs at high latitudes and the minimum at low latitudes; in the upper troposphere the response has the same sign but its variation with latitude is reversed. These results suggest that the model, if not the real world itself, exhibits something like a "normal mode", in that no matter how you disturb the system it tends to respond the same way.

References

Ohring, G. and P. Clapp, 1980: The effect of changes in cloud amount on the net radiation at the top of the atmosphere, *J. Atmos. Sci., 37*, 447-454.

Peng, L., M. D. Chou and A. Arking, 1980: Climate simulations with a multi-layer energy balance model, in preparation.

THE SENSITIVITY OF MODEL-DERIVED RADIATION FLUXES TO THE MONTHLY MEAN SPECIFICATION OF CLOUDINESS[1]

Tony Gordon and Russell Hovanec
Geophysical Fluid Dynamics Laboratory/NOAA
Princeton University
Princeton, New Jersey 08540

1. Introduction

The investigation consists of two parts. First, monthly mean fields of low, middle, and high level cloud amount, generated for January 1977 by three different methods are compared. Second, the sensitivity of model-derived radiation fluxes to the above cloudiness fields as well as to zonally symmetric vs. asymmetric cloudiness is explored. The approach consists of integrating a moderate resolution spectral general circulation model (GCM) for one time step from January 1977 monthly mean initial conditions. The basic model is described in Gordon and Stern (1981). Radiation fluxes at the top, bottom, and interior of the atmosphere were calculated by the GCM's Fels-Schwarzkopf (1975) radiation scheme and stored on tape for later analysis. NOAA satellite data was used for verification.

2. Cloudiness Data Sets

The following monthly mean fields of fractional cloud amount were generated or reconstructed.

(i) 3D-NEPH. The Air Force Global Weather Central (AFGWC) 3D-NEPH data archive for January 1977 and the northern hemisphere was truly voluminous, spanning 60 tapes. We compressed this archive to a single tape, containing daily and monthly means of low, middle, high and total cloud amount on the spectral GCM's 3.3° x 5.6° Gaussian latitude-longitude transform grid. The layered amounts were normalized to be consistent with the smoothed reported total amounts, assuming random vertical stacking. Southern hemisphere data has not been processed. Instead, southern hemisphere Meleshko cloud amounts (see below) were merged with the northern hemisphere 3D-NEPH data.

(ii) SFC OBS. Surface-based cloud observations from the level II surface data archive (which includes ship reports) were assigned to the nearest 1° x 1° grid square, time-averaged and interpolated to the 3.3° x 5.6° grid. Each 1° x 1° grid square with observations on 2 or more days per month (represented by dots in Figure 1)[2] was allowed to influence the final monthly mean analysis. The latter was terminated at 30° S, due to the scarcity of data.

(iii) Meleshko. Cloudiness at three levels was derived from monthly mean outgoing long wave flux data, vertical profiles of temperature and water vapor and 3D-NEPH total cloudiness (northern hemisphere) and SFC OBS total cloudiness (southern hemisphere). Wherever a

[1] A more comprehensive version of this manuscript is being submitted to Mon. Wea. Rev.

[2] When looking at the figures, remember that "3D-NEPH clouds" denotes 3D-NEPH cloud amounts in the northern hemisphere merged with Meleshko cloud amounts in the southern hemisphere.

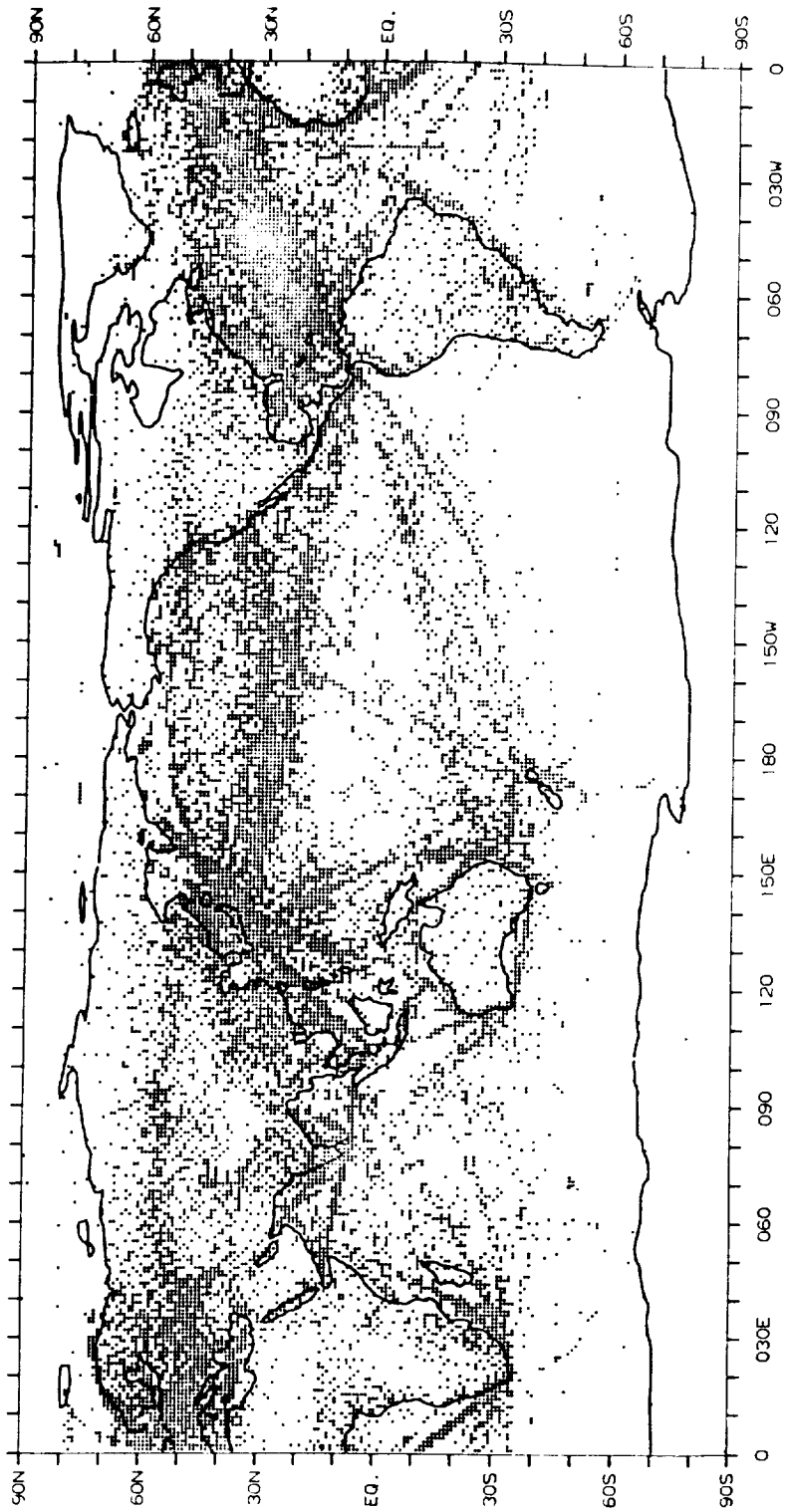

Figure 1. Geographical distribution of 1° x 1° grid squares which affected the final SFC OBS cloud amounts. Each such square is represented by a dot.

low level inversion existed, however, the low level cloud amount was set to the total while the middle and high level amounts were set to zero. The scheme was developed by Meleshko, a visiting scientist at the Geophysical Fluid Dynamics Laboratory during 1978. Refer to Meleshko and Wetherald (1981) for further details.

3. Summary of Results

(i) High level 3D-NEPH clouds are poorly correlated with SFC OBS clouds (see Figure 2). But the former are more consistent, radiatively, with NOAA satellite verification data (see Figure 4). The correlation for low level 3D-NEPH vs. SFC OBS cloudiness is fair to good overall. It is best in middle latitudes where the 3D-NEPH analysis probably incorporates numerous surface-based observations. The Meleshko cloudiness at low as well as high levels is unrealistic over land in the northern hemisphere extratropics due to the existence of low level inversions. Meleshko cloudiness is well correlated with 3D-NEPH cloudiness in the tropics where both rely on satellite data. Over Brazil and southern Africa, the Meleshko scheme senses the cold high level cloud tops but not their (optical) depth. This may help explain its bias there towards high level cloudiness.

(ii) Model-derived radiation fluxes at the top of the atmosphere are highly sensitive to cloud amount in the tropics and into the summer hemisphere, but quite insensitive to the water vapor distribution (see Figures 4, 5, and 6). In the northern hemisphere extratropics, the outgoing long wave flux is strongly dependent on surface temperature (cf. Figures 3 and 4).

(iii) Longitudinally asymmetric 3D-NEPH cloud amount fields are substantially more consistent with satellite verification data, in the tropics, than their zonal mean counterparts are (see Figures 5 and 6).

(iv) Long wave cooling rates in the interior of the atmosphere are sensitive to cloud amount even in the northern (winter) hemisphere extratropics, and somewhat sensitive to water vapor (not shown here).

4. Conclusions

(i) The 3D-NEPH cloud analysis must use a vast amount of satellite measurements of outgoing longwave and reflected short wave fluxes, despite fears to the contrary by some potential users. This enhances the consistency of the 3D-NEPH model-derived fluxes with observation.

(ii) Overall, the monthly mean 3D-NEPH cloud amounts are likely the best global cloud data set currently available and certainly a step beyond the 25-year-old London monthly zonal mean climatology. It is unfortunate that a compressed format of 3D-NEPH clouds suitable for cloud climatology or long-range forecasting applications is not readily available. The 1977-1979 period or FGGE period would be excellent for a cloud climatology comparison study which included 3D-NEPH clouds. In fact we are currently analyzing 3D-NEPH, SFC OBS and Meleshko clouds for July 1979.

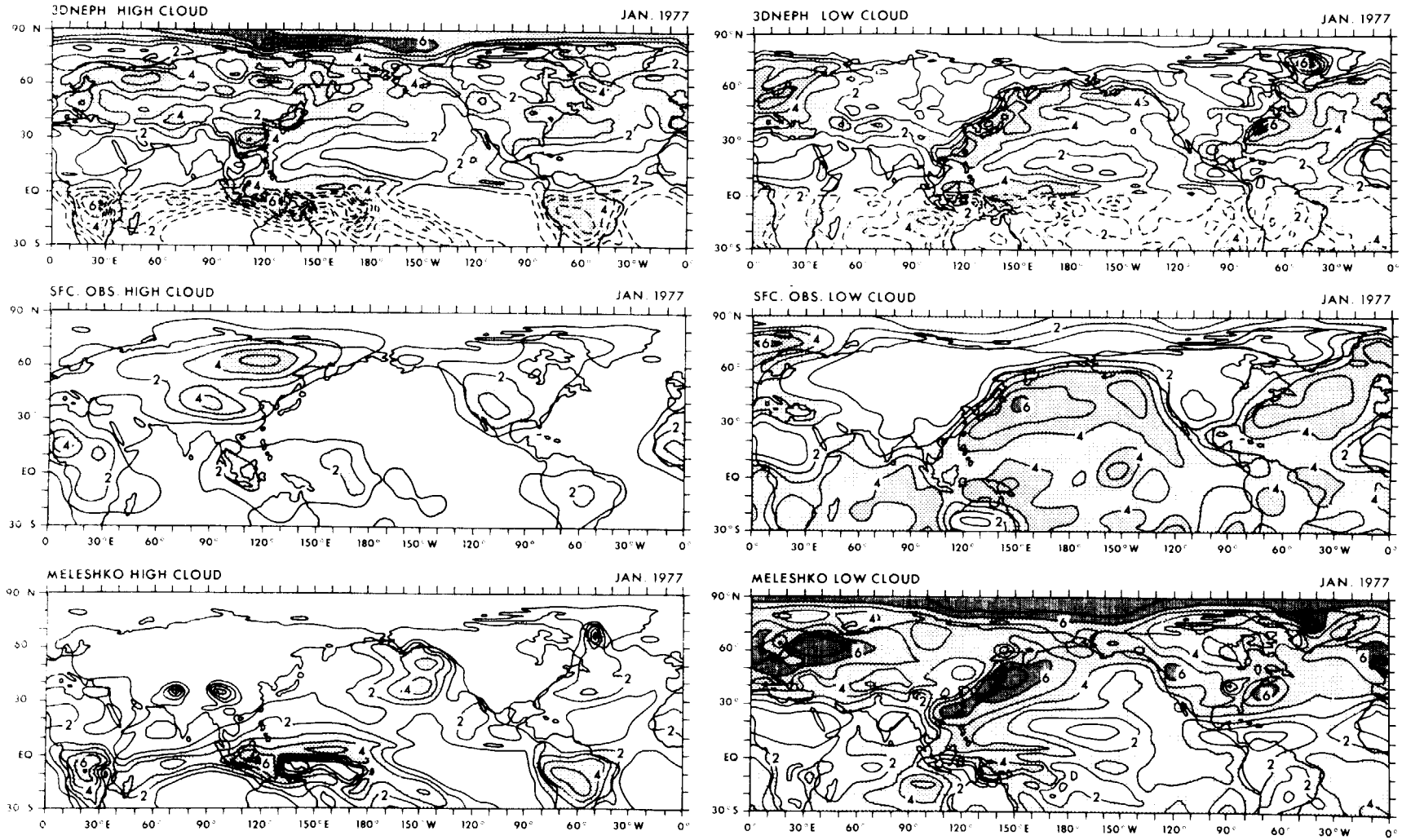

Figure 2. High and low level cloud amounts for 3D-NEPH, SFC-OBS, and Meleshko January 1977 monthly mean data sets. Domain is 90°N-30°S. Cloud interval = 0.1. Dashed contours in 3D-NEPH panels signify Meleshko cloud data.

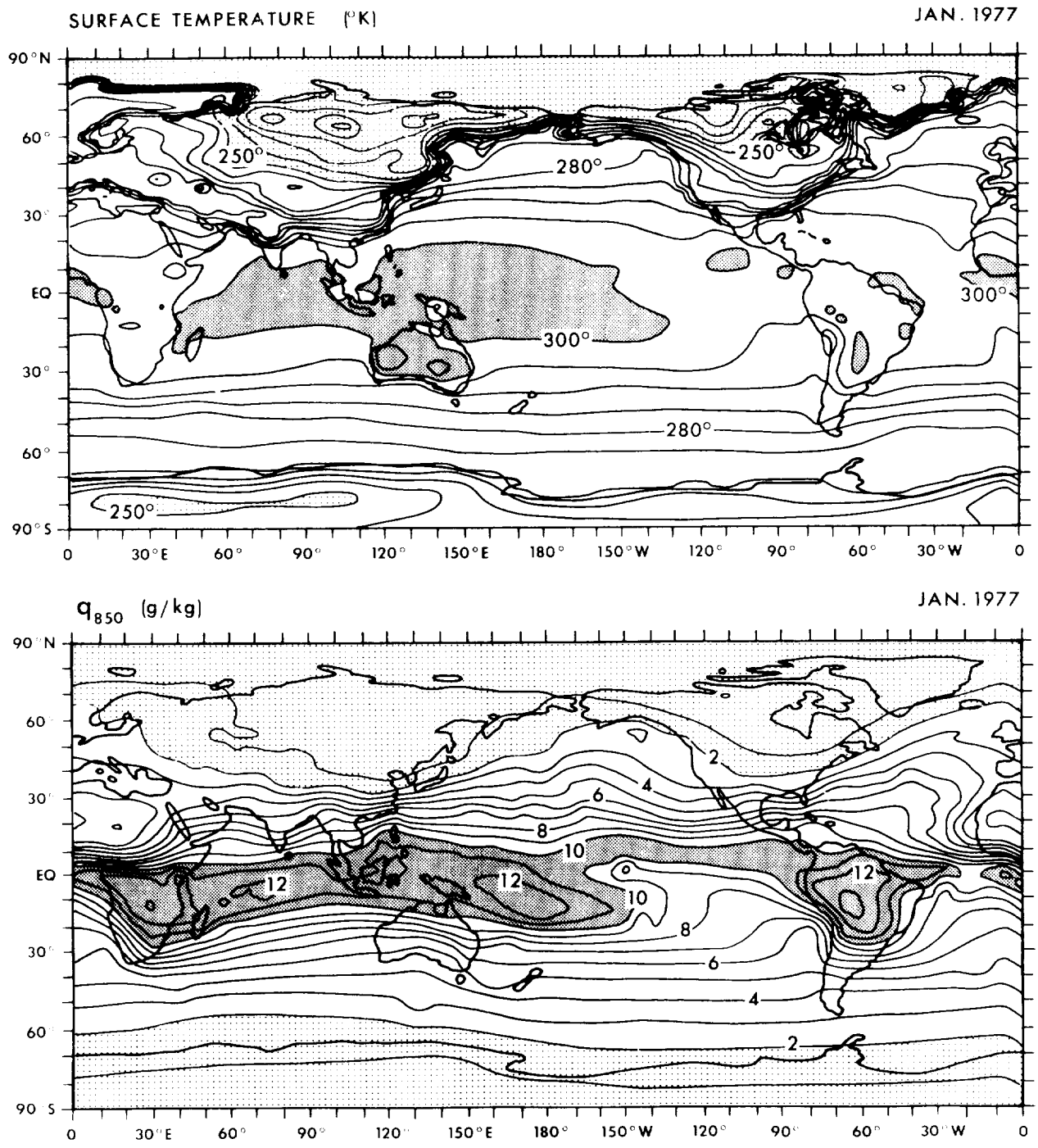

Figure 3. Monthly mean optimal interpolation analysis of water vapor mixing ratio at 850 mb (top). Contour interval = 1 g/kg. Model-computed surface temperature (bottom). Contour interval = 5°K.

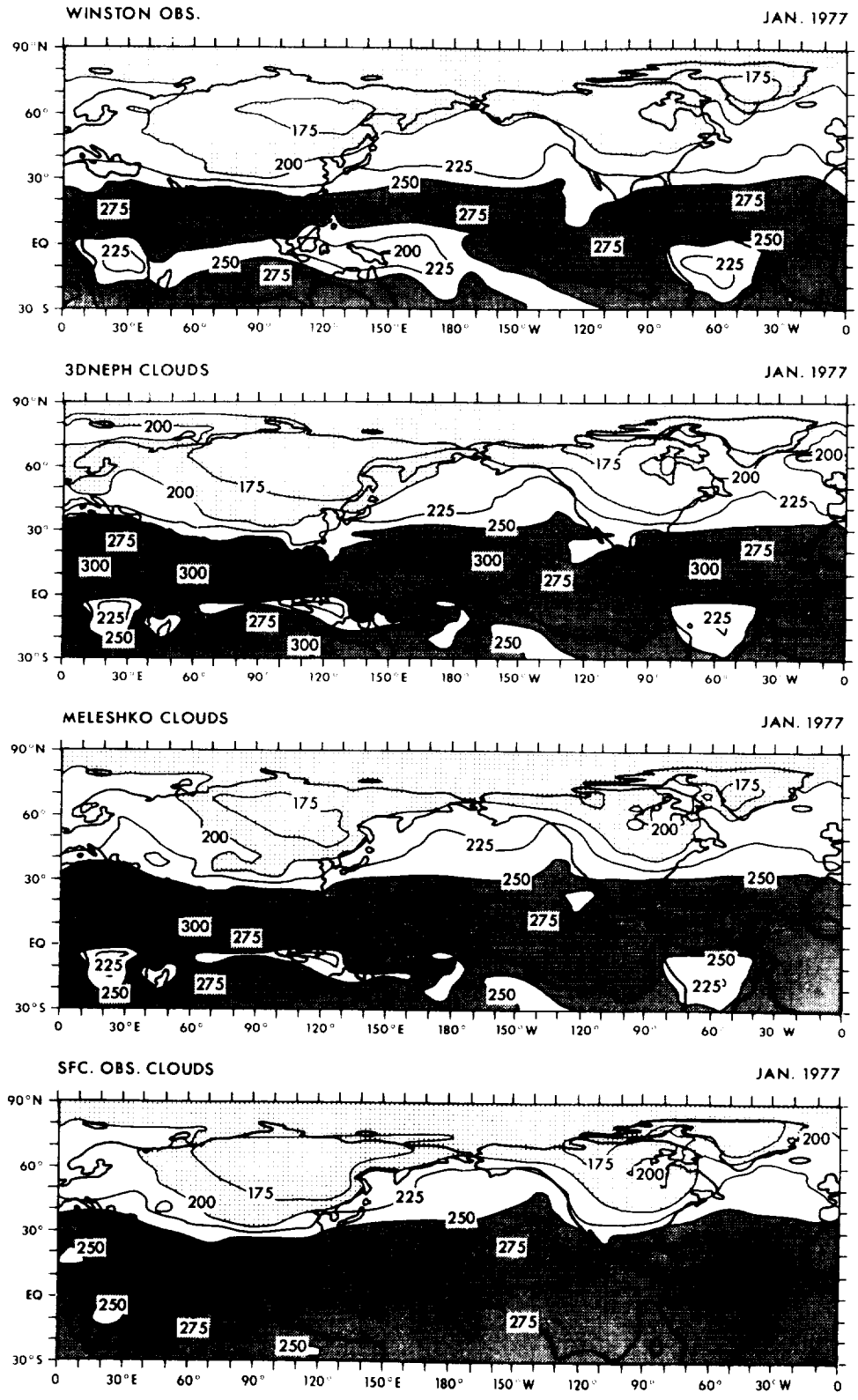

Figure 4. Outgoing long wave radiation flux. From top to bottom: (i) NOAA-5 satellite verification data (WINSTON OBS); (ii) 3D-NEPH clouds result; (iii) Meleshko clouds result; and (iv) SFC OBS cloud result. Domain is 90°N to 30°S. Contour interval = 25 w/m^2. Cloud emissivity = 1.

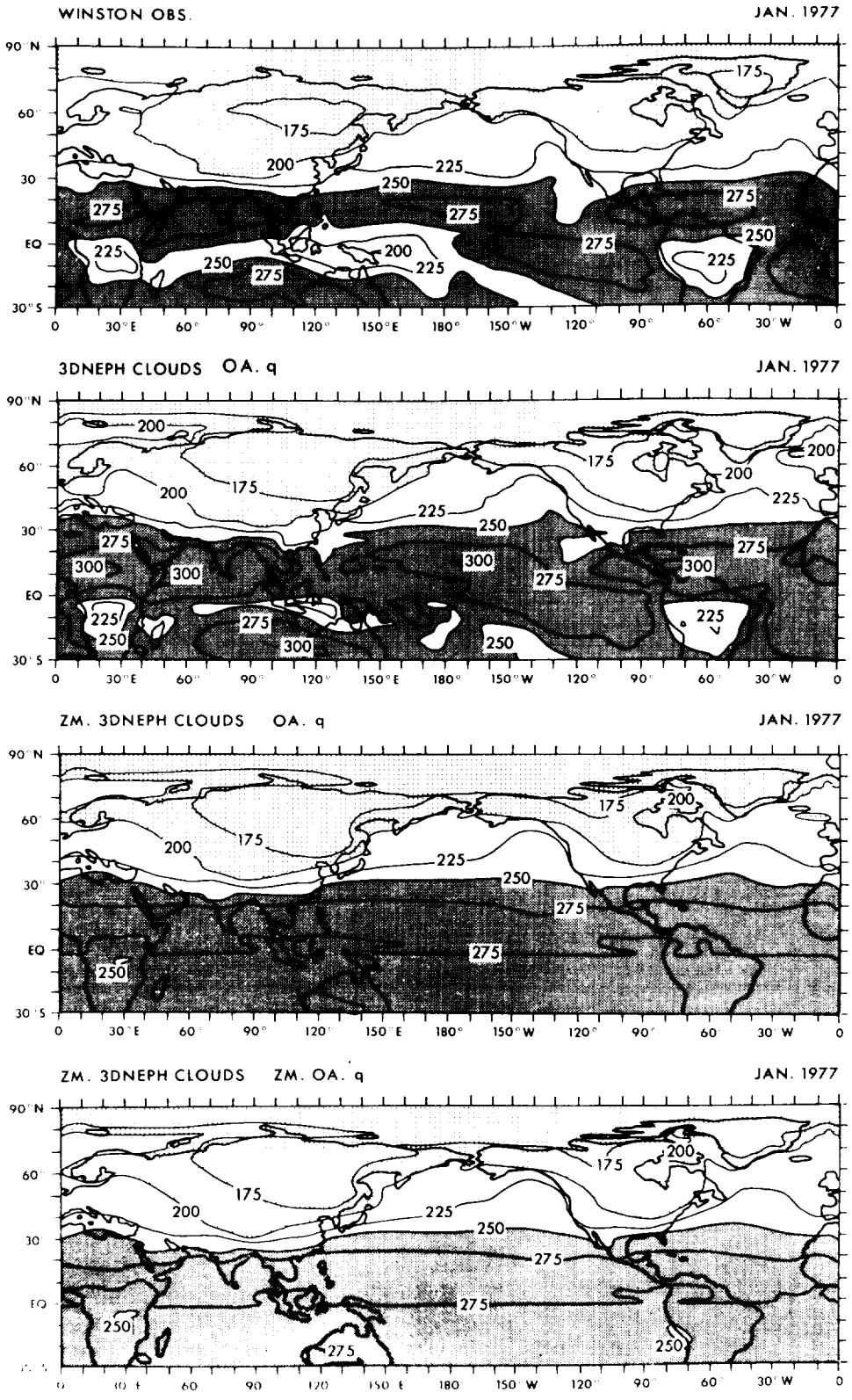

Figure 5. Outgoing long wave radiation flux. From top to bottom: (i) NOAA-satellite verification data; (ii) 3D-NEPH clouds plus optimally analyzed mixing ratio (OA.q) results; (iii) zonal mean (ZM) 3D-NEPH clouds plus ZM.OA.q. Domain = 90°N-30°S. Contour interval = 25 w/m^2. Cloud emissivity = 1.

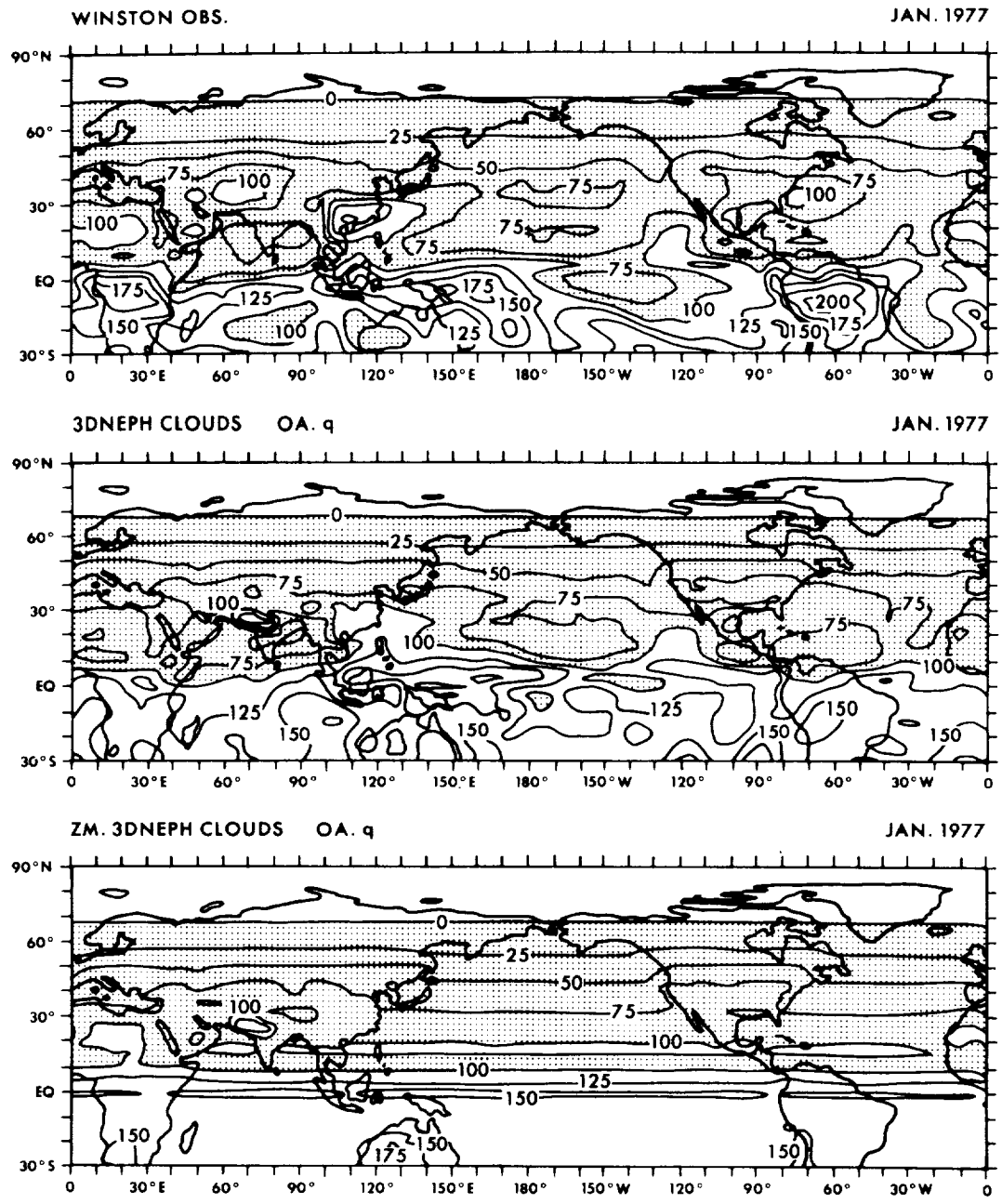

Figure 6. Reflected shortwave radiation flux at top of atmosphere. From top to bottom: (i) NOAA-5 satellite narrow band (0.5-0.7 μm) verification data; (ii) 3D-NEPH clouds broad band result; (iii) zonal mean 3D-NEPH clouds broad band result. Domain is 90°N-30°S. Contour interval = 25 w/m^2. Cloud albedo for low, middle and high cloud levels are 0.69, 0.48, and 0.21, respectively. Observed snow cover influenced the specification of surface albedo.

(iii) We suspect that like the 3D-NEPH, a good cloud climatology should incorporate surface observations of low level clouds as well as satellite observations of total and higher level clouds. If done carefully, one might be able to augment the information content of the data set without losing all capability for independent verification.

(iv) The discontinuities in our long wave cooling at 335 mb (not shown) at latitudes where the pre-specified cloud top height jumps by roughly 150 mb, underscores the need for accurate specification of cloud top heights.

(v) Improved estimates of cloud albedos and emissivities should be updated into our radiation model.

References

Fels, S. B. and M. D. Schwarzkopf (1975): The Simplified Exchange Approximation: A New Method for Radiative Transfer Calculations. *J. Atmos. Sci., 32,* 1475-1488.

Fye, Falko, K. (1978): The AFGWC Automated Cloud Analysis Model. AFGWC Technical Memorandum 78-002. 97 pp.

Gordon, C. T. and W. F. Stern (1981): A Review of the GFDL Global Spectral Model. (To be submitted for publication to *Mon. Wea. Rev.*)

Melshko, V. P. and R. T. Wetherald (1981): The Effect of a Geographical Cloud Distribution on Climate: A Numerical Experiment with an Atmosphere General Circulation Model. (Submitted for publication in *J. Geoph. Res.*)

Stephens, G. L. and P. J. Webster (1979): Sensitivity of Radiative Forcing to Variable Cloud and Moisture. *J. Atmos. Sci., 36,* 1542-1556.

3.3 SUMMARY

W. B. Rossow
NASA/Goddard Institute for Space Studies
New York, New York 10025

The discussion among the Workshop participants following each of the formal presentations generally concerned the issues raised in those presentations; however, certain key ideas seemed particularly important as evidenced by their repeated occurrence in the discussions. These ideas are briefly listed to summarize the first day's discussion.

1. Identifying the most important cloud properties for modeling or observational studies requires definition of the particular cloud–climate interaction being considered. The two key interactions recognized during the Workshop define two types of clouds: radiative clouds are those kinds of clouds that dominate the cloud–radiation interaction and transport clouds are those kinds of clouds associated with small–scale vertical transport of heat and moisture. The most important properties and cloud types constituting each of these categories have not been fully identified as yet.
2. The relation between cloud structure and cloud optical properties is one of the best understood areas of cloud physics; however, even the large general circulation climate models generally do not incorporate this understanding. In most models the radiative treatment of clouds is very crude, often improper. Improvements in radiative treatment are possible.
3. The relation between small–scale vertical transport processes and large–scale cloud and dynamic systems is one of the worst understood areas of cloud physics. Although some excellent data exist, they are not sufficiently complete or numerous to diagnose completely all the processes or to determine how typical the results are. Both cumulus convective cloud systems and boundary layer stratus systems deserve special attention.
4. Current cloud parameterizations do not make use of complete water budgets although they insure that total precipitation equals total evaporation. Some progress in parameterizing the large–scale effects of convective cloud complexes may be obtained by incorporating liquid water and vapor budgets. If cloud liquid water contents are predicted in models, more realistic parameterization of the radiative effects of clouds would be possible.
5. Most model and observational studies have focused on the correlation between cloud fractional cover and surface temperature. Other, possibly more important, correlations in the climate remain unexamined. Evaluation of cloud–climate feedbacks and climate sensitivities in terms of a single correlation may be misleading.
6. Two types of observational data are still obviously needed for further progress: detailed "process" data to improve cloud physics parameterization and global, long term climatology data to verify model performance. Emphasis was placed on climatological data to establish the cloud–radiation interaction in the climate, but verification of spatial and temporal variations of clouds predicted by climate models is an especially sensitive test of all aspects of the model performance.

4. SATELLITE OBSERVATIONS

4.1 CLOUD CLIMATOLOGIES

REVIEW OF CLOUD CLIMATOLOGIES

Eric A. Smith
Department of Atmospheric Science
Colorado State University

I am going to cover three topics in this short review. The first topic is a brief summary of what we have available now in the way of global cloud climatologies from satellite observations. Most of this material is based on a review report by Olev Avaste and a group of his colleagues, along with a group of us at C.S.U., that was done last year. This research basically involved an analysis of the Miller and Feddes (1971) data, which were derived from the ESSA satellite series from 1967 to 1970, and the Sadler et al. (1968, 1976) cloud amount data, which were based on NOAA operational satellites over the years 1965 to 1973 (also see Steiner, 1978).

After I show a few of the results that were found in that data, I would like to discuss a number of techniques that have been proposed to estimate cloudiness, cloud amount, and cloud height from satellite data. Then, if there is any time left, I will just touch on some of the highlights of the calibration, sensitivity monitoring, and inter-comparison problems, inherent with satellite data sets, along with some of the potential solutions.

What do we have right now? Avaste et al. (1979), using the two data sets I mentioned, did an analysis of the data over the regions indicated in Figure 1. These little numbers indicate a latitude-longitude coordinate system, and the large numbers indicate the oceanic region.

You will notice this is an analysis based only on oceanic clouds. A series of charts, similar to the North Atlantic chart shown here in Figure 2, were produced for each oceanic region. The two data sets were averaged in a monthly sense, some broad cloud amount categories were developed, and then analyzed for each of the individual trapezoids. Don't think of this as a latitude-longitude scale, because you are looking at the individual trapezoidal quantities across the monthly axis, and these "A", "B", "C", "D's" are basically cloud amount categories at about a 20 percent spacing.

So, there is available now, a set of these monthly cloud amount charts for the individual oceans, divided by North, South, Atlantic, Pacific, and Indian Oceans.

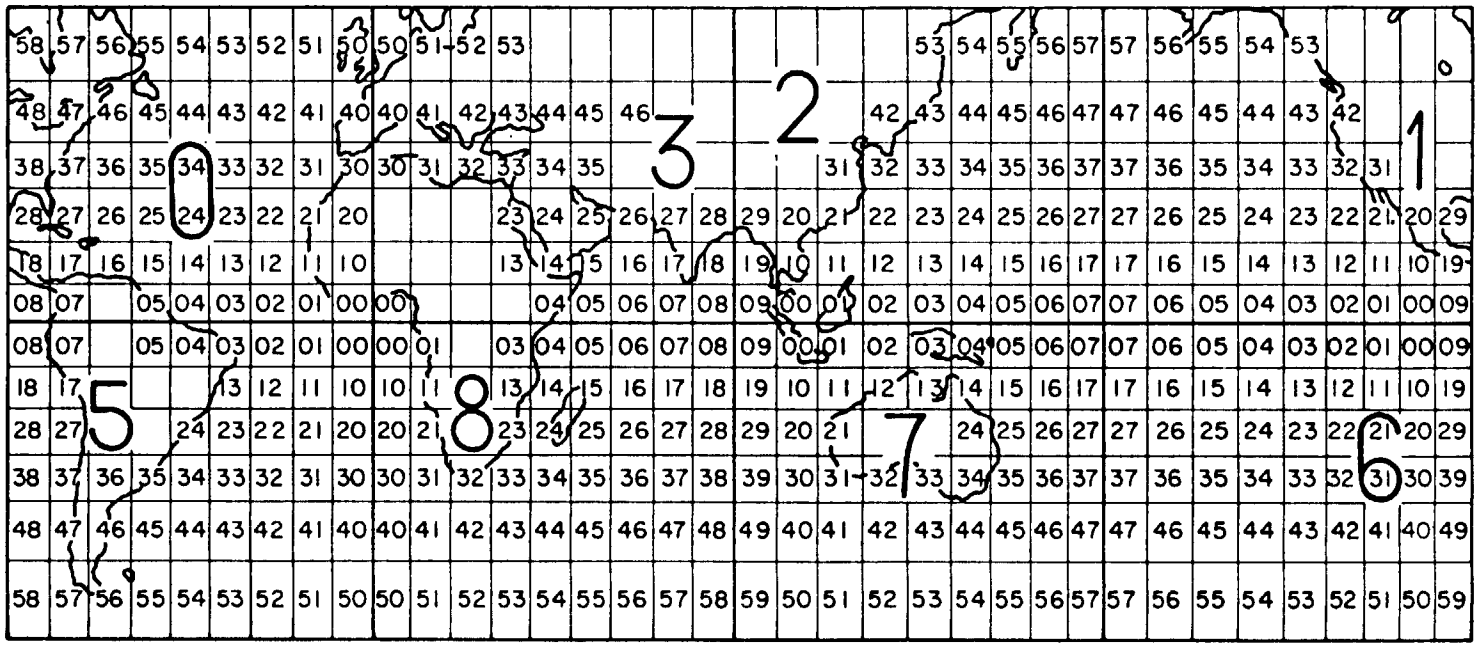

Figure 1. World map showing the trapezoid number. (After Avaste et al., 1979.)

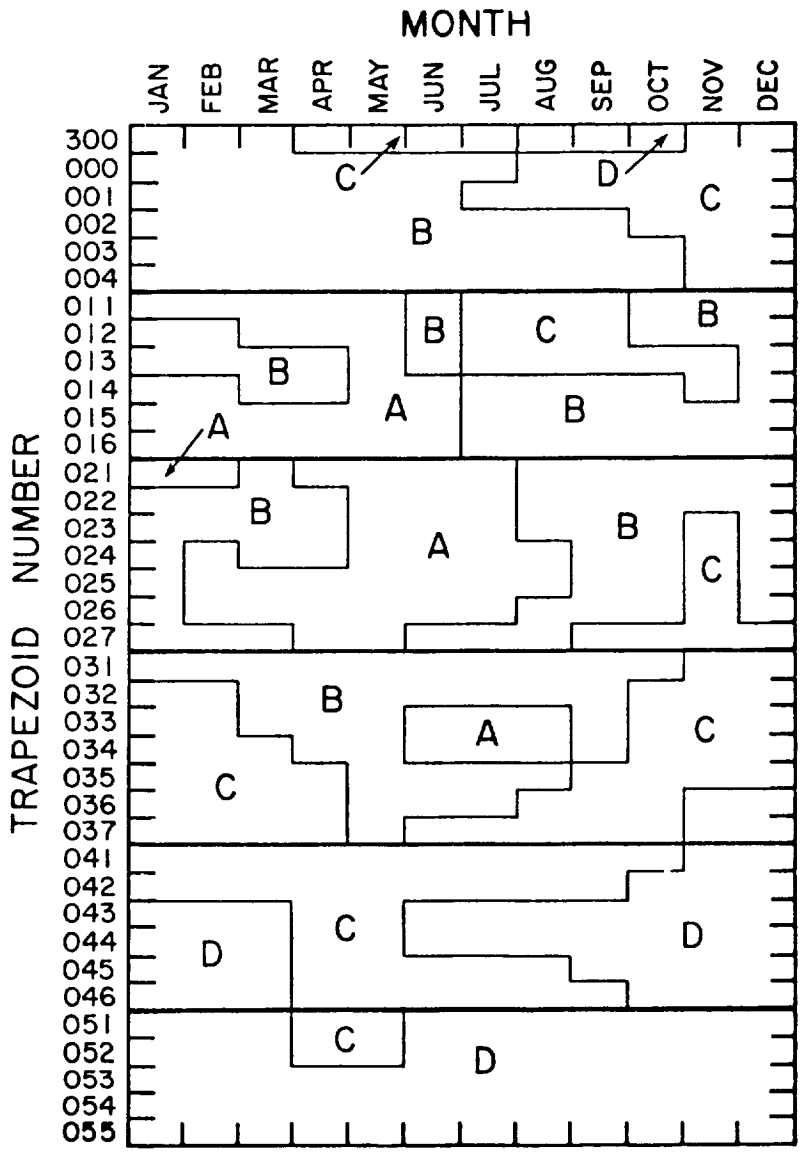

Figure 2. Annual variability in cloud amount over the northern half of the Atlantic Ocean. (After Avaste et al., 1979.)

AUDIENCE PARTICIPANT: What do those letters refer to?

MR. SMITH: These are broad cloud amount categories, 0 to 20 percent, 20 to 35 percent, 35 to 50, and greater than 50, which is a "D". "A" is the small, "D" is the large. Again, this analysis was based on the Miller and Feddes data set and the Sadler data.

Now, in addition, some trends of cloudiness were examined. Here in Figure 3, is a selection of data over the so-called GATE region, which for our purposes is just the terminology for the Eastern Atlantic. Two space scales were examined. The thinner line is the larger, 30-degree scale; the thicker line is a 10-degree scale. The data were plotted by months, and the trends investigated over the years from 1965 to about the middle of 1973.

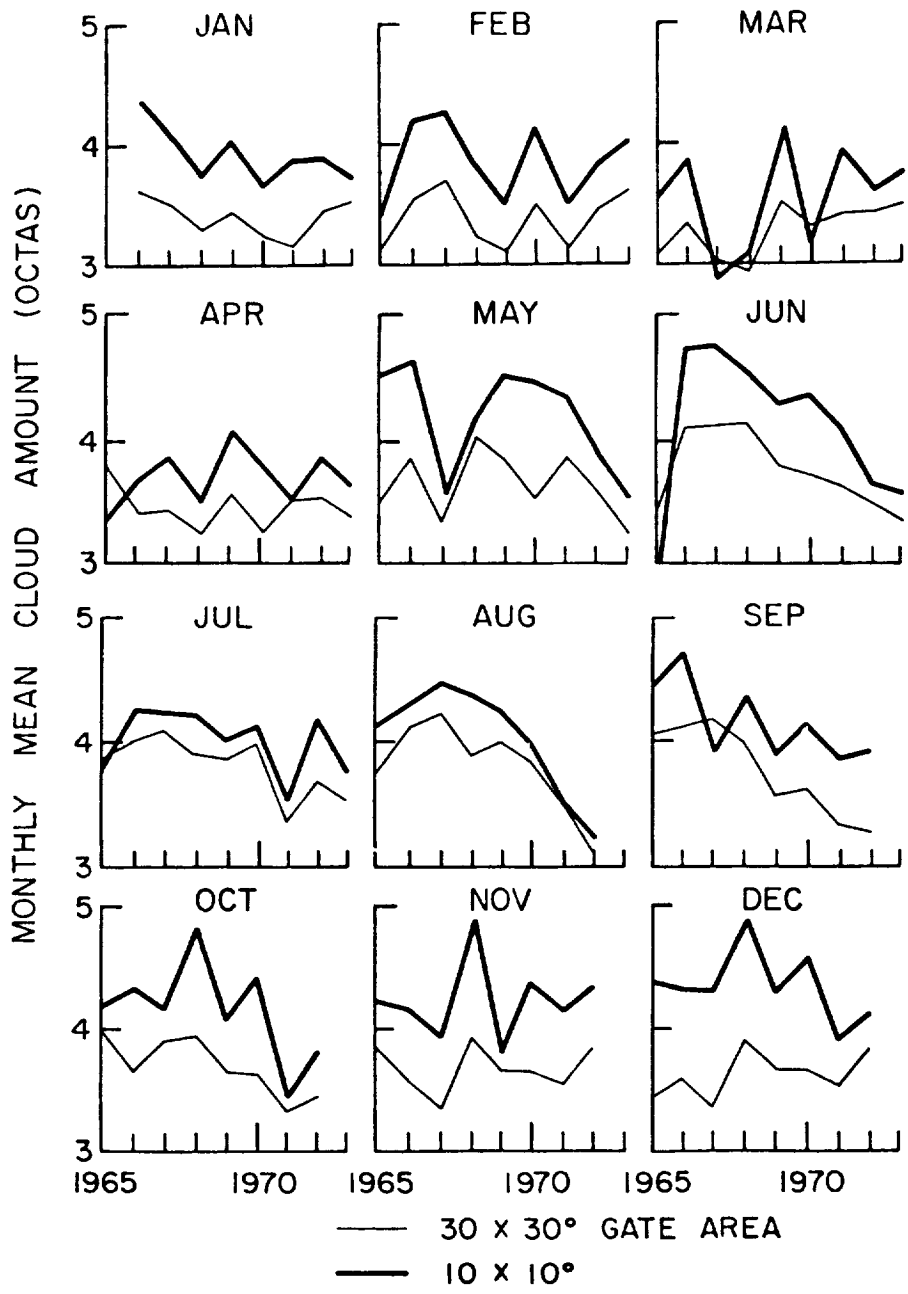

Figure 3. Trend of cloud amount in the GATE region at two scales.
(After Avaste et al., 1979.)

There are a few things in evidence from this analysis; the most obvious is that there seemed to be a decrease in overall cloudiness over the 8-year period, although it was primarily confined to the summer months. If you look at these graphs carefully, you will see that the June through October period is where the decrease was mainly contained. You will also note, if you compare the two space scales (in which the 10-degree scale was imbedded in the center of the 30-degree scale) that the 10-degree scale shows a lot more variation. Of course, part of that variation can be explained as the

expected year-to-year variability of the position and intensity of what Avaste prefers to call the maximum cloudiness zone (MCZ), which I believe is Sadler terminology for what most of us call the I.T.C.Z.

An interesting question is whether the 30° scale variability has, at its own space scale, a seasonal variability, or whether we can interpret the 30° year-to-year decrease strictly as a short-period climatic trend.

Before I go on, I will show a similar set of graphs (Figure 4) for three zones in the Pacific Ocean; 0 to 30° south, 0 to 30° north, and 30° to 60° north. Again you see the cloudiness decrease over a period primarily confined to the summer months.

One of the problems with analyzing data of this sort is choosing the appropriate grid scale resolution for studying cloud amount. What is shown in Figure 5, again for the GATE region (and I have just colored in a few cases to indicate the differences) are monthly averages for the period 1965 to 1972 for a 30-degree grid scale, a 10-degree grid scale, and a 2.5-degree grid scale. This figure shows you in a qualitative sense, that the selection of the resolution, that is the grid resolution, can determine a great deal of how you interpret cloud variability. You can see as you go to the higher scale, the structure of cloudiness, and the characteristics of the *change* in cloudiness with season, are much different.

The real question about this analysis, and the reason Avaste et al. (1979) were a little bit hesitant to go ahead and publish, is because there is a basic question concerning the accuracy of the Miller and Feddes (1971) and Sadler et al. (1968, 1976) data sets. Those data are not truly objective in the computer sense of the word. There was a great deal of human interaction with selecting cloud amount from the imagery, using what some of us would refer to as the bi-optical technique, i.e. using the eye to measure cloud amount.

These are the best satellite-derived global data we have available, however, if one compares the two data sets over the intersection period of 1967 to 1970, the comparison is not favorable. The two dimensional histogram shown in Figure 6 is used to illustrate that if there were good comparison, these points would fall along the diagonal. In fact, they fall off the diagonal, and this indicates there is no unique relationship between the two data sets. The pattern is smeared out and fairly broad. This curved line is simply an attempt at fitting the scattered points with a second-degree polynomial best fit line. The point is that the comparison is not that good and thus it opens up a lot of questions as to whether we should interpret trends and whatnot.

Another question that has come up quite often is whether we can go back to some of the radiation budget archives over the latter part of the 1960's and the early 1970's and use the budget data to re-derive cloud amount. These next two figures show how well we might do in attempting to relate cloud amount to shortwave albedo or longwave emitted flux. Figure 7 is a comparison between the Sadler cloud amount data and global albedo data derived from the scanning radiometer instruments flown on the NOAA operational weather satellites (see Winston and Gruber, 1979). Again, you see the problem of a very smeared, a very broadly smeared pattern. In other words, there does not seem to be a unique relationship between cloud amount and simple parameters available from the data

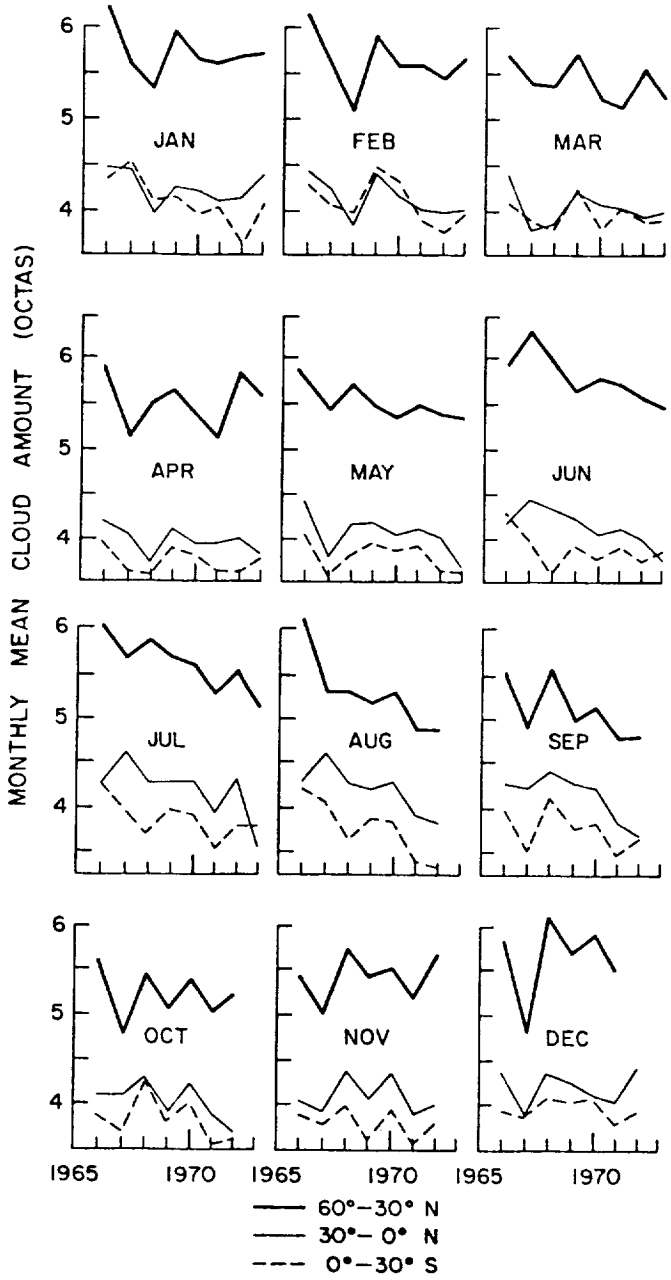

Figure 4. Monthly mean variations of cloud amount for three latitudinal zones over the Pacific Ocean. (After Avaste et al., 1979.)

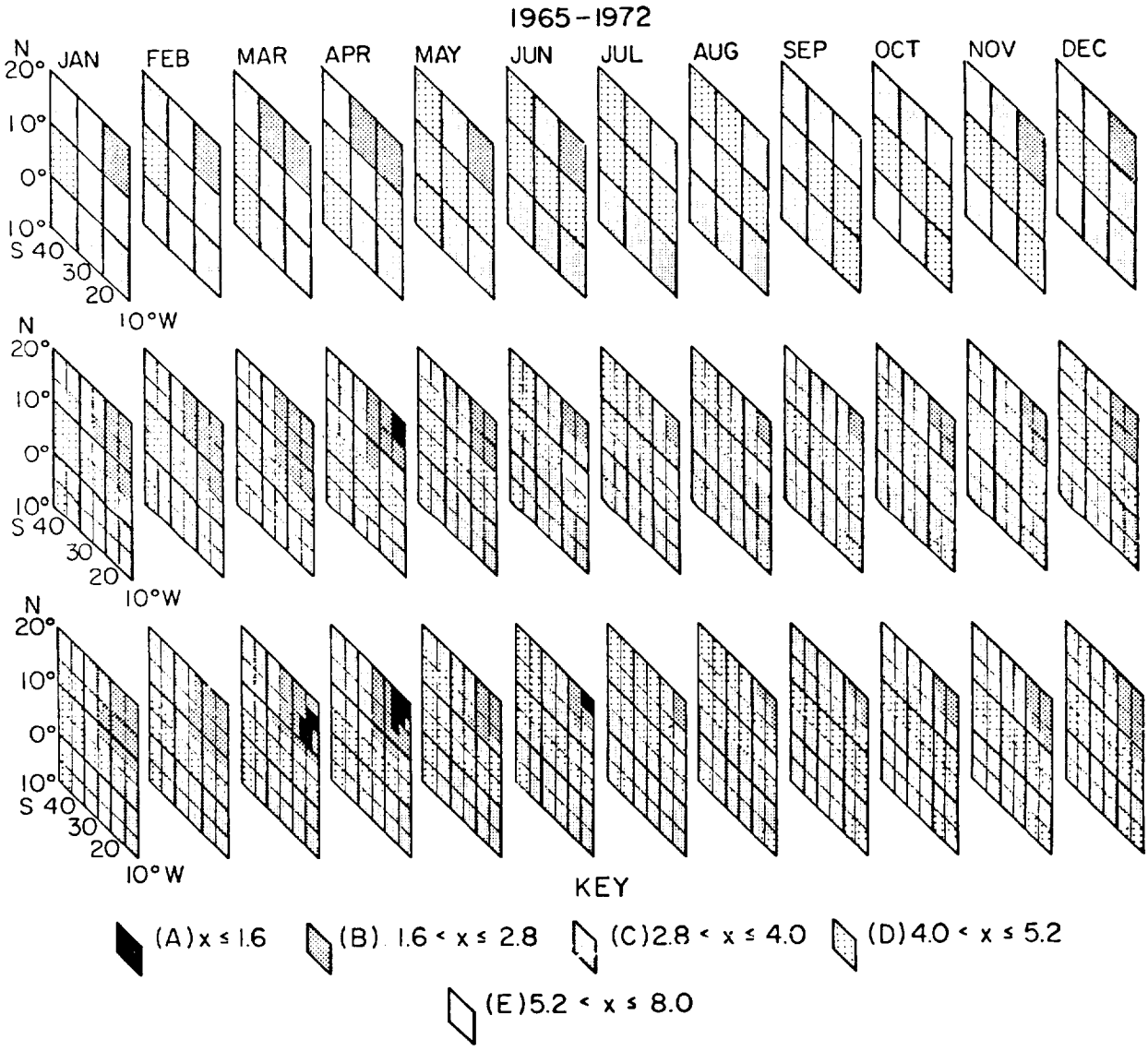

Figure 5. Monthly mean cloud amounts over the GATE area averaged over the years 1965-1972: a) 10 x 10° trapezoids; b) 5 x 5° trapezoids; c) 2.5 x 2.5° trapezoids. (After Avaste et al., 1979.)

archives such as albedo. Figure 8 shows the emitted flux comparison, and you will note, in addition to the smearing problem, that if you mentally turn the emitted flux scattergram around such that cold is going in the same sense as bright, that the albedo and emitted flux scattergram patterns have some differences in shape. This means, in addition to our other problems, that there may not be a good relationship between cloud amount derived from individual satellite channels, which can lead to confusion. I have forgotten the exact period of this comparison (see Avaste et al. (1979)).

So, in brief, there is now a period of satellite-derived estimates of cloud amount stretching over a good number of years (1965-1973). Unfortunately, there is a question concerning the overall accuracy of the data since it is difficult to evaluate error bars. Finally, there are questions as to whether we can go back, and by using simple processing techniques, make any real improvements.

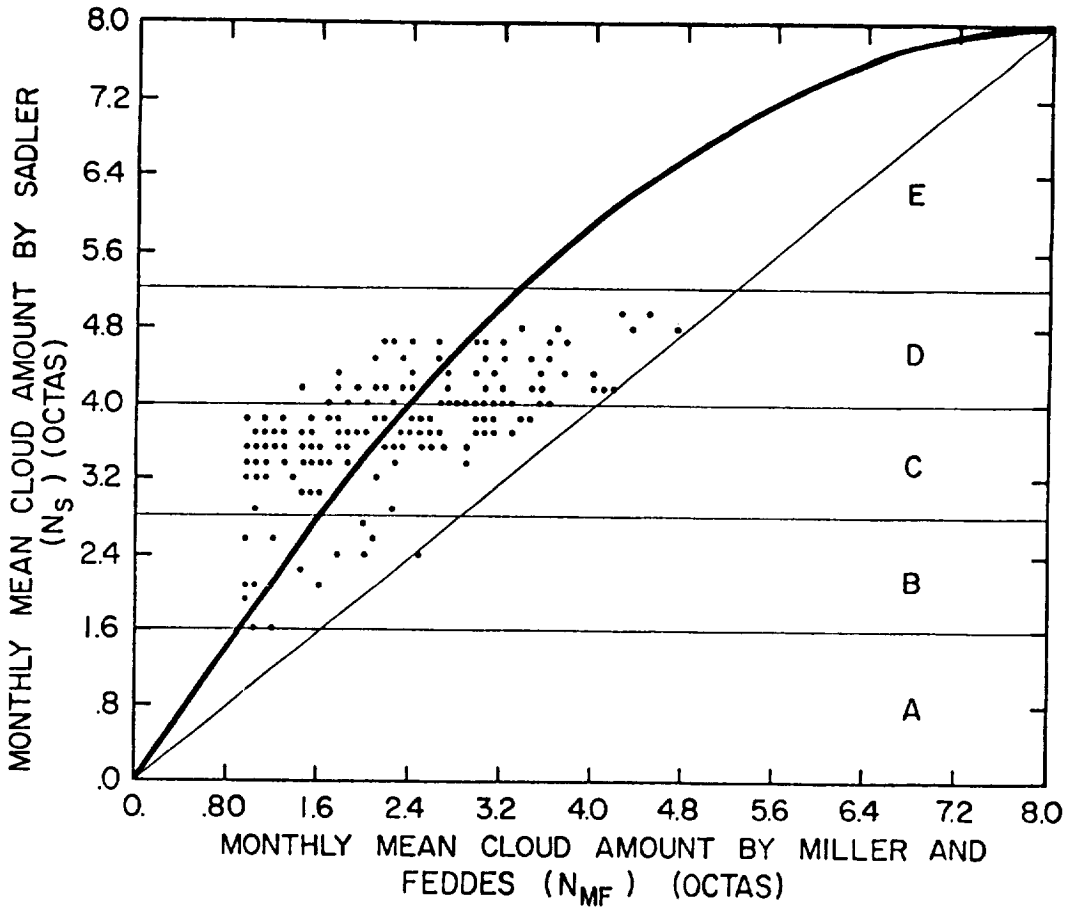

Figure 6. Comparison of Sadler's and Miller & Feddes' monthly mean cloud amounts averaged over the years 1967-1970 for the northern Atlantic Ocean. (After Avaste et al., 1979.)

I would now like to touch on some of the techniques that have been proposed, over approximately the last five years, for estimating cloud amount and cloud height from satellite data. In many ways these techniques are really geared for operational satellite systems of the latter 1970's and of the future. I have listed the techniques in Table 1.

The first is the threshold technique, which is the very simplest of the cloud measurement techniques, in which you simply select an equivalent blackbody temperature or a spectral reflectance threshold for distinguishing between cloud and non-cloud in infrared or visible satellite images.

A second technique, which was first published by Reynolds and Vonder Haar (1977), is called the bi-spectral technique. This is simply a method of combining two channels and using a few radiation calculations to try and uniquely define the cloudiness within a field of view, which is assumed to be only partially filled.

There is, of course, the 3-D neph-analysis data from the Air Force, which is their operational product used for flight forecasting, and although I will discuss this topic briefly, I am not really acquainted with the computer code that is used for this technique.

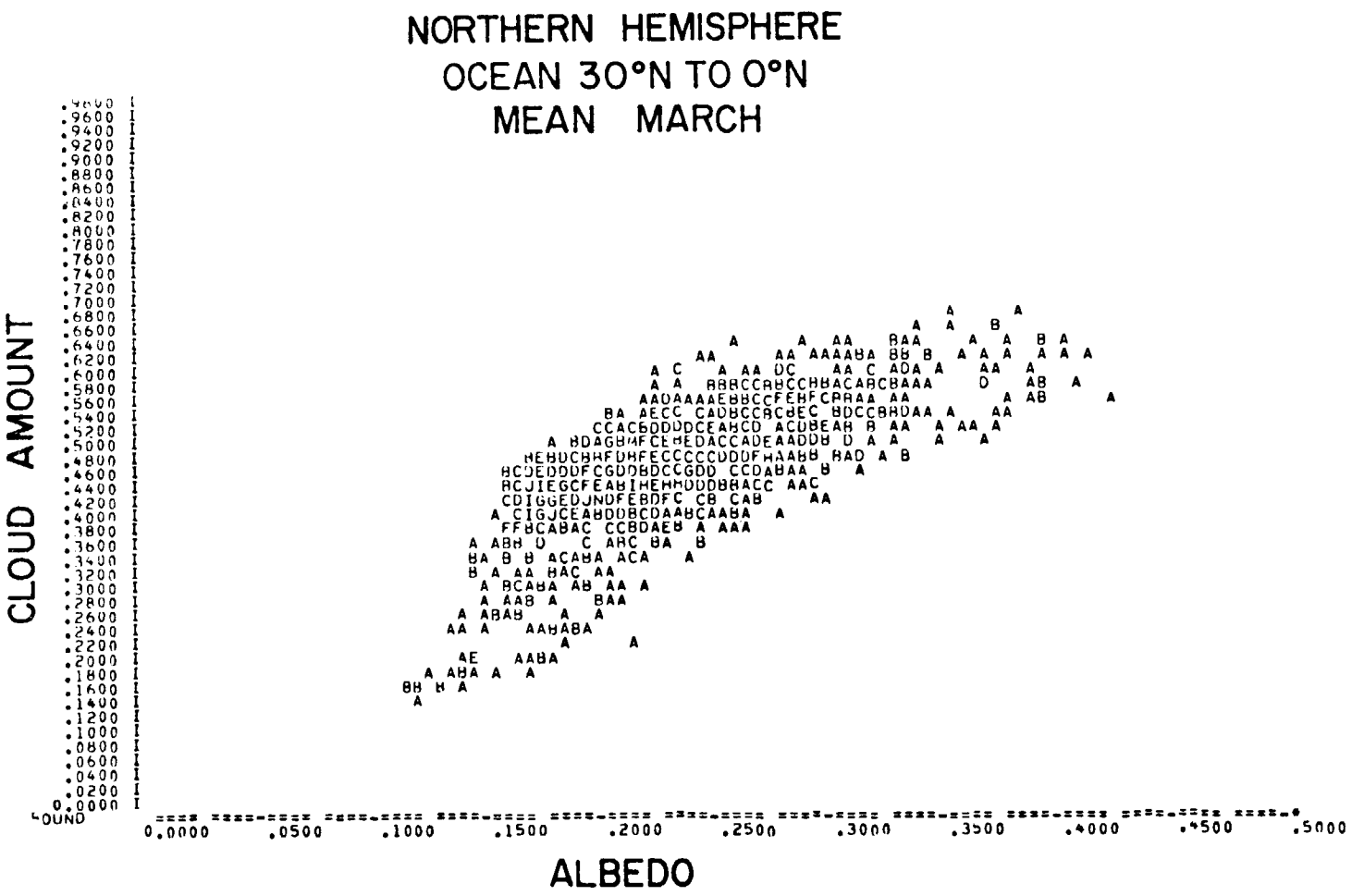

Figure 7. Spatial correlations of time mean Sadler cloud amount and time mean scanning radiometer measurements. Each letter represents a 2.5° latitude by 2.5° longitude region. The letter A represents 1 occurrence, B = 2, C = 3, etc. a) Northern Hemisphere (Albedo – Cloud Amount). (After Avaste et al., 1979.)

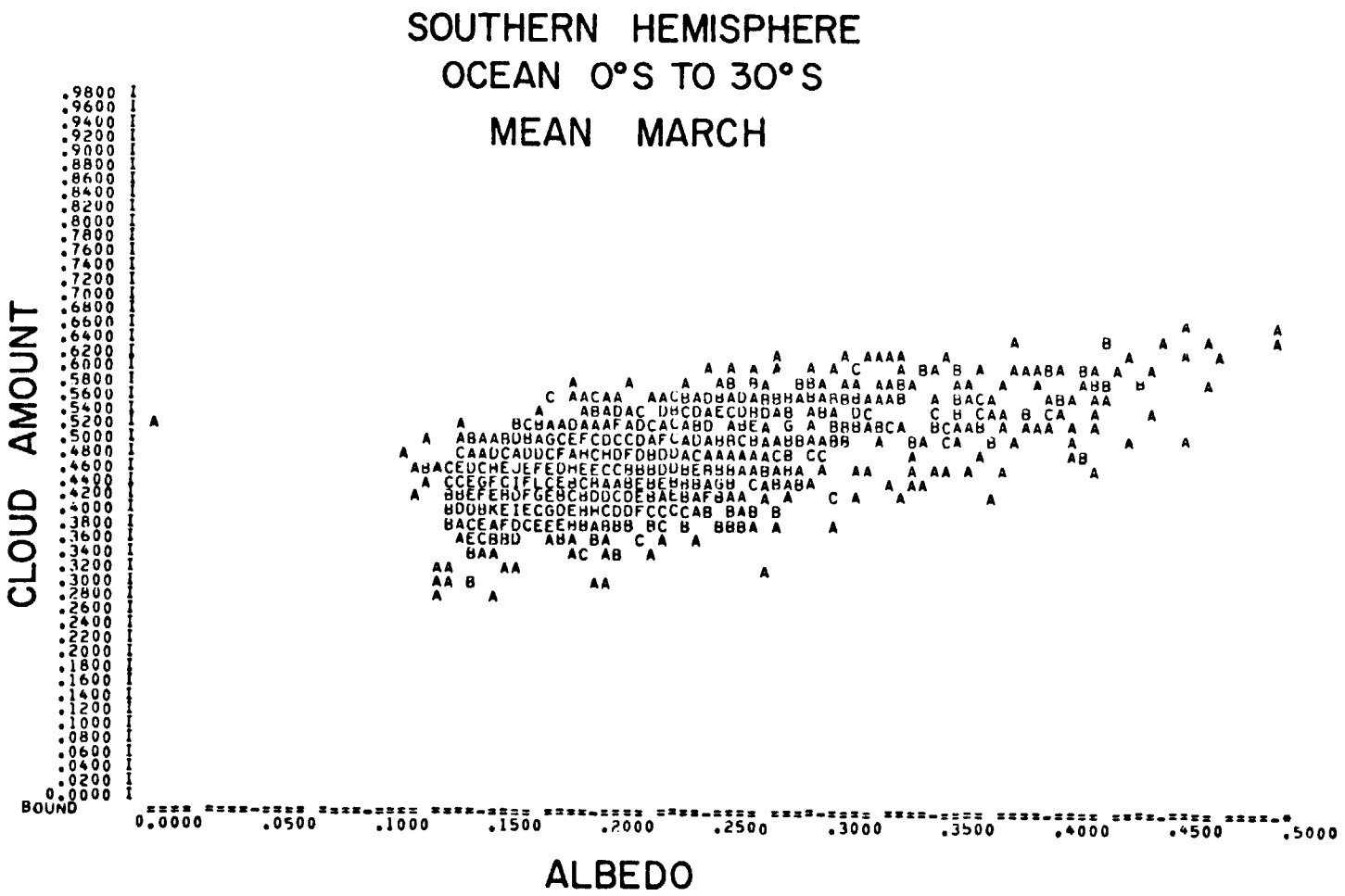

Figure 8. Southern Hemisphere (Albedo – Cloud Amount). (After Avaste et al., 1979).

Table 1
Methods Proposed for Estimating
Fractional Cloud Amount and Height

1. Threshold Technique (EBBT, VIS Reflec)
2. Bi-Spectral Technique
3. 3-D Nephanalysis – Air Force
4. 2 Channel CO_2 Absorption Technique
5. Near IR Window (3.7 μm) and Split Window Technique
6. 2-D VIS-IR Histogram Pattern Techniques

There are many less applicable techniques, in terms of obtaining global cloud climatologies, but which may prove useful for spot-checking and verification, e.g.

a) Stereo
b) Limb Scanning
c) 7600 Å 0_2 Band

The fourth technique, which is probably the most sophisticated of the techniques, and which has been discussed by Smith and Platt (1978), is the 2-channel CO_2 absorption technique, which utilizes a pair of CO_2 band measurements available from temperature sounders such as those flown on operational weather satellites.

The near IR window and split window refers to a triplicate of measurements which will be available from the future TIROS-N satellites. I hesitate to call this a technique yet; this is the material that Al Arking may be discussing this morning, and I am not yet up-to-date on what he thinks the formulation is going to be. However, I believe he has shown some convincing things already, insofar as there is a lot of additional information to be derived from multiple channels.

Finally, a more peripheral technique, involves analyzing spatial patterns from two dimensional visible-infrared histograms.

There are many other techniques that have been devised and proposed for the standard operational detectors and other more obscure channels, available on modern satellites. Many of these techniques, of course, are not really applicable for a global cloud climatology, but that does not diminish their importance in terms of their usefulness for spot-checking operational data sets and possibly using them as verification data sets. Keep in mind that it is very difficult, and at times not appropriate to compare what we like to call ground truth with satellite-derived cloudiness. I will show you an example of what I mean.

Figure 9 shows some results of Ackerman and Cox (1980) based on the thresholding method, using infrared, SMS-1 geosynchronous satellite data over the GATE region (see Smith et al. (1979)). The

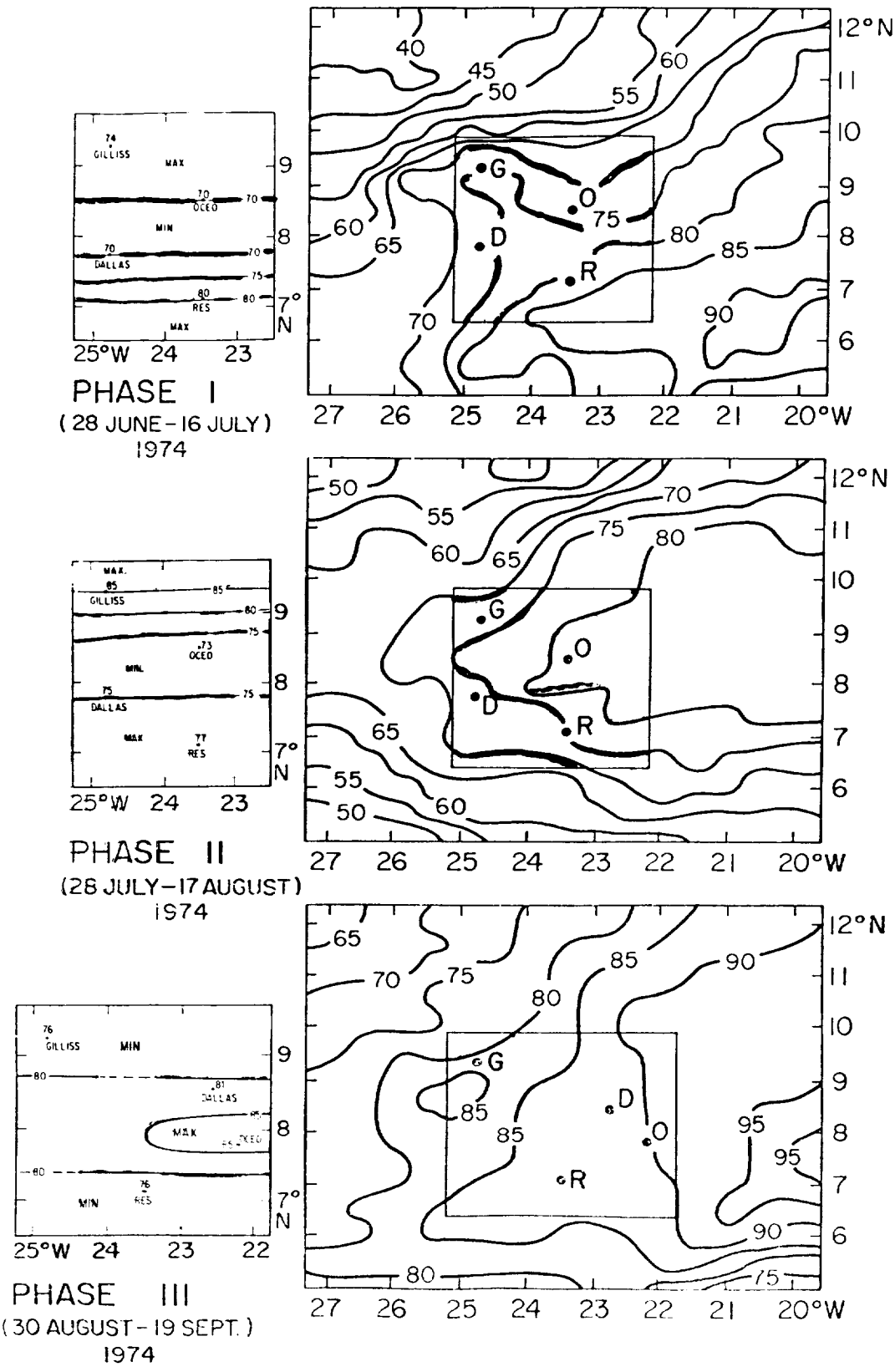

Figure 9. Comparison of satellite-derived cloudiness (right hand side) with all-sky camera-derived cloudiness (left hand side). (After Ackerman and Cox, 1980.)

little box in the center depicts the four U.S. ships in the "B" scale region during GATE. Available from each of these ships were all sky camera reports. On the left of these charts, you are looking at all sky camera results; at the right the contours represent the satellite-derived cloudiness. I have indicated with colored lines the 85, 80, 75 and 70 percent contour lines. The 3 GATE phases and an all phase averages are presented.

You will note in this comparison, between the satellite cloudiness derived from the threshold technique, and the upward looking all-sky camera cloudiness derived from careful hand analysis by Holle et al. (1979), that the basic contour levels are in the same, roughly in the same ballpark, but the patterns of cloudiness certainly are not similar. The left side shows a very zonal configuration, whereas the right side shows a lot more structure. Most of this difference, of course, is due to the sparse sampling inherent to the ship data.

Now, you might say, well, it is good that we are getting 80 and 85 degree contours together at the same time, but then, if you separate the cloud amount measurements based on low cloud and high cloud, you get a different picture. Figure 10 presents this breakdown. You will note that for the low cloud category the satellite measures less cloud, about 10 percent less cloud than the all-sky camera, whereas for the high cloud category, the satellite is seeing more cloud, 15 to 20 percent more. Now, that means that the previous comparison, which was reasonably good at the ship coordinates, may have been fortuitous in that the distribution of high and low cloud over the GATE area may have been very well balanced. In other regions of the world where you have, say, predominant low cloud, the total cloudiness derived from the surface observations would be, by definition, greater than the satellite observations.

AUDIENCE PARTICIPANT: Was the threshold only for the longwave data?

MR. SMITH: This case used an IR threshold-derived cloud amount, partly tuned by a VIS threshold procedure. See Cox and Griffith (1979) for details.

Figure 11 presents some results, based on the thresholding technique, from a paper by Campbell, et al. (1980), presented at the recent International Radiation Symposium, held in Fort Collins, Colorado. This may be a little complicated to read. The x and y directions represent space; the x direction is longitude; the y direction is latitude. Each of the 7 zones covers approximately 2 degrees of longitude. For each zone, the ordinate represents a time axis ranging from 0 to 24 hours local time. The sliding abscissa for each line represents the magnitude of the mean infrared emission given in radiance units ($W.M^{-2}sr^{-1}$). The figure thus consists of diurnal longwave emission functions for a 7 by 24 grid of 2° latitude-longitude regions.

In other words, these functions are associated with diurnal cloudiness patterns, if you will, and you are looking at the space distribution of the diurnal patterns. The geographic region you are viewing is coastal South America. The high amplitude region is approximately the coast; the center of the region is about 25 degrees south and 65 degrees west. I present this figure to illustrate that by using thresholding, which is not, in the purest sense, the best way to estimate cloudiness, you can get a first cut look at patterns of diurnal variation as a function of space.

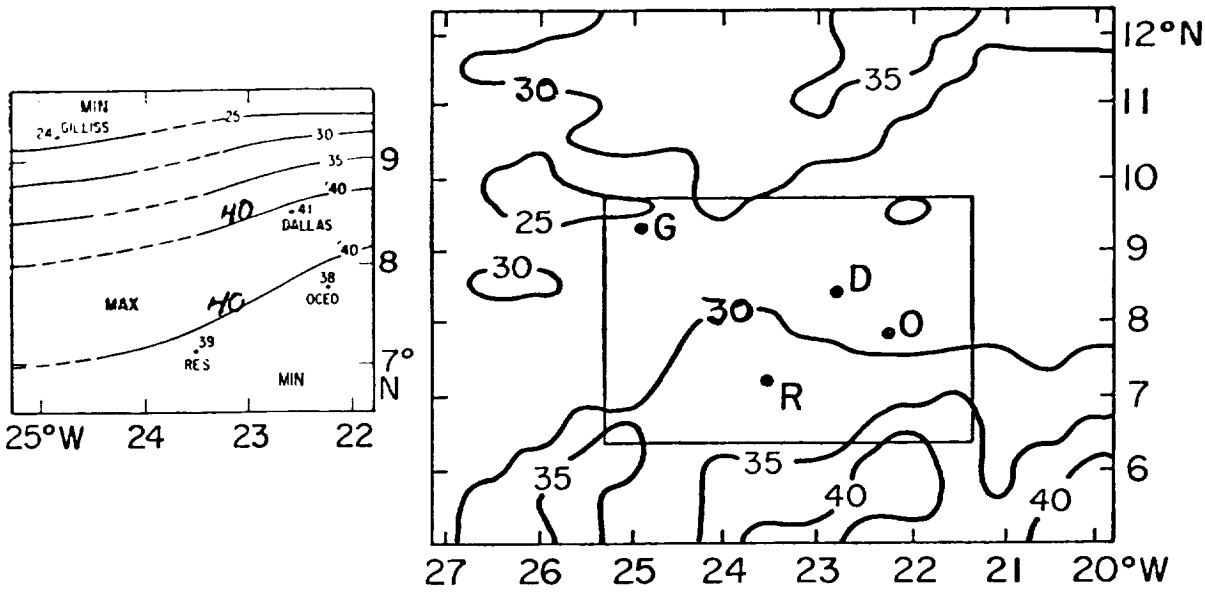

A. LOW CLOUD AMOUNT (%)

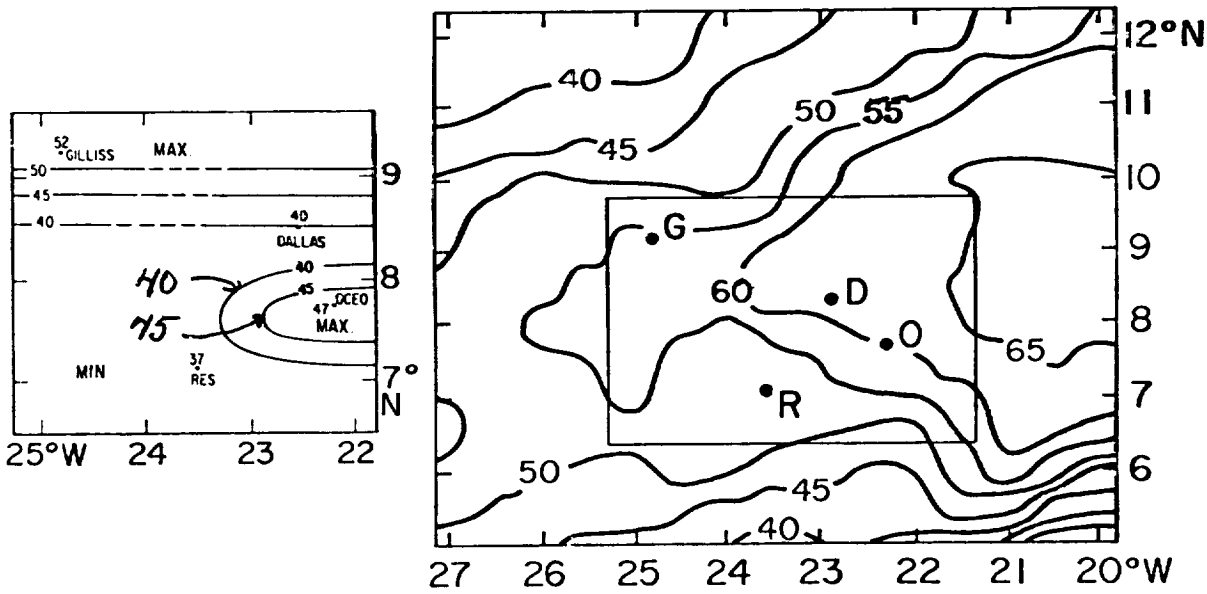

B. HIGH CLOUD AMOUNT (%)

Figure 10. Satellite cloudiness vs. all-sky camera cloudiness comparison based on a low cloud-high cloud stratification. (After Ackerman and Cox, 1980.)

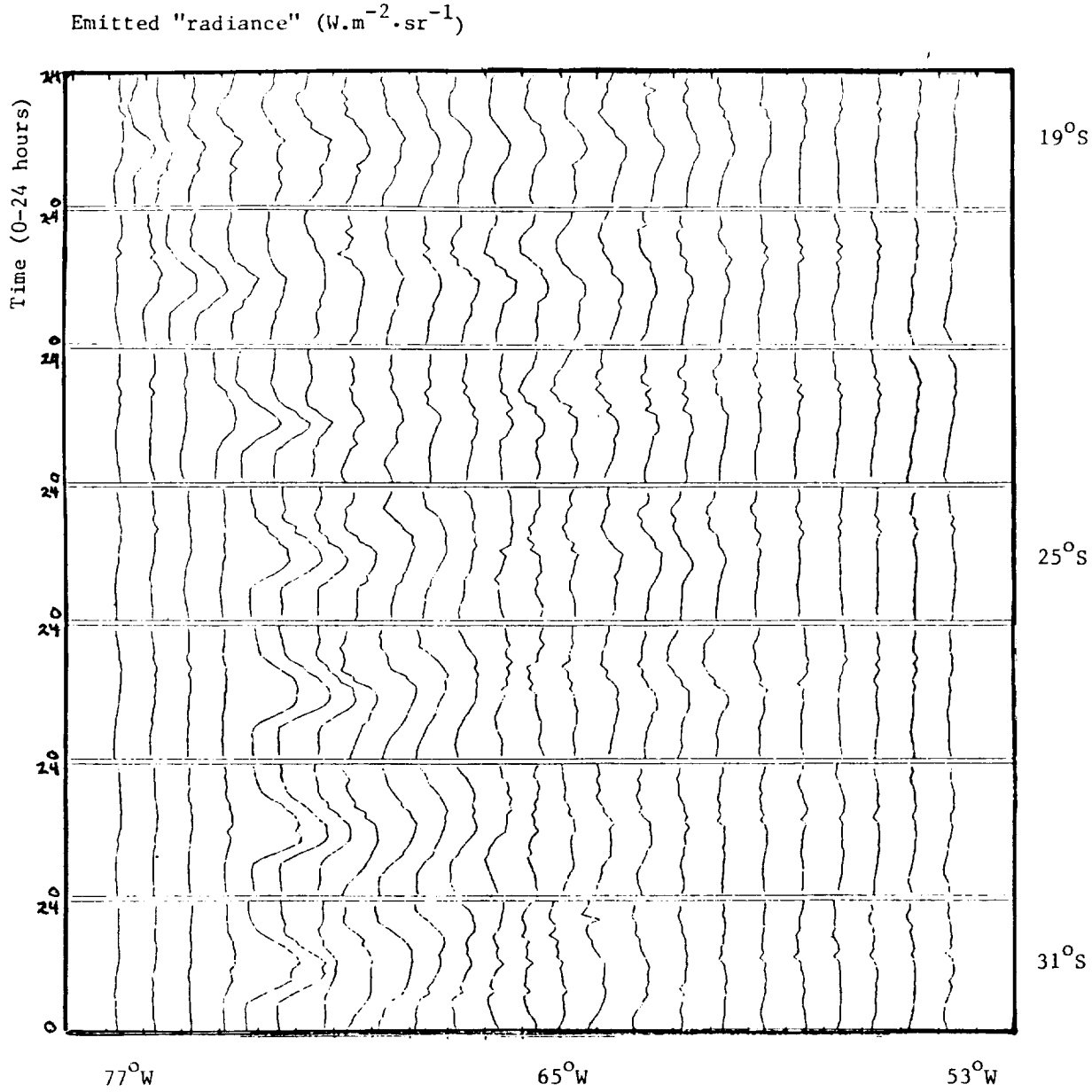

Figure 11. Depiction of the diurnal cycle (average of 10 days) in emitted "radiance" for a number of different surrounding geographical locations centered on about 25°S over the west coast of South America. Each column of curves represents the cycle at a location around 25°S. Curves sequentially displaced to the right correspond to cycles in areas sequentially separated eastward by about 200 km. Similarly curves displaced to the top of the diagram relate to regions displaced successively northward by about 2°. The transition from ocean to coastal S. America to inland S. America is clearly evident by scanning from left to right. (After Campbell et al., 1980.)

If you analyze the data in terms of an amplitude chart, you get what is shown here in Figure 12. Each of those little lines was decomposed for its first Fourier series component, and these are then the resultant amplitudes in units of watts per meter square per steradian deviation from the mean. Note that the region considered here is about 100 degrees of latitude by 100 degrees of longitude, and you will note that the peak in the amplitude falls along the west coast of South America, where you have a significant daily heating cycle.

AUDIENCE PARTICIPANT: What time of day is this?

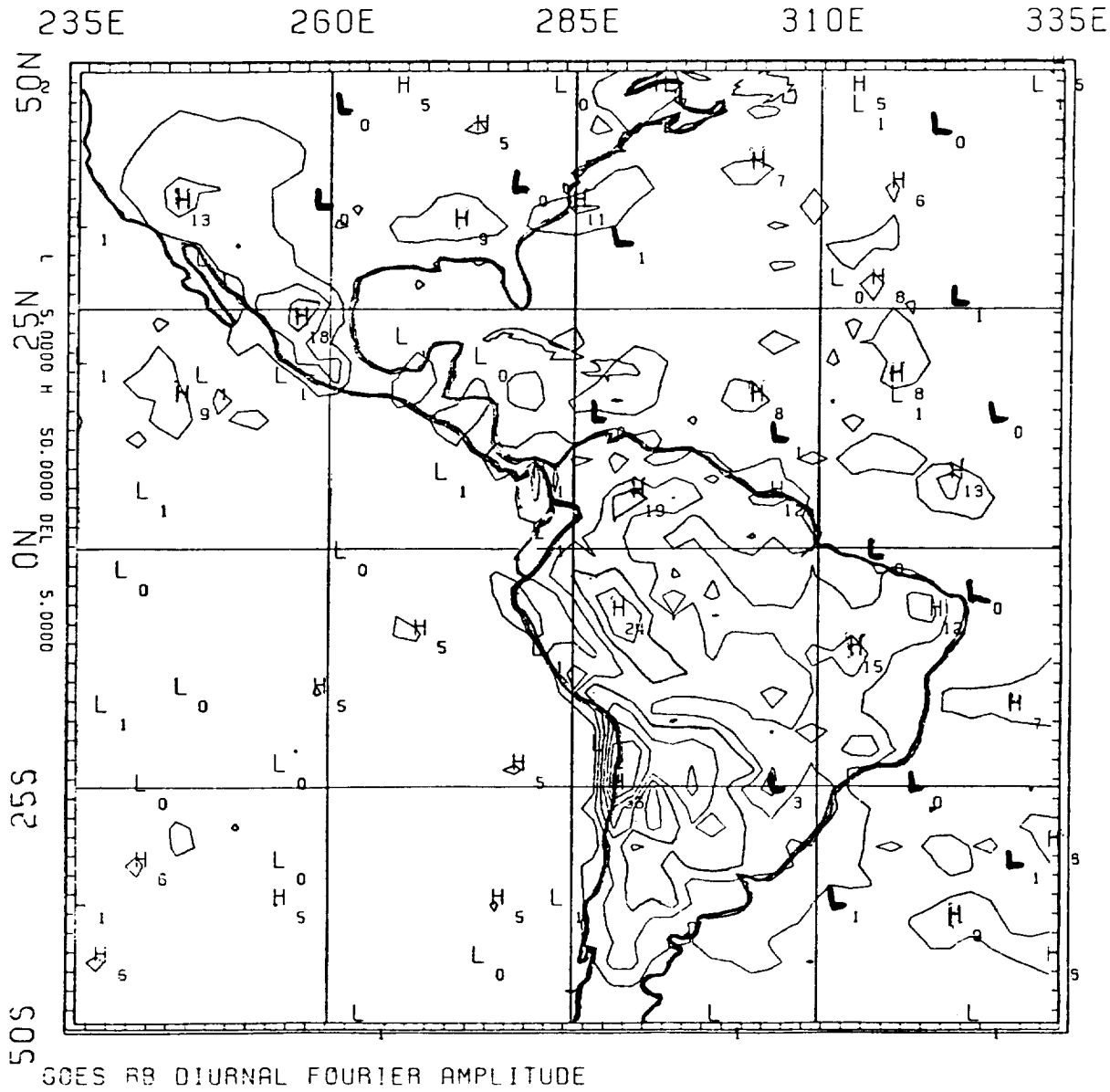

Figure 12. A map of the amplitudes (in $Wm^{-2}sr^{-1}$) of the diurnal cycles portrayed in Fig. 11 (After Campbell et al., 1980.)

MR. SMITH: This figure does not indicate time of day. This is an amplitude diagram involving the magnitude of the diurnal variation of infrared emission. It does *not* consider the phase or time of the maximum amplitude. I will show you the associated phase diagram this afternoon.

AUDIENCE PARTICIPANT: What season or month is this?

MR. SMITH: The data period is November, 1978, and it represents an average of ten days of data.

AUDIENCE PARTICIPANT: Is this the amplitude of the IR channel?

MR. SMITH: Yes, this is the amplitude based on the IR channel from the GOES-East satellite.

I am showing you this – I don't want to discuss details – I will try and get into this subject a little more this afternoon – to emphasize that with thresholding you can get some very useful products.

The bi-spectral method is a fairly straight-forward technique designed for use with 2-channel weather satellite instruments and formulated to overcome the partially filled FOV problem. You can express long and short-wave spectral radiances ($N^{SW}_{\Delta\lambda}$, $N^{LW}_{\Delta\lambda}$) as a function of fractional cloud amount and clear area, and simply solve the following pair of equations for F, the fractional cloud amount, and T_{CLD}, the equivalent blackbody temperature of the cloud. In using this method, you are required to specify a number of parameters; basically the surface conditions, that is surface temperature and emissivity, and the albedoes and angular reflectance functions of both the surface and the cloud. The latter is an area in which the method can get you a bit of trouble because of the lack of knowledge of variation of the albedo and anistropic reflectance properties of cloud, particularly cirrus. The following pair of equations are a mathematical representation of the problem:

$$N^{LW}_{\Delta\lambda} = (1 - \epsilon_c \cdot F) \cdot \left\{ \epsilon_s \cdot \int_{\Delta\lambda} B(T_s) + (1 - \epsilon_s) \cdot L^{s\downarrow}_{\Delta\lambda} / \pi \right\} + \epsilon_c \cdot F \left\{ \int_{\Delta\lambda} B(T_{CLD}) \right\}$$

$$N^{SW}_{\Delta\lambda} = (1 - F) \cdot A_s \cdot I^{s}_{\Delta\lambda} / [\pi \cdot \chi_s(\theta_\Theta, \theta_s, \Phi_r)] + F \cdot A_c \cdot I^{c}_{\Delta\lambda} / [\pi \cdot \chi_c(\theta_\Theta, \theta_s, \Phi_r)]$$

where

F	$\equiv$	Fractional Cloud Amount
T_s, T_{CLD}	$\equiv$	Surface and Cloud Top Temperatures
$L^{s\downarrow}_{\Delta\lambda}$	$\equiv$	Downward Spectral Infrared Surface Flux
ϵ_s, ϵ_c	$\equiv$	Surface and Cloud Emissivities
$I^{s}_{\Delta\lambda}$, $I^{c}_{\Delta\lambda}$	$\equiv$	Spectral Solar Fluxes Reaching Surface and Cloud Levels
A_s, A_c	$\equiv$	Surface and Cloud Spectral Albedoes
χ_s, χ_c	$\equiv$	Bi-Directional Reflectance Functions

These next figures are results from Reynolds and Vonder Haar (1977) in which they have tested the technique by comparing it to actual surface derived cloudiness reports. Figure 13 represents Denver Station results while Figure 14 shows Oklahoma City and White Sands Missile Range results. They have compared the heights of the derived cloudiness based on the technique to heights based on the surface observations.

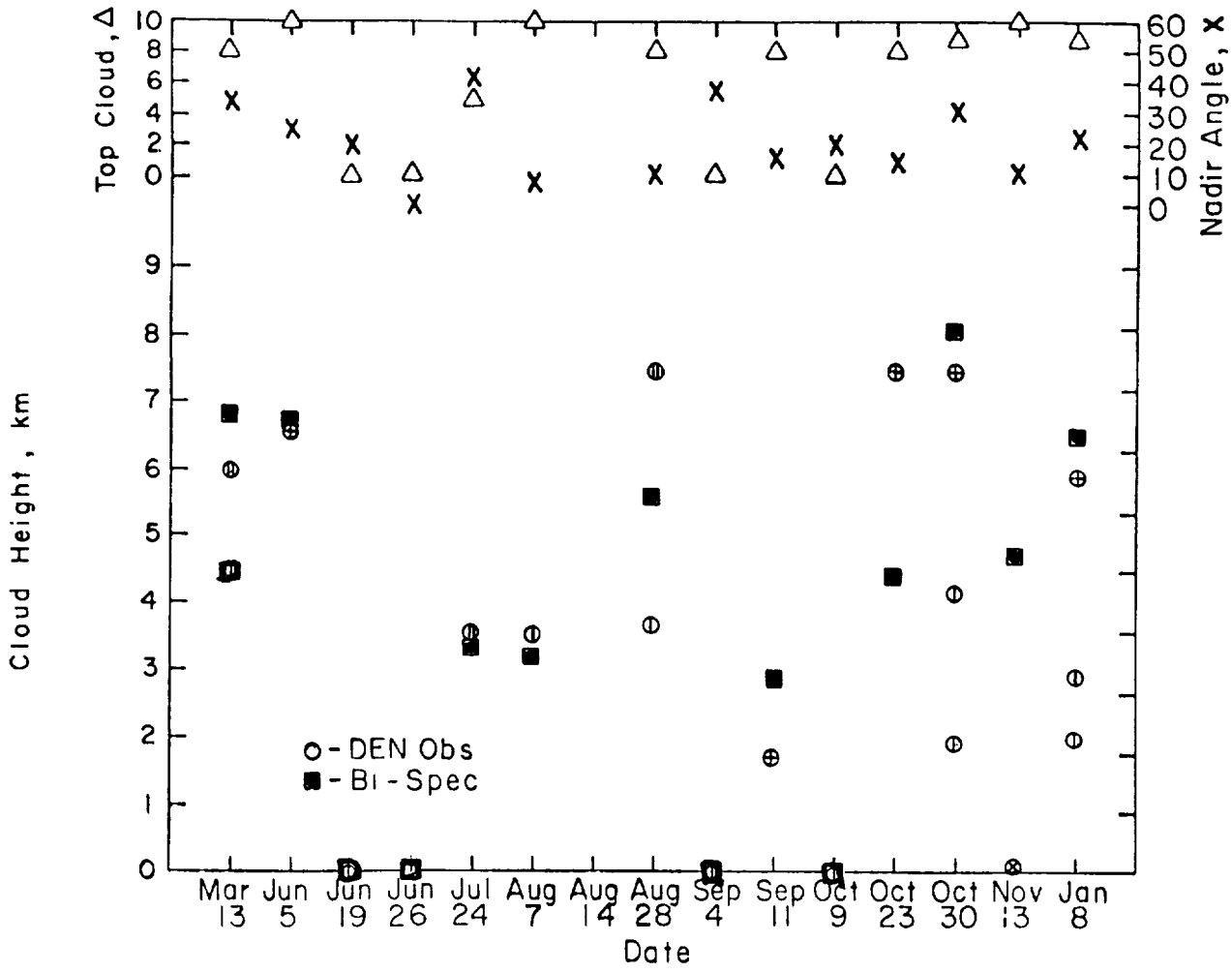

Figure 13. Results from bispectral technique for a 75 km x 75 km area over Denver, Colorado. (After Reynolds and Vonder Haar, 1977.)

To summarize their results, I have underlined a section of their paper; they show reasonably good RMS error when the cirrus cases are deleted (approximately ± 0.5 km). When the cirrus cases are considered, the RMS error goes up to on the order of four or five kilometers.

> Results from all sites, for all days chosen where direct measurements could be made, show an rms error of 0.2 in cloud amount and a slight bias toward underestimation (average deviation -0.05). The rms error in cloud height when cirrus cases are deleted is 0.5 km with a bias toward overestimation by 0.27 km. When cirrus cases are included the results show an rms error of 4.7 km and a bias or average deviation of -4.2 km. The fact that we have used an emissivity of 0.9 for all clouds including cirrus gave rise to this problem. In an . . .

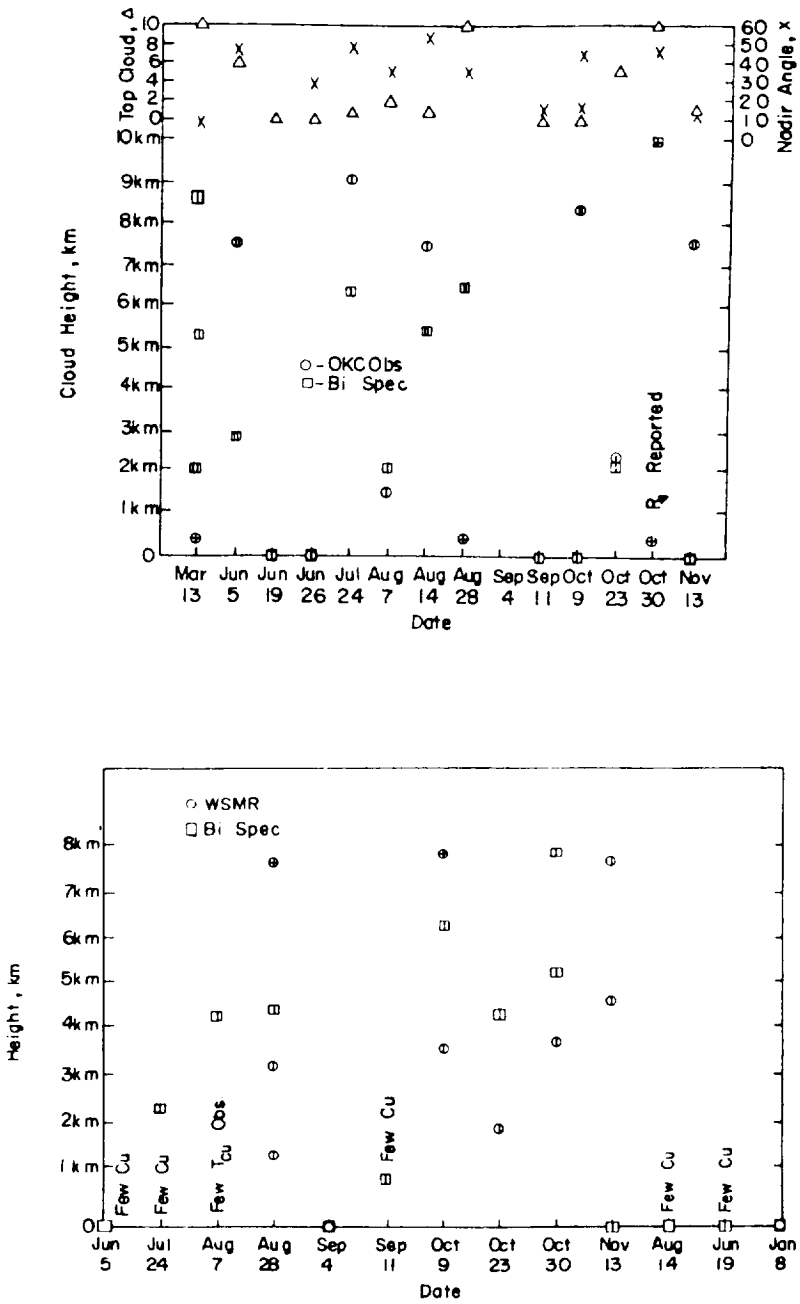

Figure 14. Results from the bispectral technique for 75 km x 75 km areas over Oklahoma City (top) and White Sands Missile Range (bottom). (After Reynolds and Vonder Haar, 1977.)

AUDIENCE PARTICIPANT: What was the observation that they were comparing with?

MR. SMITH: They were ground observations; an observer on the ground reporting bases and tops.

AUDIENCE PARTICIPANT: Estimating?

MR. SMITH: Estimating. Just another example of the problems with an inter-comparison.

This next chart, Figure 15, originates from the Air Force and highlights their three-dimensional nephanalysis. It is a reasonably good chart, because it shows that there are a lot of components to their 3-D NEPH, and I think they are taking the right attitude in showing you they do insert the satellite.

The input data (Figure 16) for their 3-D NEPH analysis involves a lot of different platforms; radio and rocket-sondes, aircraft reports, visible and infrared satellite imagery, but they also "bogus in" data when they are missing data, and they use persistence forecasting when they are missing data,

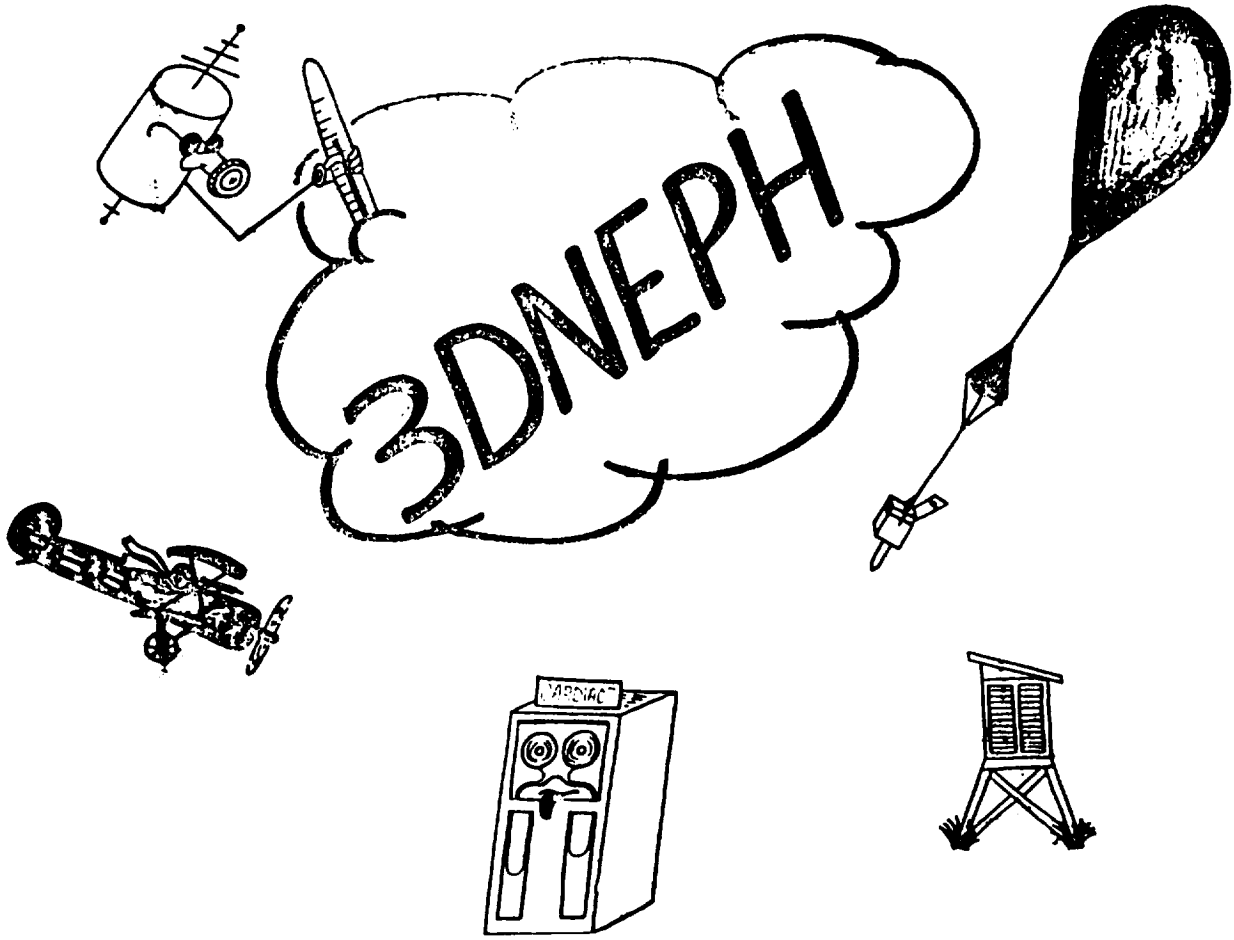

Figure 15.

INPUT DATA

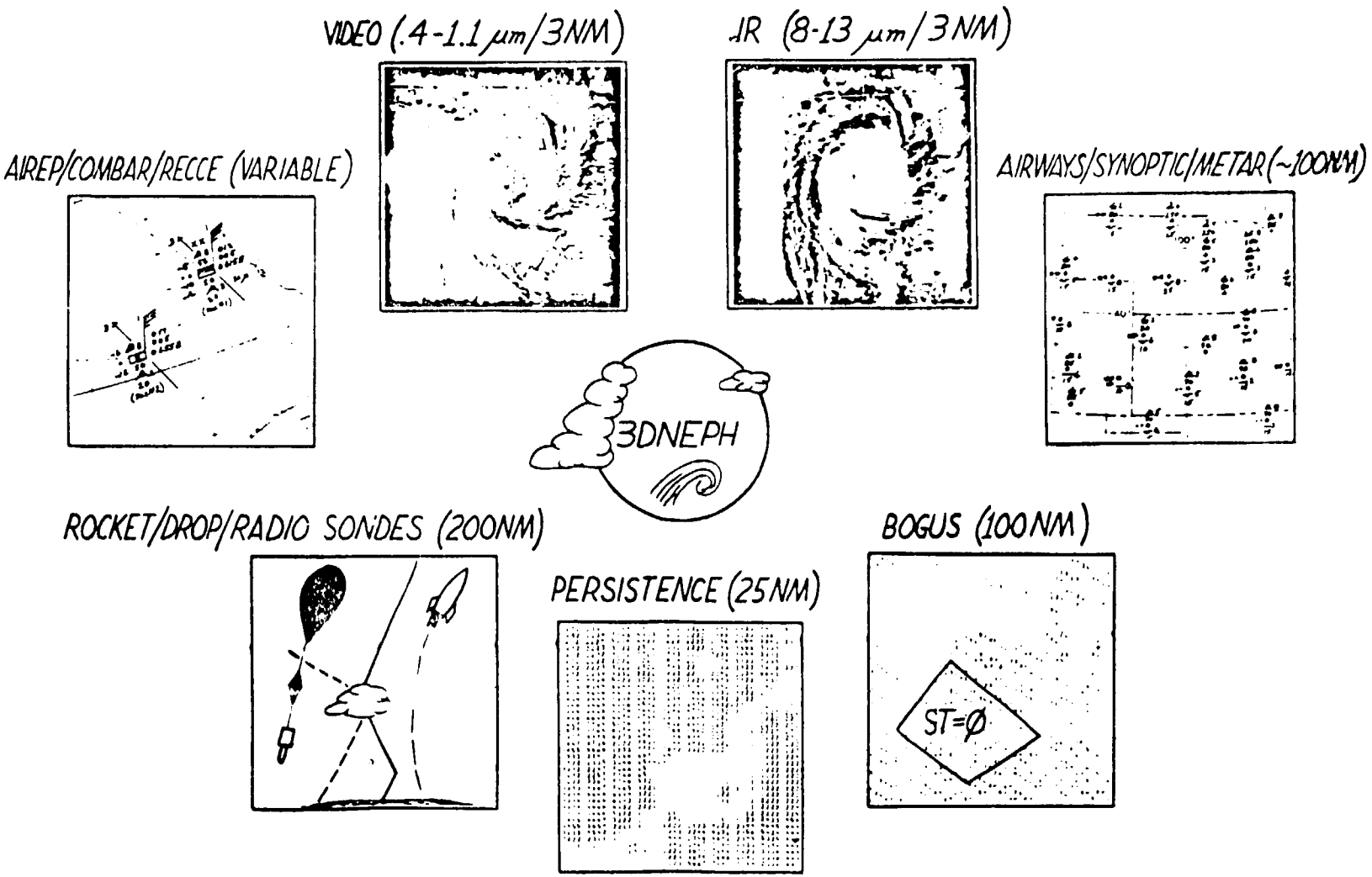

Figure 16.

and this, of course, represents one of the problems of using the 3-D NEPH quantitatively. It does not always use actual cloudiness.

I will also put up Figure 17. There is a decision tree involved in their method in which cloud amounts, from the various sensors or platforms, are given priority weights. They go through the decision tree and insert estimates as a function of these weights. This approach allows them the flexibility of utilizing data from the best available sensors (i.e. satellites) in a high priority mode. Keep in mind that the priority scheme is constantly updated as sensors are added or changed, so that the 3-D NEPH archive can not be considered a consistent record. Recall, that the 3-D NEPH is intended as an operational product, *not* a cloudiness climate archive.

The CO_2 solution, as shown in Smith and Platt (1978), is a rather interesting way of solving the problem. You first define what is called a cloud pressure function (f (ν_1, ν_2, p), which is an expression involving a pair of differences (for frequencies ν_1 and ν_2) of two column radiances (R (ν, N_1), R (ν, N_2)) of neighboring fields of view containing differing cloud amounts (N_1 and N_2), assumed

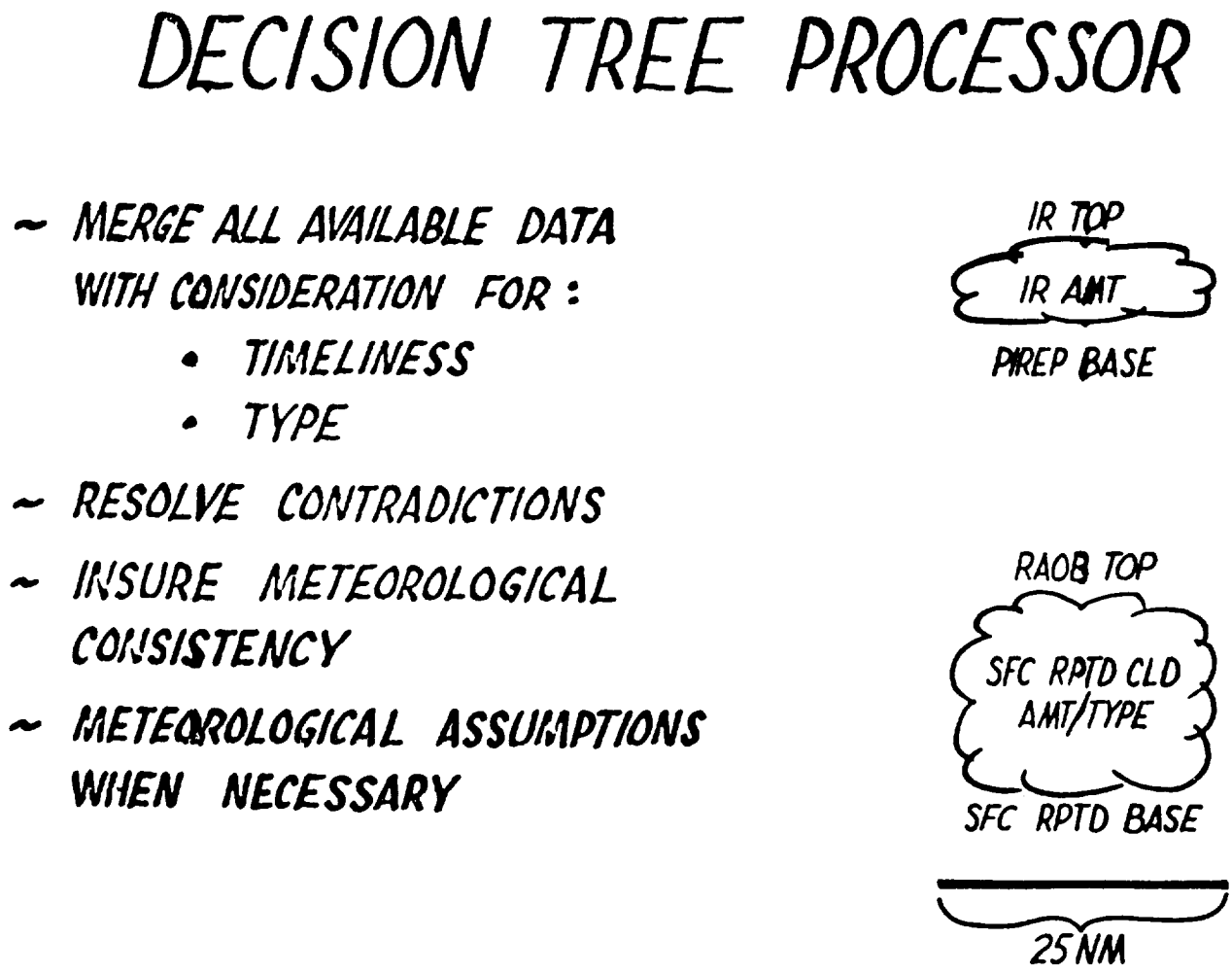

Figure 17

to be at the same pressure level (P_c). If you express these column radiances in terms of differences then the implied vertical integrations need only go from the surface to the cloud top because the above-cloud components subtract, then by ratioing two frequencies, you can remove the coefficient of cloud amount that is gotten from expanding these terms into clear and cloudy portions. It is necessary to make an assumption that the cloud is infinitesimally thin, so that you need only work with a single transmittance function (τ) below the cloud. In other words, for the clear and the cloud-covered region, you need only one transmittance function. Then, by assuming that cloud, any thin layer cloud, has equivalent transmission at the two frequencies, you can cancel the resulting cloud amount coefficient. The following is a mathematical statement of the above:

$$f(\nu_1, \nu_2, p_c) = \frac{R(\nu_1, N_1) - R(\nu_1, N_2)}{R(\nu_2, N_1) - R(\nu_2, N_2)} = \frac{\int_{p_c}^{p_0} \tau(\nu_1, p) \frac{dB[\nu_1, T(p)]}{dp} dp}{\int_{p_c}^{p_0} \tau(\nu_2, p) \frac{dB[\nu_2, T(p)]}{dp} dp} = f(\nu_1, \nu_2, p).$$

You can now evaluate the cloud pressure function, and will find that it is a single value function, which means for fields of view with differing cloud amount, you can evaluate with this function a unique cloud top pressure, for any pair of dual channel measurements. Figure 18 from Smith and Platt (1978) illustrates two such cloud pressure functions.

The practical way of applying this technique avoids using neighboring fields of view of differing cloud amount because of a singularity problem, and because of the fact that you must assume that the cloud height for the two fields of view is the same. The practical way of using the method is to

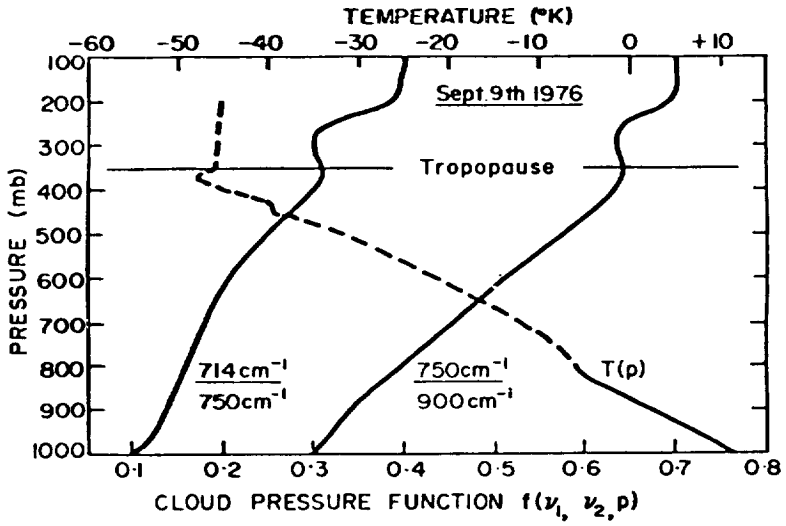

Figure 18. Cloud pressure function for two ITPR channel combinations computed from the Aspendale temperature profile on 9 September 1976. (After Smith and Platt, 1978.)

use a clear field of view or a clear column radiance, in proximity to a cloudy field of view measurement (see below):

$$f(\nu_1, \nu_2, p_c) = \frac{R(\nu_1) - R_c(\nu_1)}{R(\nu_2) - R_c(\nu_2)} = \frac{\int_{p_c}^{p_0} \tau(\nu_1, p)B'(\nu_1 p)dp}{\int_{p_c}^{p_0} \tau(\nu_2, p)B'(\nu_2 p)dp} = f(\nu_1, \nu_2, p) .$$

This approach increases the sensitivity of the technique by avoiding the ratioing of differences of large almost equivalent radiances which contain noise.

Cloud amount (N) is then calculated from a window measurement (R(w)) and surface and cloud top temperatures ($T(P_0)$, $T(P_c)$); the temperature profile is assumed to be known in this technique:

$$N = \frac{R(w) - B[w, T(p_0)]}{B[w, T(p_c)] - B[w, T(p_0)]} .$$

Smith and Platt (1978) have applied this technique, and compared the results to Lidar derived cloud tops and to cloud tops derived from examining the relative humidity along a radiosonde path. If you look at these comparisons, they are actually very good. There are not very many of them, but those that are given in Table 2 are in very good correspondence. The columns indicate the two-channel, the Lidar, and the radiosonde results.

Table 2
Summary of ITPR, Radiosonde and Lidar Indicated Cloud-Top Pressure Altitudes for Aspendale, Victoria (Australia)

Date September	Radiosonde Pressure (mb)	Lidar Pressure (mb)	ITPR* Two-Channel Method	
			Pressure	Amount (%)
9	420 (?)	440	450	31
14	830	830	800	39
15	700 (?)	630	600	13
16	400	420 (?)	450	24
21	460 (?)	–	400	100
22	330	–	300	80
23	850	830	850	25
24	500	800 (?)	500	14
28	550	550	550	65

*Values chosen are those which are in best agreement with lidar observations.

AUDIENCE PARTICIPANT: If there are several cloud layers, does the method also work?

MR. SMITH: You run into difficulty with several cloud layers because of the assumption you have to make equalizing the transmittance functions. If you put in more than one cloud, you have various points along the path in which you have to put in discontinuous transmittance. So I guess the answer is – my gut feeling would be – no it can not handle multi-level very easily. I think Wielicki and Coakley (1980) could add more to this question. I should point out that they have done an analysis of this approach and have some more to add.

Figure 19 is from a paper by Arking (1980) in which he has been investigating the TIROS-N data which consists of both the weak or lower window imagery along with the 11-micron window imagery. He has discussed various differences noted in clouds at these 2 wavelengths. Note that some of the clouds appear dark against a light surface (which indicates warm) in the 3.7 micron, whereas in the 11-micron, these clouds appear colder. The explanation here, of course, is due to the enhanced near-infrared component from the reflection of near-IR solar energy. The reason the use of these two windows together may be important, as he will go into, is because it may be possible to separate radiatively ice properties from water properties. In other words this may be the first good opportunity we have to go after the difficult problem of accurate detection and placement of high ice clouds or thin cirrus clouds.

MR. ARKING: The most obvious case is the big cloud on the left that is totally missing in the 3.7 μm image.

MR. SMITH: Finally, there has been a technique proposed, and a lot of people have looked at this sort of thing, in which you construct a two-dimensional histogram of VIS and IR samples and try and analyze the patterns that show up. Here, in Figure 20, the IR scale is on the ordinate; it goes from warm to cold. The abscissa is a visible scale, going from dim to bright, so to speak. The ideas are that these histograms break up into patterns in which the various regions may represent, for example, the higher and thicker cirrus down through the thinner cirrus, or over there the thicker warmer clouds. Unfortunately, it is difficult to be quantitative.

Well, one needs to evaluate the pros and cons of these techniques, which I have attempted to do in Table 3. The thresholding technique, of course, is simple, but it necessarily must fail when the emissivity is not one and when an FOV is only partially filled. It is also very problematic over land.

The bi-spectral technique does have a sound physical basis, tuneable with physical parameters, but by the same token, its problems lie in the fact that you need to specify surface properties and the cloud and surface albedoes. In addition, because you are dealing with a narrow field of view measurement, you run into problems with interpreting it as a reflectance because of non-flat cloud top geometry, and, of course, the technique only applies in the daytime.

The CO_2 absorption technique, has the advantage of being immediately adaptable to the operational retrieval going on now, and it is a technique based on the methods of radiative transfer. Its disadvantages lie in problems of instrument sensitivity, which Jim Coakley may have more to say about, and it is difficult to apply in the cases where you cannot retrieve a clear column radiance such as synoptic scale situations, frontal cloudiness, et cetera.

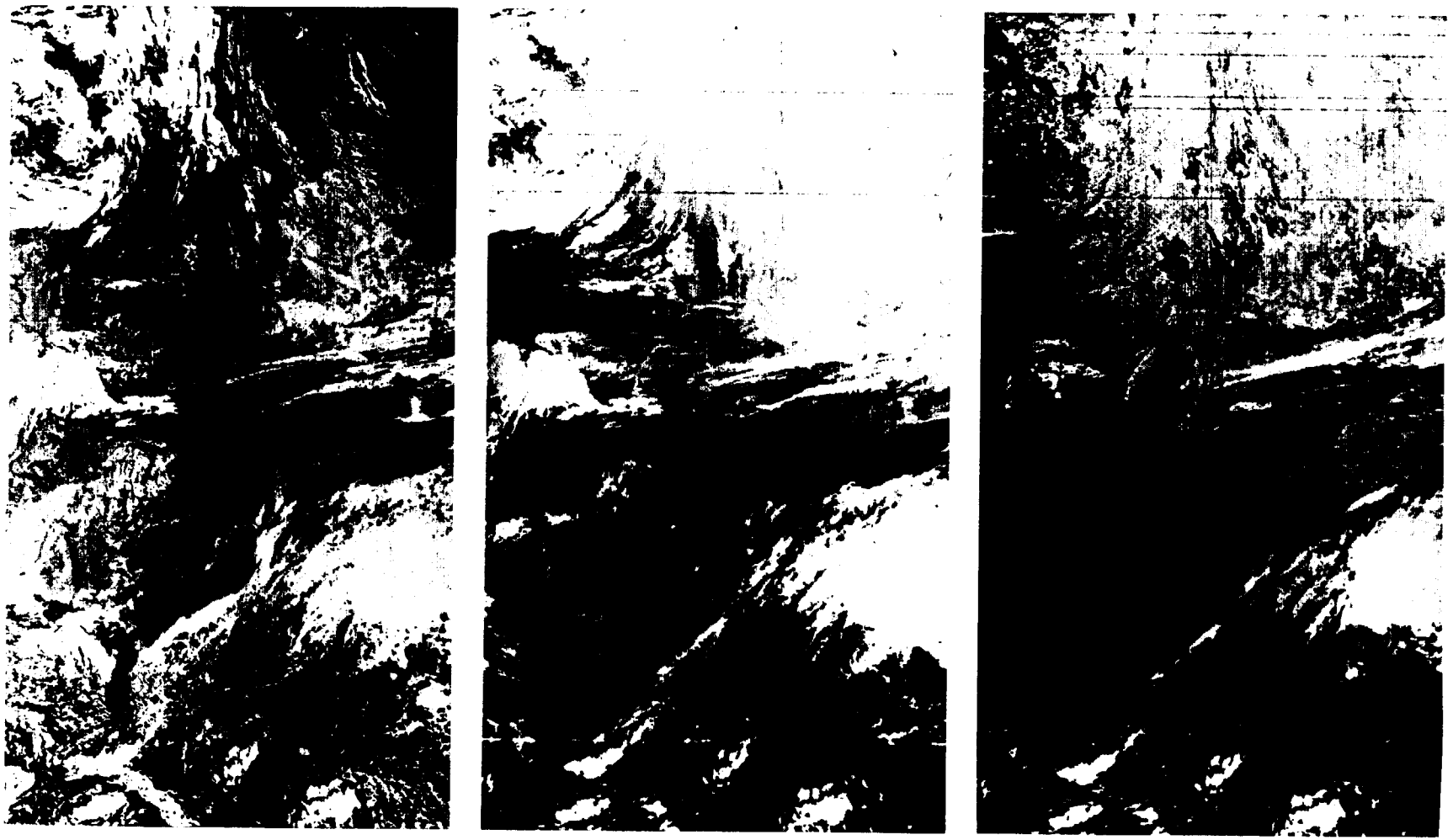

0.9 micron

11 micron

3.7 micron

Figure 19. (After Arking, 1980.)

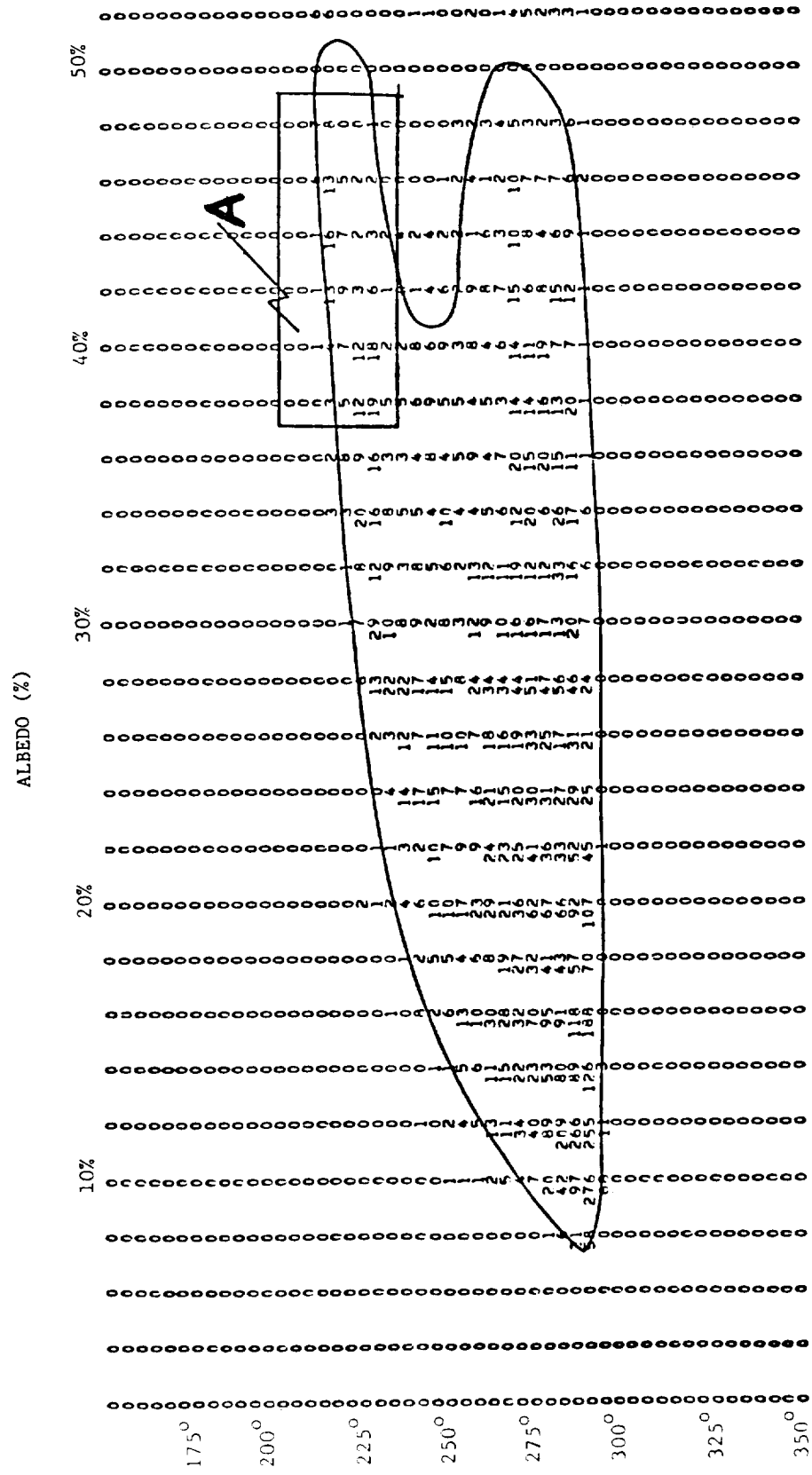

Figure 20. Two-dimensional histogram of GOES temperature and reflectance (albedo) data. The box region labeled A is presumably high thick cirrus cloud. The upper branch of the bounded region is interpreted as middle and high cloud of varying thickness and FOV coverage whereas the lower branch is interpreted as low cloud of varying thickness and FOV coverage.

Table 3
Pro's and Con's of the Various Cloud Measurement Techniques

	Pro's	Con's
1. Threshold	– Simple	– Fails when FOV not filled – Fails when $\epsilon \neq 1$ – Problematic Over Land
2. Bi-Spectral	– Physical Interpretation	– Requires Many Assumptions a) albedoes b) surface temp c) χ's and cloud top geometry d) emissivities
	– Tuneable with Physical Parameters	– Daytime Only
3. CO_2 Absorption	– Adaptable to Operational Temperature Retrieval	– Sensitive to Instrument Noise
	– Applies Principles of Radiative Transfer	– Difficult to Apply In Cases Where Clear Column Radiances Are Not Available
4. 3.7 – Split Window	– ?	– ?
5. 3-D Nephanalysis (Air Force)	– Operational Product	– Bogus Data
	– Vertical Structure Available	– Discontinuities in Method
6. 2-D Histogram	– Simple	– Highly Subjective

MR ARKING: Also, you are usually limited by resolution, because you have to rely on a sounder.

MR. COAKLEY: No, you're not. You are not limited by resolution. Modern sounders have a 20 kilometer field of view. Except for the case that Eric has pointed out, where you can't at all see the surface within thousands of kilometers of where you are looking, then you've got a problem. The higher resolution in that case won't help you.

MR. SMITH: I haven't really made a final evaluation of the 3.7 micron-split window technique that Al Arking will discuss; I prefer that he do that.

The 3-D NEPH, of course, has the advantage of being an ongoing operational product, and probably more important, it is really the only method in which you are given the vertical structure. Its problems basically are that it involves "bogusing", and that there has been a great deal of discontinuity in the method which has been used over the years, and will be used in the future. The Air Force is continually going to update this system as better products become available, so you cannot necessarily assume that the time history has uniform biases in it, which you would like to have for climate variability studies.

Finally, the 2-D histogram approach is simple, but a highly subjective approach.

There are a number of remaining problems. I think Table 4 highlights the major ones. We still have the problem that has plagued a number of the techniques over the years, that is the detection of thin cirrus and the vertical placement of it. In addition we have the multiple layer problem which is probably not resolvable with passive sensors, at least those we have now, although active sensors are coming in the near future.

We also need better methods of verification. Using ground-based observations may not be an appropriate way to go because of the unavoidable biases. We do not have much in the way of intercomparison of these techniques yet either. Thus we have no way of evaluating the variability due to the techniques themselves.

Finally, we do not have a simple technique based on spatial correlation parameters which would give us the cloud size distribution or moments; this is a parameter that has been pointed out by various scientific committees as a key element to the climate monitoring problem.

Table 4
Remaining Problems

1.	Detection and Placement of Thin Cirrus
2.	Detection and Placement of Multiple Layers
3.	Improved Verification Procedures
4.	Technique Intercomparison
5.	Development of a Simple Cloud Size Population Algorithm

AUDIENCE PARTICIPANT: You listed as an advantage of the 3-D NEPH that it is an operational product. NOAA is operationally retrieving cloud cover on their sounder system as well, using a modification of that 15 micron technique, but nobody has looked at the data, and it is probably not to be trusted. But that is another operational product which NOAA is doing now.

MR. RAMANATHAN: Eric, I am getting a feeling from your presentation that there is still quite a bit of uncertainty involved in retrieving cloud cover, and I am making this comment from the viewpoint of a climate modeler. One of the reasons why you would want to use cloud cover is to see how we are forcing the system, the forcing being the difference between the clear sky flux, which you have, and what happens when you put in the clouds. In that sense I would think one piece of information which we could really use is a clear sky climatology, so that we can compare it.

MR. SMITH: Well, I think that part of what we are meeting about here is to get off home plate on this whole issue of creating a global climatology. You know, we have many techniques for estimating cloud from satellites, some of them better than others, but I think most of them are reasonably good techniques. I think there needs to be more verification work, nevertheless my feeling is that they are good techniques, they are physically sound techniques. But, they simply haven't been applied to a global data set, and we must do that. That's what we are here for.

MR. RAMANATHAN: Still, a useful component and a very valuable set of information would be the radiation flux leaving the system under clear sky conditions.

MR. ARKING: Well, that might be necessary. But if you are going to use a threshold technique, then you will have to have that threshold as an input to your processing system.

MR. RAMANATHAN: That is what I had in mind when I made the comment. I was wondering if that information is being stored in the archives.

MR. STOWE: In the Nimbus 7 ERB program, we are going to keep minimum albedo as one of our parameters, which will be a rough indication of the clear sky.

MR. SMITH: Basically the problem right now is that the data archives that are being retained, which are basically radiance archives at various scales, simply represent too much data, too many computer tapes, too much in the way of burden and expense to immediately go in and derive global cloud climatologies including a clear sky climatology. What we want is there in the recent archives, and will be there in the future archives, but we must find better ways of retaining this data, and simpler, less expensive, and less burdensome methods of retrieving it.

AUDIENCE PARTICIPANT: I was particularly impressed by one of your points of trying to have an inter-technique comparison, which I think, for instance in the case of meso-scale models, in which people have taken several different models and made a comparison for the same cases, I think this approach would be excellent. The same kind of thing could be done with cloud data, by applying all of these five or six techniques, and see where they perform well, and in which situations.

MR. SMITH: Well, I think that can be done right now with the TIROS-N data. We have a satellite that is carrying the CO_2 channels, it is providing infrared window data, it is providing visible data. Really, it just remains for somebody to do it.

MR. POTTER: I have a question that I think we could ask all of our speakers today. Can you give us your best definition of what you mean by the terms cloudiness, cloud amount and cloud cover, and in particular, can you explain how the cloud amount, that you derived from the all-sky camera in the GATE area, how that definition of cloudiness compares?

MR. SMITH: Well, the all sky camera data was a matter of analyzing pictures and applying a hand planimetering technique. As for the definition of cloudiness, cloud amount, and cloud cover, they all mean the same thing in an automated computer sense. You consider individual pixels, and determine, for example, with a threshold technqiue, how many pixels of the total grid are above a threshold. If you are using bi-spectral or tri-spectral techniques, you derive a fractional cloud cover for each individual field of view or pixel, and then sum those up over the total grid. The definitions are all the same. They all denote mean percentage of these derived F's.

AUDIENCE PARTICIPANT: I know you have a problem with sorting it all out based on the various techniques, but doesn't the calibration problem overwhelm all of this.

MR. SMITH: I don't think that calibration is necessarily an unsolvable problem. When we consider this topic, we have to talk about the three parts of it. The first part is the relative calibration of the detectors and the determination of their response properties. This is an engineering problem that is handled fairly well prior to satellite launch by the instrument contractors.

We also have to talk about the inter-comparison of calibrated detectors as the satellites change, which gets us into the area of transfer calibrations or calibration adjustment. All calibrations are not referenced perfectly, but as we go from one satellite to another, if we have time intersection, we can transfer the original reference scale from one to another. This is a subject that has not really been considered, in a serious manner, by the satellite community.

Finally, we have the problem of sensitivity monitoring. This is not, in a pure sense, a calibration problem; this is a problem of monitoring the satellite data output.

I would like to illustrate a few of these points. Figure 21 illustrates a case in which we have combined an SMS-1 sector of data with a NOAA-2 sector of data (see Smith and Loranger, 1977). These are two visible data sectors co-located, or mapped into the same projection. We had a photometric pre-flight calibration of the NOAA-2 VIS detector. We transformed that calibration to a radiometric standard, and then transferred this over to the SMS-1 satellite, for which we did not have an absolute pre-flight calibration. Linear regression was used to accomplish the transfer.

MR. ARKING: You know, one of the things that is being neglected here is the angles at which you are viewing the target.

Figure 21. SMS-1 – NOAA-2 composite overlay, September 17, 1974 (10:00 GMT). (After Smith and Loranger, 1977.)

MR. SMITH: The angles vary, of course, but given that the photo-multipliers, or in this case a photo-multiplier and a photometer-bolometer, are linear responsive, and if we average over a region that is large, we believe the angular problem is negligible.

MR. ARKING: The SMS satellite always sees the same position at the same angle, whereas the polar orbiter would see a position from different angles at different times.

MR. SMITH: Agreed, but if we take enough of these data sets at enough times, and average, we can effectively baseline the two linear response scales.

MR. ARKING: But if you average over the same part of angular space, and if you are always averaging over one set of angles in one case, and over another set of angles in another case, you cannot compare the two averages.

MR. SMITH: I disagree. The reason I disagree is because first we use the variability of surfaces over the whole field as a sort of random variate. In addition, we are getting many looks of any given surface at many different angles. What you are driving at, is that a selected piece of real estate may bias the results.

MR. ARKING: Only if you are careful to get the angular regions of your 2π space. If you get this coverage, then you are okay.

MR. SMITH: Here is a possibility for sensitivity monitoring. Figure 22 is a picture from GOES West during March, 1979. I show this to illustrate that we can monitor the moon. The moon is not always in the earth field, so to speak, but because GOES is a spinner, and because we can control the turn on-turn off points of the detector, we could track the moon continuously. The moon is a great target for sensitivity monitoring of a space craft detector because of its invariant properties. The first part of Figure 22 is a visible image, the second part is an infrared view of the moon.

There is another interesting feature of the GOES spacecraft. It can actually monitor the sun by the use of a specialized set of prism optics. Figure 23 is a view from GOES of the sun (visible); note the limb darkening effect across the disc. We can debate about the variability of the solar constant, but the point is that the satellites we have in space are able to image planetary bodies that we can assume not to change. This could be used to our advantage in the area of sensitivity monitoring.

Finally, I will just show one more example of how we can effect a transfer calibration. Figure 24 illustrates two calibration curves of the visible detectors on SMS-1 and GOES-1 (see Smith and Vonder Haar, 1980). The photomultipliers were produced in the same batch so they should indicate similar response properties although we cannot directly measure this after launch. The first curve is for the SMS-1 (solid line) and was derived from the NOAA-3 transfer calibration which I discussed. The dashed curve was derived from Convair-990 flux data, taken during the Monsoon Experiment (MONEX) and applying a little bit of theory in the upper atmosphere. The two curves are within about 1 percent on this normalized reflectance scale. I believe this illustrates that we can use experimental aircraft to aid us in the calibration effort.

AUDIENCE PARTICIPANT: Are the radiometers really that non-linear?

MR. SMITH: I've displayed the results according to the digital quantization level or the count scale. The quantization scale itself is non-linear. The detector response properties are linear with respect to radiant energy. The reason things are done this way is to keep the signal to noise ratio a linear function of power at the detector, so the error bars can be expressed as a constant in counts.

MR. ARKING: Also, I think to get dynamic range.

MR. SMITH: Yes, the low end of the scale is divided into more levels than the high end, so as to resolve much better ocean-land differences. But really, it is done because it serves no real purpose to use high quantization resolution when the signal to noise defeats that resolution.

AUDIENCE PARTICIPANTS: Let me add one comment. NASA is planning to use White Sands as a monitoring target, in conjunction with our aircraft flights which will coincide with GOES and TIROS-N pictures.

MR. SMITH: I did not have time to show that material, although I have with me a chart which illustrates that you can monitor a presumably invariant target like the White Sands region of New Mexico. You can monitor the infrared window temperature over that target, orbit after orbit, or monitor the reflectance level at the same time each day. This is another way of spot-checking the change in sensitivity of a detector. You do run into the atmosphere transmittance variation problem doing that, but it is a very useful method.

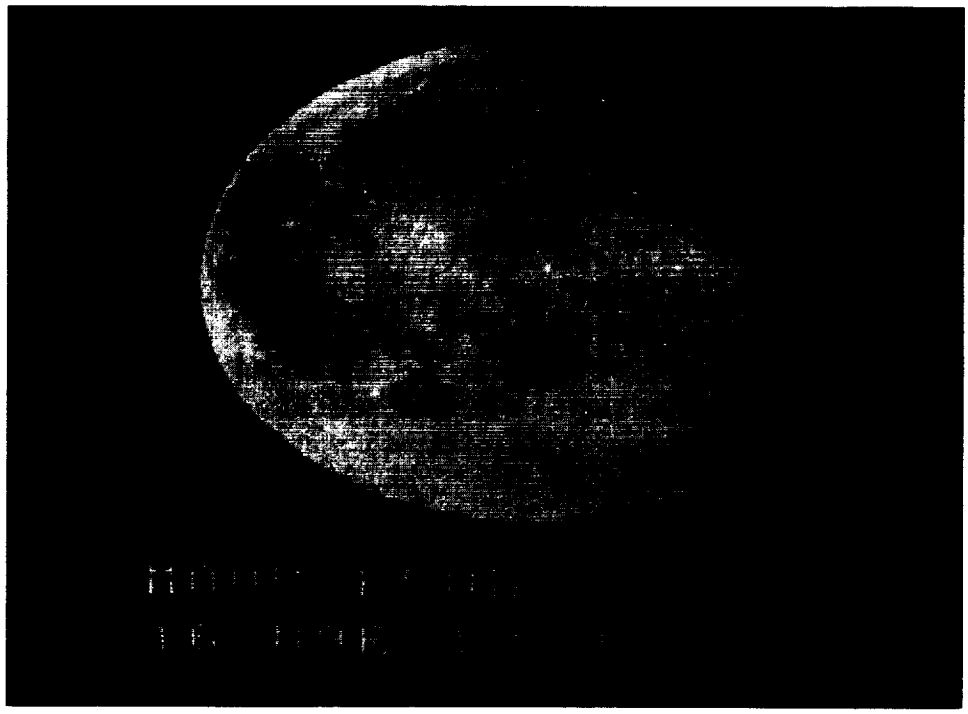

Figure 22a. Visible image of the Moon taken from the GOES-West satellite.

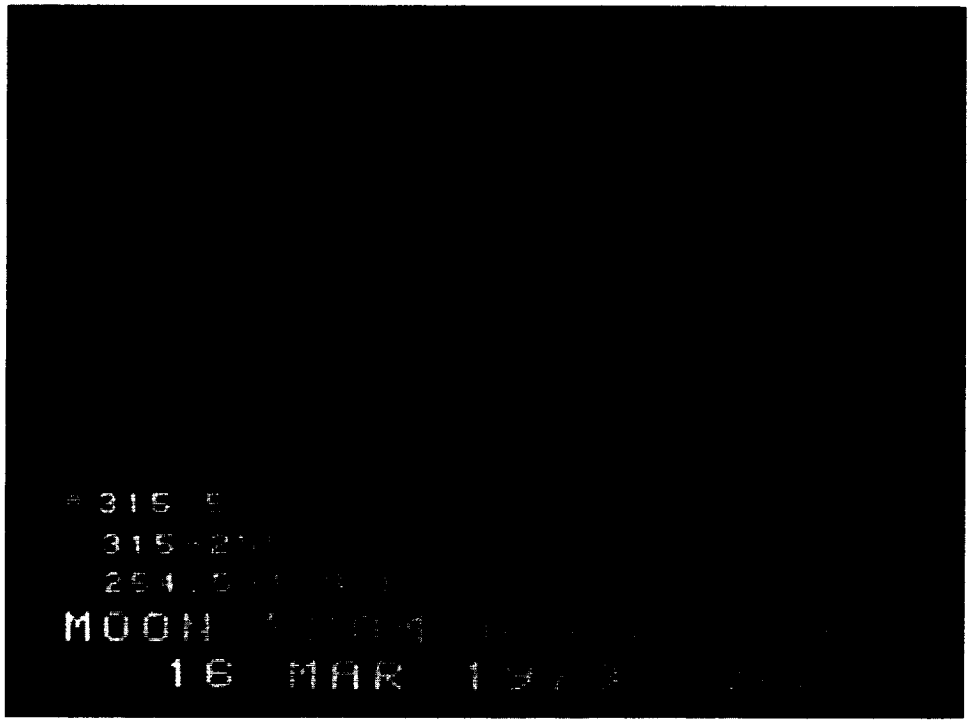

Figure 22b. Infrared image of the Moon taken from the GOES-West satellite.

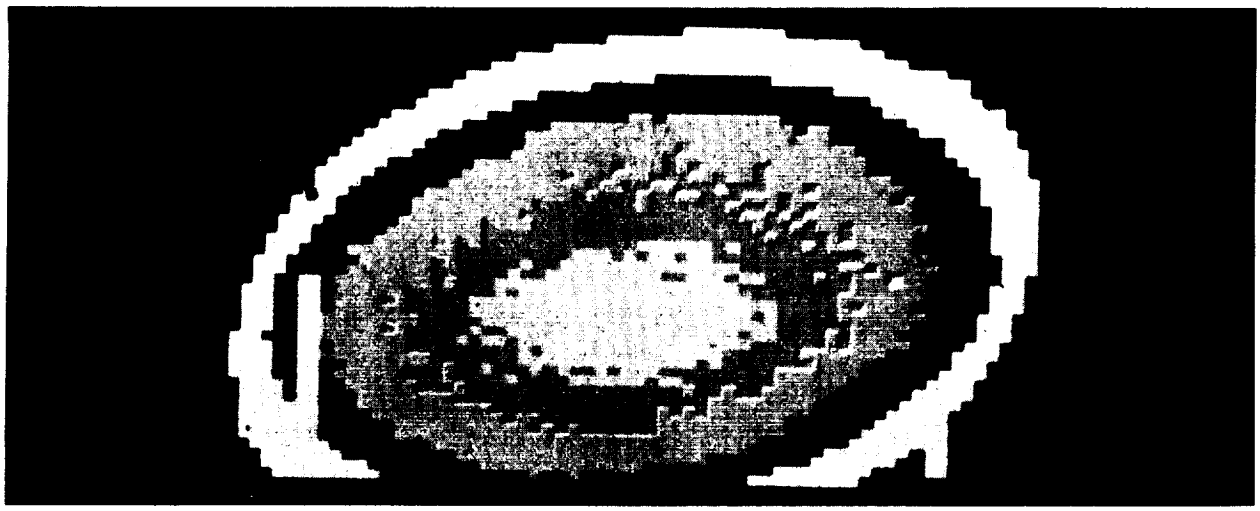

Figure 23. Visible image of the Sun taken from the SMS-1 satellite. (After Smith and Loranger, 1977.)

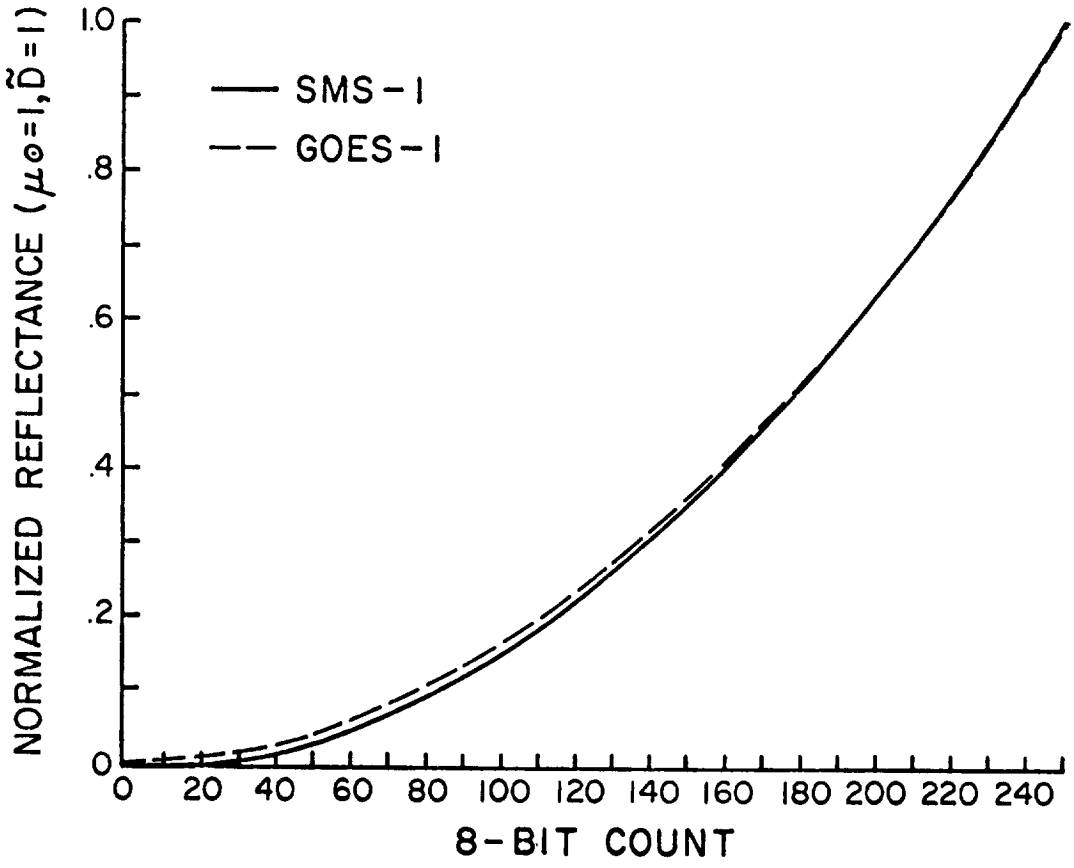

Figure 24. Comparison of the GOES-1 VIS detector calibration curve (derived from CV-990 flux radiometer data in a Rayleigh atmosphere with ozone absorption considered) with the SMS-1 calibration curve (derived from a NOAA-2 transfer calibration). (After Smith and Vonder Haar, 1980.)

MR. ARKING: It is not so simple. The reflectance of White Sands does change, particularly when it rains.

MR. SMITH: Well, that is true. In addition there are seasonal effects. There were actually two targets proposed for the monitoring effort. The other is lava flow near the White Sands monument which goes through a definite seasonal vegetation cycle.

MR. ARKING: Okay, let's turn now to the first of the contributing papers. Thanks very much for filling in for Professor Vonder Haar, and we are sorry for the circumstances which made him unable to come.

References

Ackerman, S. A., and S. K. Cox, 1980: Comparison of Satellite and All-Sky Camera Estimates of Cloud Cover During GATE. Accepted for Publication in *J. Appl. Met.*, 25 p. manuscript.

Arking, A., 1980: Use of 3.7 μm AVHRR Images to Detect Liquid/Ice Phase of Clouds. Presented at Meeting on Global Cloud Data Sets, April 23, World Weather Building, Chaired by Rex Fleming, 7 p.

Avaste, O. A., G. G. Campbell, S. K. Cox, D. Demasters, O. Ü. Karner, K. S. Shifrin, E. A. Smith, E. J. Steiner, and T. H. Vonder Haar, 1979: On the Estimation of Cloud-Amount Distribution Above the World Oceans. Atmospheric Science Paper No. 309, Dept. of Atmospheric Science, Colorado State University, Fort Collins, CO, 73 p.

Campbell, G. G., E. A. Smith, and T. H. Vonder Haar, 1980: Cloud Amount Estimation from Geosynchronous Satellites: A Demonstration of Diurnal Variations. Volume of Extended Abstracts, International Radiation Symposium, August 11-16, Fort Collins, CO, pp. 312-314.

Cox, S. K., and K. T. Griffith, 1979: Estimates of Radiative Divergence During Phase III of the GARP Atlantic Tropical Experiment, Part I. Meteorology. *J. Atmos. Sci., 36,* 576-585.

Holle, R. L., J. Simpson, and S. W. Leavitt, 1979: GATE B-scale Cloudiness from Whole-sky Cameras on Four U.S. Ships. *Mon. Wea. Rev., 107,* 874-895.

Miller, D. B., and R. G. Feddes, 1971: Global Atlas of Relative Cloud Cover 1967-1970. U.S. National Environmental Satellite Service and USAF Environmental Technical Applications Center, AD739434-Report No. 1, Washington, D.C., 237 p.

Reynolds, D. W., and T. H. Vonder Haar, 1977: A Bispectral Method for Cloud Parameter Determination. *Mon. Wea. Rev., 105,* 446-457.

Sadler, J. C., 1969: Average Cloudiness in the Tropics from Satellite Observations. Int. Indian Ocean Expedition Meteorological Monographs No. 2, East-West Center press, Honolulu, 22 p. and 12 plates.

Sadler, J. C., L. Oda, and B. J. Kilonsky, 1976: Pacific Ocean Cloudiness from Satellite Observations. Technical Report, Dept. of Meteorology, Univ. Hawaii, 137 p.

Smith, E. A., and D. C. Loranger, 1977: Radiometric Calibration of Polar and Geosynchronous Satellite Shortwave Detectors for Albedo Measurements. Technical Report, Dept. Atmospheric Science, Colorado State University, Fort Collins, CO, 92 p.

Smith, E. A., T. H. Vonder Haar, and M. Whitcomb, 1979: GATE Satellite-Surface Radiation Data Archives. Technical Report, Dept. Atmospheric Science, Colorado State University, Fort Collins, CO, 210 p.

Smith, E. A., and T. H. Vonder Haar, 1980: A First Look at the Summer MONEX GOES Satellite Data. Pre-prints of the AIAA 15th Thermophysics Conference, July 14-16, Snow Mass, CO, 16 pp.

Smith, W. L., and C. M. R. Platt, 1978: Comparison of Satellite-Deduced Cloud Heights with Indications from Radiosonde and Ground-Based Laser Measurements. *J. Appl. Met., 17*, 1796-1802.

Steiner, E. J., 1978: A Comparison of Surface Wind Parameters, Cloud Amount, and Sea Surface Temperature in Tropical Pacific. 3rd NOAA Climate Conference, Miami, FL, pp. 10-78.

Wielicki, B. A., and J. A. Coakley, 1980: Cloud Retrieval Using Infrared Sounder Data: Error Analysis. Submitted for Publication in *J. Appl. Met.*, 32 p. Manuscript.

Winston, J. S., A. Gruber, 1979: Earth-Atmosphere Radiation Budget Analyses Derived from NOAA Satellite Data June 1974-February 1978: Volume 1. NOAA-NESS, U.S. Dept. Commerce, Washington, D.C.

EXAMPLES OF CLOUD COVER AND DIURNAL VARIATION STUDIES USING GEOSTATIONARY SATELLITE DATA

Edwin F. Harrison
NASA Langley Research Center
Hampton, VA 23665

and

Patrick Minnis
Kentron International, Inc.
Hampton, VA 23666

INTRODUCTION

Clouds play a significant role in the Earth radiation budget as they influence the solar-reflected and Earth-emitted radiation and, in turn, affect our climate. Cloud cover varies greatly with geographical location and time. Satellites are the most effective means of measuring cloud distribution over the Earth. The Geostationary Operational Environmental Satellite (GOES) provides hourly radiance data from which cloud information can be extracted over a substantial portion of the Earth. A large set of the high-resolution, GOES, visible (0.55 – 0.75 μm) and infrared (10.5 – 12.5 μm) digital data has been collected at the Colorado State University Ground Station and processed and analyzed at the NASA Langley Research Center. Cloud cover amounts have been determined for each daylight hour of each day of November 1978 over 1600 regions, each 250 km by 250 km. These regions, located between 45°N and 45°S latitudes and 30°W and 120°W longitudes, encompass most

of the United States and South America, and parts of the Atlantic and Pacific Oceans. The hourly radiance data for these regions were obtained from the GOES-East Satellite, located over the equator at a longitude of 75°W and an altitude of 37,800 km.

CLOUD COVER ANALYSIS AND RESULTS

An adaptation of the bispectral method first developed by Reynolds and Vonder Haar (1977) and applied to digital data by Mendola and Cox (1978) is the basis of the technique used here to derive cloud cover. This method is based on the following relationship.

$$A_c = (D^2 - D_s^2)/(D_c^2 - D_s^2), \quad (1)$$

where A_c is the effective cloud fraction, D is the measured visible brightness count, D_s is the land or water background count, and D_c is the cloud model brightness. This equation is derived from an energy balance model which assumes that a measured radiance is the area-weighted summation of the respective radiance reflected by the cloudy and cloud-free areas of the scene. Effective cloud cover, rather than apparent cloud cover, is used in this analysis of the GOES data because of its appropriateness for Earth radiation budget studies. Effective cloud cover is a parameter which accounts for the total integrated effect of clouds from the reflected visible window channel. It is the fraction of the scene which would be entirely covered with a reference cloud model to yield the same radiance as that measured. An optically thick cloud model with a maximum albedo is used as the reference cloud.

An example of the effective cloud cover amount for each daytime local hour of each day of November 1978 and the monthly mean hourly effective cloud amount for a 250-km by 250-km region near the west coast of South America is shown in Figure 1. While it is apparent that the cloud amounts do not recur exactly each day, the daily maximum cloud amount nearly always occurs in the morning. This tendency is easily seen in the plot of the lower right side of the figure which indicates the monthly mean hourly cloud cover. The reason for this distribution is that a layer of clouds tends to form every night in the moist lower atmosphere over the relatively cool ocean surface. As the cloud cover reaches a maximum in the morning, the clouds and surrounding air begin to absorb the Sun's energy. This solar heating gradually dissipates the cloud cover in the afternoon by evaporation and mixing of the low, moist air with the warm, dry air above. This change in cloud cover as a function of local time is an example of diurnal variability of cloudiness.

Figure 2 shows the distribution of monthly mean diurnal variation of effective cloud cover over 1600 regions for November 1978. The largest diurnal variation of cloudiness is over a significant portion of the Southeast Pacific Ocean. The maximum amount of cloudiness in this region occurs in the morning between the hours of 0700 and 1000, whereas the maximum cloudiness over South America generally occurs after 1000. The peak cloudiness over the United States usually takes place between 1000 and 1400. Little mean diurnal variation of cloud amount was observed in most regions of the North Atlantic Ocean. However, monthly mean cloud cover in this same area ranged from less than 10 percent up to about 40 percent.

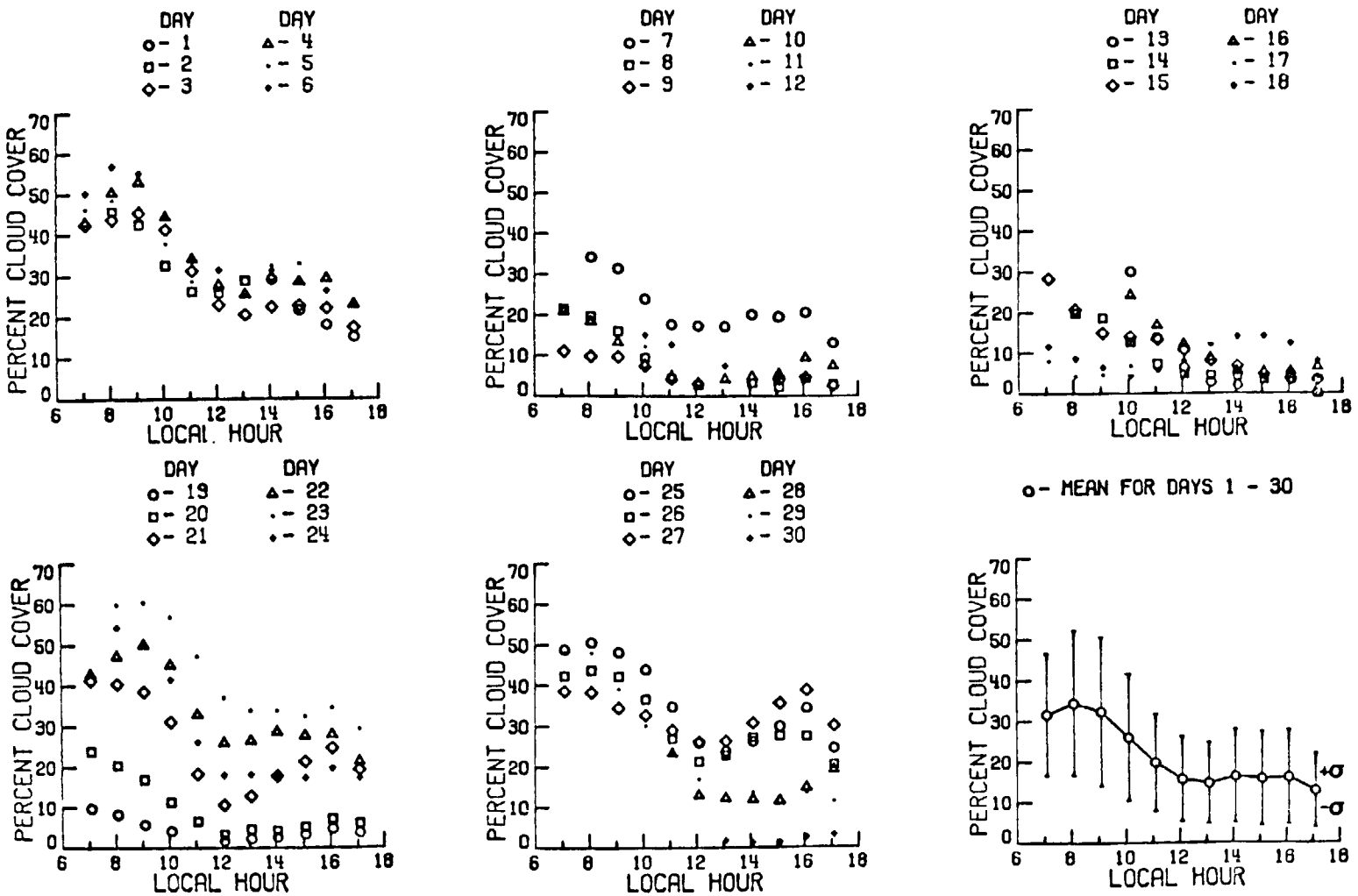

Figure 1. Hourly daytime effective cloud cover amounts from GOES for a 250 x 250 km region at 21.4°S and 73.8°W during Nov. 1978.

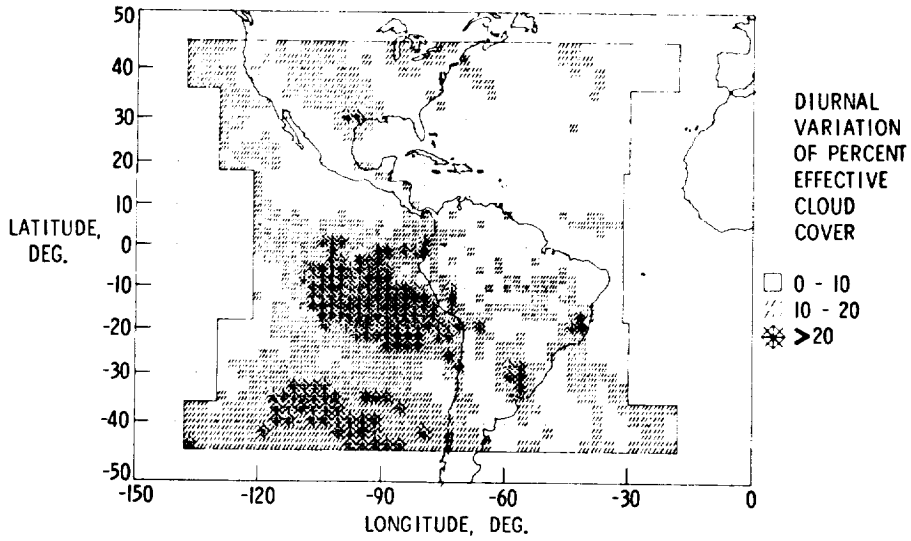

Figure 2. Monthly mean diurnal variability of regional cloudiness from GOES for Nov. 1978.

The distribution of the monthly mean and standard deviation of effective cloud cover as a function of latitude are presented in Figure 3. The lowest observed cloud amounts exist in the tropics and the highest amounts are in the middle latitudes. Two portions of the intertropical convergence zone are apparent as relative maxima at 7.5°N and 15°S. The results are consistent with the trends found in other studies (e.g., Raschke and Preuss, 1979).

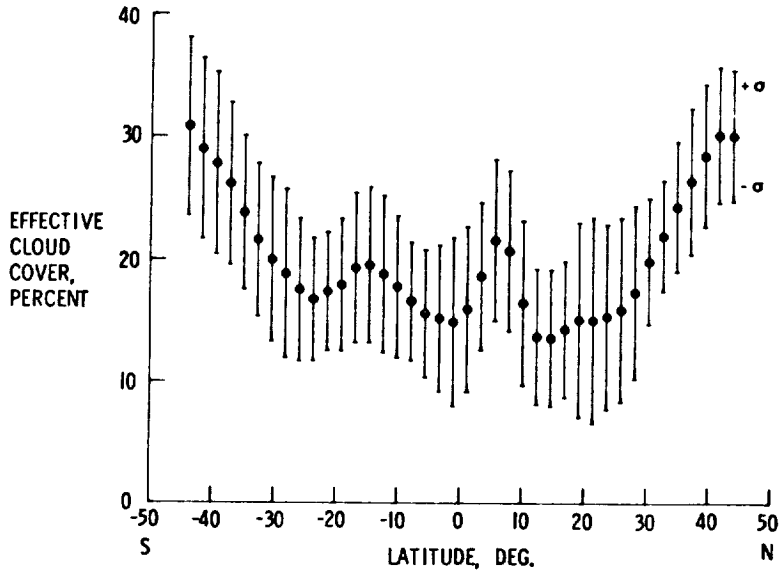

Figure 3. Zonal mean effective cloud cover from GOES for Nov. 1978. (40 regions/zone).

The GOES visible data were also used in conjunction with the infrared data to determine various temperature quantities. The equivalent blackbody temperature, T_c, of the effective cloud was calculated from the following equation.

$$T_c = TBD\,[(BB[T] - BB[T_s]\,(1 - A_c))/A_c]\,, \tag{2}$$

where T and T_s are the measured mean total and surface equivalent blackbody temperatures, respectively; BB is the Planck function and TBB is its inverse evaluated at 11.5 μm. A clear visible radiance technique is used to determine T_s. All measured thermal radiances are normalized to a viewing zenith angle of 0° with an infrared window limb-darkening model derived with a radiative transfer routine using standard atmospheres.

An example of the mean values retrieved by this method for 1 month for a region off the west coast of South America is shown in Figure 4. The morning peak of the effective cloud amount decreases to a minimum in the late afternoon, which is consistent with the climatology of the area (see lower portion of the figure). Gradual increase of T and decrease of T_c throughout the day may indicate the dissipation of a low cloud layer.

In summary, a methodology has been described which yields effective cloud parameters and temperatures from geostationary satellites. Examples of hourly variability of daytime cloud cover have been quantified and analyzed on regional and zonal scales for November 1978 from the GOES-East satellite. These cloud results provide an initial data base toward the development of global cloud quantification information for the International Satellite Cloud Climatology Project.

Analyses are also underway to determine cloud cover amounts for other months, seasons, and years from existing GOES data. These results will be used to develop statistical diurnal cloud models. Correlations will be performed between the simultaneous measurements of Nimbus-7 ERB broadband data and GOES narrowband data. Cloud amounts at 3 altitude levels (e.g., low, middle, and high) will also be determined from using a combination of the visible and infrared GOES data. These results will have important applications to Earth radiation measurements and climate modeling studies.

References

Mendola, C. and S. K. Cox, 1978: Cloud Analysis from Bispectral Satellite Data. Atmos. Sci. Paper No. 295, Colorado State University, Ft. Collins.

Raschke, E. and H. J. Preuss, 1979: The Determination of the Solar Radiation Budget of the Earth's Surface from Satellite Measurements. Meteorol. Rdsch., 32, 18-28, February.

Reynolds, D. W. and T. H. Vonder Haar, 1977: A Bispectral Method for Cloud Parameter Determination. *Mon. Wea. Rev., 105,* 446-457.

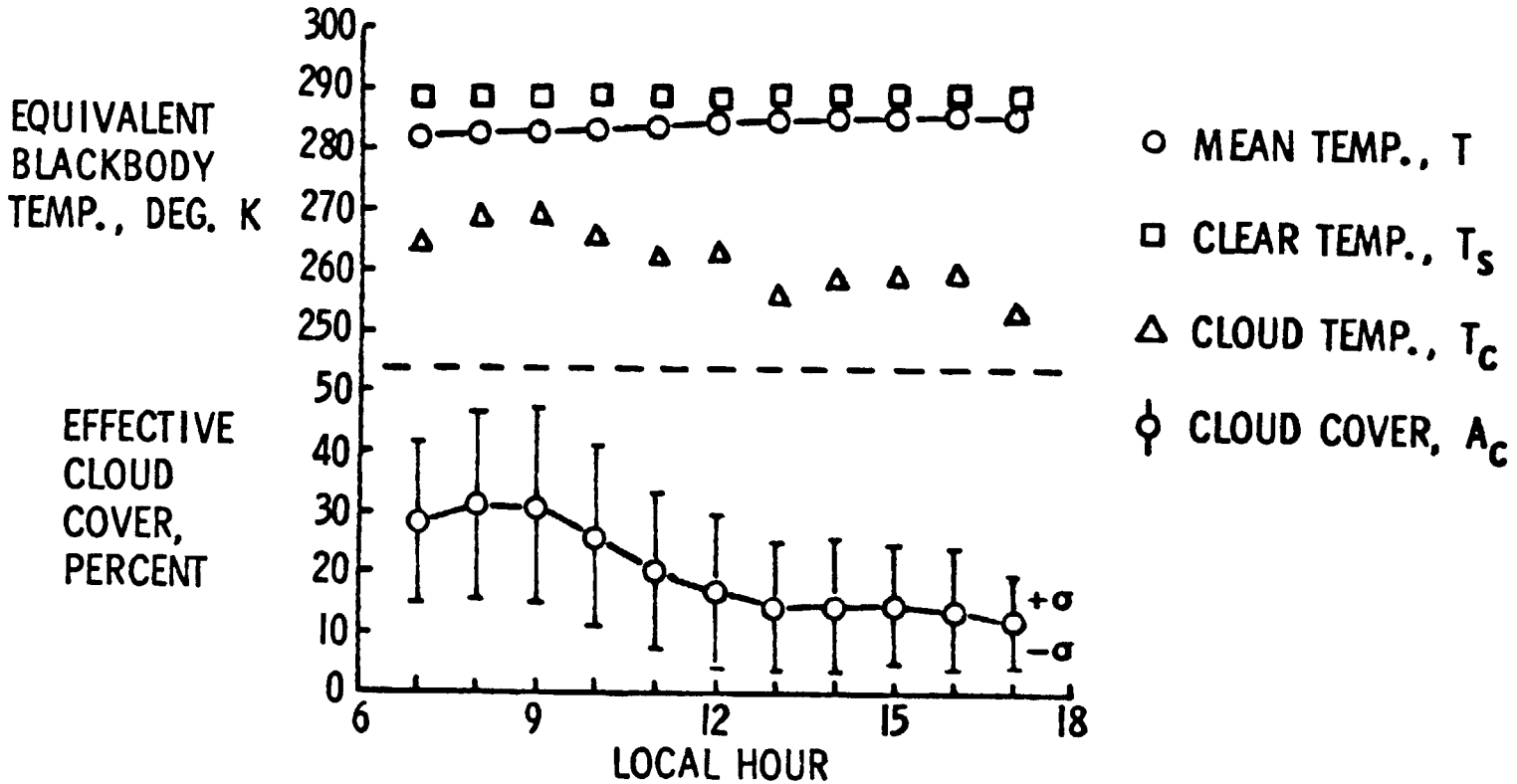

Figure 4. Mean effective cloud parameters derived from GOES for a 250 x 250 km region at 21.4°S and 78.8°W during Nov. 1978.

ERRORS IN CLOUD AMOUNT OBTAINED USING THRESHOLD TECHNIQUES

James A. Coakley
National Center for Atmospheric Research
Boulder, Colorado 80307

Errors in cloud-cover area obtained with popular threshold techniques are inversely proportional to the square root of the area covered by a typical cloud. Because of this nonlinear dependence, errors become small only when the size of clouds are many times the scan spot size of the viewing instrument. In addition, the errors depend on the cloud areal size distribution. An alternate procedure for obtaining cloud cover is to use the spatial structure of the IR radiance field to identify radiance associated with cloud-free, completely cloud-covered and partially cloud-covered fields of view. This identification is shown in Figure 1. For single layered systems the separation of completely covered from partially covered fields of view allows an estimate of the cloud-areal size distribution and thus the errors associated with threshold techniques. For such systems the errors that result from threshold methods can be appreciable as is shown in Figure 2. When the errors are large the retrieved cloud cover is found to be highly sensitive to the applied threshold, but when clouds are uniform and large so that the errors are small the retrieved cloud cover is found to be insensitive to the applied threshold. Observations of radiances at visible wavelengths reveal considerable spatial structure in the radiance field as is shown in Figure 3. Because of this structure, estimates of cloud reflectivities for completely covered fields of view will have large uncertainties. These uncertainties will give rise to unreliable estimates of cloud cover when only the visible radiance field is used.

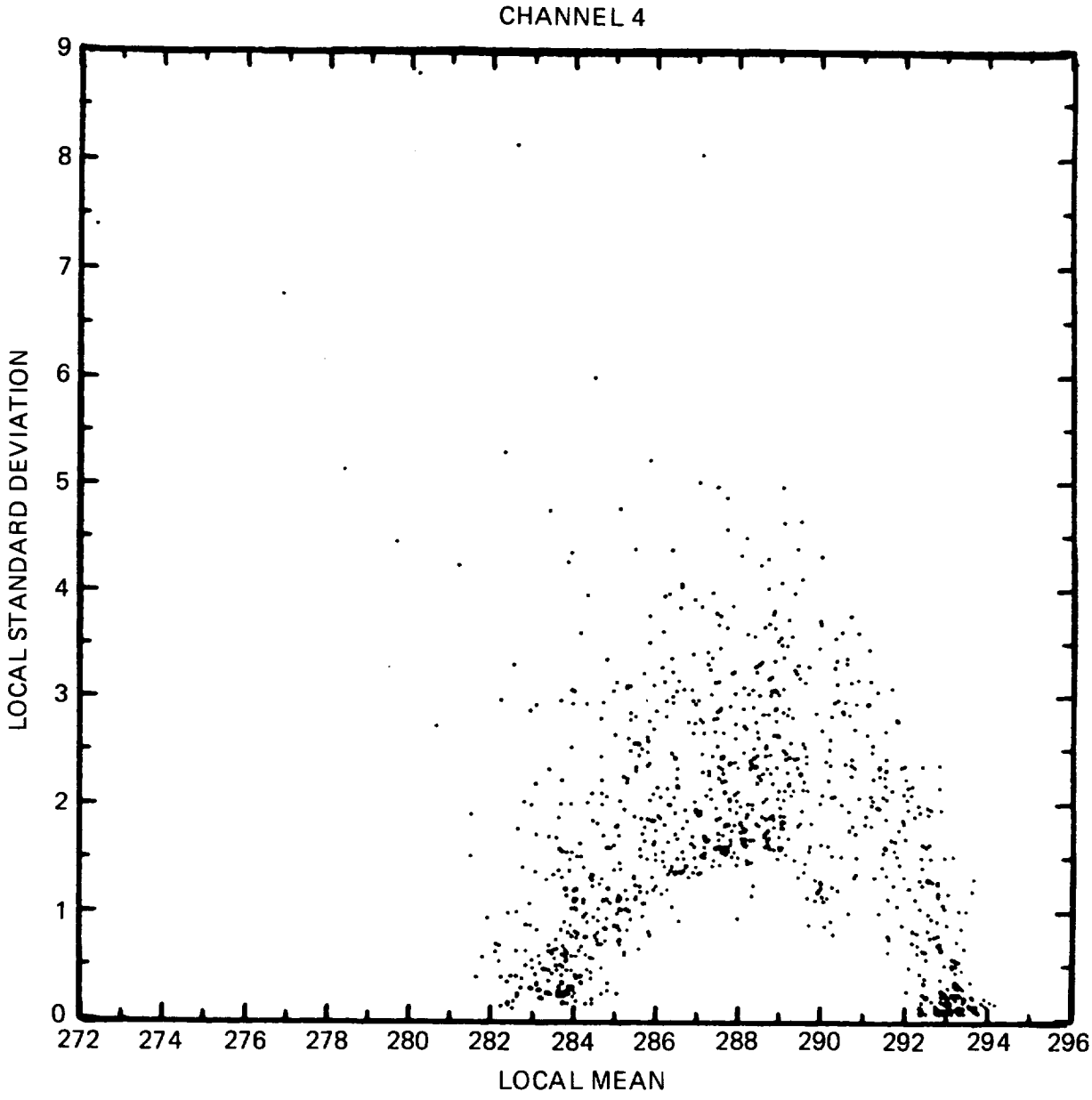

Figure 1. Local mean vs. local variance constructed from 8x8 arrays of 4 km, 10.5-11.5μm AVHRR scan spots for a (1000 km)^2 region centered at 22.3 N, 136.7 W on June 8, 1979 at 0000 GMT. The cluster of points with low spatial structure at a radiating temperature near 293 K represents clear fields of view, the cluster near 283.5 K represents completely cloud-filled fields of view; the points in between exhibiting high local spatial structure represents partially filled fields. From the clear sky radiance, the cloudy sky radiance and the mean radiance for this (1000 km)^2 region, the total cloud cover is estimated to be 0.54 ± 0.04.

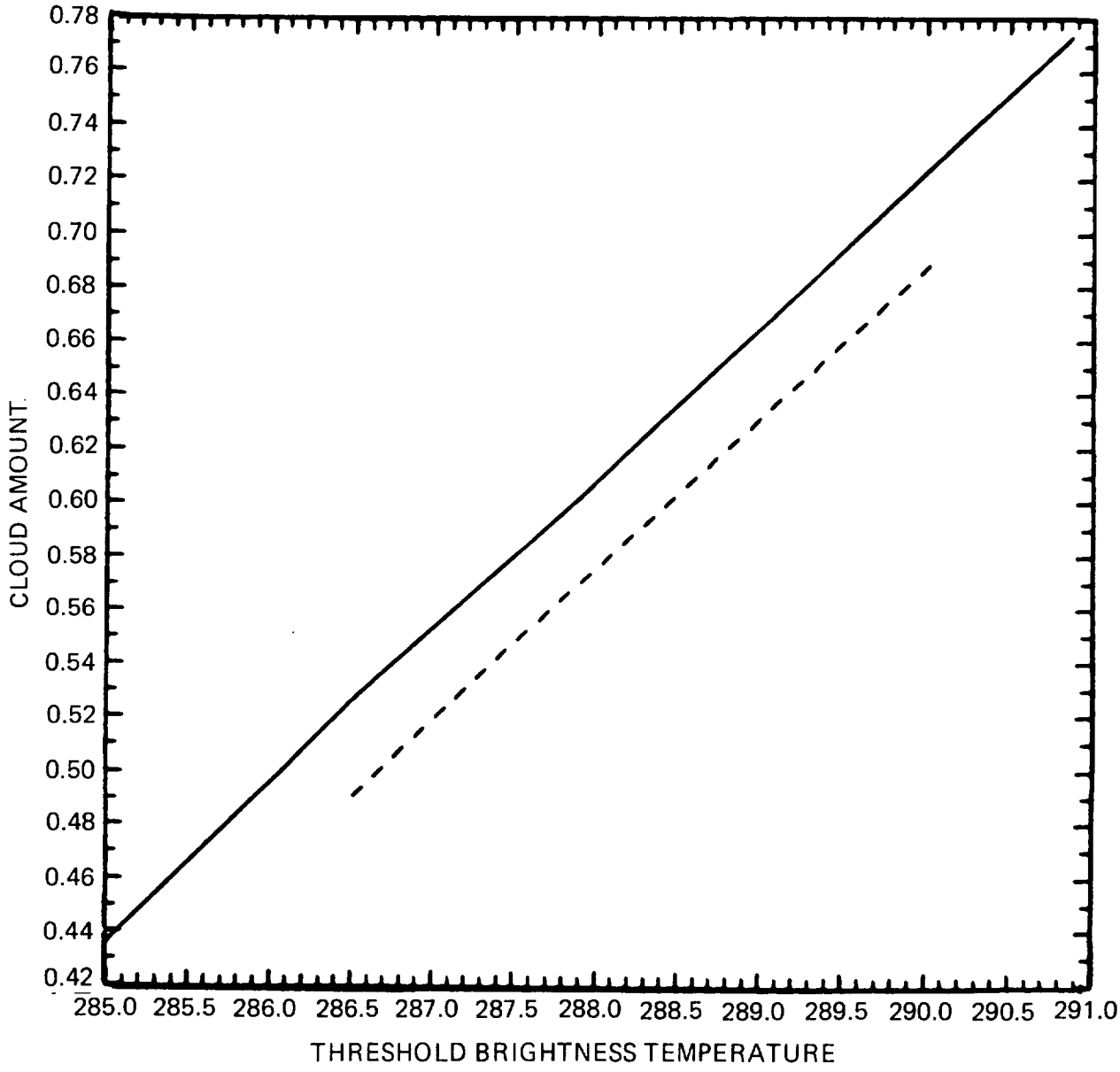

Figure 2. Estimated cloud amount as a function of assumed threshold for data displayed in Figure 1. For the solid curve, clear sky radiating temperatures are assumed to be greater than 292.3 K; cloudy sky radiating temperatures are assumed to be less than 285.0 K. For the dashed curve, clear skies are greater than 290.9 K; cloudy skies less than 286.5 K.

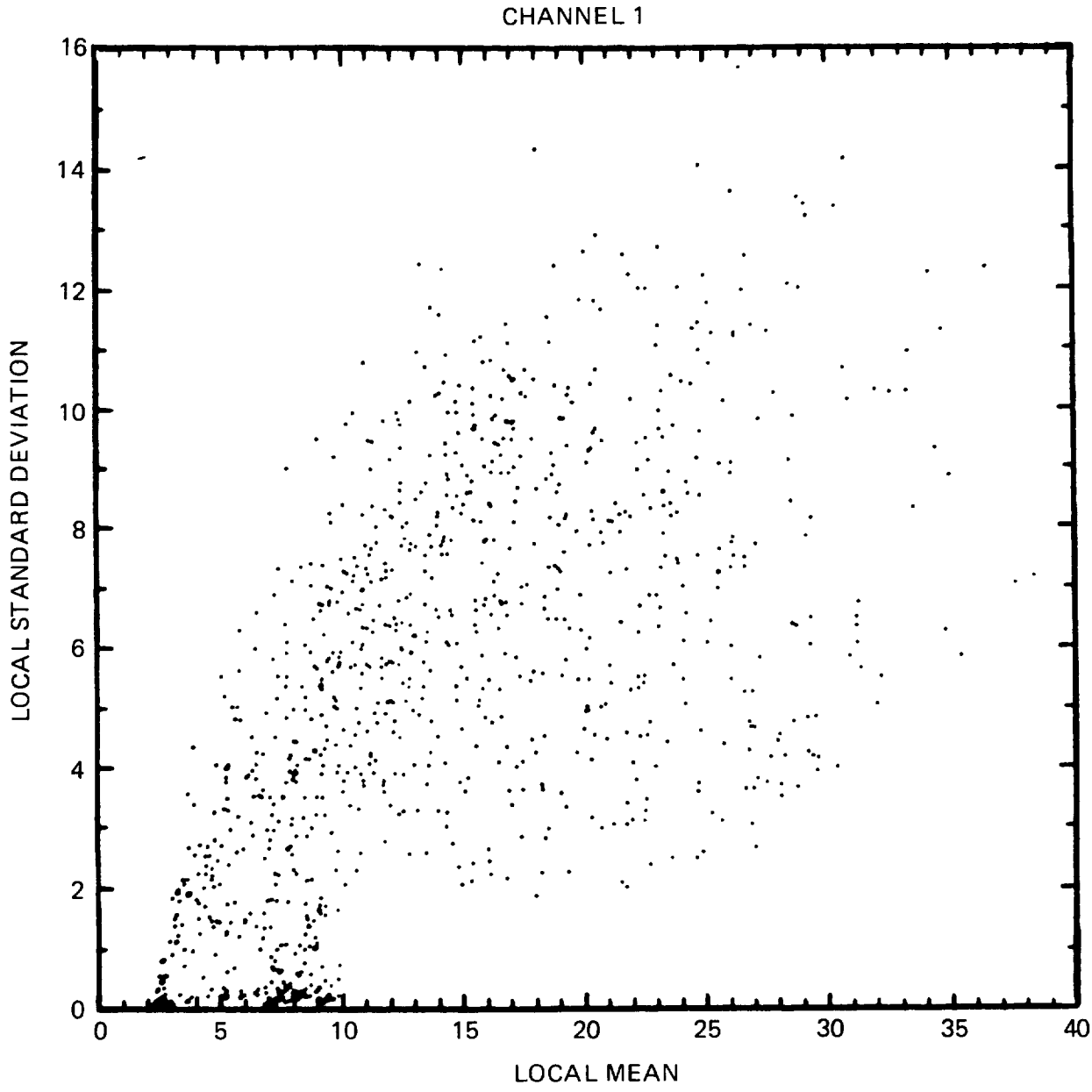

Figure 3. Local mean vs. variance of visible reflectivities (0.55–0.9 μ m) for same scene as in Figure 1.

COMPARISONS OF VISIBLE AND INFRARED DISTRIBUTION OF GLOBAL CLOUD COVERS

Moustafa T. Chahine
Jet Propulsion Laboratory
California Institute of Technology
Pasadena, California 91103

Day and night mapping of the global distributions of the horizontal cloud cover and the corresponding cloud-top pressure levels can be obtained from the same set of infrared radiance data used to retrieve clear-column temperature profiles. General formulation of the problem is presented with illustrations for the simple case of a single layer of non-reflecting clouds. Experimental verifications are obtained using 15 μm data measured by the NOAA-VTPR infrared sounder.

APPROACH

The upwelling radiance from a planetary atmosphere is a function of the thermal state of the atmosphere, the concentration of radiatively active gases, and the extents, heights, and radiative transfer properties of clouds and aerosols. Thus, in principle, it should be possible to recover useful information about the physical and chemical structure of an atmosphere from analysis of the upwelling radiance. However, the problem in analyzing such data lies in finding ways to uncouple the effects of these variables and retrieve the true values of each unknown parameter separately. *By treating the cloud effects as short period oscillations over the clear column radiance,* an analytical method was developed by Chahine to retrieve clear-column vertical temperature profiles from radiance measurements made in the presence of clouds. The method requires radiance data from two spectral regions measured over two adjacent fields of view having different amounts of clouds. The uncoupling of the effects of clouds is carried out analytically without any *a priori* information about the amounts, heights and optical properties of the clouds in the fields of view. Once the clear-column temperature profiles are determined the same radiance data could then be used to determine the heights, amounts, and radiative transfer properties of clouds.

APPLICATION TO VTPR DATA

The determination of the clear-column temperature profiles from the VTPR data requires *a priori* knowledge of the surface temperature T_S. We obtained T_S from the NOAA surface analysis. We investigated the effects of errors in the assumed surface temperature on the accuracy of the values of the effective cloud cover $\tilde{N}$ which is the product of the geometrical cover N and the cloud emissivity ϵ_ν and the mean cloud top pressure, P_C. We concluded that the effects of an error in T_S of ± 2 K on $\tilde{N}$ and P_C are small, especially for $P_C < 700$ mb. Correction for the effects of water vapor on the atmospheric transmission functions were made before generating the clear-column radiances.

It should be noted here that while the determination of the clear-column radiance is obtained without any assumptions about the properties of clouds, the determination of the amount and height of

clouds requires the use of cloud models. In the case of the VTPR data we assumed that the difference between the reconstructed clear-column radiance and the radiance measured in a given field of view is due to the presence of a single layer of non-reflecting cloud. We applied the non-reflecting cloud model to analyze radiance data from the NOAA-VTPR sounder for a period of one week from January 1-7, 1975. The VTPR global cloud distributions were calculated in 1977. The results were then averaged for a grid size of 4° latitude by 5° longitude, and only the averaged results were stored on a magnetic tape for subsequent comparison with other cloud maps to be obtained from other sources. A typical comparison of the results is shown in Figures 1, 2 and 3.

Figure 1 shows contours of cloud amounts for a region across the Pacific Ocean between 40°N-30°S and 75°W-255°W. Figure 2 shows contours of cloud amounts derived from computations made by J. Sadler of the University of Hawaii for the same period of time and the region from photographs obtained from the Vidicon cameras of NOAA's satellite.

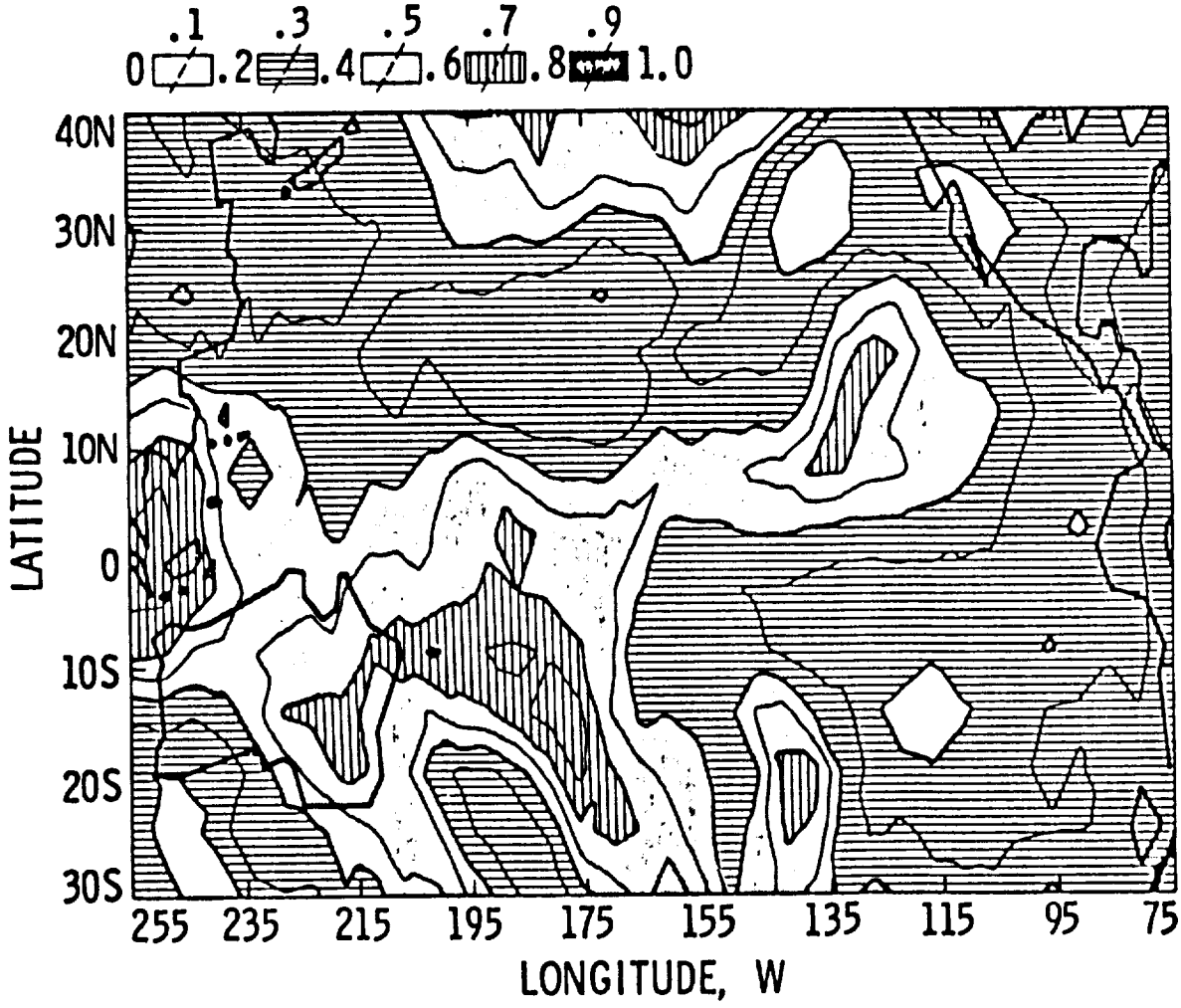

Figure 1. Contours of cloud amounts in decimals derived from 15 μm satellite data for the period of January 1-7, 1975.

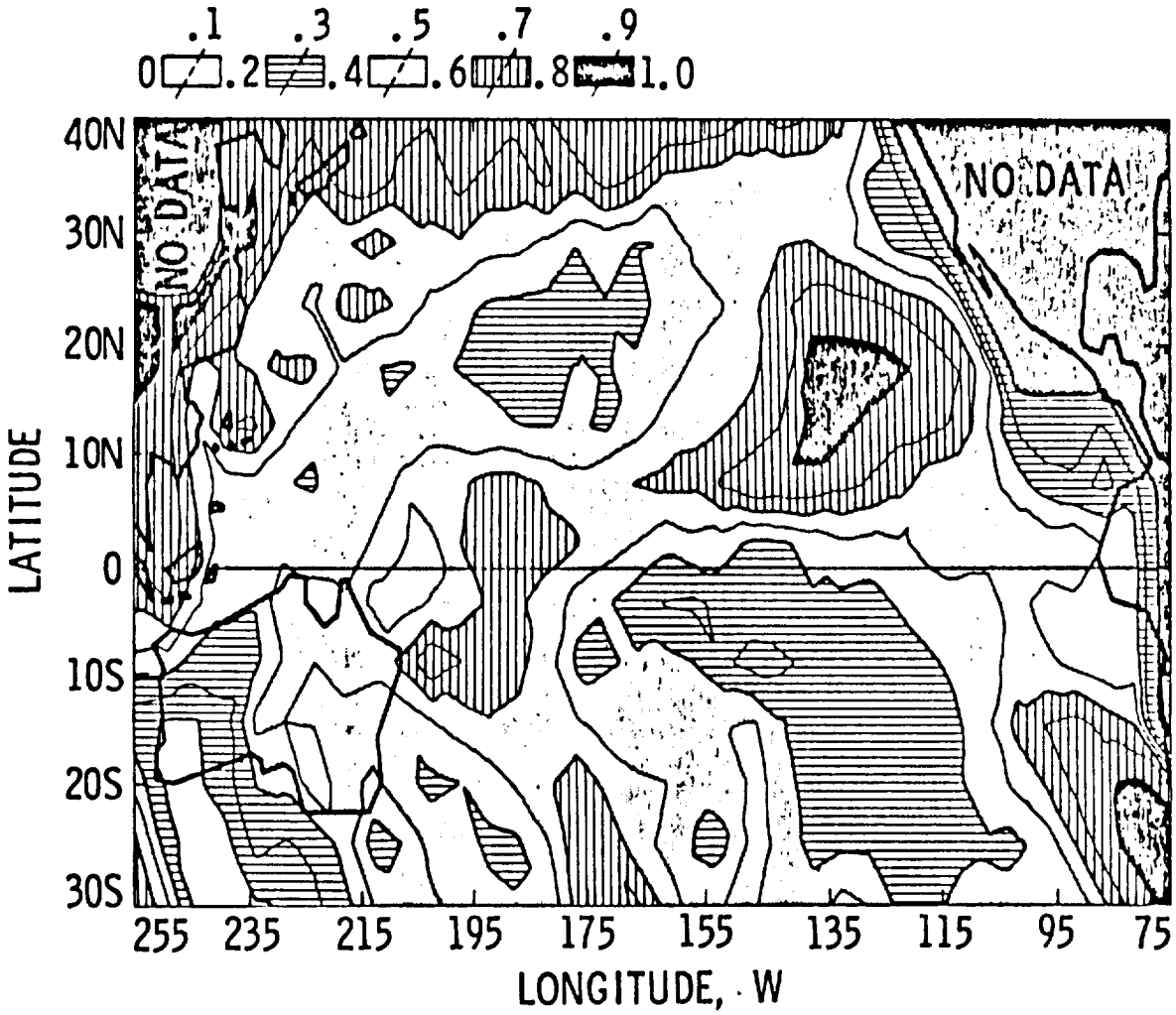

Figure 2. Contours of cloud amounts in decimals derived from visible data by Sadler for the period of January 1-7, 1975.

The results shown in Figures 1 and 2, therefore, compare asynoptic infrared cloud maps and synoptic visual maps. Consequently only persisting cloudiness appears to be common between the two cloud maps. For this reason the zonally averaged values shown in Figure 3 give a more realistic comparison between the amount of clouds observed in the infrared and visible. The conclusion that the effective infrared cloud amount $\tilde{N} = N\epsilon$ is smaller than the cloud amount observed in the visible could be due to the facts that the cloud emissivity in the 15 μm is less than one, and the VTPR sounding channels are not sensitive to detecting low level clouds below 800 mb. The average cloudiness for the region shown in Figures 1 and 2 is 0.39 for the infrared and 0.52 for the visible, and the ratio of the infrared to the visible cloud cover is ~0.75.

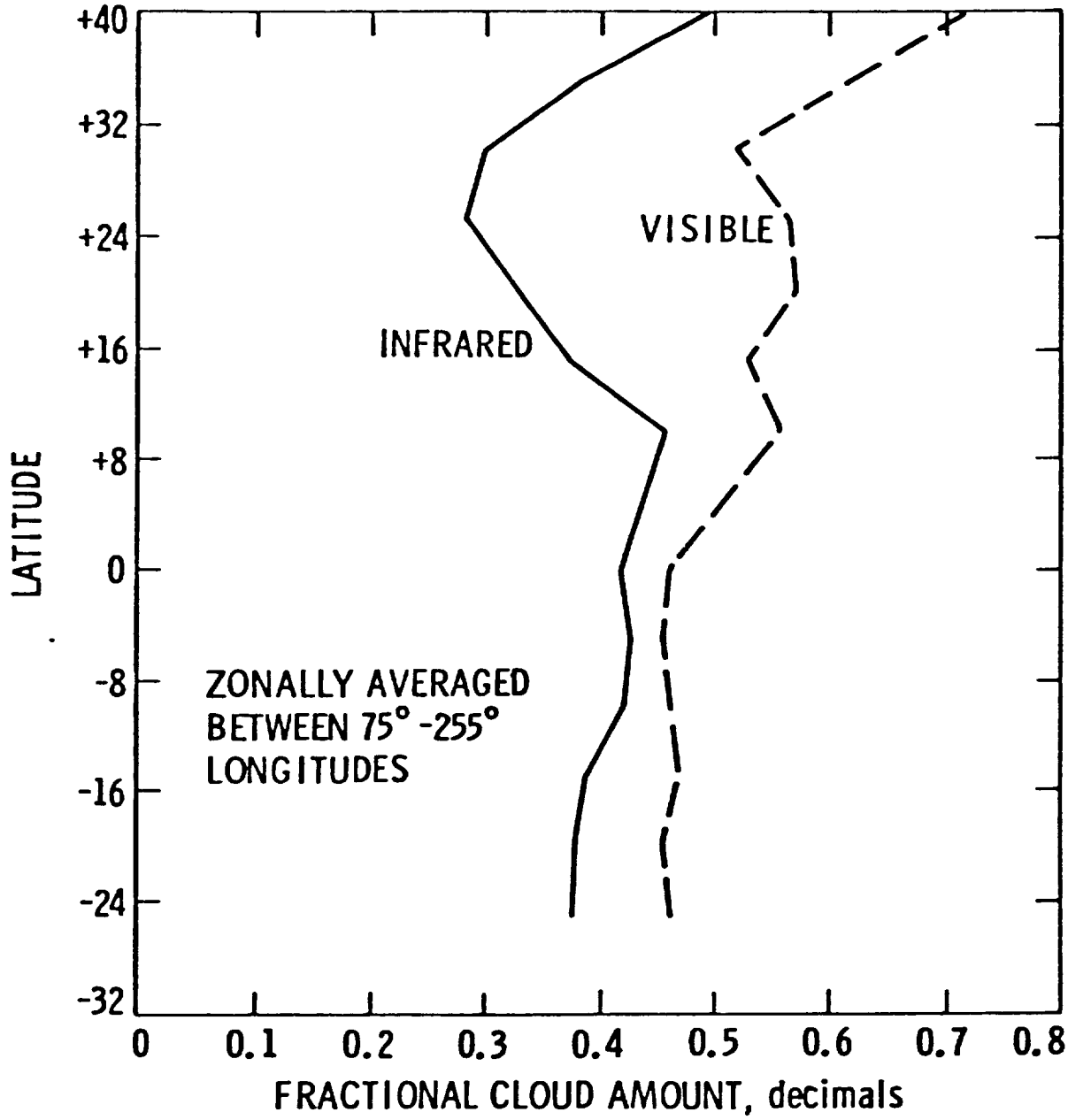

Figure 3. Meridional profiles of zonally averaged distribution of fractional cloud cover for the data given in Figures 1 & 2.

CLASSIFICATION OF CLOUDS USING THIR DATA FROM NIMBUS 7 SATELLITE

T. S. Chen, L. L. Stowe, V. R. Taylor
MSL, NOAA, Washington, D.C.

P. F. Clapp
CAC, NMC, NOAA, Washington, D.C.

1. INTRODUCTION

This paper describes the development of a method to obtain cloud features on a global basis through the interpretation of the THIR instrument's (Temperature Humidity Infrared Radiometer) 11 μm window and 6.7 μm water vapor absorption channel measurements made on board Nimbus-7. Derived products such as clear, low, middle and high cloud amounts and their associated statistics in a four-level histogram for each of 18,630 fixed subtarget areas (STA), each approximately 160 km on a side, are analyzed and compared with other available satellite and conventional cloud data. Initially, this study was undertaken to support the Earth Radiation Budget Experiment (ERB) flown on Nimbus-7, by specifying mathematical models of the earth's surface and clouds. However, it appears likely that this approach can also be modified to developed a cloud climatology needed for climate modeling and climate variability diagnostic applications.

2. FORMULATION OF TECHNIQUE

Basic principles used to derive the cloud amounts and heights have been reported in detail by Stowe, et al. (1978). A brief review here is intended to provide readers with some minimal background and continuity.

An abbreviated cloud-type classification as described in the International Cloud Atlas (1956) is adopted in the present study. It is defined in terms of altitude above mean sea level. Thus, low cloud is defined as having tops below 2 km; middle clouds between 2 km and 7 km in the tropics, 2 km and 6 km in mid-latitude and 2 km and 4 km in polar regions; high clouds above these levels. The monthly-mean climatological temperature profiles compiled at NCAR by Jenne, et al. (1974) and Crutcher, et al. (1970) have been used, with linear interpolation, to relate these cloud altitude boundaries to atmospheric temperature for a given STA. But the climatological temperatures at the surface and at 2 km have to be corrected for atmospheric attenuation, as functions of surface temperature and local satellite zenith angle of the radiating surface, in order to bring them close to the effective radiative temperature measured by THIR. Thus, for a given STA, the boundary temperatures at the surface/low, low/middle and middle/high are set.

The THIR data, after being converted from filtered radiance to the black-body temperatures (Cherrix, 1978) are then processed into four histograms giving the fraction of clear and three layer cloud coverages. Also for each bin the 11 μm and 6.7 μm mean temperatures are listed, along with several "flags" based on certain values of temperature standard deviations, to provide adequate information for cloud interpretations.

An algorithm using statistical and meteorological information is developed to read the cloud-ERB tape which contains cloud data in the four histogram bins mentioned above, to produce final products such as those listed in Table 1.

Table 1
Sample of THIR Cloud Products

Clr Amt = 0.30	Low Cld Amt = 0.28	Mid Cld Amt = 0.29	Hi Cld Amt = 0.13
Clear Flags	Low Cld Flags	Mid Cld Flags	Hi Cld Flags
Ambig Low = 0	Ambig Clr = 0	Thin Cirrus = 0	Ice = 1
Low Cld = 0	Clear = 0	Convctv = 1	Brkn Srts = 0
Thin Cirrus = 0	Thin Cirrus = 0	Ambig Clear = 0	Thk Srts = 0
Ambigs = 1	Ambigs = 1	Ambig Low = 0	Thin Srts = 0
		Ambig High = 0	Ambig Middle = 0
			Convctv = 1

3. DISCUSSION OF RESULTS

Cloud types and amounts derived from THIR are verified against a direct visual comparison with enhanced infrared and visible GOES pictures. Favorable agreement is generally obtained for those STA's limited to tropical regions. This was expected because of the small daily temperature anomalies there. At higher latitudes, however, the use of climatology becomes a problem particularly over land and in snow and ice covered regions.

Figure 1 shows a plot of THIR clear amount (percent) against subjective estimates which include, besides the sectorized GOES images and upper-air soundings, available surface observations concurrent with THIR both in space and time. This limited sample includes data in the western hemisphere from 15° and 45° north or south latitude and for November 15 and 18, 1978. Note that for the 11 ocean cases, there is very good agreement, with a correlation coefficient of $\gamma = 0.95$. Over land, however, the agreement is poor with $\gamma = 0.53$. In the ocean case, the subjective data seem to underestimate the clear amount, perhaps, due to overestimation of cloud amounts reported from surface observers. In the land case, occasionally large temperature anomalies seem to produce poor results.

The THIR high clouds compare well with the subjective ones for both ocean and land cases (not shown) even though the THIR clear estimates do not appear satisfactory over land. This may also be related to temperature anomalies. At high elevations, temperature anomalies are small, even over land. Therefore, the THIR estimates of high clouds should still be good over land even though the surface temperatures may depart considerably from climatology.

For low and middle clouds over ocean, THIR also compares well with the subjective estimates, with $\gamma = 0.82$ for low and 0.98 for high clouds.

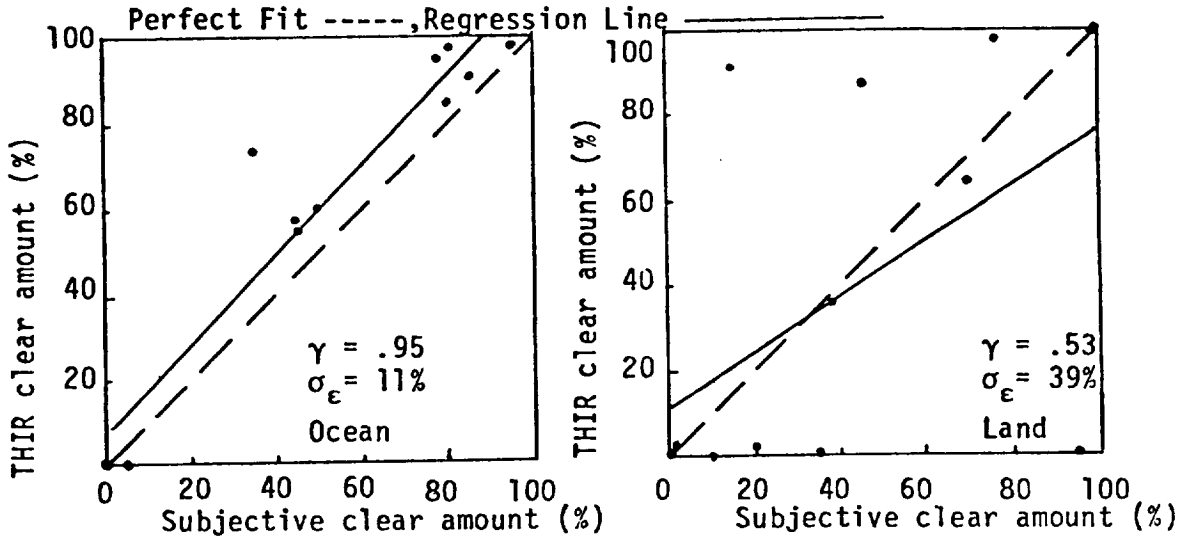

Figure 1. Plot of subjective versus THIR clear amount.

4. CONCLUDING REMARKS

Results indicate that at present THIR-derived cloud information is adequate for middle and high clouds. However, over land there is an uncertainty in the determination of clear and low cloud amounts. For computerized sorting of Nimbus-7 ERB scanning channel data into uniformly clear and cloudy categories, this ambiguity can be eliminated through quality control processes to meet our initial objective. The best way to improve THIR products however, is to bring in the daily global surface temperatures.

Since our THIR cloud products possess many broad aspects such as global coverage, compatibility with ground-based observations, and high resolution of cloud characteristics and statistics, there is a potential in using this technique as a basis for developing a cloud climatology.

References

Cherrix, G. T., 1978: The Temperature Humidity Infrared Radiometer (THIR) Subsystem. The Nimbus 7 User's Guide, GSFC, 247-263.

Crutcher, H. L. and J. M. Meserve, 1970: Selected Level Heights, Temperatures and Dewpoints for the Northern Hemisphere, NAVAIR 50-1C-52.

International Cloud Atlas, Vol. 1, WMO 1956, Geneva, Switzerland.

Jenne, R. L., H. L. Crutcher, H. Van Loon, and J. J. Taljaard, 1974: A selected climatology of the southern hemisphere: computer methods and data availability. NCAR-TN/STR-92, 91 pgs., Boulder, Colorado.

Stowe, L. L., M. Chen, H. Jacobowitz, and I. Ruff, 1978: Classification of clouds for the Nimbus Satellite ERB Experiment using THIR data. Preprint, Third Conference on Atmospheric Radiation, 103-106.

PRELIMINARY GLOBAL CLOUD PROPERTIES RETRIEVED FROM TWO-CHANNEL SCANNING RADIOMETER DATA FOR JULY 1977

W. B. Rossow, S. Vemury, S. Davis, E. Kinsella, A. A. Lacis
NASA/Goddard Institute for Space Studies
New York, New York 10025

The objectives of this project are to derive a one year global climatology of cloud fractional cover, visible optical thickness, and cloud top height and to evaluate the utility of scanning radiometer observations for determining cloud effects on the atmosphere's radiation budget. Preliminary analysis results are presented here. The data used for this analysis are:

1. visible (0.5–0.7 μm) and infrared (10.5–12.5 μm) scanning radiometer data from the NOAA 5 satellite for January to December 1977,
2. daily NMC temperature and humidity profiles, including surface temperature, for 1977, and
3. global vegetation/land use survey and monthly mean sea ice extent data for 1977, both converted to seasonal surface reflectance maps.

The ocean reflectance is obtained by calculating the Fresnel reflection coefficients using an empirical wave slope distribution. The instrument field-of-view is 4x4 km for the visible channel and 8x8 km for the infrared channel at nadir, but the data employed are samples of the full resolution data producing a nominal 12–25 km sampling.

The analysis method proceeds by reconstructing the viewing geometry of the satellite observations and then comparing the observed radiances to theoretical radiances calculated assuming that the instrument field-of-view is either completely cloud-filled or cloud-free. The theoretical visible radiance is derived as a function of viewing geometry, surface reflectance and cloud optical thickness with a complete multiple scattering calculation assuming plane-parallel clouds, a droplet single scattering albedo of one, and no atmospheric scattering or absorption. The theoretical infrared radiance is derived as a function of viewing geometry and cloud top height with a complete radiative transfer calculation using the daily vertical profiles of temperature and humidity. Diurnal variations of temperature and humidity are not accounted for.

Figure 1 illustrates, in polar stereo projection, the optical thickness and cloud top height distribution obtained for a single day in July 1977 for the northern hemisphere. The numbered arrows indicate several interesting features.

1. The clouds in the eastern Pacific ITCZ exhibit characteristic small scale, large optical thickness features embedded in large scale, high altitude features extending westward from the cumulus features.
2. Trade wind cumulus cloud fields are recognizable as patchy, low altitude features.
3. Distinctive frontal cloudiness associated with midlatitude systems display embedded small, high optical thickness, high altitude features characteristic of precipitating systems.

The highly complex longitudinal variations of cloud structures is readily apparent in the figure.

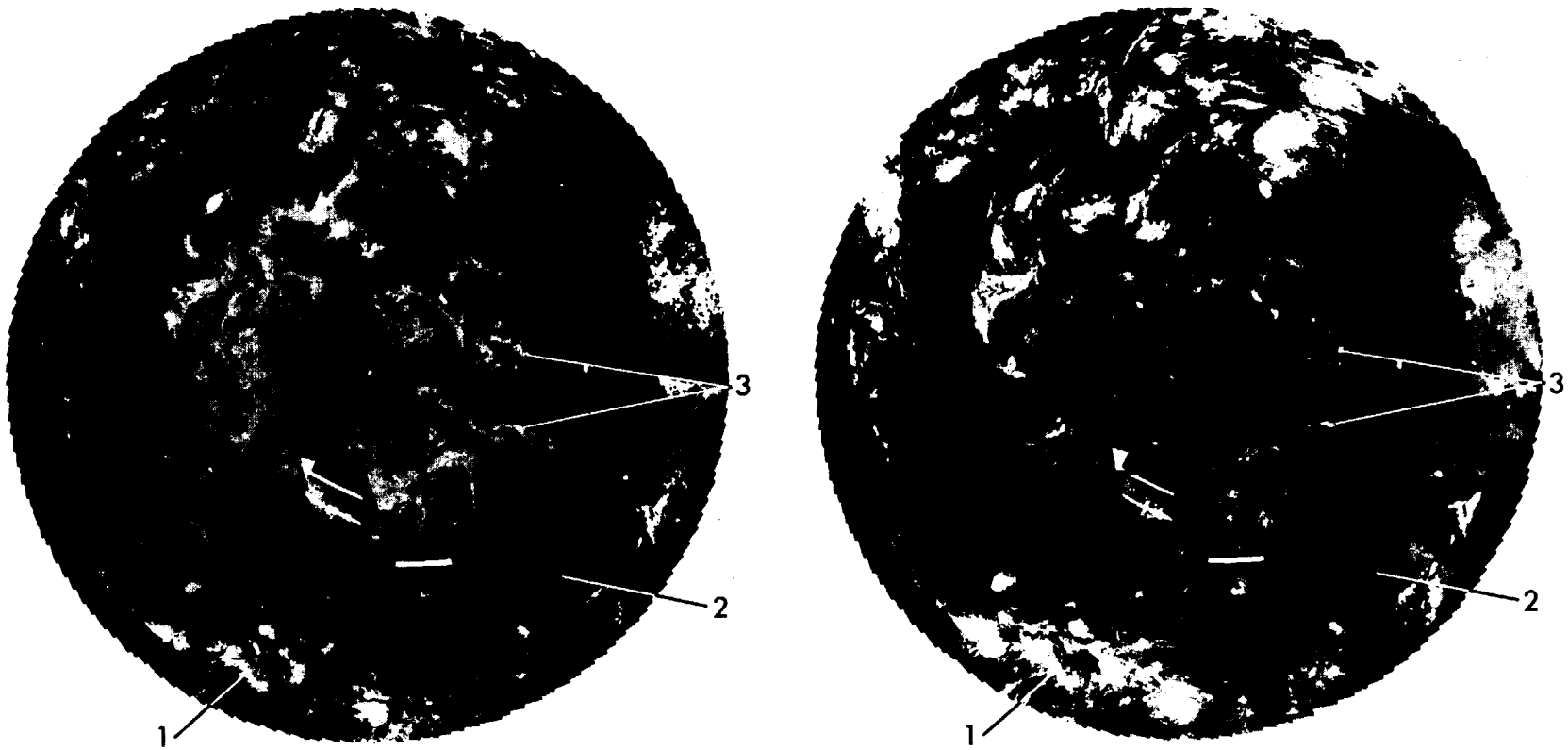

(a) (b)

Figure 1. Cloud properties in the northern hemisphere for 5 July 1977 from NOAA 5 Scanning Radiometer. In this polar stereo projection North America is below center, North Africa to the right and Asia above center. The arrows point to features described in the text. The white bands are missing data. (a) Cloud optical thicknesses derived from the visible channel data are displayed in four ranges: 0-1 (black), 1-8 (dark gray), 8-32 (light gray) and >32 (white). (b) Cloud top altitudes derived from the infrared channel data are displayed in four ranges: 0-1 km (black), 1-3 km (dark gray), 3-7 km (light gray) and >7 km (white).

Key problems revealed by this analysis are difficulties in reconstructing the observation geometry and in determining the optical thickness of clouds over bright surfaces. The first problem is caused by the operational sampling strategy employed to produce the data archive, together with poor documentation of the orbital characteristics. Improper reconstruction of the viewing geometry is partly responsible for the pattern marking orbital swaths in Figure 1a. The second problem is caused by the uncertainty in sea ice reflectance and by the multivalued relation between reflectance and cloud optical thickness for bright surfaces. The latter effect is caused by the large difference in scattering phase function between a nearly isotropic surface and the cloud particles. This second difficulty is illustrated by the differences in the cloud patterns over the Arctic Basin in Figures 1a and 1b.

Two important advantages of this analysis method are that:

1. determination of cloud top height allows height-dependent atmospheric scattering effects to be incorporated, and
2. determination of cloud visible optical thickness allows more realistic infrared emissivities to be used to avoid incorrect cirrus cloud altitude determinations.

SATELLITE CLOUD ANALYSIS DURING GATE

JoAnne Parikh
Southern Connecticut State College
New Haven, CT 06515

and

Marshall Atwater
Center for Environment of Man
Hartford, CT 06120

A method for analysis of cloud types and cloud amounts during GATE was developed using SMS infrared data. The method, described by Parikh and Ball (1980), is based on histograms for 1) clear, 2) partial, and 3) overcast cloud amounts, and on spectral and textural features represented by a variation of the Roberts Gradient. Five cloud types defined were 1) low clouds, 2) middle clouds with no significant high clouds, 3) high clouds with no significant lower clouds, 4) high clouds with significant lower clouds, and 5) cumulonimbus clouds. Results are shown in Figures 1-3 from the 4th of September 1974 at 1200 GMT.

The data were used to derive cloud coverage characteristics for Phase III of GATE, as reported by Ball, et al., (1980) for use in a solar radiation and infrared radiation model for GATE (Atwater and Ball, 1981).

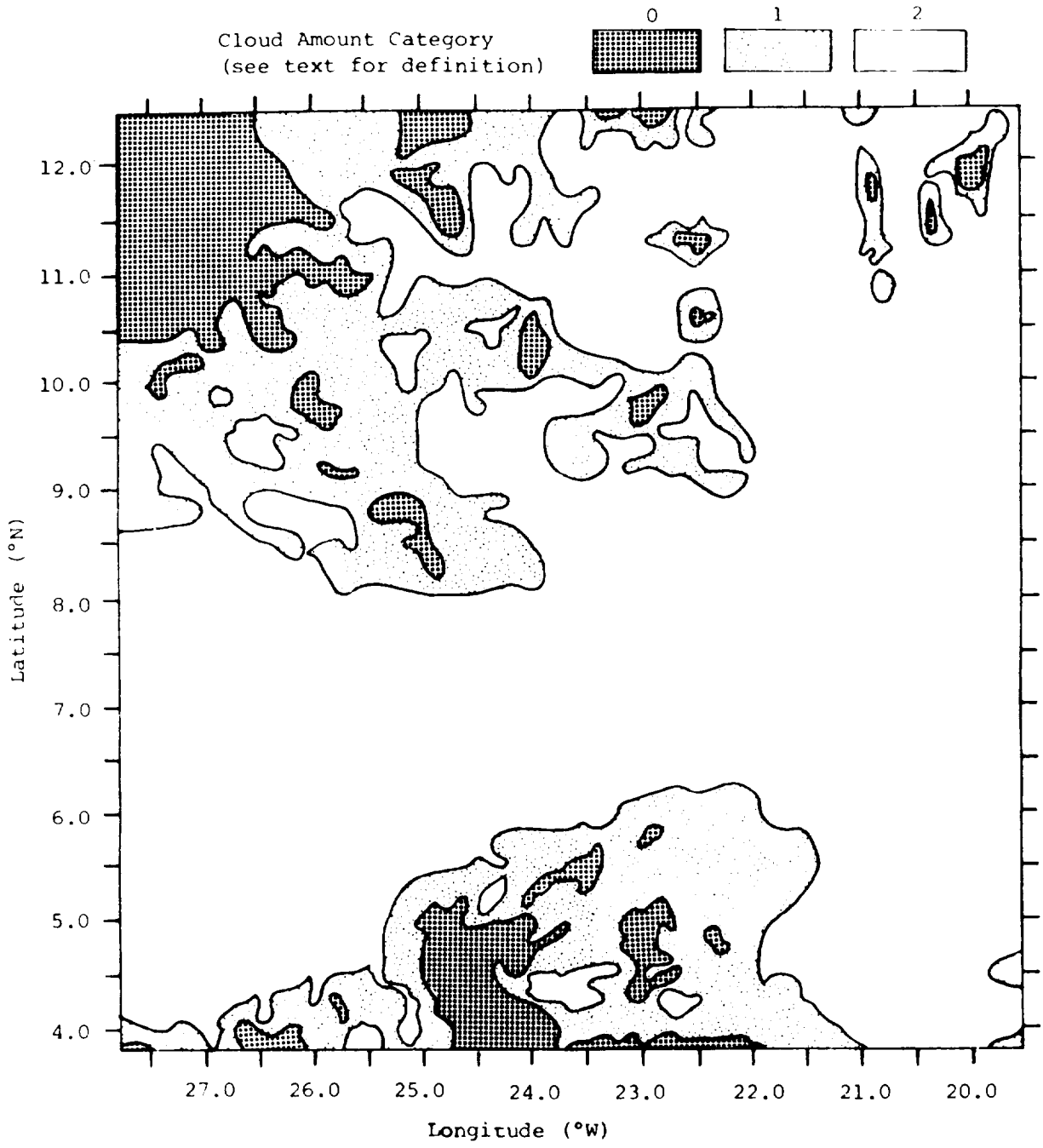

Figure 1. Cloud amount analysis from SMS-1 IR data in the region of interest on 4 September 1974 at 1200 GMT.

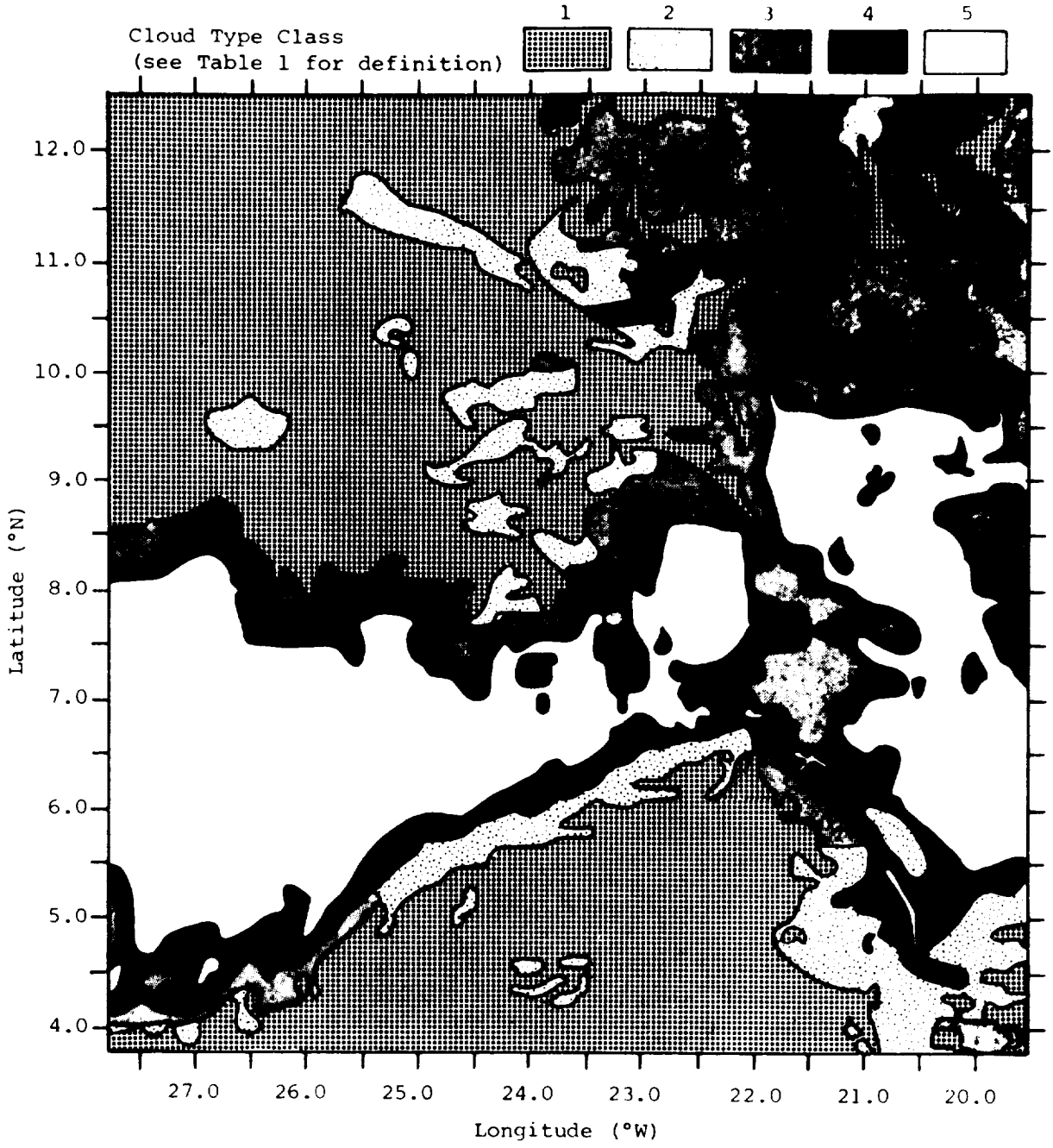

Figure 2. Cloud type analysis from SMS-1 IR data in the region of interest on 4 September 1974 at 1200 GMT.

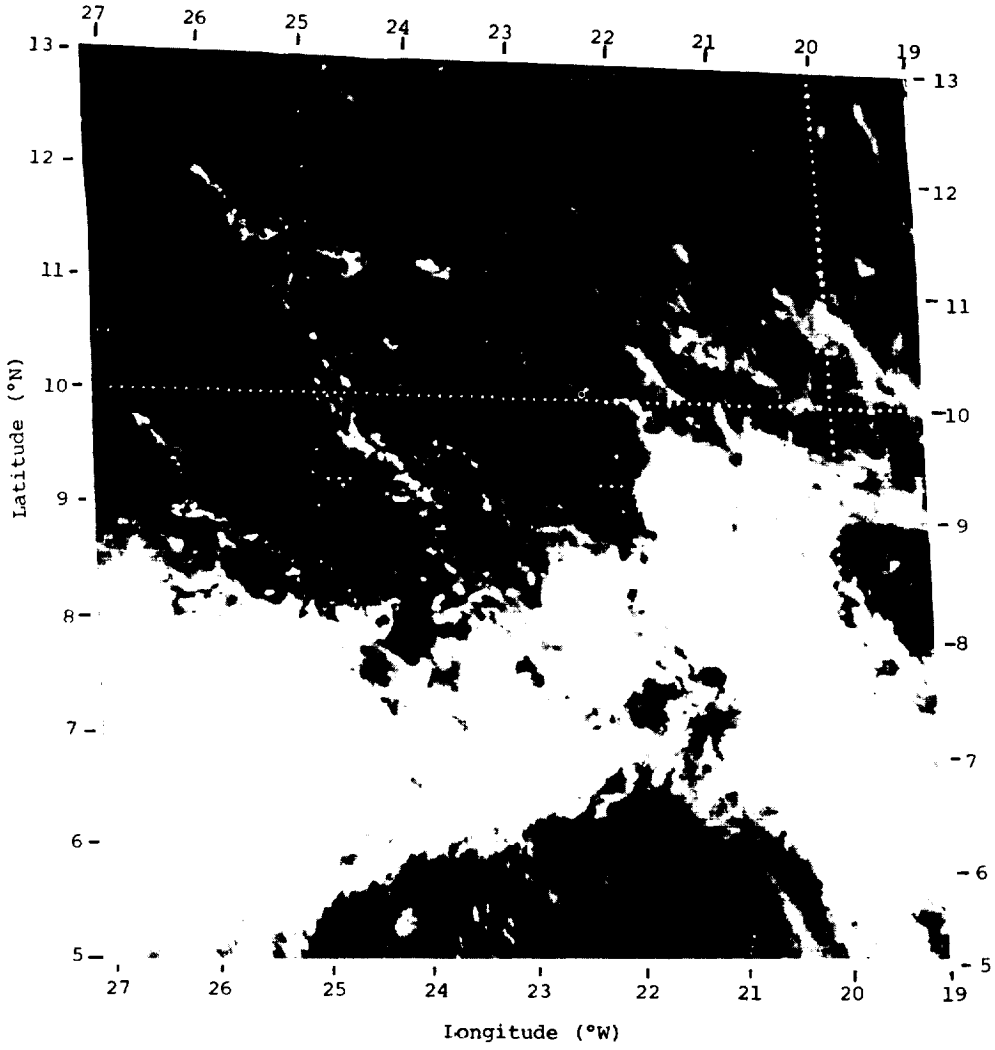

Figure 3. SMS-1 visible picture of the region of interest on 4 September 1974 at 1200 GMT.

When daily averages of the high cloud amount for days with *enhanced* convection and days with *depressed* convection are compared, higher cloud amounts are observed at the end of the day and generally persist to nearly sunrise of the next morning. Results are shown in Figure 4.

The major reason the current method is applicable is the rather uniform surface temperature during the analysis period. In other regions, and over land, similar methods could be developed, possibly incorporated multi-channels or other data sources.

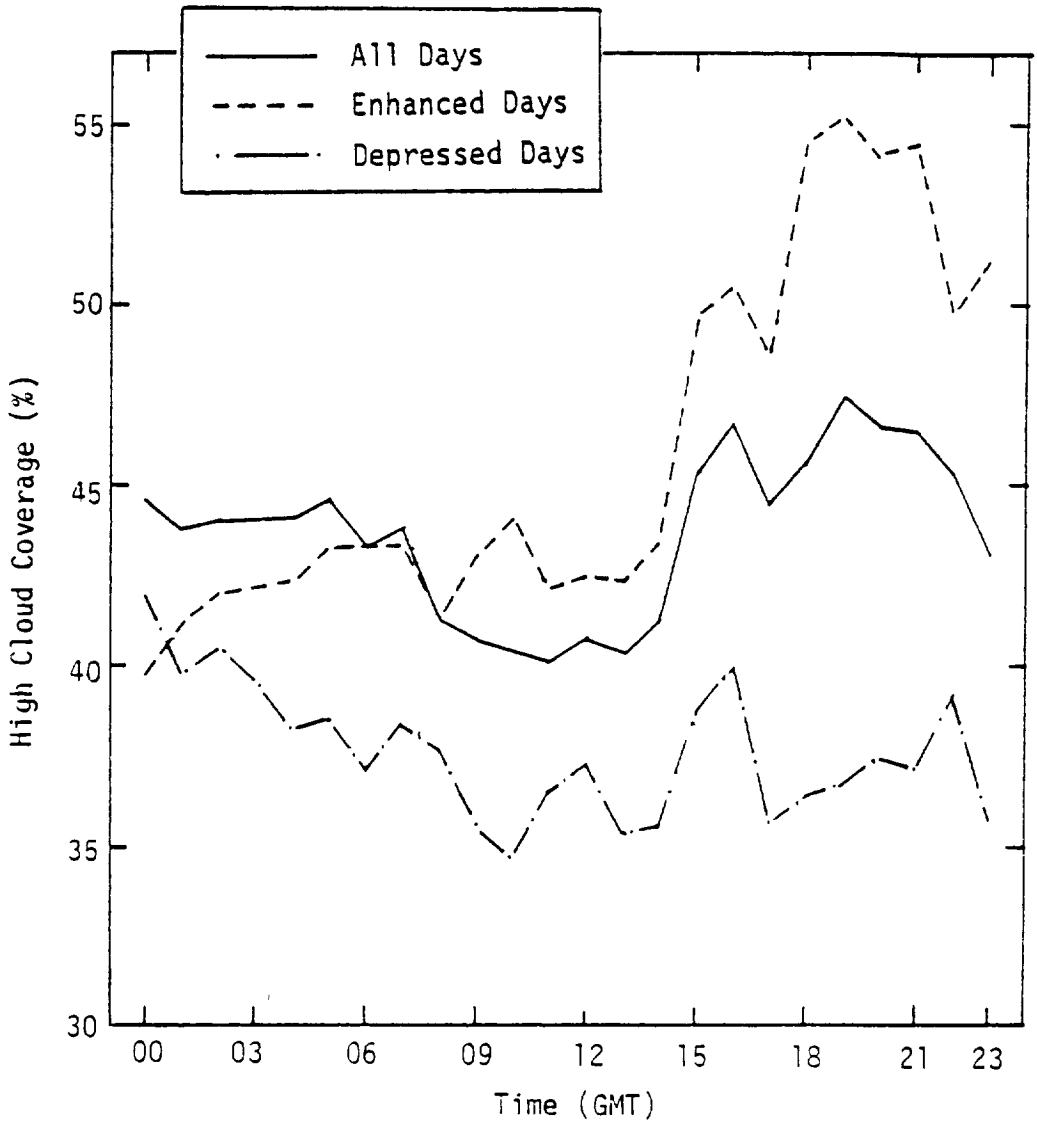

Figure 4.

References

Atwater, M. A. and J. T. Ball, 1981: "A Radiation Model for Realistic Atmospheres. Part I: Methodology," to be submitted to the *Journal of Atmospheric Sciences.*

Ball, J. T., S. J. Thoren, M. A. Atwater, 1980: "Cloud Coverage Characteristics During Phase III of GATE as Derived From Satellite and Ship Data," *Mon. Wea. Rev., 109,* 1419-1429.

Parikh, J. and J. T. Ball, 1980: "Analyses of Cloud Type and Cloud Amount During GATE From SMS Infrared Data," *Remote Sensing of Env., 9,* 225-245.

DETECTION OF THIN CIRRUS CLOUDS AND WATER/ICE PHASE WITH THE AVHRR

Albert Arking
Laboratory for Atmospheric Sciences
Goddard Space Flight Center
Greenbelt, MD 20771

New channels introduced in the imaging radiometers on the TIROS-N series of polar orbiting meteorological satellites provide a capability for detecting thin cirrus clouds and for discriminating between the water and ice phase at the cloud top. There are two versions of the Advanced Very High Resolution Radiometer (AVHRR): a four-channel instrument (AVHRR/1) such as that on the TIROS-N and NOAA-6 satellites, now in operation, and a five-channel instrument (AVHRR/2) which will be introduced on the next satellite in the series (with a probable launch in the first half of 1981). In addition to the visible channel (0.6 μm) and an infrared window channel (11 μm) the AVHRR/1 has channels at 0.9 μm and 3.7 μm. On the AVHRR/2, a fifth channel is obtained by splitting the 11 μm window into two channels; at 10.8 μm and at 12.0 μm.

Phase discrimination is achieved during daytime by the amount of reflection of solar radiation at 3.7 μm. Because of differences in the index of refraction of water and ice at that wavelength, and the non-sphericity of ice particles, water clouds reflect about four times as much solar radiation as ice clouds. Hence, the ratio of reflectance at 3.7 μm to that in the visible channel is a parameter that indicates phase with a high degree of sensitivity.

The detection of very thin cirrus clouds is based upon a comparison between the radiance at 3.7 μm and at 11 μm, using the split window channels to correct for the effects of water vapor. This technique will detect cirrus clouds at night with optical thickness as small as 0.1 (which is several times smaller than what could be detected during daytime with the visible channel alone) and in daytime it is more sensitive, detecting clouds with optical thickness much smaller than 0.1.

SENSING SNOW AND CLOUDS AT 1.6 μm

James T. Bunting
Air Force Geophysics Laboratory
Meteorology Division
Mesoscale Forecasting Branch

Current cloud climatologies such as the Air Force 3DNEPH are limited in their ability to distinguish snow from clouds since they both reflect sunlight well in visible channels (0.5 to 1.0 μm) on satellites. The Air Weather Service and Geophysics Laboratory are evaluating data from a near IR channel near 1.6 μm at which snow cover reflects poorly and appears much darker than cloud cover. The

channel can also be used with visible and IR (10–12 μm) channels to distinguish water clouds from ice clouds. If this channel is available in the future, improvements are expected for automated detection of snow cover and cloud cover in the 3DNEPH.

GROUND-BASED OBSERVATIONS OF CLOUDINESS FOR CROSS-VALIDATION OF SATELLITE OBSERVATIONS

Stephen G. Warren,[1] Carole Hahn,[1,2] and Julius London[2]
[1]*CIRES and* [2]*Dept. of Astrogeophysics, Univ. of Colorado*
Boulder, CO 80309

Ground-based cloud observations can provide data for comparison with satellite-derived cloud parameters. In addition, such observations provide cloud information not normally accessible to satellites; viz, the distribution and base-heights of low clouds, etc., which represent essential input data for surface radiation budget studies. Because cloud observations have been made routinely over an extended period of time as part of the regular meteorological reporting network, they can also be used to determine long-term cloudiness trends. Synoptic cloud data are presently available on tapes for the period 1901–1980 from land station observations, and for the period 1854–1980 from ship observations.

We have analyzed the cloudiness data from individual ship observations for the period 1946–1978 that have been compiled by the U.S. Navy Fleet Numerical Weather Central (FNWC). For this data set, 99 percent of the observations reported total cloud cover amounts and about 90 percent reported low cloud amount, type and base height. Our preliminary study involved total cloud-cover information over all oceans and primarily involved geographic and seasonal distribution, as well as diurnal, interannual and long-term variations of total cloudiness. In subsequent studies we plan to extend this work to include analysis of cloudiness variations by cloud type.

The individual observations of total cloud cover were grouped into 8 three-hour periods, 4 three-month seasons (December-January-February, etc.) and 5°x5° latitude-longitude grid boxes. The motivation for this time-space resolution was to:

a. reduce the data volume to a convenient subset (the total data volume was approximately 20 million individual synoptic observations);

b. have a sufficiently fine time-space resolution to provide useable information, but still contain sufficient numbers of individual observations to produce representative mean cloud values and statistics.

We have compared the ship observations with analogous cloud-cover distributions derived from satellite data (Sadler, *et al.*, 1976). The geographic and seasonal patterns of cloud cover for 30°N–30°S from these subjective NESS-nephanalyses are very similar to those reported by the ships, but

there is a consistent difference. On average, the ships reported 8% higher cloud cover than did Sadler *et al.* This difference may be partly due to each of several biases: differences in projection from the two viewpoints above and below cloud, the inability of the satellite to detect small or thin clouds, and the somewhat arbitrary classification procedure used to convert the nephanalysts' categories to cloud amounts. The interannual anomalies (Figure 1) parallel each other moderately well for 5°x5° boxes that were well-sampled by the ships (Figure 1ab, 200-300 observations per season). The agreement is poorest for sparsely-sampled boxes (e.g. Figure 1d, 25 obs. per season). This is consistent with our conclusion (discussed below) that about 150 observations in 90 days are necessary to obtain a representative season-mean.

The ship observations are made every 6 hours (and less-frequently every 3 hours), with little tendency for fewer observations at night. Thus, diurnal variations in cloudiness can be partially resolved by the surface reports in most areas. The eastern subtropical oceans consistently show early-morning cloud-cover maxima in summer, and late-morning maxima in winter. In other places where the diurnal cycle is significant, there is a preponderance of cloud maxima near noon. This may not be real, but may instead be due to a tendency of nighttime observers not to detect thin cirrus. This problem can be resolved with analysis of variations for each cloud type.

Some of the diurnal cycles in cloud cover reported by ships are compared (Figure 2) with "effective" cloud cover from GOES brightness data (Harrison, *et al.*, 1980ab). In all cases the cloud cover from ships is higher, probably due to the operational definition of "effective" cloud by which clouds are weighted according to their relative brightness. Off the Atacama coast (Figure 2a), the average total cloud cover seen by the ships for SON (1946-1978) is 50% higher than the "effective" cloud cover for Nov. 1978, but the 10% amplitude and 7 AM maximum are in excellent agreement. In other areas (Figure 2bc), however, there is no similarity between the two results. Here we cannot rule out sampling errors as a cause for the discrepancy. We are comparing a single month of satellite data with 32 seasons of ship observations because the single month (Nov. 1978) lacked sufficient transient ship observations to establish a characteristic diurnal cycle.

We have also analyzed the Air Force Three-Dimensional Nephanalysis (3DNEPH) reports of total cloudiness for a six-month period (Dec. 1977-May 1978) in the northeastern Pacific for which data were readily available to us. The seasonal averages for the total area (containing seventeen full 5° x 5° boxes) agree to within ±2-3% with the ship observations for the same two three-month periods. But the diurnal cycle for DJF (not shown here) is 12 hours out-of-phase with that reported by the ships. The diurnal cycles for MAM are also in disagreement with the ship observations, but there is no such consistent relation. Part of the disagreement may reflect the use of different data sources for the 3DNEPH during day than at night.

In addition to these kinds of seasonal comparisons with satellite data, we plan in subsequent work to do *simultaneous* comparison of satellite-derived cloud parameters with selected individual synoptic observations.

The interannual variability of season means of total cloud cover at 5°x5° resolution can only be obtained for the North Pacific and North Atlantic where it averages about 4% (standard deviation, in percent cloud cover, of individual season-means about the long-term mean). Elsewhere the apparent

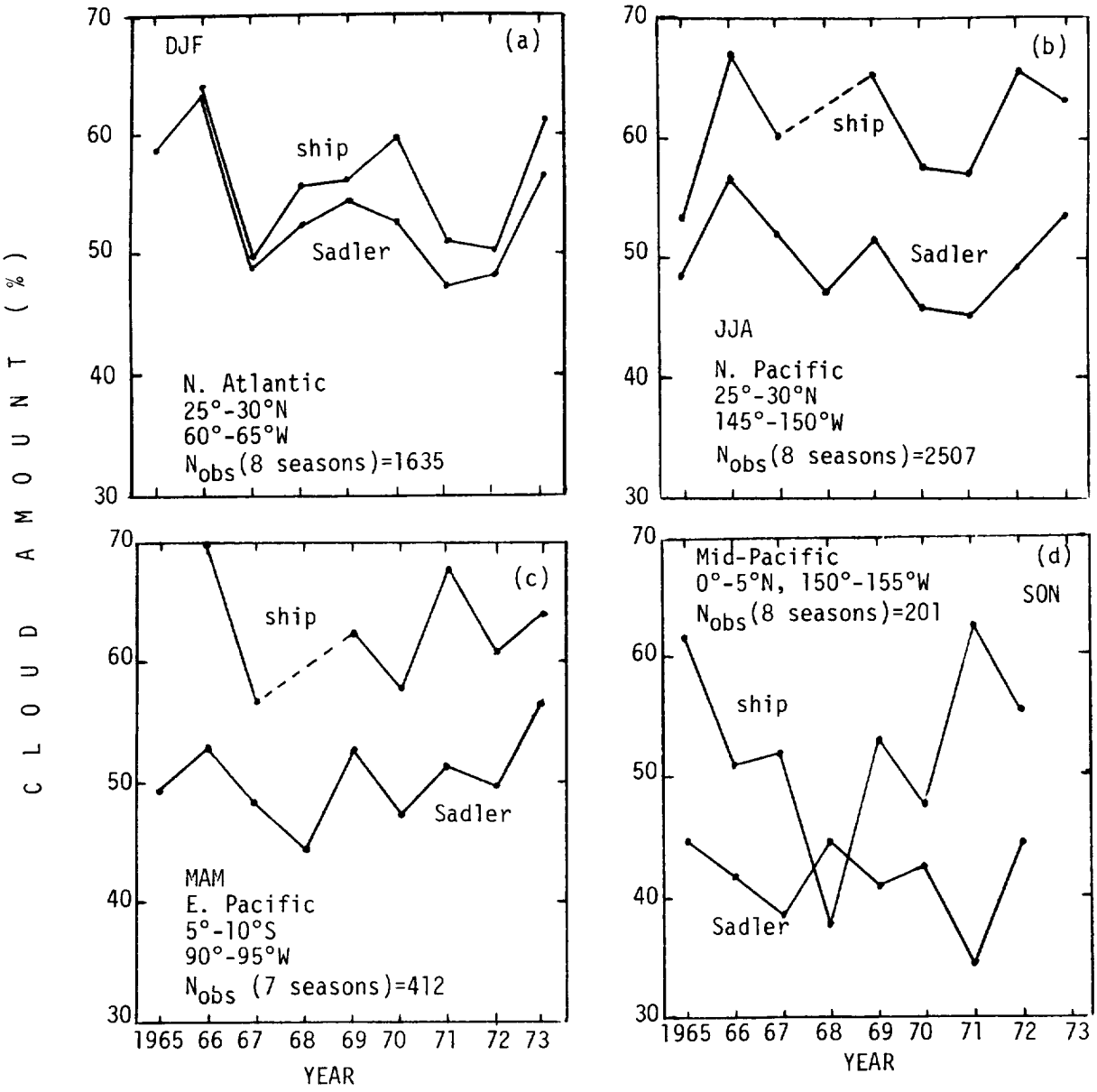

Figure 1. Comparison of seasonal cloud-cover anomalies for 5°x5° latitude-longitude boxes, 1965-1973, as seen from ship and satellite. The upper line in each case is from the ship synoptic observations, which on average give 8% higher cloud cover than do the satellite nephanalyses of Sadler *et al.* (1976). Examples of boxes well-sampled (a,b) and poorly sampled (c,d) are shown. Average number of observations per season was (a) 200 (b) 300 (c) 60 (d) 25. [Dashed lines (b,c): No data point for 1968 appears in the ship data for MAM, JJA 1968, because the tape containing those ship data was temporarily unavailable to us.]

interannual variation is larger, due to poor sampling, than the true interannual variation. It was found empirically that about 150 independent (i.e. no two in the same three-hour period) observations in 90 days are necessary to represent adequately the individual season mean for a 5°x5° box. The interannual variability for stationary weatherships ranges from 1% to 7%. For 5°x5° boxes in

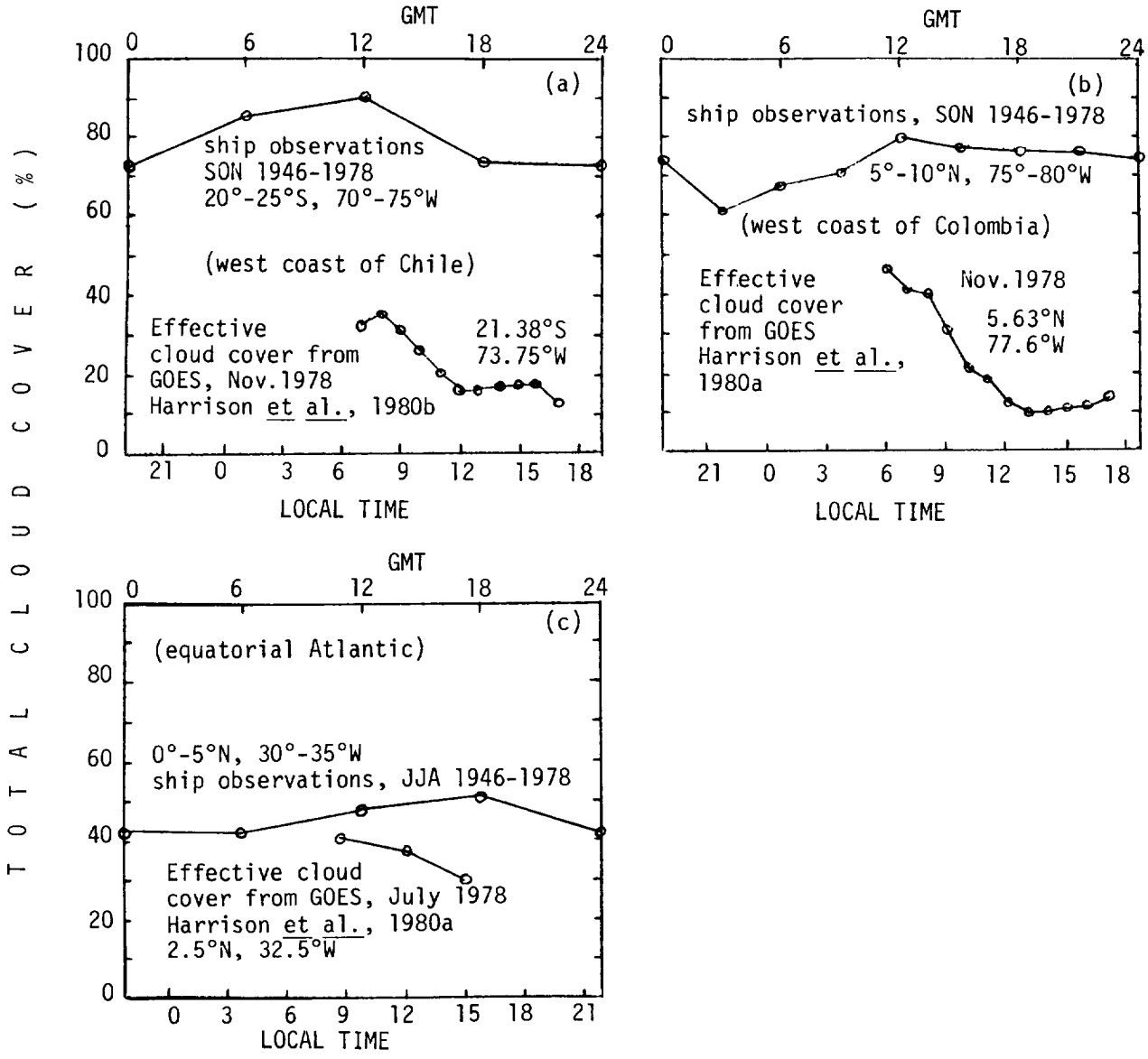

Figure 2. Diurnal variation of cloudiness: comparison of ship observations of total cloud cover with "effective" cloud cover from GOES brightness data (Harrison *et al.*, 1980ab).

the open ocean the standard deviations are between 2% and 7%, and as large as 8-9% over some coastal areas.

It is of considerable interest for climate and climate model studies to establish the existence of long-term changes in total cloudiness. Cloud-cover trends were calculated at 5°x5° resolution, at 15° lat. x 30° long. resolution, and as 15° zonal averages. In each season there are more areas with positive trends than with negative trends. The resulting 2% increase in global-average ocean cloud cover over the period 1946-1978 is qualitatively consistent with the 6-8% difference we find when we compare the average hemispheric ocean cloud cover for 1946-1978 with that of the earlier period

1880–1934 summarized by London (1957) and van Loon (1972). The old and new values for mean annual global ocean cloud cover are 52% and 60%, respectively, for NH; 59% and 65% for SH. The distribution of trends for 15°-wide latitude zones exhibits a recognizable pattern (Figure 3), with large positive trends near the equator and small negative trends toward the pole. This latitudinal variation is most apparent for the 6-month period December–May.

Some of these observed trends may not be real but due instead to changes in sampling bias such as the "fair-weather bias." This will be investigated by doing a separate examination of trends in the records of ocean weather station ships, and by determining which cloud types are contributing to these trends.

Perspective error enters into comparison of satellite with ground-based observations. Sky cover reported by ground observers is normally higher than earth cover as determined from nadir observations from satellites. For different radiation budget purposes, both sky and earth cover data are needed. It would be extremely useful to have these two observation systems provide a consistent set of cloud data.

The full paper will be submitted to *Monthly Weather Review* for publication. The work is supported by the U.S. GARP Office (NOAA). The data were made available to us by Ralph Slutz, Joseph Fletcher and Garth Paltridge. Robert Chervin helped us with the computer graphics for producing atlas maps. We thank Roger Barry, Robert Chervin, Roy Jenne and Bruce Wielicki for helpful discussion.

References

Harrison, E. F., P. Minnis and D. R. Brooks, 1980a: Diurnal studies of cloudiness and earth radiation budget. *Minutes of the First ERBE Science Team Meeting,* Hampton, VA, January 1980, pp. Y1–Y12.

Harrison, E. F., P. Minnis and G. G. Gibson, 1980b: Temporal and spatial variability of cloud cover from GOES data for radiation budget studies. *International Radiation Symposium Abstracts,* Fort Collins, CO, August 1980, 361–363.

London, J., 1957: A study of the atmospheric heat balance. AFCRC-TR-57-287. New York University College of Engineering, 99 pp.

Sadler, J. C., L. Oda and B. J. Kilonsky, 1976: *Pacific Ocean Cloudiness from Satellite Observations.* University of Hawaii Report UHMET-76-01, 137 pp.

van Loon, H., 1972: Cloudiness and precipitation in the southern hemisphere. *Meteor. Monographs, 13,* 101–111.

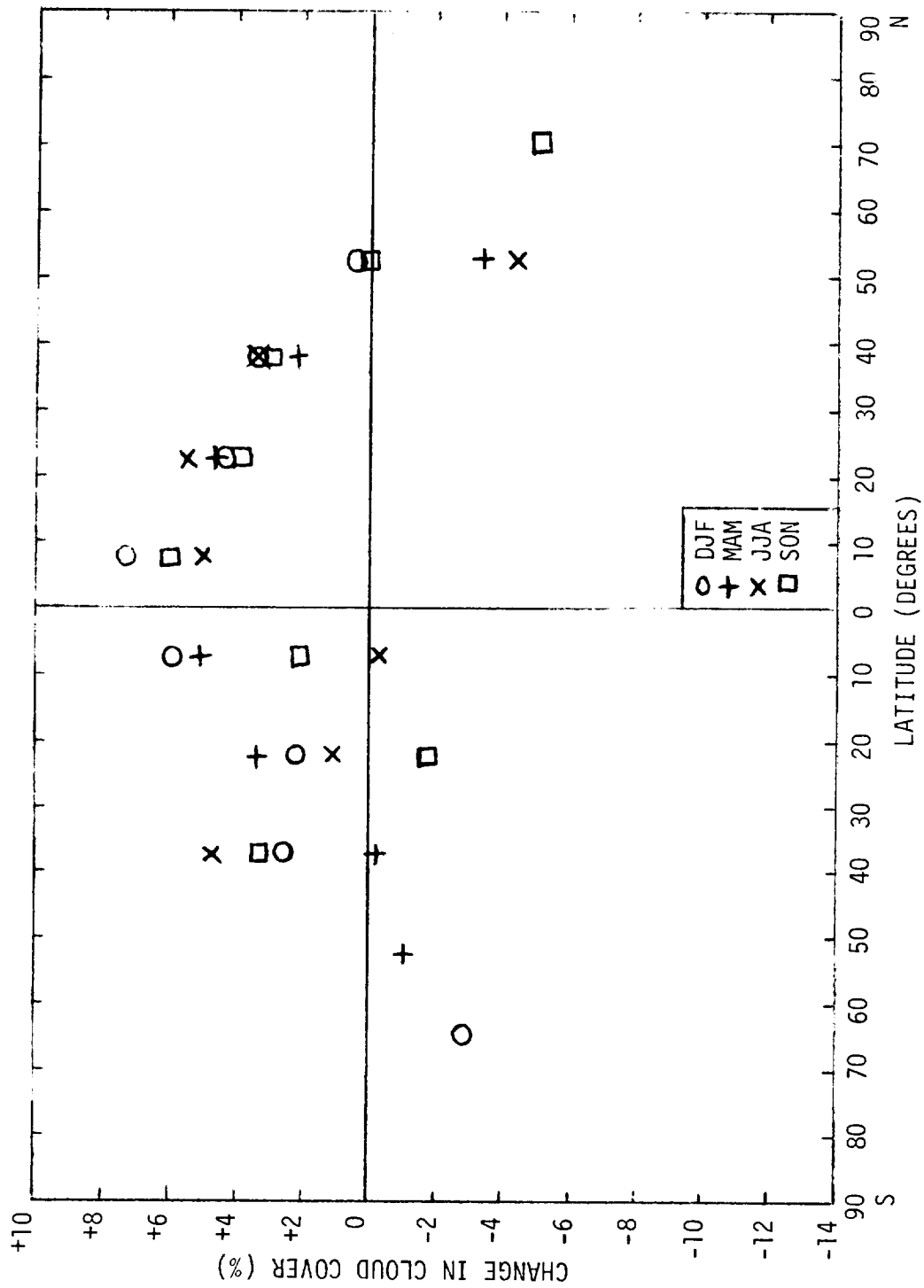

Figure 3. Change in average seasonal cloud cover (absolute-%) for the ocean part of 15°-wide latitude zones, over a 32-year interval 1946-1978 (from slope of least-squares trend line). Slopes are plotted only if the uncertainty in slope was ⩽3%/32 years, so the full set of 4 seasons is not plotted for some latitude zones. The uncertainties in the slopes plotted average ±1% in the NH; ±1.5% in the SH.

4.2 DATA COMPRESSION

PROJECTED CLOUD DATA ARCHIVES AND 3-D NEPH STATISTICS

Roy L. Jenne
National Center for Atmospheric Research
Boulder, Colorado

A Selected Archive of Cloud Data

The satellite data that are needed for cloud studies are primarily visible and IR spots with a fine enough resolution that they can observe many of the breaks in clouds rather than just seeing an average of cloud and land conditions. It is also necessary to obtain the relationship between visible and IR data (and sometimes other channels as well). That is, we need to know whether a bright spot has a cold or warm temperature. One way to obtain such relationships is to save histograms with 2 or more dimensions. If adequate resolution is provided, the 2-D histograms have a large volume and are difficult to produce. Therefore, it is proposed to obtain such information by sampling the spots, probably at the highest resolution possible but ignoring many of the spots. A distance of 8 km between spots in the first sampled archive is proposed with another subset at 16 or 32 km intervals.

Cloud element size information is also necessary. A one-dimensional histogram has been proposed (by F. Mosher, University of Wisconsin) to save this information.

Separate one-dimensional histograms of visible and IR data are proposed. They should be made from all highest resolution spots within areas about 100 to 250 km in size. It would be useful to have them closer to 100 km in size over land areas so that they also can help to assess snow cover and precipitation in the appropriate drainage basin. Tables 1 and 2 summarize many of the different possible intermediate sized archives.

The spot samples will also be used to obtain land surface temperature, to estimate surface radiation, to derive sea surface temperature, and to use for estimates of rainfall.

Data Volume, Archive Selection, Formats, and Costs

By considering the examples of full resolution synchronous satellite data, and USAF 3-D nephanalysis data, it will become evident how certain strategies can reduce the volume of the data. Some reductions can be made with no loss of information and almost no change in complexity. Other decreases in volume require a loss of some information.

Table 1

Data sets proposed for the pilot cloud and climate archive. The data bits only include basic data. The "tapes per year" include 25% overhead and assume 300 million bits per tape (1600 BPI).

From Each GOES	Space Resolution	Time Resol. Hours	Bits Each Sample	Grids Per Day	Data Bits Each Year ($*10^8$)	1600 BPI Tapes Per Year
1. Average radiation	100 km	1 h	8 bit	24IR, 13 Vis	13.5	5.6
2. IR histogram	250 km	3	8 bit, 83 lvl	8IR	11.7	4.9
3. Visible histogram	250 km	3	8 bit, 64 lvl	5Vis	6.0	2.5
4. Neighbor IR hist.	250 km	3	8 bit, 64 lvl	8IR	11.7	4.9
5a. Spot samples	16 km	3	8 bit	8IR, 5Vis	171	71
5b. Spot samples	32 km	3	8 bit	8IR, 5Vis	43	18
6. Land and Coastal For 30 boxes (750 km) per satellite	8 km	6	8, 6 bit	4IR, 2Vis	42	18
7a. High Resolution For 5 boxes (100 km) per satellite	1 km vis, 8 km IR	1	8 bit	24IR, 13Vis	20	8.3
Orbiting Satellite						
7b. High Resolution For one orbiter, 25 boxes, 300 km	4 km	12	8 bit	2IR, 1Vis	12.3	5.1
8. Scanner (Items 1 thru 4 and 5b above)				2IR, 1Vis	~86	~36
9a. Sounder data	250 km 20 chan	12	8 bit per chan	2	~75	~25
9b. Sounder data	E42 km 4 chan	12	8 bit per chan	2	~76	~30

NOTE: The yearly volume of archives 1-4, and 5b is 36 tapes for each GOES.

Table 2
Cloud Archive

Tapes/yr each GOES		
5.6	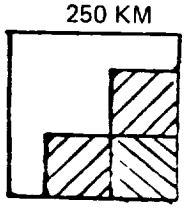	100 Km Ave, 1 hr
4.9		IR Histogram, 3 hr 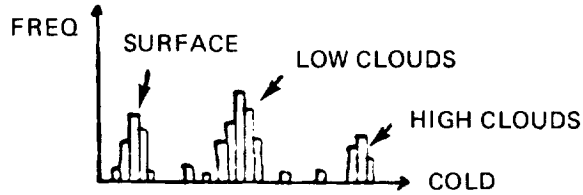
2.5		Visible histogram, 3 hr 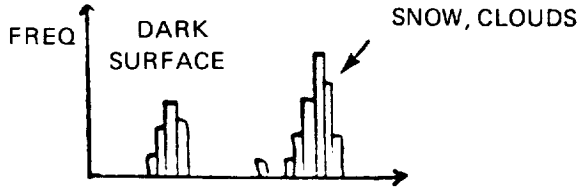
71	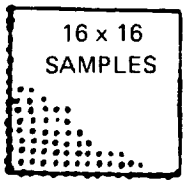	Spot samples, 16 Km, 3 hr
18	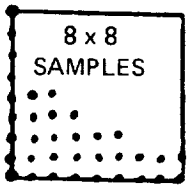	Spot samples, 32 Km, 3 hr
18	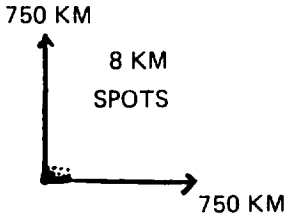	Regional cloud and land sfc. archive -30 Boxes (750 Km) each GOES -8 Km resolution, 6 hr
8.3		High Resolution Boxes -5 boxes (100 Km) each Goes -Resolution 1 Km vis, 8 Km IR

Synchronous Satellites

Table 3 gives data resolution and volume from the geostationary satellites. Note that if visible data is not saved over the dark areas, half the volume is saved, but a *complete* half-hourly save of data from one GOES would still require 33.4 tapes (6250 BPI) per day for visible data and 1.39 tapes for IR. If the data looking into space is dropped, about 9149 tapes/year would be needed for the visible and 381 for IR. If spots each 8 km are saved for both (only each 3 hours), then 25 tapes/year are needed for the visible and 66 for the IR. A subset of these data would be prepared where the sampling is reduced to one in 16 or 32 km, which reduces the volume by a factor of 4 or 16. The visible spots should be individual spots near the center of the IR spots, not averages over the 8 km area. During the initial processing, histograms of all the visible spots (within 100 km boxes) should be prepared each 3 hours. These boxes would be along scan lines. A histogram showing cloud element size relationships within 200 km boxes should also be made at that time. If hourly 100 km averages can be prepared at low cost, they would be useful, but a high cost process is not warranted. Some of the reduced volume archives have already been discussed in more detail in WCRP, 1980.

3-D Nephanalysis Data

The analyses for the N. Hemisphere start in 1971; the S. Hemisphere starts in May 1974. The data are thought to be most useful starting in 1976. Satellite and ground-based cloud observations are used. Sometimes there is no new data at a grid point or there isn't machine time to make a full analysis. Then the old data is carried along. The grid resolution varies from 48 km at 60N to 26 km at the equator. The higher resolution scanning data were always averaged to 3 nmi resolution (6 km) before it was used in the 3-D neph program. An 11 km resolution cloud descriminator channel was available July through December 1979 but was not used in the 3-D neph.

With high volumes of data, it is useful to examine whether the grid mapping strategy that is used is causing very large numbers of points for some areas. In the Lat-longitude grids there is often a very large number of points near the poles. When the NMC-polar stereographic grid mapping (as in 3-D neph) is used, it gives a large number of points in low latitudes, and in the opposite hemisphere. In the 3-D neph, nearly 25% of the 245,760 points are off the hemisphere, and 130,544 of the 195,805 hemispheric points are between the equator and 30° latitude. Thus, 25% could be cut from the archive volume by simply not storing the off hemisphere data. Another large reduction could be obtained by using a lat-lon grid to latitude 30°. Table 4 shows that further large reductions in volume can be obtained by using variable length formats in which a clear sky case requires less space than one of several cloud layers.

Table 4 (from Jenne, 1980b) shows that 254 tapes (6250 BPI) would be needed to save a year of the present 3-D neph data. This would be cut to 86 tapes if a variable format were used, and decreased another 25% if off-hemisphere points were eliminated. The table shows a volume reduction to about 45 tapes per year if a new variable length format is used together with 0.5° lat-lon mapping to 30° latitude. Optimistic processing costs are also shown for the different archives. The present archive of 3-D neph data takes one tape per box-month or 1440 tapes/year compared to the 45 to 254 higher density tapes discussed above. It is interesting that all of the 3 nmi (6 km) IR and visible that is the major input to produce the 3-D neph could be archived on about 160 tapes per year (6250 BPI). Saving only every other spot (ea 12 km) would give 40 tapes.

Table 3

Data from Geostationary Satellites. Note that saving all data from one GOES satellite would take 9149 tapes/year (6250 BPI) for visible data but only 25 tapes when the data is sampled each 8 km. The data volume includes several percent for overhead.

	ESA Meteosat	GMS Japan	GOES USA
Spin scan	100 RPM	100	100
No. of steps	2500	2500	1820
Visible resolution (km)	2.5	1.25	0.9
IR resolution (km)	5	5	0.9
Water vapor resolution (km)	5		
Visible resolution (μr)	65 μr	35	21 (E-W) x 25 (N-S)
Angle between vis spots (E-W)	62.5 μr	24	21
IR resolution (μr)	140 μr	140	250 x 250
Angle between IR spots	125 μr	48	84
Wave Length Vis	0.4-1.1 μm	0.5-0.75	0.55-0.75
IR	10.5-12.5 μm	same	same
Vis samples in scan line	5000	13376	15292
Vis lines in picture	5000	10000	14560
IR spots in scan line	2500	6688	3823
IR lines	2500	2500	1820
Vis Bits/picture (6 bit spot)	1.58×10^8	8.12×10^8	13.9×10^8
IR Bits/picture (8, 9, 9 bit spots)	5.26×10^7	1.57×10^8	6.51×10^7
Data from Satellite		Each Day	
Vis Bits/day (6 bit) (10^9)	7.57 (48 p)	11.4 (14P)*	66.7 (48P)
IR Bits/day (8, 9, 9 bit) (10^9)	2.52 (48 p)	2.20 (14P)	3.12 (48P)
Cut vis at dark line, drop IR overlap			
Vis Bits/day (6 bit) (10^9)	3.79 (48 p)	5.69 (14P)	33.4 (48p)
IR Bits/day (8 bit) (10^9)	2.52 (48 p)	0.98 (14p)(5 km)	1.39 (48p) (9 km)
Cut most space data (25%)		Each Year	
Vis Bits/year (6 bit) (10^9)	1037 (48p)	1558 (14p)	9149 (48p) (year)
IR Bits/year (8 bit) (10^9)	691 (48p)	268 (14p)	381 (48p)
3-Hourly spots each 8 to 10 km	(10 km)	(10 km)	(9 km)
Vis Bits/year (6 bit) (10^9)	13 (8P)	15 (8p)	25 (8p)
IR Bits/year (8 bit) (10^9)	31 (8P)	40 (8p)	66 (8p)
Points each vis, IR picture	0.75(1250x1250)	0.75 (1672x1250)	0.75(1912x1820)

*(14p) means 14 pictures/day

NOTE: A 1600 BPI tape holds 0.3×10^9 bits
A 6250 BPI tape holds 1.0×10^9 bits
A U. Wisc. recorder tape holds 22.3×10^9 bits

Table 4

For different 3-D neph options the average number of bits for the cloud stack at each grid point is multiplied by the number of points to give yearly volume. The machine cost (rather cheap rates) to read or write the yearly data 4 times is shown. The yearly cost (with no processing) to archive 5 years of data off-line on 6250 BPI tape is also shown. Each tape holds 10^9 bits.

3-D NEPH: Volume and Costs for Options

	Ave. Bits Per Point	Yearly Points Over Earth (10^9)	Bits Per Year Earth (10^9)	Machine Cost to Read 4 Times	Yearly Partial Cost to Archive 5-Year Data
a. Present 3-D neph	177	1.436	254	$31,000**	$2540*
b. Present, vrbl form.	60	1.436	86	10,500	860
c. New-Plans-fixed	170	1.436	244	29,750	2440
d. New-Perhaps-vrbl	87	1.436	125	15,250	1250
e. New-Possible-vrbl	70	1.436	101	12,300	1010
f. Drop off-hem points	70	1.15	81	9,890	810
g. Lat-long (0.5°) to lat 30	70	0.64	45	5,500	450

*These off-line archival costs are unrealistically low because they don't include the cost of a data copy each 6-8 years, or certain personnel costs. On-line archival costs on mass storage systems are typically higher by a factor of 150 to 250 or more. Thus, it is now unreasonable to plan for archival of all data on-line. The off-line archival costs vary directly with the number of tapes archived. Thus, the present 3-D Neph archive costs about 6 times as much.

**The reading costs are based on $17.0 for I/O and $13.5 for CPU for simple read processing (not writing) of 10^9 bits on a CDC 7600 priced at low rates. As long as simple data packing structures are used, the read costs will decrease almost directly with data volume. The costs are 82% higher with 1600 BPI tapes.

Processing and Archive Costs

Table 5 summarizes archive and processing costs. Note that hardware maintenance is not included in the on-line archival costs. The off-line archival costs do not include archival costs such as copying the archive each 5 to 7 years, and the cost of keeping track of the archive. More information about machine costs, channel speeds, etc. is contained in Jenne, 1980.

Table 5

Data storage and processing costs. The cost is given for both on-line and off-line storage. The costs generally assumed a hardware lifetime of 5 to 6 years. The processing costs are optimistically low because inexpensive rates on a fast computer (CDC-7600) were used.

	Cost/yr Per 10^{10} Bits		I/O and Computing Costs for 10^{10} Bits		
	On-Line Hardware Storage Costs (No Maintenance)	Off-Line Costs Media and Storage	I/O Minutes	I/O Cost	CPU Cost Minimum Processing
1600 BPI Tapes	$170,000	$66*	92	$340	$135
6250 BPI Tapes	51,000	20	24	88	135
Auto Tape Library (2000 Tapes – 6250 BPI	835	20	24	88	135
Disk Packs (300 mbytes)	36,000	1000+			
Large Disks (2400 mbytes)	E4,700	–			
TBM Mass Store	7,600	29	76	281	135
Optical Disk	E3,600	E2	35	124	135
Core Disk Transfer	–	–	10	37	

*These costs assume relatively full tapes. If tapes average only 25% full, multiply these costs by 4.

E. Cloud Statistics from 3-D Neph

A selection of cloud statistics have been calculated from USAF 3-D nephanalysis data. The calculations, Tables 6-8, have been done for two boxes of data, 5 months in 1978 for each. Each box is 8 x 8 NMC grid squares, thus about 3000 km on a side. One is over the U.S. (Box 44), the other over the Eastern Pacific (Box 43). The archive of 3-D neph data has 15 fixed layers with tops at 150, 300 feet, 600, 1000, 2000 feet AGL (above ground level), 3500 feet MSL, 5000, 6500, 10K, 14K, 18K, 22K, 26K, 35K, and 55K (55,000 feet MSL).

The statistics in Tables 6 and 7 include the percentage of the time that there are no clouds, using all points, 8 times a day, for each month. The total cloud coverage including the clear cases is given. It is recorded for each point in the archived data. If clouds were recorded at two (or more) continuous layers (given above), they were counted as one layer. The coverage assigned was the maximum of the two. The data for Jan., Box 43, shows that each cloud layer spanned an average of 2.60 levels in the format. The average number of cloud layers per point (including clear cases as zero) was 1.36 in January.

Low clouds were defined as those having either tops $\leq$2000 feet AGL or tops $\leq$10,000 feet MSL. In high terrain the low clouds can go up to about 7000 feet AGL. Middle clouds have tops $\leq$22,000 feet MSL and are not low clouds. Clouds above are high. The archive has a more accurate lowest base and top cloud height than is possible using the top and bottom of the vertical segments in the format. The more accurate data are used when possible.

The base of low clouds is an average of AGL and MSL values. The table shows the percentage of time that a low or middle cloud layer is also the highest cloud layer. For the top layer, this can be computed by subtracting the percent of cases with no high clouds from 100.

For each of the low-middle-high cloud categories, the average coverage is given; it includes the cases with no clouds. If clouds were always overcast when they occured, the coverage plus the cases with no clouds would add up to 100%.

Table 8 shows diurnal cloud changes in the two 3-D neph boxes for 1978.

Table 9 shows a very limited comparison between London, 1957 and these few calculations from the 3-D nephanalysis. Table 9 shows London's zonal means, as well as an estimate from his charts of the averages over the 3-D neph boxes. Many of the comparisons are surprisingly close considering that a long-term mean is being compared to individual months of data. However, the 3-D neph shows significantly more clouds than London in the E. Pacific box in winter, and it shows few high clouds in the summer.

Table 6
Cloud Statistics Calculated from USAF 3-D Neph Box 43 in the Eastern Pacific, 1978

	Jan.	Feb.	Apr.	May	July
Percent Clear	11.5	14.7	15.1	26.5	29.4
Total Coverage	71.7	66.7	63.7	54.9	52.2
Average # Cloud Layers	1.36	1.30	1.27	0.96	0.93
Average Lvls per Layer	2.60	2.61	2.36	2.68	2.56
Low Clouds					
Cases with no Low Clouds (%)	43.9	42.9	37.4	41.5	43.8
Average Coverage (%)	37.9	36.7	39.0	41.3	41.0
Average Cloud Top (ft)	4963	4535	4963	4688	4596
Average Cloud Base (ft)	1954	1728	2092	1712	1654
This is Top Layer (%)	32.4	34.3	42.4	47.1	44.6
Middle Clouds					
Cases with no Middle Clouds (%)	61.9	68.1	71.2	81.7	79.5
Average Coverage (%)	24.6	19.6	17.4	9.9	9.9
Average Cloud Top (ft)	16720	16774	16439	16014	16147
Average Cloud Base (ft)	8881	9064	9232	9302	9596
This is Top Layer (%)	24.1	19.3	18.9	12.3	12.2
High Clouds					
Cases with no High Clouds (%)	68.1	68.3	76.4	85.8	86.3
Average Coverage (%)	19.3	19.1	12.5	6.4	5.4
Average Cloud Top (ft)	33029	33634	33502	33269	33126
Average Cloud Base (ft)	20188	20201	21754	22510	21246

Table 7
Cloud Statistics Calculated from the USAF 3-D Neph Box 44 Over North America, 1978

	Jan.	Feb.	Apr.	May	July
Percent Clear	24.1	20.7	19.7	18.3	22.6
Total Coverage	55.0	56.2	58.6	58.7	47.3
Average # Cloud Layers	0.95	1.00	1.08	1.13	1.12
Average Lvls per Layer	3.22	3.04	2.66	2.56	2.12
Low Clouds					
Cases with no Low Clouds (%)	81.8	77.9	74.1	70.2	67.9
Average Coverage (%)	10.2	11.9	13.6	14.9	13.4
Average Cloud Top (ft)	6545	6720	6857	6871	6772
Average Cloud Base (ft)	3803	3943	4114	4102	4116
This is Top Layer (%)	10.7	13.8	15.2	16.4	16.7
Middle Clouds					
Cases with no Middle Clouds (%)	55.3	55.0	56.5	56.9	57.7
Average Coverage (%)	31.1	30.5	29.1	27.8	21.8
Average Cloud Top (ft)	17095	16848	16743	16649	16537
Average Cloud Base (ft)	7724	7843	8448	8572	9424
This is Top Layer (%)	34.4	34.3	29.5	28.4	26.4
High Clouds					
Cases with no High Clouds (%)	69.1	68.8	64.3	63.2	65.8
Average Coverage (%)	19.8	19.7	22.5	22.9	17.8
Average Cloud Top (ft)	31930	31996	32515	32630	32991
Average Cloud Base (ft)	17831	18286	19021	19307	20432

Table 8
Mean Total Cloud Coverage by Hour for 3-D Neph, 1978

	Box 43					Box 44				
	JAN	FEB	APR	MAY	JUL	JAN	FEB	APR	MAY	JUL
00Z	67.9	65.5	60.2	58.0	59.5	57.4	58.6	62.2	60.3	49.2
03Z	66.8	64.7	59.3	57.4	59.0	53.1	54.4	57.4	57.1	47.3
06Z	77.0	67.0	62.4	52.7	37.5	50.3	51.1	54.4	59.0	47.7
09Z	75.1	66.7	67.4	51.4	43.2	51.4	51.6	52.3	52.0	40.4
12Z	75.4	67.1	67.4	52.5	50.1	53.9	54.6	55.0	56.7	45.2
15Z	71.6	68.0	66.8	53.1	53.3	58.3	61.0	58.8	57.7	45.6
18Z	71.4	68.0	64.6	57.2	56.6	58.5	58.9	65.4	65.5	53.9
21Z	68.6	66.8	61.6	57.1	60.0	57.3	59.2	63.4	61.4	49.9

Table 9
Comparison of London's 1957 Long Period Cloud Data With
3-D Cloud Statistics for 1978

	3-D Box 43 East Pacific		3-D Box 44 US		Zonal Cloud Cover by Type (London)	
	Total Clouds	High Clouds	Total Clouds	High Clouds		
Zonal Mean, London	59 %		59		Ci	19.7%
					As	11.2
Clouds over 3-D Box (London)	55		53		Ns	12.6
3-D neph Jan 1978	71.7	19.3	55.0	19.8	St	18.4
					Cu	10.2
3-D neph Feb 1978	66.7	19.1	56.2	19.7	Cb	1.4
			Summer			
Zonal Mean, London	55		55		Ci	17.8
					As	8.8
Clouds over 3-D Box (London)	52		47		Ns	9.0
3-D neph June 1978	48.0	5.4	50.1	19.6	St	16.9
					Cu	4.4
3-D neph July 1978	52.2	5.4	47.3	17.8	Cb	4.4

References

Jenne, R. L., 1975: Data Sets for Meteorological Research, NCAR TN/IA-111, Boulder, Co., 194 pp.

Jenne, R. L., 1980a: Data for cloud studies, notes. NCAR (unpublished).

Jenne, R. L., 1980b: Format of 3-D Neph Data, a memo to ETAC. (unpublished).

Jenne, R. L., 1980c: Data handling and its costs in large computing systems. NCAR, Boulder, Co., (unpublished).

London, J., 1957: A study of the atmospheric heat balance. College of Engr., N.Y. Univ., Final Rept., Contract AF19(122)-165.

Miller, D. B., and G. F. Feddes, 1971: Global Atlas of Relative Cloud Cover, 1967-70. National Envr. Satellite Service, Washington, D.C., 237 pp.

Telegados, Kosta, and Julius London, 1954: A physical model of the N. Hemisphere Troposphere for winter and summer, Sci. Rpt. #1, AF19(122)-165 AFCRL, N. York Univ. Col. Engr., 55 pp.

WCRP, 1980: The international satellite cloud climatology project. Appendix 1: Status of Cloud Archives, WMO, Geneva.

Fye, Falko, K., 1978: The AFGWC Automated Cloud Analysis Model, AFGWC TM 78-002. A F Global Weather Central, Offutt AFB, Nb 68113, 97 pp.

DATA STORAGE AND COMPRESSION OF GEOSTATIONARY IMAGE DATA FOR CLOUD CLIMATOLOGIES

Anne LeBlanc and Frederick R. Mosher

Space Science and Engineering Center

University of Wisconsin, Madison, Wisconsin 53706

I plan to present information on why one would want to use data compression for either reducing the data storage volume or increasing the information content of the data (different strategies are used to obtain each objective). Modern technology making use of high density recording devices (such as slant track archives and the 6250 bpi tape drive) has reduced the need to use data compression for data storage. An example is the GOES Sony slant track archive which stores 25 gigabits per $25 tape with no data compression. Play back of the stored data is close to real time rates, so the cloud climatology is a *data processing* problem rather than a *data storage* problem. The best way to increase the information content of data is to process it into the desired answer as quickly as possible and store only the correct answer. If one does not know how to process the data, or wants to try several methods of processing, they can preprocess the data into a form which still preserves the "important" information at a much reduced data volume so that the final processing can be done quickly (or several times if need be). Methods such as storing n-dimensional histogram,

sampled data, or spectral components have been suggested for preprocessing. These methods have problems in that they don't store what everyone considers "important". Hence my recommendations are to:

1. Store all the raw data on high density storage devices.
2. Decide what products one wants and develop algorithms to extract these from the raw data.
3. Process the raw data in real time into as many of the final products as is possible.
4. Use preprocessed compressed data only as a back-up for processing historic data into cloud climatology information in the event that the real time processing has problems.

THE IMPACT OF GOES SATELLITE DATA COMPACTION ON THE ESTIMATES OF CLOUD PARAMETERS

Eric A. Smith, Thomas H. Vonder Haar and John Graffy
Department of Atmospheric Science
Colorado State University
Fort Collins, CO 80523

Satellite data compaction is a necessary evil insofar as setting the stage for an operational global cloud climatology. We are investigating the impact of data compaction on cloud parameters, using digital hourly GOES imagery as the test data set. We have selected two methods for compaction; the first is a 2-dimensional VIS-IR histogram approach, in which the spatial dimension of samples is reduced to approximately 8 km and the quantization resolution is reduced to 4 bits or 16 levels. The second approach involves a decomposition of the GOES imagery into a set of empirical orthogonal basis functions.

2-Dimensional Histograms

The 2-D histogram tables have been used to analyze the amplitude and phase of the diurnal variation of cloudiness over the earth sector viewed by the GOES-East Satellite. The histogram or grid scale used here was 2° latitude by 2° longitude. A comparison of the bit storage requirements between standard image matrix format and 2-D histogram format is given in Table 1. Note the various tradeoffs as the space scale and quantization scale are varied. Figure 1 illustrates a more complete breakdown of bit density requirements for conventional matrix format with regards to GOES VIS-IR data.

Figure 12 from the Smith review on Cloud Climatologies contained in this document, presented the amplitude diagram for an average of 10 days of infrared data taken during November, 1978. Figure 2 presents the associated local-time phase diagram. The diagram can be interpreted as follows. The

Table 1
Comparison of Image Sector Storage with
Cross-Histogram Storage (1 Satellite)

Bit Resolution	225 Points 1° x 1°	1406 Points 2.5° x 2.5°	5625 Points 5° x 5°	22,500 Points 10° x 10°	
8 x 8 (256 LEV)	$3.6.10^3$	$2.3.10^4$	$9.0.10^4$	$3.6.10^5$	Sector
	$5.2.10^5$	$5.2.10^5$	$5.2.10^5$	$5.2.10^5$	Hist
7 x 7 (128 LEV)	$3.2.10^3$	$2.0.10^4$	$7.9.10^4$	$3.2.10^5$	Sector
	$1.3.10^5$	$1.3.10^5$	$1.3.10^5$	$1.3.10^5$	Hist
6 x 6 (64 LEV)	$2.7.10^3$	$1.7.10^4$	$6.8.10^4$	$2.7.10^5$	Sector
	$3.3.10^4$	$3.3.10^4$	$3.3.10^4$	$3.3.10^4$	Hist
5 x 5 (32 LEV)	$2.3.10^3$	$1.4.10^4$	$5.6.10^4$	$2.3.10^5$	Sector
	$8.2.10^3$	$8.2.10^3$	$8.2.10^3$	$8.2.10^3$	Hist
4 x 4 (16 LEV)	$1.8.10^3$	$1.1.10^4$	$4.5.10^4$	$1.8.10^5$	Sector
	$2.1.10^3$	$2.1.10^3$	$2.1.10^3$	$2.1.10^3$	Hist
	10,000 Regions	1600 Regions	400 Regions	100 Regions	

Based on 4 x 4 Mile Data. Tape Requirements Based on 8 Times a Day for 30 Days.

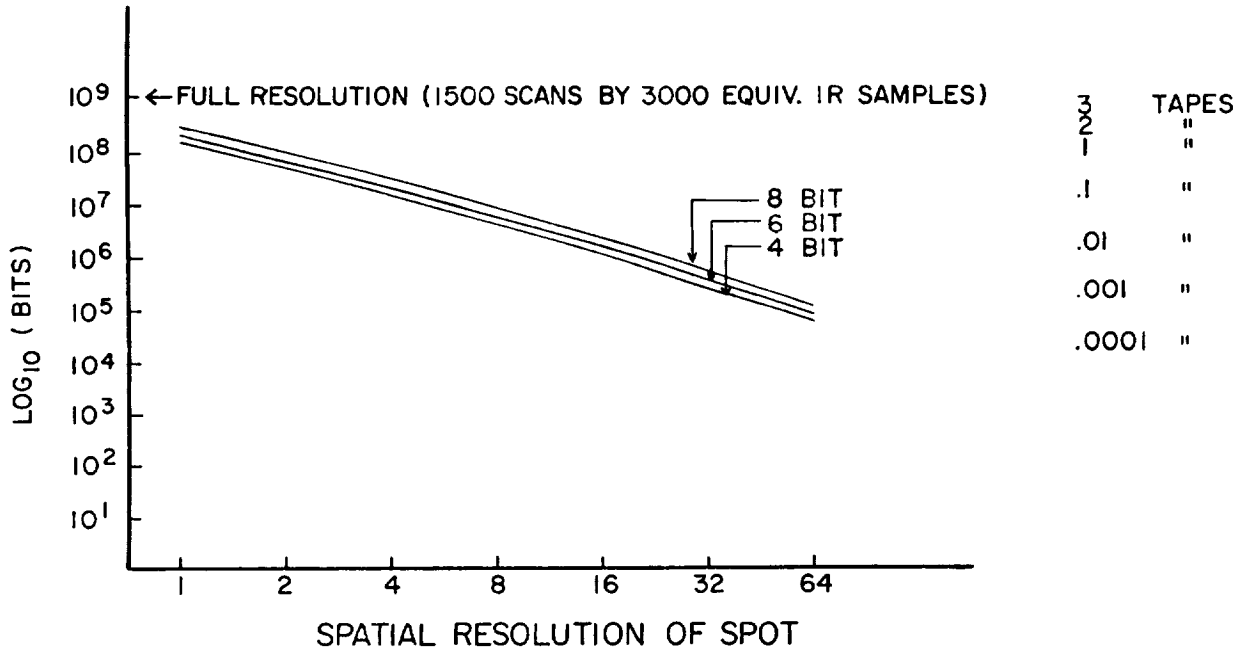

Figure 1. Bit density of day time GOES imagery as a function of spot resolution and quantization.
(Note: 1 1600 BPI tape will hold 3.10^8 bits.)

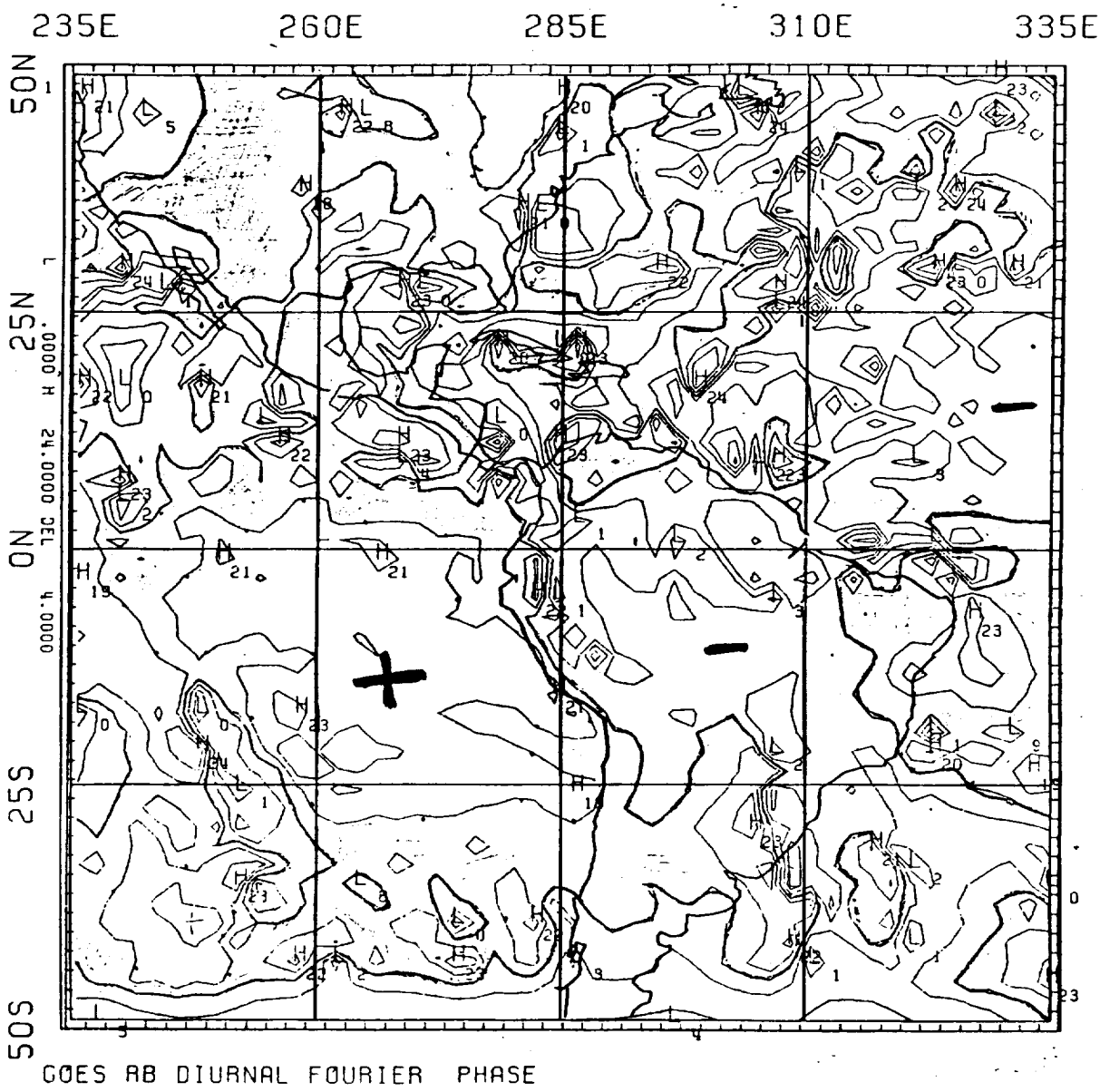

Figure 2. Phase (in local time) of maximum diurnal amplitude in the infrared emission (– indicates a pre-noon maximum; + indicates a post-noon maximum).

positive regions indicate an afternoon maximum in longwave emission or most likely an afternoon minimum in cloudiness. Note the coastal stratus regions west of South America are characterized by a large positive area. Presumably, the stratus cloud decks are warmed and evaporated as the day progresses, leading to the increased emission. It is assumed that the sea surface temperature remains fairly constant throughout.

The western portion of the South American Continent shows a dramatic rise in the amplitude of diurnal variation, decreasing from the coast to the interior. The phase of the diurnal cycle indicates a pre-noon maximum in emission or a post-noon maximum in cloudiness, i.e. a buildup in convection after surface heating takes place. In addition there is a fairly smooth phase shift toward later afternoon, as we proceed east of the Andes barrier. These results have been selected to illustrate that much of the physical nature of the diurnal cloud cycle is recoverable from 8 km, 4-bit hourly GOES data transformed to 2° x 2° two-dimensional histograms.

Use of Empirical Orthogonal Functions

Our second technique for data compaction involves the decomposition of 40 km resolution GOES data into a set of eigenvectors and expansion coefficient vectors (principle components) of the latitudinal covariance matrix. In this technique, the corresponding eigenvalues under the transformation, are proportional to the variance accounted for by the associated eigenvectors and principle components. The two important results from this analysis are:

1. The lower order eigenvectors are extremely stable on a time scale of 3-6 hours, as shown in Figure 3. This figure illustrates the first 10 eigenvectors from a sequence of 5 hourly infrared images on November 18, 1978. Note that the first 4 eigenvectors are virtually invariant with time.
2. Only 10% of the basis functions are required to recover 85% of the variance in the original data. Table 2 indicates a more complete breakdown of Explained Variance vs. Required Basis Functions.

These results imply that an order of magnitude in data reduction is achievable without severely impacting the larger scale cloud features. In addition, alluding to point 1, it is likely, due to the nearly time invarient properties of the lower order basis functions, that part of the time dimension could be retained in a much more reduced form.

Table 2
Information Reduction

Percentage of Variance Explained	Percentage of Basis Functions Required
95%	25%
90%	15%
85%	10%
80%	7%

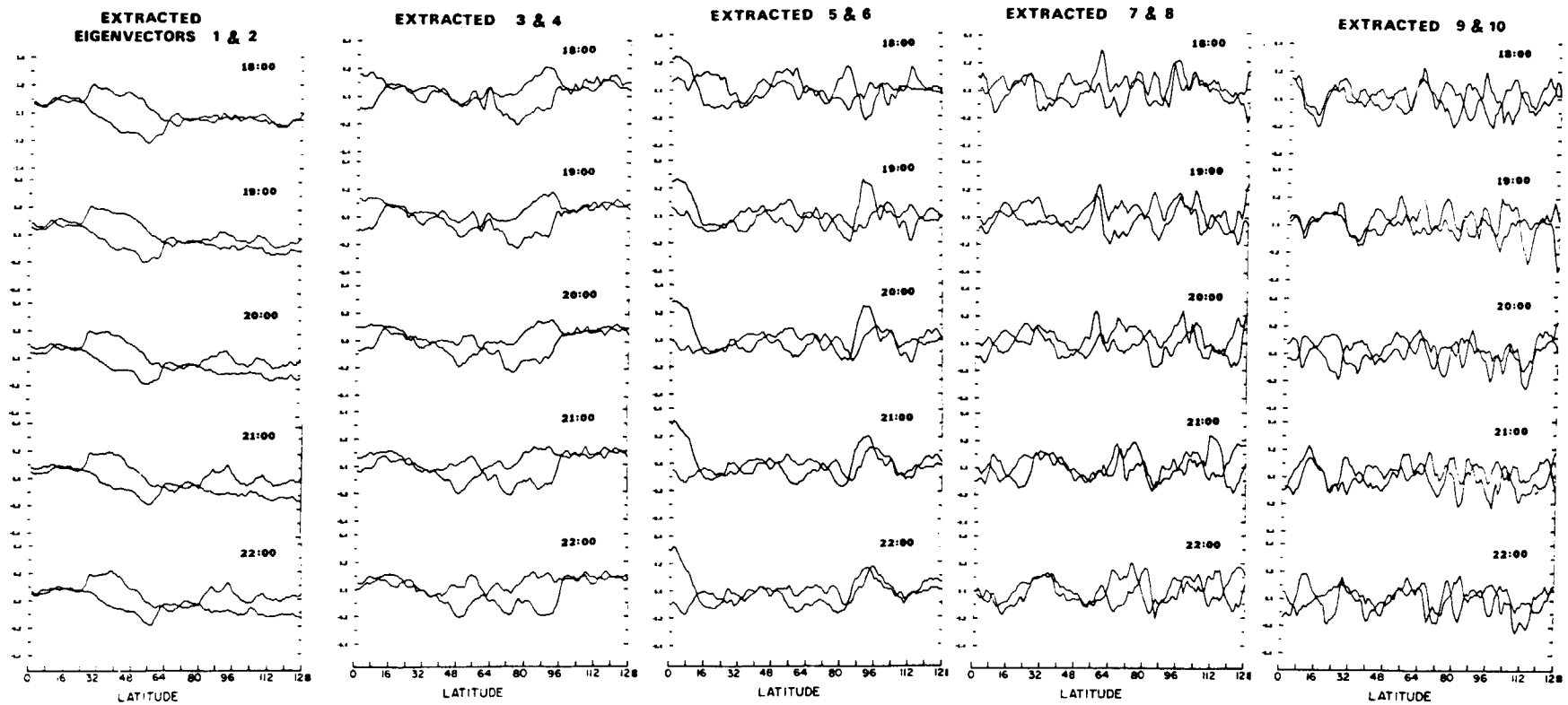

Figure 3. First 10 eigenvectors of the latitudinal covariance matrices of 5 hourly GOES-East image sectors (November 18, 1978: Northern Hemisphere). The original space scale resolution is 40 km.

4.3 SUMMARY

W. B. Rossow
NASA Goddard Institute for Space Studies
New York, New York 10025

Key ideas discussed during the second day are briefly listed as a summary.

1. Most current techniques for deducing cloud properties from satellite measured radiances do not account for variations of cloud albedo and the corresponding variation of cloud emissivity of thinner clouds. Consequently, these techniques do not reliably define cirrus cloud properties and distributions. Furthermore, these techniques do not reliably characterize the multi-layer cloud systems which probably produce the larger portion of global precipitation.
2. Available observations indicate that the diurnal, seasonal, and interannual variations of clouds on all length scales are substantial. Consequently, the statistics describing the global cloud distribution and its variation may depend on the time and length scales used to form averages. Differing definitions of the averaging scales in different data sets makes verification of satellite techniques by data comparisons especially difficult.
3. Any data set comprised of some form of satellite measured radiances must include enough orbital information as a function of time so that the observational geometry and ground location of the observations can be accurately reconstructed. This type of information is not always a part of current operational products.
4. To reduce a cloud climatology to a useable size, it should contain statistics computed on large spatial (~1000-3000 km) and time (~1-3 months) scales, but these statistics must contain information on cloud variations on smaller spatial and time scales. For a radiative climatology, a climatology of clear sky radiances may be important.
5. Even though current satellite data sets may not contain enough information to deduce all of the critical cloud properties, these data sets are, nevertheless, so large that most research groups are reluctant to analyze them thoroughly. Formulation of data compression schemes to reduce the volume of future climatology data sets to a manageable size is necessary.
6. None of the more sophisticated techniques for deducing cloud properties from satellite measured radiances has yet been applied to a global and seasonal data set. Furthermore, no systematic intercomparison of these techniques on such data sets has been performed. Since the satellite data available in the next several years are similar to recent data, pilot studies testing and comparing such techniques on existing satellite data are necessary for further progress.

5. RECOMMENDED STUDIES

SUMMARY OF PANEL DISCUSSION

W. B. Rossow
NASA Goddard Institute for Space Studies
New York, New York 10025

5.1 Panel on Cloud/Climate Modeling Studies

The discussion focused on identification and definition of the types of data needed most for climate modeling research. Three types are emphasized: 1) detailed "process" data used to improve and verify cloud process parameterizations in climate models, 2) diagnostic data on cloud/climate sensitivities to verify model sensitivities, and 3) cloud climatology data to evaluate model simulations of the climate. These types of data differ primarily in the amount of detail included and in the spatial and temporal scales which must be resolved. Although recent modeling research and observation programs have largely concerned cloud process and sensitivity studies, the critical parameters and proper averaging scales for these two kinds of data are not yet well-defined. The data characteristics must be properly matched to those of the model considered, since the average cloud behavior deduced from the data can be scale-dependent. For example, a global general circulation climate model designed to represent mean monthly atmospheric statistics should not be expected to produce daily cloud variations in detail. Much further modeling work is needed to specify the key data needed for improvements in model climates.

A key obstacle to further modeling progress at this time seems to be the lack of a cloud climatology to compare to the model-produced climatologies. This type of data has received less attention than the process and sensitivity data. The kind of data which comprises a cloud climatology depends, somewhat, on the particular cloud process being considered; convection, precipitation and radiation processes were emphasized. A cloud-radiation climatology should be the first goal of research during the next few years since this process is the best understood and most readily incorporated in current climate models. This climatology would also contribute valuable information for climatologies of convection and precipitation.

There are two general problems with comparisons of model output and data. First, the link between the radiative and cloud quantities calculated by the model and those derived from the data is not usually straightforward. Instead the two sets of quantities are linked by complicated theoretical relationships which require supplementary assumptions. Second, the models, like the atmosphere, produce cloud distributions influenced by many physical processes, all represented by uncertain parameterizations. Hence, a problem revealed by a comparison with data may not be related only to the cloud parameterization. These two problems suggest that the number of quantities calculated by models and derived from data should be expanded to include quantities which are simply related

to the parameterization scheme or actual measurements as well as quantities which are derived with more theoretical input and assumptions. Much further modeling study of these problems is necessary to optimize the comparisons between models and data.

No one data set or analysis scheme seems capable of producing all of the quantities desired for model-observation comparisons. Further, the uncertainties of the data and analysis can only be determined by comparison to other observations of the "truth" which contain their own uncertainties. These facts suggest that cloud climatologies must be composed of several data types analyzed in several different ways. Definition of the optimum data mix and determination of the errors in the resulting climatology is not yet possible. These can only be determined by pilot programs to evaluate the capabilities of each data type and analysis scheme and to intercompare the results from different data and schemes.

The Workshop participants identified the FGGE data set as most likely to be a suitable test bed for resolving some of the issues discussed and summarized above. This data set contains most of the types of satellite data that will be available in the near future, plus a large quantity of several other types of data (e.g., ground-based observations, intensive field and diagnostic data) that can provide a thorough testing of proposed analysis schemes. With this data set different analysis techniques can be readily compared to each other and errors evaluated. Furthermore, different types of numerical models can be tested against the varied data types to compare the fidelity of their simulations. Pilot studies concerning these issues and using the FGGE data could produce significant improvement in our understanding of clouds in climate and climate models.

5.2 Panel on Analysis/Data Compression Schemes

Since we cannot yet specify the type and amount of data needed in a cloud climatology, study of data analysis schemes must necessarily be considered to be in a research rather than a development mode. One fact is, however, clear: even current data volumes are already so large that the time and cost of data storage and analysis are prohibitive for most research groups. Therefore, data compression schemes are necessary to make these and future data accessible to climate model research groups, even if storage of the complete data stream should prove feasible. We don't know how to optimize data compression to facilitate analysis for climate research.

Because the nature of data compression depends on the type of derived quantities desired for model comparisons, research on data compression schemes must be coordinated with research on analysis schemes and climate models. Further, coordination of research is desirable so that technique comparisons can be performed. The feasibility of saving all of the data should be investigated, but some of the full data stream must be saved to evaluate proposed compression schemes. The FGGE data set seems to be a suitable testbed for these studies, but some samples of current operational data are necessary to test the feasibility of real time data compression.

The Workshop participants outlined a study program which must precede a program to obtain the data for a cloud climatology. The first step is to collect and document the FGGE and other data sets, plus some samples of current operational data, to make them available to the research groups working on these problems. Then a coordinated program of pilot studies to test various compression and

related analysis schemes should be carried out. These pilot studies should all produce test cloud climatologies with thorough error analyses. These results should be widely distributed so that technique intercomparison is possible.

The recommendations of the Workshop participants are given in section 1. A short summary of these recommendations was prepared by J. Hansen and presented at the NOAA User's Workshop on December 4–5, 1980. That summary is given in Appendix E.

6. APPENDICES

6.1 APPENDIX A

ORGANIZING COMMITTEE

William B. Rossow (co-chairman)
NASA Goddard Institute for Space Studies

James E. Hansen (co-chairman)
NASA Goddard Institute for Space Studies

Akio Arakawa
UCLA, Department of Atmospheric Sciences

Albert Arking
NASA Goddard Space Flight Center

Robert E. Dickinson
National Center for Atmospheric Research

P. K. Rao
NOAA National Environmental Satellite Service

Robert A. Schiffer
NASA Headquarters, Climate Program Manager

6.2 APPENDIX B

WORKSHOP PARTICIPANTS

A. Arakawa
UCLA

A. Arking
NASA-GSFC

M. Atwater
Center for the Environment of Man

R. S. Bogart
NASA-Ames Research Center

J. Boyte
ETAC

J. T. Bunting
Air Force Geophysics Lab

A. Carlton
Institute of Arctic & Alpine Research

R. D. Cess
SUNY Stony Brook

M. Chahine
JPL

T. Charlock
CIAMS

J. A. Coakley
NCAR

S. Davis
NASA-GISS

A. Del Genio
NASA-GISS

R. E. Dickinson
NCAR

J. Ellis
Lawrence Livermore Lab

R. J. Fleming
U.S. GARP Office

A. Gordon
NOAA/GFDL

D. Graves
NASA-Langley Research Center

E. F. Harrison
NASA-Langley Research Center

J. E. Hansen
NASA-GISS

Dr. Harshvardhan
NASA-GSFC

G. F. Herman
University of Wiconsin

K. Jayaweera
University of Alaska

R. Jenne
NCAR

R. S. Kandel
Service D'Aeronomie

E. Kinsella
NASA-GISS

A. Lacis
NASA-GISS

A. Le Blanc
University of Wisconsin

H. Le Treut
Lab for Dynamic Meteorology

R. S. Lindzen
Harvard University

R. Lutz
University of Maryland

M. C. MacCracken
Lawrence Livermore Lab

S. Manabe
NOAA/GFDL

F. Mosher
University of Wisconsin

J. A. Parikh
Southern Connecticut State College

G. L. Potter
Lawrence Livermore Lab

V. Ramanathan
NCAR

P. K. Rao
NOAA/NESS

J. L. Raper
NASA-Langley Research Center

R. A. Reck
General Motors Lab

D. Rind
NASA-GISS

A. Robock
University of Maryland

W. B. Rossow
NASA-GISS

G. Russell
NASA-GISS

J. C. Sadler
University of Hawaii

E. Sarachik
Harvard University

R. Schiffer
NASA HQ

M. E. Schlesinger
Oregon State University

J. Shukla
NASA-GSFC

E. Smith
Colorado State University

G. L. Stephens
CSIRO-Australia

P. Stone
MIT

L. L. Stowe
NOAA/NESS

O. Thiele
NASA-GSFC

L. Travis
NASA-GISS

S. Vemury
NASA-GISS

W. C. Wang
Atmos. & Environ. Res., Inc.

S. Warren
University of Colorado

P. Webster
CSIRO-Australia

R. Wetherald
NOAA/GFDL

M. L. Wu
NASA-GSFC

6.3 APPENDIX C

AVAILABILITY OF DATA FOR CLOUD STUDIES

Roy L. Jenne
National Center for Atmospheric Research
Boulder, Colorado

A survey will be made of major sets of observations (surface-based and satellite) that are useful for cloud studies. Cloud analyses that have been made will also be briefly considered. More extensive information about data is contained in WCRP, 1980; Jenne, 1980; and Jenne, 1975.

Figure 1 summarizes the cloud data and satellite data sets that are available. It includes data from scanning radiometers, and atmospheric sounders as well as cloud data such as the 3-D neph analysis prepared by the Air Force. The periods of available digital data from synchronous satellites are also shown. The archive of picture data covers time periods when digital data were not prepared.

Figure 2 includes information about satellite heat budget data, stratospheric data, and microwave data in addition to much of the cloud data from Figure 1.

1. SATELLITE DATA FOR CLOUD STUDIES

Archives of satellite radiance data that are useful for cloud studies will now be briefly described. Cloud wind data prepared from satellites are also available. These include an estimated height for the clouds (or wind).

1.1 Geosynchronous Satellite Data (US)

The routine US archive of 3-hourly data for 2 synchronous satellites started 3 September 1978 with a more limited archive from 9 August 1976 (8 km data). These present archives only cover 40S–50N and 100 degrees of longitude centered on the satellite subpoint. Volume: 3 tapes/day, each satellite, but could fit on fewer tapes. These are available from WDC-A (NCC – satellite data services). Many pictures and film loops are also available.

The University of Wisconsin has full resolution data (1 km visible, 8 km IR for US synchronous satellites for the FGGE year and selected data for other periods.

- full resolution, half hourly data for GOES-E starts March 1978 and continues with minor gaps to the present
- full resolution, GOES-W data starts November 1978
- all half-hourly Indian Ocean data December 1978 through November 1979
- full resolution data for the GATE experiment period, June – September 1974.

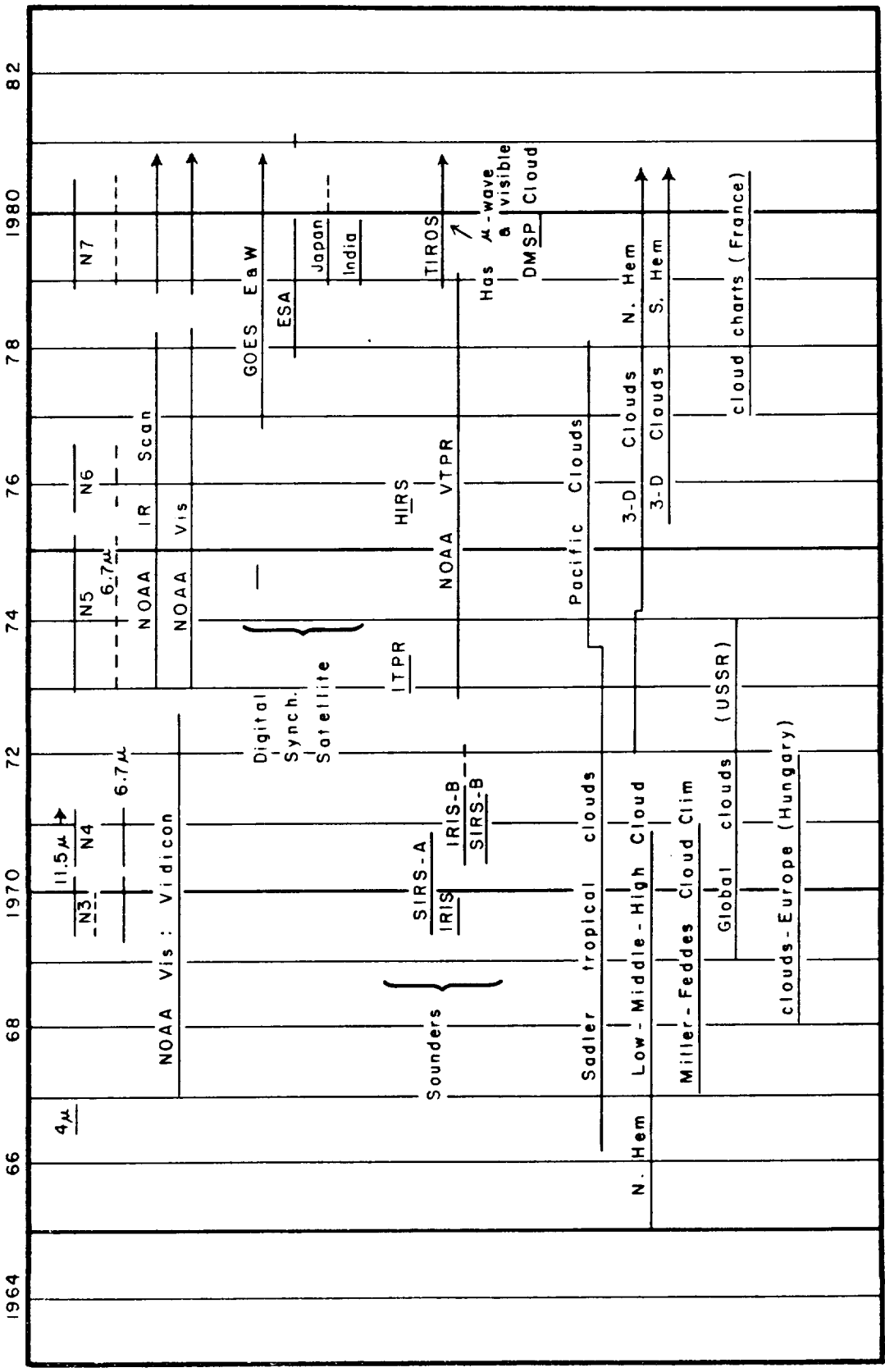

Figure 1. A summary of selected data sets of cloud data and of available satellite data that can be used for cloud studies.

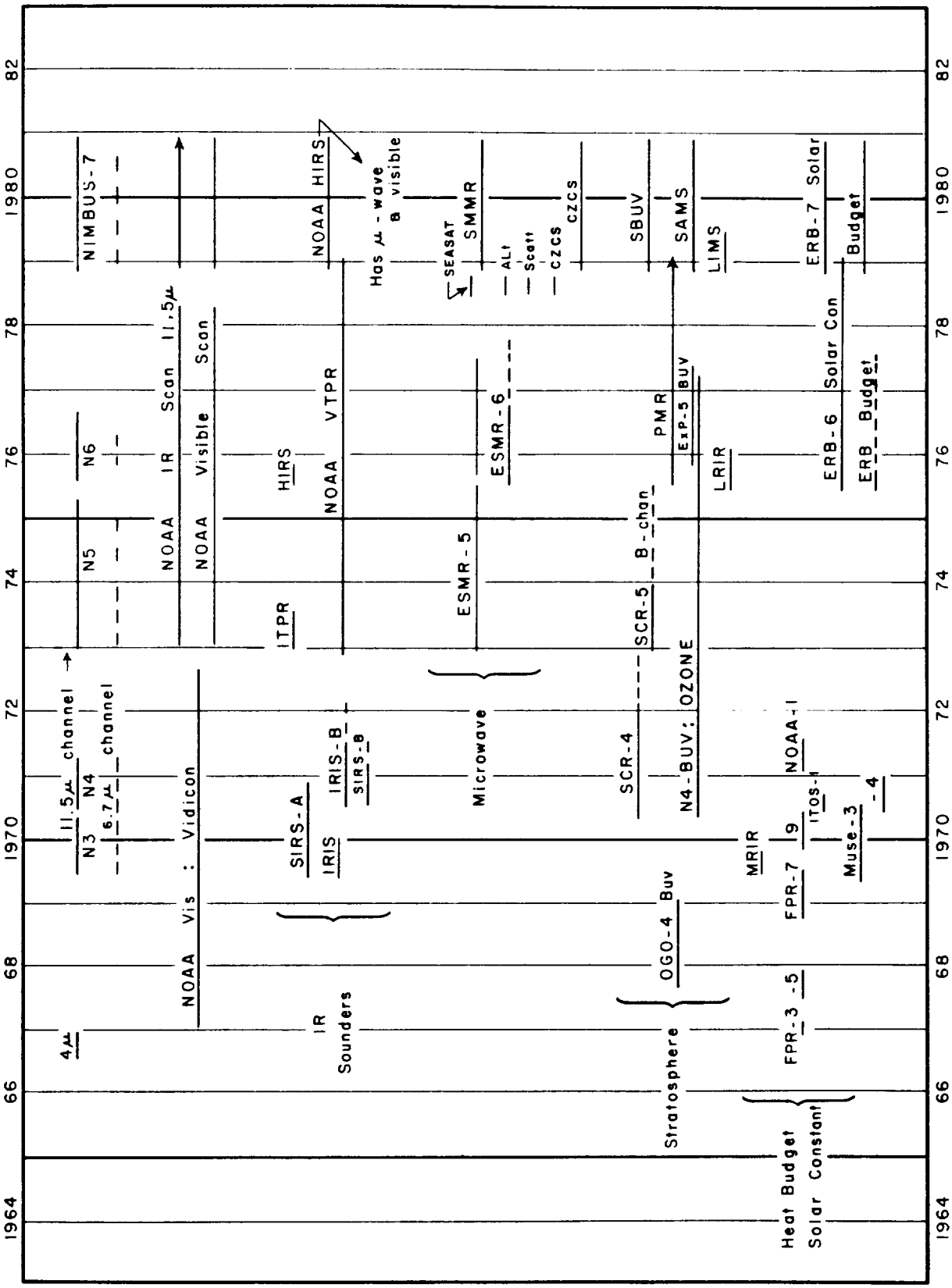

Figure 2. Satellite digital data. Data are also available from synchronous satellites.

A condensed set of 2 km, hourly data for the GATE area (10S-25N, 60W-10E) is on 83 tapes, 1600 bpi, at NCAR and Colorado State University. Associated radar-rainfall data are available for portions of the region.

1.2 Geosynchronous Satellite Data: ESA/Meteosat

The original raw Meteosat-1 digital image data at full resolution in three spectral channels, at half-hour intervals, have been archived for the two years of the life of this satellite (November 1977 – November 1979). Access to this data set will probably continue to be possible until about December 1982, but retrieval cannot be guaranteed after this date. There are three types of data: (1) visible with a resolution of 2.5 km at nadir, sampled each 2.5 km along the scan, (2) window IR with a resolution of 5 km sampled each 5 km, and (3) water vapor with a 5 km resolution. The scanning is usually done with 2 visible scans together (separated by 2.5 km), and one IR scan. When water vapor is sampled, it replaces one of the two visible scans; data are sampled each 5 km, but the format carries repeated data each 2.5 km.

1.3 Japan/GMS Satellite

The archive of the GMS is stored on 6250 bpi tape. The satellite has a visible resolution of approximately 1.25 km and infrared at approximately 5 km. The satellite is operated for a single image every 3 hours except at 0 and 12 Z when four images with half-hour separation are scanned for wind determination purposes. An archive of the full output of the GMS from 1 December 1978 – 30 November 1979 (= 7000 tapes) is maintained at the University of Wisconsin for FGGE research. The Japanese maintain a limited rotating archive of GMS data. The rotating archive may be retained for less than two years (details are not known).

1.4 NOAA Gridded IR and Visible Data

Grids of 1024 x 1024 points per hemisphere, prepared from NOAA scanner data (IR and visible) are available from January 1973 – 16 March 1978 and November 1978 – on. The resolution is 25 km at 60°N, 13 km at equator. The data at a gird point is made up of the latest observed spot. It is not an average of spots. The orbits were processed in time order during 1973-1978. For the TIROS-N data series, about one day in ten may have at least one orbit out of order; then it is not entirely possible to predict which orbit a grid value came from. The data could be put on 315 tapes through March 1978, but it is on 2600 tapes in Washington, D.C. Part of the data were prepared at a higher resolution.

Daily hemispheric pictures have been published each month. Some associated mean pictures were made.

The above data have also been mapped on a 65 x 65 grid per hemisphere starting June 1974. The data are on 7 tapes at NCAR. A 2.5° global grid is also available.

Global daily brightness data for 1 January 1967 – 31 August 1972 is on one tape at NCAR on a 5-degree lat-lon grid. It was prepared from vidicon tube data which cannot be calibrated as accurately as the above scanner data.

1.5 NOAA VTPR Sounder Data

All soundings are available for November 1972 – January 1979 on 1125 tapes. The data could be written on 130 tapes (1600 bpi). The spot resolution is about 55 km. There are 8 IR channels.

1.6 Tiros-N Series Satellites

The global archive of 4 km scanner data (GAC data – 4 channels) from Tiros-N started 21 October 1978. It has 2 visible and 2 IR channels. There are 95.2 minutes of data per tape, about 5800 tapes/year.

The sounder data started 21 October 1978. There is a scan each 6.4 sec, 56 steps in a scan, nadir resolution 17.4 km. There are 42 km between spots, 20 channels including IR, visible and microwave data. The archive has 610 tapes/year.

A data set of clear-column IR radiances, microwave channels, and derived soundings each 250 km is prepared on 25 tapes each year, starting January 1979. This archive also contains some cloud coverage data, derived from all the spots.

There is also a limited archive (near readout station) of AVHRR 1.1 km visible and IR data, starting 19 October 1978.

1.7 DMSP Satellite Sounders

Archives of these soundings were started in about 1977. The recent satellite included microwave channels. Visible data was taken with the separate scanner but not archived. A 11 km resolution cloud discriminator channel was saved for July – December 1979. The DMSP data stopped on 8 August 1980.

2. CLOUD DATA

Several sets of cloud analyses are described in WCRP, 1980. These include a cloud climatology by Telegades and London (1954) and London (1959). It is still one of the only sets giving information on mean heights and amounts for various cloud types. A summary of monthly total cloud cover, based on 1500 local time vidicon tube data, 1967 – 1970, was prepared by Miller and Feddes, 1971. Sadler, University of Hawaii, has prepared total cloud cover data for the tropical strip and the N. Pacific for February 1965 through February 1978. ESA plans to prepare cloud cluster analyses (200 km resolution) from Meteosat-2.

2.1 3-D Nephanalyses Data

These data give cloud coverage for 15 levels, 50 km resolution, each 3 hours. The N. Hemisphere is available from January 1971, S. Hemisphere from May 1974. The analysis methods used to combine satellite data, conventional data, and forecast or persistence information (for the derivation of cloud variables) have changed with time. The data from about 1975 are judged to be most

useful. The data are divided into 120 boxes covering the globe. There is one tape per box-month, thus 1440 tapes/year.

There are plans to change the basic archive to store bases, tops and coverage for up to four cloud levels.

3. CONVENTIONAL DATA TO SUPPORT CLOUD STUDIES

The conventional data from ground-based observing systems and aircraft will now be discussed.

3.1 Ship Synoptic

About 50 million surface synoptic observations are available from ships along shipping lanes starting in 1860. Most of these reports are now available on several hundred magnetic tapes.

3.2 Land Synoptic

Many synoptic reports are also available on tape from land stations, some decoded from telecommunications data and some prepared in delayed time. Many of the data have been prepared in station time series order (see Jenne, 1975, for details). Some of the data are still difficult to access.

3.3 Airways Observations

Airways reports from airports have sometimes been prepared into data sets at hourly or 3-hourly intervals. These contain more detailed cloud data than the synoptic data.

3.4 Ceilometer Observations

Measurements of ceiling height are routinely made at most major airports, using ceilometers, some of which are the lidar-type. In general these observations are only made when the ceiling is below a certain level, usually below 1 km or so. These data can provide an objective specification of the cloud base, but they represent point readings in the extreme sense, and they are not horizontally representative in chaotic sky conditions.

In Australia, the CSIRO have used a lidar and infrared radiometer to construct a climatology of cirrus clouds over 2 periods – March to August 1978 and November 1979 to May 1980. Data were obtained for approximately 70% of the time for which cirrus was visible. The climatology includes statistics on cloud base and top altitudes, mean cloud temperatures, visible optical depths and infrared emittances.

3.5 Aircraft Data

Aircraft sometimes observe the base and tops of clouds or "overcast below, clear above", etc. Most of these observations have not been saved in archives.

3.6 Rawinsonde Observations

These data are available both as decoded in real-time from GTS and also as prepared later by many countries into better checked archives. They are useful to identify the relationship between temperature and height and the humidity at different levels.

3.7 Analyses

To relate cloud temperature data to heights, one needs the relationship between temperature and height at the observation time.

N. Hemisphere tropospheric analyses of temperature and height are available from about 1963 with some earlier grids.

S. Hemisphere analyses are available from about 1972, prepared by Australia.

Global analyses are available from 1976, prepared by Washington.

3.8 Solar Data

Solar energy data could be used for cloud amount ground truth. Data on direct solar input, minutes of sunshine, and hemispheric radiometer data are available for many locations around the world. Direct solar input and minutes of sunshine give cloud/no cloud information as a function of time for a given point. These data can be processed into fractional cloud cover for climatological verification.

3.8.1 U.S. hourly total solar data

The U.S. has hourly solar total irradiance data from 26 stations starting in 1951. The data include the original hourly values as well as the "corrected" values. Corrections were added because of various bad calibrations and drifts in the sensors. There are problems in the corrections too.

3.8.2 Daily U.S. solar data

An additional 25 U.S. stations started measuring total daily solar starting about 1951.

A tape will have daily solar data, (reported and corrected) for the 26 + 25 U.S. stations. This will include max-min temperature, etc. (Whole period or only from 1965?)

3.8.3 New solar network – global radiation, direct, diffuse

The new global data started for 38 stations in January 1977. Most of the diffuse measurements were being made (I think) by mid 1977. In January 1978, the tracking pyrohelimeters were installed to measure the direct radiation. About 40 stations will be added to the 38, mostly just global radiation, many volunteer.

3.8.4 World-wide daily and monthly solar and net radiation at the surface

The USSR has maintained an archive of total radiation gathered from about 600 world-wide stations. The period of record generally starts about 1965. I have heard that many of the data are of relatively low quality, because many of the observing networks weren't well maintained. However, the data are still valuable when used properly. The USSR prepares a monthly publication with daily and monthly net radiation for about 65 stations and solar radiation for a few more stations. Data from about 5 U.S. stations are included.

3.8.5 U.S. sunshine data

The data gives minutes of bright sunshine. About 10 stations in 1890's, about 100 1978. Hourly and daily data are often available.

6.4 APPENDIX D

DATA ARCHIVES AND ANALYSIS/DATA COMPRESSION SCHEMES

Roy L. Jenne
National Center for Atmospheric Research
Boulder, Colorado

Methods for coping with the high volumes of satellite data by preparing intermediate-sized data sets will first be considered. Some complete sets of data at full resolution, perhaps limited by time or area, are also needed. The surfaced-based observations and data from older satellites are treated briefly, followed by major activities necessary to collect and prepare the cloud data.

In his discussion of data compression methods E. Smith of Colorado State University noted that data typically must be processed several times in different ways in order to obtain the necessary results. A. LeBlanc from the University of Wisconsin put the main emphasis on saving all of the data and doing all of the cloud calculations in real time. However, she also feels that an intermediate archive provides good insurance to meet needs for reprocessing.

Recommendation for Intermediate-Sized Archives

We should proceed with the definition of an intermediate archive that has enough components to permit a variety of calculations. Straw-man components are shown in Table 1 and include averages, one-dimensional histograms (Vis and IR), cloud element-size histograms, and spot samples. The samples should first be made by heavy sampling at the highest resolution (each 8-10 km). An archive with fewer samples should also be made (such as each 16 to 32 km). The numbers on the right column of Table 1 show the approximate numbers of 6250 BPI tapes per year from each satellite. These archives would also support calculations of other quantities such as convective rainfall, solar energy, surface temperature, etc.

High Resolution Data Archive

Some (or all) of the highest resolution data (with all samples saved) are also needed. The University of Wisconsin can save all data from one GOES satellite at a cost of about $125,000 per year. The recorder tapes have higher error rates and somewhat shorter lifetimes than ordinary tapes.

The following non-exclusive options for saving "full resolution" data should be considered for the cloud program:

- Save all the data
- Save all the data but at a lower time frequency than each half hour
- Save all of the data for a number of selected earth boxes.

Table 1
Components of Pilot Intermediate-Sized Archive for Cloud Research

	Space Resolution	Time Resol. Hours	Bits Each Sample	Grids Each Day	Bits/Year per Satl ($x10^9$)
For Each GOES					
1. Average radiation	80 km	3 (1 if easy)	8 bit	24IR, 13 Vis	2.1
2. IR histogram	250 km	3	(8 bit 83 lvl)	8 IR	1.17
3. Vis histogram	250 km	3	(8 bit 64 lvl)	5 Vis	0.6
4. Size histogram	250 km	3	–	8 IR, 5 Vis	2.0
5. Spot samples (IR)	8 km	3	8	8 IR	66*
(Vis)	8 km	3	6	5 Vis	25*
Each Orbiting Satel. Scanner**					
1. Sample the spots	8 km	cont.	8, 6	Vis, IR	85*
2. Average spots	80 km	cont.			2
Sounder					
3. All channels	250 km	cont.	8, 6		9
4. Four channels	40 km	cont.	8, 6		9

*Also, prepare a subset sampled each 16 km (or 32 km) having about ¼ (or 16) the volume. The 8 km data should perhaps be saved in boxes 1000 to 2000 km on a side. Sample other channels only each 16 or 32 km, at the same location as the above channels.

**Vis and IR histograms should be saved from the orbiter if 0.5–2 km resolution data is available. Otherwise they can be calculated with little loss from the 4 km data sampled each 8 km.

Work is needed on the following tasks and questions

- Define simple methods to eliminate unnecessary off-earth data and eliminate visible data at night from the archive. Preserve necessary calibration data.
- Summarize the information about instrumental noise of a spot sample vs its resolution.

- Determine whether there are any major problems when a 1 or 4 km resolution visible spot is used with a 8 km IR spot at the same location (to determine inter-relationships) instead of degrading the resolution of the visible samples through averaging.
- From future satellite in the TIROS-N series, we could probably obtain 1 km samples each 4 km rather than the present 4 km averages. Which is preferred?

Data Sets Needed

Both satellite data and conventional surface-based observations are needed to support necessary cloud studies. Data from orbiting satellites are needed as well as from geosynchronous ones. To obtain information about cloud variability, older data are needed in addition to current observations. Table 2 summarizes a selection of the ground-based data archives, and the satellite archives that are useful for cloud research. In most cases, the reduced numbers of tapes will be obtained by saving all of the data on higher density tapes, using better formats rather than by saving only part of the data. For the high volume geosynchronous satellites and for TIROS, the reduced volume is achieved by preparing intermediate archives.

Research Projects Needed

Research projects must continue to test the adequacy of given intermediate data sets for use in deriving cloud data. This will insure that the desired cloud information can be derived from the archives that finally will be provided.

International Experiment

Work has been underway for more than two years to plan an International Satellite Cloud Climatology Experiment, probably for 1983 through 1987. Because of national satellite schedules and and research needs, it would not be desirable to delay this experiment. The panel *recommends* U.S. participation. This means that there is an urgency to completing enough research to insure that the plans for the experiment provide adequate data sets.

FGGE Cloud Data

The FGGE year was ideal for the preparation of cloud information because it provided data from all five geosynchronous satellites, and from TIROS-N. Nimbus-7 provided heat budget and microwave data in addition to THIR 8 km IR data. The problem is that the costs would be relatively high to obtain subsets of all FGGE data for use in cloud studies.

Costs should be estimated for developing intermediate archives of the following most difficult data sets:

- For each geosynchronous satellite estimate a cost to prepare the strawman archives.
  - 8 km samples each 3 hours.
  - One-Dimensional histograms each 3 hours.
  - 80 km averages each one or 3 hours.

Table 2
Summary of Basic Cloud Data Set Options

		Tapes Now	Planned Tapes (6250)
Old surface synop	~1901-1965	1414	70
Sfc synop from teletype	1965-1980	400 to 2500	90-135
Ship log data	1850-on	500+	30-50
Scanners			
NOAA SR grids (20 km)	Jan 73 – Mar 78	2600	95
TIROS 4 km (ea 8 km)	21 Oct 78-on	5800/yr	85/yr**
NASA SR (N4, 5, 6, 7)	Apr 1970-on (breaks)	8700/yr	62/yr
DMSP (6 km spot ea 12 km)		none	40/yr
Geosynchronous			
Each US GOES (8 km)	FGGE on	all orig* 9530/yr	91/yr
ESA Meteosat (10 km)	FGGE on (break)	all orig 1728/yr	44/yr
GMS Japan (10 km)	FGGE on	all orig 1826/yr	55/yr
Sounders			
VTPR	Nov 72 – Jan 79	1130	40
TIROS (all chan, 250 km)	Nov 78-on	50/yr	9/yr
TIROS (all spots, 4 chan)	Nov 78-on	610/yr	9/yr
Clouds			
3-D neph	1971-1980	11460	700
(only do this now)	10 boxes, 1978-80	360	30

*The geosynchronous satellite now has much more volume than this.

**Only 2 channels.

- TIROS-N: Cost to prepare samples each 8 km of GAC 4 km data and in more compact format. Are 2 channels sufficient?
- NIMBUS-7 THIR: Cost to prepare all data in a more compact format.

If the projected costs for reducing all of the data are too high, a strategy such as processing only one full day in three from the geosynchronous satellites might be used.

History of Procedures Used

For the operational archiving of basic data and analyses, the data producers need to prepare condensed listings that describe the history of changes in procedures used, analysis methods, usual data inputs to analyses, and format changes. Satellite pictures are often navigated more precisely than indicated by the navigation on the tapes. Such precise correction information should also be archived.

6.5 APPENDIX E

CLOUD CLIMATOLOGY NEEDS OF CLIMATE MODELERS SUMMARY OF RECOMMENDATIONS PRESENTED TO NOAA USER'S WORKSHOP, DECEMBER 4-5, 1980

J. E. Hansen
NASA Goddard Institute for Space Studies
New York, New York 10025

The NASA/GISS Cloud/Climate Workshop was coordinated with the NOAA User's Workshop on Satellite-Derived Cloud Data, December 4-5, 1980, such that the cloud climatology needs of climate modelers defined at the GISS workshop could be presented at the User's workshop. The following two displays represent the requirements as I summarized them at the User's workshop. Display 1 is based primarily on a viewgraph shown by Bob Dickinson during the Panel 1 discussion at the GISS workshop, while Display 2 is based on a viewgraph I presented during the Panel 2 discussion. An attempt was made to incorporate suggestions which arose during our workshop, but we would welcome further suggestions of improvements for future discussions. You may also want to provide suggestions directly to the relevant program administrators, Robert Schiffer of NASA Headquarters and Rex Fleming of NOAA.

Display 1
Cloud Climatology Needs of Climate Modelers – Key Characteristics

1. Prime Objective in Next Decade: Cloud/Radiation Interaction
   - represents first-order impact of clouds on climate; is consistent with emphasis planned on radiation budget in mid 1980's
   - other important objectives include: *moist convection* (better description of occurence and structure of associated clouds); *rainfall* (correlation with clouds; heights of associated clouds and latent heat release)

2. Spatial Coverage: Global
   - needed for relation to global radiation

3. Temporal Coverage: Characterization of Annual Cycle
   - required for first-order cloud/climate relationships
   - implies need for at least *several years* of *consistent* cloud climatology to yield true mean annual cycle and interannual variability
   - implies need for information on *diurnal cycle* to obtain correct mean as well as to examine diurnal processes

4. Coincident Data Sets
   - radiation fields, temperature, humidity, surface albedo, others desirable

5. Cloud Characteristics
   - cloud altitude (at least 3 categories)
   - T_{top}
   - τ ($\rightarrow \epsilon$ for high clouds)
   - fractional cloud coverage
   - cloud brokenness, cloud scale (cloud type)

6. Resolution
   - prime need: 2½° x 2½°, monthly mean
   - some daily data and diurnal cycle needed

Display 2
Strawman Cloud Data Set Activity, which could be initiated now and is consistent with climate modeling needs.

1. Set of Pilot Studies using Existing Data
   - coordinated: in time period covered; to assure comparability of cloud data extracted from geosynchronous satellites and polar orbiters; etc.
   - regular meetings of participants
   - resulting data sets should be promptly and widely available, including prescriptions employed
   - include mechanism for exchange of information on data set status and modeling/analysis status (newsletter, e.g.)

2. Real Time Data Set Extraction
   - small group to work with operational system to define and test algorithms; should include expertise in ('inverse') radiative transfer ane in cloud modeling
   - same algorithms should be applied to both polar orbiting and geosynchronous satellite data
   - resulting data sets should be made widely available
   - entire data stream should also be saved for at least some time intervals during algorithm tests

3. Store Current Data Streams
   - investigate feasibility of storing full data streams
   - if this is impractical, implement a partial storage scheme, e.g., bursts of global data, complete time coverage for some regions, etc.

4. Organize Existing Data Sets onto Minimum Number of Tapes and Make Them Available
   - choice of data sets should be based on an overall cloud climatology strategy, possibly guided by an ad hoc group of experts

6.6 APPENDIX F

SELECTED BIBLIOGRAPHY

Cloud Parameterization

Arakawa, A., 1975: Modelling clouds and cloud processes for use in climate models. Appendix 4 in *The Physical Basis of Climate and Climate Modelling*. GARP Publication Series No. 16, World Meteorological Organization.

Cho, H-R., 1975: Cumulus cloud population and its parameterization. *Pageoph, 13*, 837-849.

Herman, G.F., and R. Goody, 1976: Formation and persistence of summertime Arctic stratus clouds. *J. Atmos. Sci., 33*, 1537-1553.

Heymsfield, A., 1975: Cirrus uncinus generating cells and the evolution of cirriform clouds. Parts I, II, III. *J. Atmos. Sci., 32*, 799-830.

Lilly, D. K., 1968: Models of cloud-topped mixed layers under a strong inversion. *Quart. J. Roy. Met. Soc., 94*, 292-309.

Lord, S. J., and A. Arakawa, 1980: Interaction of a cumulus cloud ensemble with the large-scale environment. Part II. *J. Atmos. Sci., 37*, 2677-2692.

Moeng, C-H., and A. Arakawa, 1980: A numerical study of a marine subtropical stratus cloud layer and its stability. *J. Atmos. Sci., 37*, 2661-2676.

Randall, D. A., 1980: Entrainment into a stratocumulus layer with distributed radiative cooling. *J. Atmos. Sci., 37*, 148-159.

Smagorinsky, J., 1960: On the dynamical prediction of large-scale condensation by numerical methods. *Physics of Precipitation, Geophys. Mongr.*, No. 5, Amer. Geophys. Union, 71-98.

Sensitivity Studies

Cess, R. D., 1976: Climate change: An appraisal of atmospheric feedback mechanisms employing zonal climatology. *J. Atmos. Sci., 33*, 1831-1843.

Cess, R. D., and V. Ramanathan, 1978: Averaging of infrared cloud opacities for climate modeling. *J. Atmos. Sci., 35*, 919-922.

Cox, S. K., 1971: Cirus clouds and climate. *J. Atmos. Sci., 28*, 1513-1515.

Hartmann, D. L., and D. A. Short, 1980: On the use of Earth radiation budget statistics for studies of clouds and climate. *J. Atmos. Sci., 37*, 1233-1250.

Manabe, S., and R. T. Wetherald, 1967: Thermal equilibrium model of the atmosphere with a given distribution of relative humidity. *J. Atmos. Sci., 24*, 241-259.

Ohring, G., and P. Clapp, 1980: The effect of changes in cloud amount on the net radiation at the top of the atmosphere. *J. Atmos. Sci., 37*, 447-454.

Ramanathan, V., and J. A. Coakley, 1978: Climate modeling through radiative-convective models. *Rev. Geophys. Space Phys., 16*, 465-489.

Roads, J. O., 1978: Numerical experiments on the climate sensitivity of an atmospheric hydrologic cycle. *J. Atmos. Sci., 35*, 753-773.

Schneider, S. H., 1972: Cloudiness as a global climate feedback mechanism: The effects on the radiative balance and surface temperature of variations in cloudiness. *J. Atmos. Sci., 29,* 1413-1422.

Schneider, S. H., and R. E. Dickinson, 1974: Climate modeling. *Rev. Geophys. Space Phys., 12,* 447-493.

Stephens, G. L., and P. J. Webster, 1979: Sensitivity of radiative forcing to variable cloud and moisture. *J. Atmos. Sci., 36,* 1542-1556.

Temkin, R. L., B. C. Weare, and F. M. Snell, 1975: Feedback coupling of absorbed solar radiation by three model atmospheres with clouds. *J. Atmos. Sci., 32,* 873-880.

Wang, W-C., W. B. Rossow, M-S. Yao, and M. Wolfson, 1981: Climate sensitivity of a one-dimensional radiative-convective model with cloud feedback. *J. Atmos. Sci.* (in press).

Climate Model Cloud Studies

Gates, W. L., 1976: The numerical simulation of ice-age climate with a global general circulation model. *J. Atmos. Sci., 33,* 1844-1873.

Miyakoda, K., and J. Sirutis, 1977: Comparative integrations of global models with various parameterized processes of subgrid-scale vertical transports: Description of the parameterizations. *Beit. Phys. Atmos., 50,* 445-487.

Schneider, S. H., W. M. Washington, and R. M. Chervin, 1978: Cloudiness as a climatic feedback mechanism: Effects on cloud amounts of prescribed global and regional surface temperature changes in the NCAR GCM. *J. Atmos. Sci., 35,* 2207-2221.

Wetherald, R. T., and S. Manabe, 1980: Cloud cover and climate sensitivity. *J. Atmos. Sci., 37,* 1485-1510.

Cloud Data

Avaste, O. A., G. G. Campbell, S. K. Cox, D. DeMasters, O. V. Karner, K. S. Shifrin, E. A. Smith, E. J. Steiner, T. H. Vonder Haar, 1979: On the estimation of cloud-amount distribution above the world oceans. Atmos. Sci. Paper No. 309, Colorado State Univ., Ft. Collins, 73 p.

Ball, J. T., S. J. Thoren, and M. A. Atwater, 1980: Cloud coverage characteristics during Phase III of GATE as derived from satellite and ship data. *Mon. Wea. Rev., 109,* 1419-1429.

Berlyand, T. G., and L. A. Strokina, 1974: Cloudiness regime over the globe. *Phys. Climatology, MGO,* Trudy, Vol. 338, 3-20.

Ellis, J. S., and T. H. Vonder Haar, 1976: Zonal average earth radiation budget measurements from satellites for climate studies. Atmos. Sci. Paper No. 240, Colorado State Univ., Ft. Collins.

Holle, R. L., J. Simpson, and S. W. Leavitt, 1979: GATE B-scale cloudiness from whole-sky cameras on four U.S. ships. *Mon. Wea. Rev., 107,* 874-895.

Houze, R. A., C-P. Cheng, C. A. Leary, and J. F. Gamache, 1980: Diagnosis of cloud mass and heat fluxes from radar and synoptic data. *J. Atmos. Sci., 37,* 754-773.

Johnson, R. H., 1980: Diagnosis of convective and mesoscale motions during Phase III of GATE. *J. Atmos. Sci., 37,* 733-753.

London, J., 1957: A study of the atmospheric heat balance. AFCRC-TR-57-287. New York Univ. College of Engineering, 99 pp. [NTIS PB 115626].

Miller, D. B., and R. G. Feddes, 1971: Global Atlas of Relative Cloud Cover 1967–1970. U.S. National Environmental Satellite Service and USAF Environmental Technical Applications Center, AD739434 – Report No. 1, Washington, D.C., 237 pp.

Reed, R. J., and E. E. Recker, 1971: Structure and properties of synoptic scale wave disturbances in the equatorial western Pacific. *J. Atmos. Sci., 28,* 1117–1133.

Reynolds, D. W., and T. H. Vonder Haar, 1977: A bispectral method for cloud parameter determination. *Mon. Wea. Rev., 105,* 446–457.

Sadler, J. C., 1969: Average Cloudiness in the Tropics from Satellite Observations. Int. Indian Ocean Expedition Meteor. Monogr. No. 2, East-West Center Press, Honolulu, 22 pp.

Sadler, J. C., L. Oda, and B. J. Kilonsky, 1976: Pacific Ocean Cloudiness from Satellite Observations. Technical Rept. of Meteorology, University of Hawaii, 137 pp.

Schutz, C., and W. L. Gates, 1971: Global Climatic Data for Surface, 800 mb, 400 mb: January. R-915-ARPA Order No. 189-1, Rand, Santa Monica, 173 pp. [also (1972) for July, R-1029-ARPA, 180 pp; (1973) for April, R-1317-ARPA, 192 pp.; (1974) for October, R-1425-ARPA, 192 pp.]

Telegados, K., and J. London, 1954: A physical model of the northern hemisphere troposphere for winter and summer. New York Univ. Sci. Rept. No. 1, Contract AF 19(122)–165, 55 pp.

Thompson, R. M., S. W. Payne, E. E. Recker, and R. J. Reed, 1979: Structure and properties of synoptic-scale wave disturbances in the intertropical convergence zone of the eastern Atlantic. *J. Atmos. Sci., 36,* 53–72.

Van Loon, H., 1972: Cloudiness and precipitation in the southern hemisphere. *Meteor. Monogr.* No. 13, 101–111.

Other Reports

GARP, 1975: *The Physical Basis of Climate and Climate Modelling.* GARP Publications Series No. 16, World Meteorological Organization, 265 pp.

GATE, 1980: Proceedings of the NAS Symposium on the Impact of GATE on Large-Scale Numerical Modelling of the Atmosphere and Ocean. Woods Hole Oceanographic Institution, 1979.

Jenne, R., 1980: Planning Guidance for the World Climate Data System. World Meteorological Organization.

Oort, A. H., and E. Rasmussen, 1971: Atmospheric Circulation Statistics. NOAA Professional Paper No. 5, U.S. Dept. of Commerce, 323 pp.

Oxford, 1978: JOC Study Conference on Parameterization of Extended Cloudiness and Radiation for Climate Models, Oxford, England, 1978, GARP Climate Dynamics Sub-programme, World Meteorological Organization.